

***Applications of Precision Agriculture (PA) tools
to manage climate variability in pastures in
Southeast Australia.***

James Gough (199022954)

ORCID iD: 0009-0002-2289-5303

Submitted in total fulfilment of the requirements of the degree of
Doctor of Philosophy

The School of Agriculture, Food and Ecosystem Sciences (SAFES)
The University of Melbourne, Australia.

March 2024

ABSTRACT	6
DECLARATION	8
PREFACE	9
ACKNOWLEDGEMENTS	10
ABBREVIATIONS	11
LIST OF TABLES	12
LIST OF FIGURES	13
1 INTRODUCTION	17
2 LITERATURE REVIEW	22
2.1 Scope of the Literature Review	22
2.2 Pasture-based livestock production in SE Australia	22
2.3 Climate in SE Australia.	26
2.3.1 Managing Variability	29
2.4 Use of biophysical models to understand climate variability impacts on agricultural production.	30
2.4.1 Agricultural Models History	30
2.4.2 Types of Agricultural Models	31
2.4.3 Australian Agricultural Models	32
2.4.4 Model and data output quality	36
2.4.5 Forecasting	36
2.4.6 Soil Moisture	40
2.4.7 Summary	40
2.5 What is Precision Agriculture?	41
2.5.1 Precision agriculture – tools and techniques	41
2.5.2 Remote Sensing	41
2.5.3 Imaging technologies	43
2.6 Monitoring Plant water stress using Remote Sensing	44
2.6.1 Monitoring soil moisture	48
2.6.2 Reliability, Interpretation, Cost	49
2.6.3 Capturing plant canopy Temperature in the field.	52
2.6.4 Crop water stress index (CWSI)	53
2.6.5 Issues Developing baselines.	55
2.6.6 Baselines and their development	56
2.6.7 Comparing baselines	57
2.6.8 Use of CWSI to understand spatial variability in agriculture.	59

2.7 Knowledge Gaps	60
3 UTILISING SOIL WATER CONTENT TO PREDICT PASTURE GROWTH RATES IN VICTORIA, AUSTRALIA.	
3.1 Introduction	62
3.2 Materials and Methods	63
3.2.1 Site Descriptions	63
3.2.2 Validation of predicted SWC	66
3.2.3 Modelling the effect of SWC on pasture growth rate	67
3.3 Results	69
3.3.1 Validation of predicted SWC	69
3.3.2 Pasture Growth Rates	70
3.3.3 Pasture growth predictions using SWC	72
3.4 Discussion	76
3.5 Conclusion	77
3.6 Supplementary Material	79
4 A CROP WATER STRESS INDEX FOR A PHALARIS (<i>PHALARIS AQUATICA L</i>) AND SUBTERRANEAN CLOVER (<i>TRIFOLIUM SUBTERRANEUM L</i>) PASTURE IN SOUTHEASTERN AUSTRALIA.	
	81
4.1 Introduction	81
4.2 Material and Methods	82
4.2.1 Experimental design and plot management	83
4.2.2 Meteorological Conditions throughout the experiment	84
4.2.3 Air Temperature during the Monitoring Period	86
4.2.4 Validation of canopy temperature sensors	89
4.2.5 Calculation of baselines	89
4.2.6 CWSI Calculations	90
4.2.7 Airborne thermal imagery acquisition	90
4.2.8 Processing of Thermal Images	91
4.2.9 Ground Truthing sites Species Composition – broader farm area	91
4.2.10 Calculating CWSI of the paddocks	93
4.3 Results	94
4.3.1 Diurnal Sampling	94
4.3.2 Validation of canopy temperature measurements using ground-truthing sites.	97
4.3.3 Time series of Canopy Temperatures	98
4.3.4 Baselines	99
4.3.5 Canopy temperature of field plots from flights	102
4.3.6 CWSI from flights	104
4.3.7 Comparison of canopy temperature and CWSI	104
4.4 Discussion	106
4.4.1 CWSI vs Pasture mass comparison	108
4.4.2 Spatial CWSI Discussion	109
4.4.3 Comparing Flight data to ground data.	110
4.4.4 Cloud Cover	110

4.4.5	Further Research	111
4.5	Conclusions	112
5 A CROP WATER STRESS INDEX OF ANNUAL RYEGRASS PASTURES IN SOUTHERN AUSTRALIA.		113
5.1	Introduction	113
5.2	Materials and Methods	113
5.2.1	Experimental design and plot management	113
5.2.2	Meteorological Conditions throughout the experiment	113
5.2.3	Baseline Calculations	114
5.2.4	CWSI Calculations	114
5.3	Results	115
5.3.1	Temperature	115
5.3.2	Diurnal Sampling	116
5.3.3	Soil Moisture	117
5.3.4	Baselines	118
5.3.5	Resulting CWSI	119
5.4	Discussion	120
5.5	Conclusion	123
6 COMPARISON OF EMPIRICAL, ADAPTIVE, AND BASELINE-DERIVED CROP WATER STRESS INDEX (CWSI) METHODS TO ASSESS PLANT WATER STRESS IN PASTURES IN SOUTHEAST AUSTRALIA.		124
6.1	Introduction	124
6.2	Materials and Methods	125
6.2.1	Experimental design and plot management	125
6.2.2	Meteorological Conditions throughout the experiment	126
6.2.3	Field Plots	126
6.2.4	Study Area	127
6.2.5	Thermal Image Acquisition Remote	128
6.2.6	Processing of Thermal Images	128
6.2.7	CWSI Calculations	128
6.2.8	Data analysis	128
6.3	Results	129
6.3.1	Baseline approach	129
6.3.2	Empirical Approach	129
6.3.3	Adaptive Approach	130
6.3.4	Comparison of the CWSI's generated	130
6.3.5	CWSI of paddocks	132
6.4	Discussion	136
6.5	Conclusion	139
7 GENERAL DISCUSSION		140

7.1	Introduction	140
7.2	Aims	140
7.3	Key findings and original contributions	140
7.4	Future Research	145
7.4.1	Pasture Growth Forecasting	145
7.4.2	CWSI/Baselines	146
7.5	Conclusions	147
8	REFERENCES	148

Abstract

Maximising the availability and use of grazed pasture is extremely important for grazing systems because it is usually the cheapest feed source for livestock. With increasing risks caused by variability in climate, precision agriculture (PA) technologies provide opportunities to routinely measure the current state of their pasture and to predict future pasture growth which may assist in risk management, but there has been relatively little research on PA application in pasture systems.

Some Australian farmers are utilising PA by using soil moisture probes to monitor soil water content (SWC) to assist in acquiring an indication of seasonal conditions. Farmers could utilise this knowledge of SWC to predict pasture growth in the weeks and months ahead. One pasture model being used to estimate pasture growth rates is the Sustainable Grazing Systems (SGS) pasture model which incorporates the farms soil moisture content and historical weather records to estimate pasture growth rates over the months ahead. This work explored the potential to link infield measurements of soil water content to pasture growth models, in order to predict future pasture growth. A study was undertaken to determine the usefulness of SWC as a predictor of pasture growth at three sites (Pigeon Ponds, Baynton and Dartmoor) in Victoria, Australia, with different climatic conditions and pasture types.

The SGS pasture model was used to predict monthly pasture growth rates based on historically dry (10th percentile), moderate (50th percentile) or wet (90th percentile) SWC, simulated using local climate data from 1990-2020. Results were presented as the probability that pasture growth will be in the lowest, middle or top tercile (third) of expected growth rates for the month.

The SGS modelling work demonstrated that the pasture growth forecast skill was mostly demonstrated at intervals within the main growing season with variation between each site. For Baynton, the forecasting skill was highest in October (Spring) and April and May (Autumn), at Pigeon Ponds it was in October and November (Spring) and April and May (Autumn) whilst at Dartmoor the forecasting skill was January through to April (Summer and Autumn).

In horticulture and other broadacre cropping PA is used to measure plant water stress using canopy temperatures. Numerous studies have been undertaken using stressed and non-stressed plants to develop the Crop Water Stress Index (CWSI) and accompanying baselines in horticulture and broadacre cropping over the years. Limited work has been undertaken on using the CWSI and associated baselines for annual ryegrass and pastures with mixed species in southeast Australia.

We developed field experiments set up on a commercial farm in Murroon, in the Otway's (38°27'S. 143°50'S, 273m alt.) in southwest Victoria which ran from October 2020 to January 2022. Two treatment plots were set up in the paddock: a well-watered (non-stressed) and a rainfall-only (stressed) plot. The pastures were predominantly phalaris (*Phalaris aquatica L*) with a small amount of clover (*Trifolium subterraneum L*) and dandelion (*Taraxacum officinalis*) weeds. A permanent thermal canopy sensor was installed in each plot, along with soil moisture probes and a weather station.

Field plots were set up to simulate a stressed and non stressed pasture, from which data was collected to develop the stressed and non stressed baselines. Canopy temperatures were collected remotely, using infield canopy temperature sensors and utilising a flir thermal camera from a plane, to examine the use of CWSI spatially, at the plot and paddock scale. The field experiments showed that the baselines could be developed in the Australian pasture context, with clear canopy temperature differentials observed between stressed and non-stressed field plots during stressed conditions which made it possible to then calculate the CWSI. This work also showed that the CWSI could be applied spatially for pastures, highlighting areas of stressed and non stressed pastures across the paddock and farm scale. A comparison between the baselines, empirical and adaptive CWSI was undertaken, with the baseline appearing more robust and useful as a method to determine the requirements for irrigation.

Future research should aim to expand the available CWSI baselines for pastures in southeast Australia and examine how the phenological stages of pasture growth may affect the baselines. SWC has utility in predicting pasture production, which varies from site to site, but this predictive power could be further enhanced by integrating seasonal climate forecasts.

Effective use of PA to monitor plant water stress by using the CWSI and improving accuracy in predicting pasture production can both assist with improving fodder management, quality and quantity in the weeks and months ahead, which is critical in an increasingly variable climate.

Declaration

This is to certify that:

1. The thesis comprises my original work towards the degree of Doctor of Philosophy except where acknowledged in the chapters.
2. Acknowledgement has been made in the text to all other material used.
3. This thesis is less than 100,000 words in length, exclusive of figures, tables and references.

James Gough
March 2024

Preface

The work in this thesis is original and was conducted during my PhD candidature (2019-2024) at the University of Melbourne.

The research was supervised by Associate Professor Brendan R. Cullen, Professor Pablo J. Zarco-Tejada and Professor Richard Eckard from The University of Melbourne.

Covid impacts

This work was undertaken during COVID-19, where in Melbourne we had 262 days of lockdown over 2020-2021 (Macreadie). As a result of the lockdowns, it was difficult to set up and run field experiments. For Chapter 3, we adapted by making it purely a desktop modelling exercise on data that we could obtain remotely, excluding field pasture cuts we had initially planned. For Chapter 4 and Chapter 5, we had to alter the field experiments from a number of sites spread across Victoria to one site that we could get intermittent access to. Whilst using one site was better than no sites, having a few sites would have been excellent to compare field results in different geographic locations.

Conference Attendance and Presentation

Attended the 63rd Annual Conference for the Grassland Society of Southern Australia (GSSA)

Presented Two posters at the GSSA conference.

Gough J (2022). Development of a Crop Water Stress Index (CWSI) for pastures. In 'Proceedings of the 63rd Annual Conference for the Grassland Society of Southern Australia – Sowing the Seeds of Success' Lardner Park, Victoria. Page 42.

Gough J (2022). Using Soil Water Content (SWC) to predict pasture growth rates in pastures in Victoria. In 'Proceedings of the 63rd Annual Conference for the Grassland Society of Southern Australia – Sowing the Seeds of Success" Lardner Park, Victoria. Page 42.

Acknowledgements

I would like to thank my supervisors, Associate Professor Brendan R. Cullen, Professor Pablo J. Zarco-Tejada and Professor Richard Eckard from The University of Melbourne for their guidance, advice, and patience.

In addition, I would like to thank Professor Kevin Smith at the Department of Agriculture for his input and advice, ensuring I reached the finishing line.

A special thanks to my wife and daughters, Sophia, and Zoe.

Finally, I'd like to thank those who have helped along the way, from my peers to my friends and relatives.

It was a long, challenging and yet rewarding journey, especially with the addition of COVID 19.

Abbreviations

- ABARES - Australian Bureau of Agricultural and Resource Economics and Science
- APSIM - Agricultural Production Systems sIMulator
- APSRU - Agricultural Production Systems Research Unit
- BOM - Bureau of Meteorology
- CERES - Crop Environment Resource Synthesis
- CSIRO - Commonwealth Scientific and Industrial Research Organisation
- CWSI - Crop water stressed Index.
- DM - Dry Matter
- EM - Electromagnetic spectrum
- FOV - Field of View
- Ha - Hectare
- LWI - Leaf Wilting index
- MLA - Meat livestock Australia
- NDVI - Normalised difference vegetation index
- NWSB - Non-water stressed baseline.
- PA - Precision agriculture
- PAW - Plant available water
- PAWC - Plant available water content
- RS - Remote Sensing
- SWC - Soil water content.
- TIR - Thermal Infrared
- UAV - Unmanned aerial vehicle
- VPD - Vapour pressure deficit.
- VRT – Variable rate technology

List of Tables

Table 1. Physical characteristics and soil water holding parameters, including saturated water content, field capacity and wilting point (all % volumetric) at the three sites.....	66
Table 2. Summarised results for Pigeon Ponds showing percent chance of predicted pasture growth being in the Low, Mid and Upper tercile. Upper tercile above 43 shaded in green, mid tercile above 43 shaded in grey and lower tercile above 43 shaded in orange.	73
Table 3. Summarised results for Baynton showing the percent chance of predicted pasture growth being in the Low, Mid and Upper tercile. Upper tercile above 43 shaded in green, mid tercile above 43 shaded in grey and lower tercile above 43 shaded in orange.	74
Table 4. Temperatures and CWSI of stressed and non-stressed field plots using flight canopy temperatures and baselines (non-stressed $y=-2.8212x+7.2968$. Stressed = 16) during the three flights.	104
Table 5. CWSI generated using baselines	129
Table 6. Maximum and minimum canopy temperatures for the stressed and non-stressed plots and empirically developed CWSI.	129
Table 7. CWSI results for the adaptive approach.....	130

List of Figures

Figure 1. Seasonal average pasture production (kg DM/ha.day) from 1960 to 2015 in 14-year time intervals at (a) Wagga Wagga without C4 grasses, (b) Wagga Wagga with C4 grasses, (c) Dookie, (d) Hamilton, (e) Ellinbank and (f) Elliott. (source Perera <i>et al.</i> (2020)	23
Figure 2. The varied Species composition at four sites in Southeast Australia (a) Attunga NSW, (b) Cargo NSW, (c) Hall ACT and (d) Nile Tasmania (Garden <i>et al.</i> 2000).....	25
Figure 3. Major Droughts and MDB (Murray Darling Basin) rainfall anomaly from seasonal average %. (King <i>et al.</i> 2020)	26
Figure 4. Climate Classification of Australia (Bureau of Meteorology).....	26
Figure 5. Rainfall anomaly southeast Australia (April – October) (CSIRO State of the Climate 2022).....	27
Figure 6. Annual mean temperature anomaly, Victoria. (http://www.bom.gov.au/cgi-bin/climate/change/timeseries.cgi?graph=sst&area=vic&season=0112&ave_yr=T).....	28
Figure 7. Anomalies in annual temperature over land in the Australian region (CSIRO State of the Climate 2022).	28
Figure 8. Australian Beef, Sheep and Lamb flock size fluctuations (Source – ABS, Agricultural commodities, Australia 2021-2022).....	29
Figure 9. Looking back at the last 70 years and the main drivers for developing agricultural system modelling (Source Jones <i>et al.</i> 2016).....	31
Figure 10. Varying Levels at which agricultural models are developed and operate at. (Jones <i>et al.</i> 2016)	32
Figure 11. Yield prophet simulation overview. (Source – Yield prophet website).....	34
Figure 12. Overview of the farm-predict system (Source - www.agriculture.gov.au)	35
Figure 13. Rainfall, three-month outlook, December to February (2023-2024). The chance of exceeding median rainfall (Source - Bureau of Meteorology).....	37
Figure 14. Accuracy for chance of above Median rainfall, November-JANUARY (Source Bureau of Meteorology).....	38
Figure 15. Projected green herbage forecast available to farmers using the CSIRO “Farming Forecaster.”	39
Figure 16. (a) Plant available water content (PAWC) v (b) Plant available water (PAW). Source Verburg <i>et al.</i> 2020.....	40
Figure 17. The Electromagnetic Spectrum. (Source- https://www.e-education.psu.edu/geog160/node/1958)	43
Figure 18. Components of plants and the vegetation spectrum. (Source - www.dronezon.com)	44
Figure 19. Relationship between the stresses, plants response and applicable remote sensing technique (Source - Jones <i>et al</i> 2010)	46
Figure 20. Water flow through a plant (Source - Plants and Microclimate, Jones 1992).....	47
Figure 21. Stomata open and closed (Source - Plant Physiology, 2nd Edition, p. 523, edited by Taiz and Zeiger.)	47
Figure 22. Remote measurement of canopy temperature (Source - Ahmad <i>et al.</i> 2021).....	48
Figure 23. Annual Soil Moisture measured at different depths, including annual rainfall for Harrow in South-west Victoria. (Source – https://extensionaus.com.au/soilmoisturemonitoring/)	49
Figure 24. Satellites and their spatial resolution since 1999 (Khanal <i>et al.</i> 2020).....	50
Figure 25. Summary of agriculture remote studies by geographic region by (a) platform and (b) sensor type. (Khanal <i>et al.</i> 2020).....	51
Figure 26. Plant canopy minus air temperature v's time for three guayule cultivars under wet (I_1), medium (I_2) and dry (I_3) irrigation treatments. Source – Bucks <i>et al.</i> (1985)	52
Figure 27. CWSI Formulae.....	53
Figure 28. Visual representation of how CWSI can be calculated from baselines.	54
Figure 29. UAV sourced thermal data to develop the CWSI for an olive orchard in Spain (Berni <i>et al.</i> 2009).	54
Figure 30. (a) NON-STRESSED Alfalfa (b) Stressed soybeans (Source - Idso <i>et al.</i> (1982))	57
Figure 31. Comparing baselines across a broad selection of species.....	58
Figure 32. Comparing baselines of fescue, Turfgrass and bermudagrass.....	58

Figure 33. NON-WATER stressed baselines reported by various researchers for Alfalfa (Payero <i>et al.</i> (2005)).....	59
Figure 34. Climate summary with average monthly rainfall (grey bars), and average monthly maximum (bold line) and minimum temperatures (lighter line) at (a) Pigeon Ponds, (b) Baynton, (c) Dartmoor from 1990-2021.....	65
Figure 35. Plant available water for three percentiles "dry" (0.1 percentile), 'moderate' (0.5 percentile), 'wet' (0.9 percentile) on the first day of each month at (a) Pigeon Ponds, (b) Baynton, and (c) Dartmoor.....	68
Figure 36. Daily measured relative SWC and predicted SWC from the SGS pasture model at 20 cm at (a) Pigeon Ponds, (b) Baynton, (c) Dartmoor.....	70
Figure 37. Simulated monthly average pasture growth rates (kg DM/ha.day) at (a) Pigeon Ponds, (b) Baynton, (c) Dartmoor. The shaded area shows the range of pasture growth rates, the dark line the 33 rd percentile and light line the 66 th percentile. Shaded areas below the 33 rd percentile line represents the low tercile, between the 33 rd and 66 th percentile line the mid tercile), and above the 66 th percentile the high tercile.....	71
Figure 38. Topographic map of the property with a black circle indicating the location of stressed and non-stressed field plots. (source - https://mapshare.vic.gov.au/vicplan).....	83
Figure 39. Annual total rainfall (mm) from 1980 to 2022.....	85
Figure 40. Monthly rainfall (mm) averaged between 1980 and 2022, and 2021 and 2022 as a comparison.....	85
Figure 41. Maximum monthly temperatures (°C) averaged between 1980 and 2022, including 2021 and 2022 as a comparison.....	86
Figure 42. Air temperatures (°C, 12.00 noon – 1.00 pm) throughout period of the field experiments with flight dates (red arrows).....	86
Figure 43. Soil moisture, rainfall and watering throughout the field experiments. Red arrows indicate the time of the flights.....	87
Figure 44. VPD comparison between calculated and collected from the sensor (HT.w Sensor, SensorPush).....	88
Figure 45. (A) Field plot set up, showing soil moisture probe and thermal camera, fenced off to restrict stock and wildlife. (B) aerial view of two field plots within the paddock.....	88
Figure 46. Pasture composition (% DM) within the plots on the 11/9/2021.....	89
Figure 47. Flight path taken to collect aerial canopy data, the red box indicates the farm boundary where field experiments were conducted (14/12/2020). Red box indicates area of farm.....	91
Figure 48. Locations where species composition and pasture mass (kg DM/ha) were collected....	92
Figure 49. Species composition and pasture mass (kg DM/ha). (a) 29/11/2021 (b) 14/12/2021.	93
Figure 50. Outline (in black) of the two paddocks used for the following CWSI calculations.....	94
Figure 51. Diurnal sampling canopy temperature (°C) undertaken on stressed and non-stressed plots on 1/1/2022.....	95
Figure 52. Canopy Temperature (Deg C) spread recorded by handheld thermal sensor (a) stressed pasture (b) non-stressed pasture on 21/1/2022.....	96
Figure 53. Validation of canopy temperature comparing handheld thermal sensor to Goanna Ag field sensor (A, stressed field plot, B, Non-stressed field plot).....	97
Figure 54. Comparison of handheld temperatures (13 sites around the farm) and flight data (a) 29/11/2021, (b) 14/12/2021.....	98
Figure 55. (a) Daily canopy temperatures (Tc) of the stressed and non-stressed pasture. (b) Daily Tc – Ta of stressed and non-stressed pastures between 1-2 pm.....	99
Figure 56. Non-stressed baseline development, (a) excluding wet days and solar radiation under 700 W/m ² , (b) excluding wet days and solar radiation under 1,000 W/m ² , (c) excluding wet days and solar radiation under 1,100 W/m ²	100
Figure 57. Stressed baseline development (a) Tc – Ta, less rain and solar radiation under 1200 W/m ² . (b) Tc – Ta, less rain and solar radiation under 1250 W/m ²	101
Figure 58. CWSI calculated from the ground canopy sensors screening for wet days and solar radiation under 900 W/m ²	102
Figure 59. CWSI was calculated from the ground canopy sensors, excluding wet weather and solar radiation under 1200 W/m ² using 16 Deg C as the stressed baseline (y = -2.9289x + 7.286).....	102

Figure 60. Canopy temperature (Deg C) variation across non-stressed and stressed plots from aerial flight (14/12/2020). The average temperature of the stressed plot was 40.88 °C, and the non-stressed plot was 38.15 °C.....	103
Figure 61. A broader view of pasture canopy temperatures (Deg C) recorded during the flight (14/12/2020) from the FLIR camera. Field trial plots in square boxes (canopy temperatures). ...	103
Figure 62. CWSI was derived from flight 1 (14/12/2020). Field trial areas in black squares. Non-stressed compound CWSI =0.15 Stressed compound CWSI=0.48.	104
Figure 63. CWSI of flights (a) Flight 1. 14/12/2020, (b) Flight 2. 29/11/2021, (c) Flight 3. 14/12/2021. Using the baselines (non-stressed $y=-2.9289x+7.286$. Stressed = 16).....	106
Figure 64. Analysis of the % per cwsi range across the paddocks for flights 1, 2 and 3. The average CWSI range for Flight 1 was 0.45, for Flight 2, it was 0.18 and for Flight 3, it was 0.27.	106
Figure 65. Pasture non-stressed baseline compared against other baselines developed by Idso <i>et al.</i> (1981).....	107
Figure 66. CWSI over time, less wet days and days where solar radiation are below 600 w/m ²	108
Figure 67. comparison comparing the CWSI and pasture mass (kg DM/ha).....	109
Figure 68. Thermal temperature issues. Pasture and non-pasture-based thermal temperatures were recorded with a FLIR camera during flight data acquisition.	110
Figure 69. Average cloud cover between 9 am and 3 pm for Australia (source BOM). Red circle indicates location of field site.	111
Figure 70. Waterings (mm) and Rainfall (mm) throughout the experiment.	114
Figure 71. CWSI Formulae.....	115
Figure 72. Canopy temperature of stressed and non-stressed plants, including air temperature..	116
Figure 73. Diurnal sampling of ryegrass 2/1/2022.....	116
Figure 74. Canopy Temperature (Deg C) spread recorded by handheld thermal sensor (a) stressed pasture (b) non-stressed pasture on 2/1/2022.....	117
Figure 75. Soil moisture (mm) of the stressed and non-stressed plot areas.....	118
Figure 76. Baselines (stressed and non-stressed) with manually adjusted stressed baseline.	118
Figure 77. CWSI during periods of higher ambient temperature, experienced in late December and January (21/12/2021).....	119
Figure 78. CWSI between 21/12/2021 and 31/1/2022 during hotter periods of year, putting the plants under water stress.....	119
Figure 79. Comparison of annual ryegrass baseline to Tall Fescue (Haghverdi <i>et al</i> 2021), Hybrid Bermuda (Haghverdi <i>et al</i> 2021) and Turfgrass (Gonzalez-Dugo <i>et al</i> 2022).....	120
Figure 80. Rainfall (mm) collected from an on-site weather station.	126
Figure 81. Dates and amounts (mm) of water added to non-stressed plot during field trials.	127
Figure 82. Field plots (blue squares) and Area A used to develop the histogram.	127
Figure 83. Frequency distribution histogram of field Canopy Temperatures (°C) of area in figure 6 for each flight.	130
Figure 84. Comparing the three flights' (baseline, empirical and adaptive) generated CWSI results. (a) Flight 1, (b) Flight 2, (c) Flight 3 of the field plots. (note: Empirical will always result in a CWSI of 0 to 1.)	131
Figure 85. Pasture canopy temperatures (°C) were obtained remotely (by plane) on 14/12/2020. Stressed and non-stressed field plots and a broader area (paddocks) are shown. Area within black outline is the paddock boundary.....	132
Figure 86. Pasture canopy temperatures (Deg C) were obtained remotely (by plane) on 29/11/2021. Stressed and non-stressed field plots and a broader area (paddocks) are shown. Area within black outline is the paddock boundary.....	133
Figure 87. Pasture canopy temperatures (Deg C) were obtained remotely (by plane) on 14/12/2021. Stressed and non-stressed field plots and a broader area (paddocks) are shown. Area within black outline is the paddock boundary.....	133
Figure 88. Analysis of the CWSI range for flight 1 over several paddocks, using the (a) baseline, (b) empirical and (c) adaptive CWSI methods.....	134
Figure 89. Analysis of the % CWSI range for (a) flight 1 (14/12/2020) and (b) flight 2 (29/11/2021) using the baseline, empirical and adaptive CWSI methods.	135
Figure 90. Average CWSI for (a) flight 1 (b) flight 2, using the different CWSI calculation methods.	136

Figure 91. Comparing pasture and annual ryegrass stressed and NON-STRESSED baselines developed in SE Australia as part of the field work undertaken for this thesis.....	142
Figure 92. Comparing the pasture and annual ryegrass NON-STRESSED baselines developed as part of this thesis against a number of other plants.....	143

1 Introduction

Use of canopy temperature and biophysical modelling to improve management of climate variability in grazed pastures.

Background

Field-grown pasture is the primary and cheapest feedstock for cattle and sheep in southern Australia (Perera *et al.* 2020, Chapman *et al.* 2009) and many other regions worldwide. Climate, particularly rainfall variability, is one of the significant sources of intra and inter-annual variation in pasture growth (Chapman *et al.* 2009). In the temperate and Mediterranean climates of southern Australia, pasture growth is primarily limited by water availability from mid-late spring to the time of the opening rains in autumn, while appropriate spring and autumn temperatures, nutrients, disease and other management practices (overgrazing) can also affect pasture growth. If the farmer can more accurately predict the fodder available in their paddocks in the coming weeks and months, they can improve their resource management and produce more fodder with fewer resources. The first part of this thesis examines the ability to model soil water content (SWC) to predict pasture growth rates in pastures in Victoria.

The second related topic involved using precision agriculture and remote sensing to remotely monitor plant water stress in pastures using canopy temperature sensors and generate stressed and non-stressed baselines for a CWSI (Crop Water Stress Index) for pastures. The CWSI relies on recording the canopy temperatures of the plants to identify stressed and non-stressed plants. Water deficits occur in plants when evaporative demand exceeds the supply of water in the soil (Slatyer, 1967). When there is inadequate water for the plant, the water stress causes partial stomatal closure and reduction in transpiration rates, and the reduced evaporative cooling raises the canopy temperature in relation to the ambient temperature (Jones, 1999). This canopy temperature difference can be measured and used to identify stressed and non-stressed plants in a plot or at a broader scale, such as across a paddock or farm. Using the CWSI can assist farmers in quickly identifying plant water stress over broad areas such as a paddock, vineyard or orchard, using the canopy temperature to measure the plants' water stress status. The CWSI has been extensively used in horticultural and other crops internationally (Idso 1982) and in parts of Australia (Park, *et al.* 2015) to measure the canopy temperature difference between a stressed and non-stressed plants; however, more work needs to be done on using the CWSI on pastures globally.

Literature review overview

Livestock producers in SE Australia experience fluctuations in pasture production within a season and from season to season and managing the pasture production and undertaking feedstock budgeting from month to month is critical to animal health and for the economic performance of farmers. The uneven pasture production is primarily governed by climate variability, ultimately affecting soil

moisture (Perera *et al.* 2020). In SE Australia, pasture production and quality are largely driven by the amount and timing of rainfall, with the peak pasture growth period being in the spring season for temperate pasture species (Chapman *et al.* (2009). Phalaris (*Phalaris aquatica*), an important perennial grass in south-eastern Australia due to its high productivity (Anderson *et al.* 1999; Reed *et al.* 2008a) and its ability to survive drought (Robinson *et al.* 1966, Hutchinson, 1979) and its drought tolerance is becoming more critical as summer droughts become more frequent and more severe (Kiem *et al.* 2016). Whilst phalaris is seen as an important pasture in the Australian grazing context, it can be affected by stresses related to climate, soil and grazing pressure, which can affect its persistence (Culvenor *et al.* 2014).

Biophysical agricultural models can simulate biological systems, assisting farmers in predicting the pasture growth that they can expect in the weeks and months ahead. These models can utilise local historic climate data and current on-farm conditions to simulate a range of pasture growth possibilities ahead. Several biophysical models are used in cropping, dairy, and weather forecasting, with the SGS pasture model being developed for southeast Australian conditions. In rain-fed cropping systems, SWC or Plant Available Water (PAW) is well established as a valuable indicator of future yield potential (Carberry *et al.* 2002, Foale *et al.* 2004), and systems have been developed to store soil moisture prior to planting in order to minimise climate risk (Hunt *et al.* 2011). Tools such as 'Yield Prophet' have been developed to improve the understanding of seasonal climate risk in cropping systems (Hochman *et al.* 2009) and to evaluate management input decisions (such as nitrogen fertiliser rates) to improve decision-making for grain growers (Hunt *et al.* 2006). However, there needs to be more research on the value of SWC for managing climate risk in pasture-based livestock production systems. Pasture systems differ from crop systems because they are often based on perennial plants rather than annual species and aim to supply year-round feed to meet livestock demands rather than a single crop harvest.

Precision agriculture (PA) can assist with managing some of the risks around pasture production. The tools and techniques of PA are examined along with work to date using remote sensing in agriculture. It examines the use of PA to measure plant water stress and how the soil water content or canopy temperature can indirectly monitor it. Canopy temperature is generally accepted as an indirect, rapid, accurate and a large-scale indicator of crop water stress (Gonzalez-Dugo *et al.* 2022). Canopy temperature is considered a reliable proxy for plant water stress monitoring and irrigation scheduling (Tanner, 1963; Idso *et al.* 1984; Steele *et al.* 1994). The issues of using the CWSI and baselines are also examined when developing the baselines; clear sky conditions (Idso, 1982) are required, as well as consideration of the growth stage of the plant (i.e. for grain crops pre-heading or post-heading, (Idso, 1982)).

The CWSI has been used extensively in orchards and vineyards in Europe and the United States to monitor plant water stress. Initial studies undertaken by Idso *et al.* (1981) also developed baselines for numerous vegetable crops across sites in the USA. Continuing studies are being undertaken using the CWSI in other geographic

locations, looking at similar species with different varieties (i.e. vines with different cultivars) and looking into using the CWSI as a tool for controlling irrigation. However, minimal work has been undertaken on developing baselines and using the CWSI for pastures in southeast Australia, with limited information on the CWSI of annual ryegrasses or pastures in southeast Australia specifically. The CWSI can be calculated from baselines, empirically and theoretically. To develop stressed and non stressed baselines, the canopy temperature, air temperature and VPD needs to be recorded for stressed and non stressed plants and plotted. The empirical approach uses the formulae suggested by Idso (1981) and involves gathering canopy temperature for the canopy being measured, the air temperature, the canopy temperature of a stressed and non stressed canopy. Having a stressed and non stressed plant in order to undertake CWSI calculations is not always practical. A form of adaptive CWSI has also been used, using a histogram to assess the canopy temperatures in the area of interest and then using the high and low points in the histogram as the stressed and non stressed temperatures for the formulae. Jackson *et al.* (1981) also developed a theoretical CWSI, which requires canopy temperature, air temperature, relative humidity, net radiation wind speed and crop height.

Aims of the study

The research aimed to develop approaches to manage climate variability in pastures in south-eastern Australia, with a particular focus on water stress. Biophysical modelling was used to predict the impact of soil water on pasture growth and precision agriculture approaches were used to record canopy temperatures of stressed and non stressed pastures to develop baselines and calculate the CWSI.

The specific research questions and hypothesis were:

1. Is soil water content (SWC) a reliable predictor of pasture growth? How reliable is the prediction of pasture growth, and does it predict more reliably at certain times of the year? How does the pasture growth prediction vary due to climate and pasture types?

Hypothesis: Wet/dry SWC will result in model predictions of high/low pasture growth rates

Hypothesis: Pasture growth predictions will show most differences in the spring season.

2. Do water stressed (non-irrigated) and non-stressed (irrigated) pastures show different canopy temperatures?

Hypothesis: The stressed canopy will have a higher temperature than the non-stressed canopy (based on literature from other species).

3. Can the canopy temperatures of water-stressed (non-irrigated) and non-stressed (irrigated) pastures (Phalaris, Clover, and Dandelion) in southeast Australia be used to create the baselines and CWSI for pasture?

What are the issues of calculating the CWSI and baselines on pastures in southeast Australia?

Hypothesis: The stressed and non-stressed baselines and CWSI will be able to be developed for pastures and will be similar to the annual ryegrass pastures.

4. Can the stressed and non stressed baselines and the CWSI be developed remotely for an annual ryegrass pasture in southeast Australia? What are the issues of calculating the CWSI and baselines on annual ryegrass in southeast Australia?

Hypothesis: The stressed and non-stressed baselines and CWSI will be able to be developed for the annual ryegrass pasture.

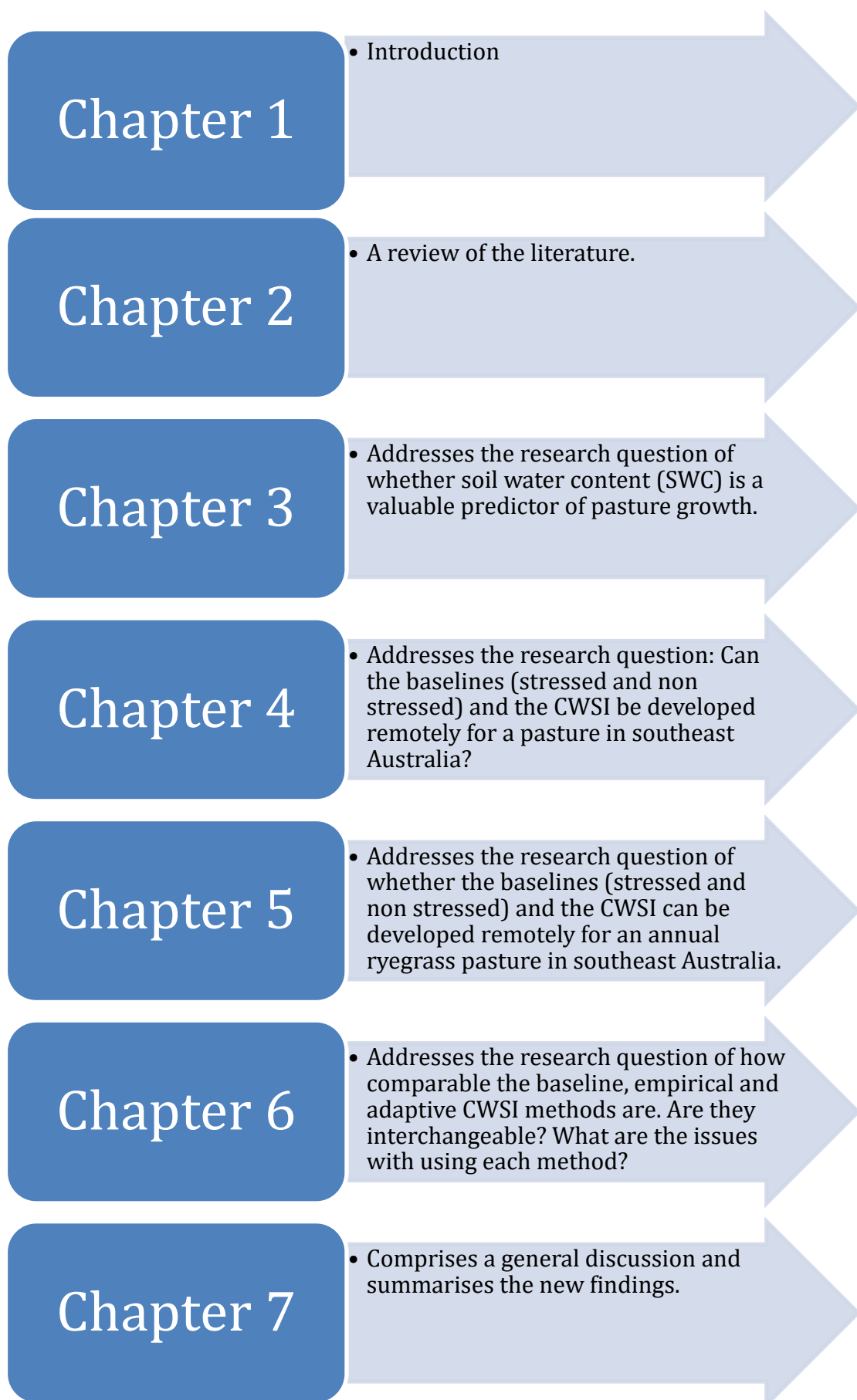
5. Can the CWSI and baselines be applied spatially? Can this data be used spatially to project the CWSI across a paddock, property, and surrounds? What are the issues of calculating the CWSI and baselines from aerially derived data on pastures in southeast Australia?

Hypothesis: The CWSI method developed will be able to detect spatial variation in pasture water stress, and temporal variation (flights on different days).

6. How comparable are the baseline, empirical and adaptive CWSI methods? Are they interchangeable? What are the issues with using each method?

Hypothesis: The baseline and empirical CWSI method will provide a more realistic result for plant water stress, and the adaptive CWSI will be less accurate than the conventional CWSI; however, the adaptive CWSI will still highlight areas of plant water stress in the field over a broad area (farm-scale).

Thesis Structure



2 Literature review

2.1 Scope of the Literature Review

The scope of the literature review was to investigate what biophysical models are used in agriculture and the pasture systems in Southeast Australia. The specific focus of this was on pasture modelling tools and forecasting, how they are used, and how fodder growth forecasts are presented to end users for pastures in Southeast Australia. This review does not cover all the plant species, management variables, soil conditions, fertilisation rates, etc., that can contribute to the variability of pasture fodder production.

The literature review also considers the use of the Crop Water Stress Index (CWSI) and the development of baselines (stressed and non-stressed) as a way of evaluating plant water stress and how and where it has been applied in the field. The review examined the use of the CWSI across the globe and examines potential limitations for using the CWSI in Southeast Australia with regard to pastures.

2.2 Pasture-based livestock production in SE Australia

Livestock producers in SE Australia experience fluctuations in pasture production within a season and from season to season. Managing pasture production and undertaking feedstock budgeting from month to month is critical to animal health and the farmers' profitability. Agricultural production is also significant to Victoria. The gross value of agricultural production in Victoria was \$17.5 billion (2020-21), which was 25% of the total gross value of agricultural production in Australia (Victorian Agriculture Industry Snapshot, January 2023). Livestock production in Victoria also plays a significant role in the state's economy. In Victoria, the gross value of agricultural milk production was \$2.86 billion, beef was \$2.58 billion, and sheep meat was \$1.90 billion. Most of South West Victoria's sheep and cattle production is based on dryland pasture systems of summer dormant cultivars of perennial ryegrass (*Lolium perenne*) or phalaris (*Phalaris aquatica L*) with subterranean clover (*Trifolium subterraneum*) (Waller *et al.* 2001).

One major issue for Australian farmers is the uneven pasture production within a year (seasonal variation) and between years (inter-annual variation) (Perera *et al.* 2020). The uneven pasture production is primarily governed by climate variability, ultimately affecting soil moisture (Perera *et al.* 2020). Work undertaken by Perera *et al.* (2020) examining the seasonal average pasture production (kg DM/ha.day) from 1960 to 2015 across five different sites clearly shows the increase in pasture production in Spring, with the least amount of pasture production typically in Summer in southeast Australia (Figure 1). Perera *et al.* (2020) also found that year-to-year pasture yield variability had increased from 2002 -2015 compared with an earlier period (1998-2001).

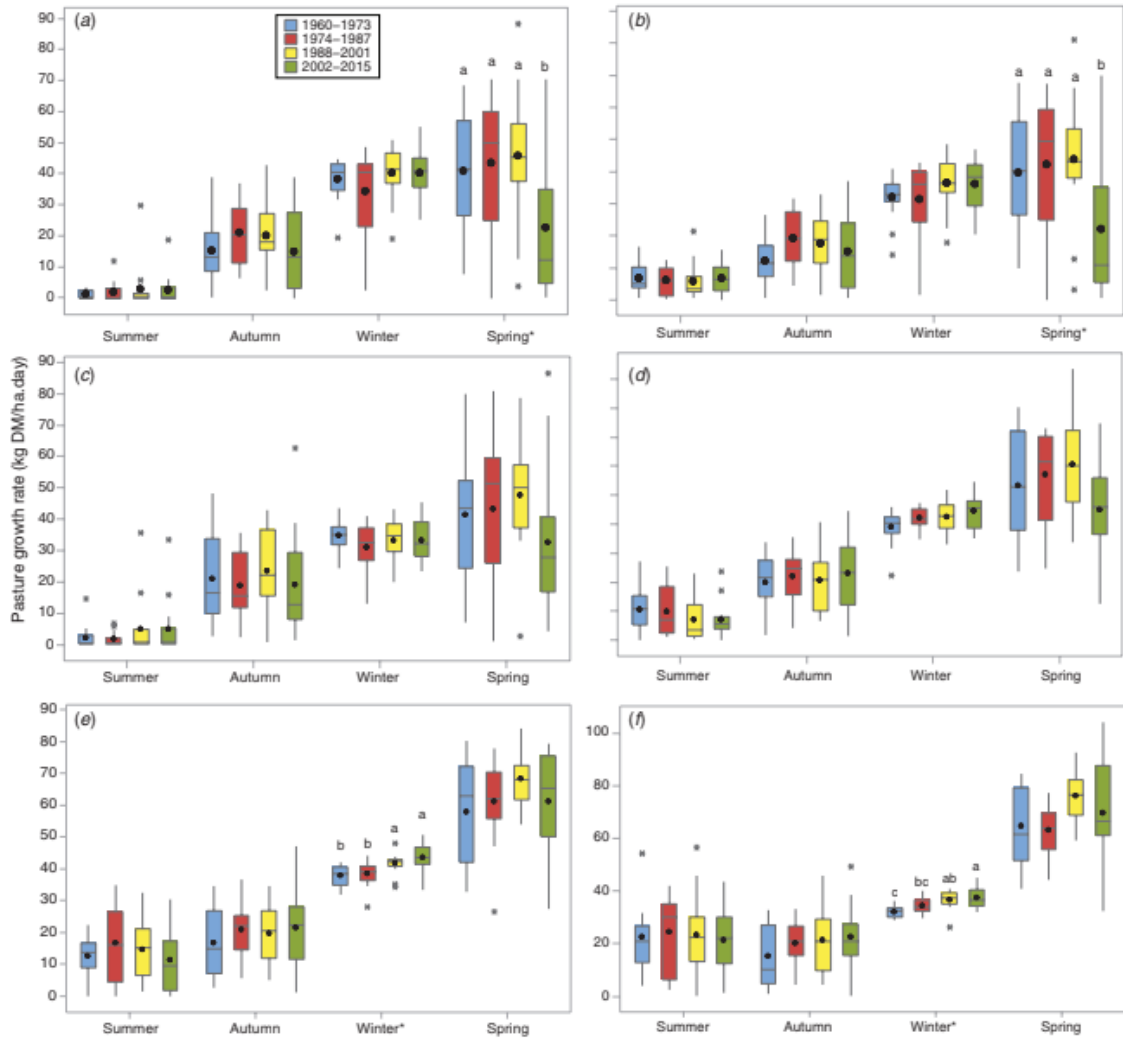


FIGURE 1. SEASONAL AVERAGE PASTURE PRODUCTION (KG DM/HA.DAY) FROM 1960 TO 2015 IN 14-YEAR TIME INTERVALS AT (A) WAGGA WAGGA WITHOUT C4 GRASSES, (B) WAGGA WAGGA WITH C4 GRASSES, (C) DOOKIE, (D) HAMILTON, (E) ELLINBANK AND (F) ELLIOTT. (SOURCE PERERA *ET AL.* (2020)

One of the most important perennial pasture grasses in southeastern Australia is phalaris due to its high productivity (Anderson *et al.* 1999; Reed *et al.* 2008a) and its ability to survive drought (Robinson & Simpson, 1966; Hutchinson, 1970). Its ability to survive summer drought is due to deep roots and partial summer dormancy (Culvenor, 2009). While phalaris is considered an essential pasture in the Australian grazing context, it can be affected by climate, soil, and grazing pressure stresses, affecting its persistence (Culvenor *et al.* 2014). Disease and interplant competition can also affect its persistence (Culvenor *et al.* 2014). Cocksfoot (*Dactylis glomerata L.*), tall fescue (*Festuca arundinacea*) and phalaris (*Phalaris aquatica*) are the major sown permanent, perennial grasses in areas of high rainfall in southeast Australia considered too dry for perennial ryegrass (*Lolium perenne L.*) (Culvenor *et al.* 2016).

Since European settlement, the botanical composition of native pastures in high-rainfall temperate areas of Australia has changed (Moore, 1970). Grazing,

accidental and deliberate introduction of exotic species and fertiliser applications have generated many pastures with a mix of native and exotic perennial grasses, annual grasses and native and exotic legumes (Garden *et al.* 2000). Some pastures may contain sown exotic pastures, sown to create feed for grazing stock (Garden *et al.* 1996).

Seed supply companies and researchers have been undertaking field trials looking at improving the cultivars (Culvenor *et al.* 2016) and genetics of the pastures used in the Australian grazing industry with overseas species being brought in and trialled to see how they survive, how much biomass they yield, their persistence, etc in the Australian environment (Culvenor *et al.* 2016).

In Europe, agriculture production has relied on the application of nitrogen fertiliser for the production of grasses. In contrast, Australia has relied on using legumes in pastoral agriculture to maintain low-cost farming (Ledgard *et al.* 1992). However, in more recent times, the use of nitrogen has increased in Australia (Rawnsley *et al.* 2019). Legumes have been identified as important in the Australian grazing environment as they fix atmospheric nitrogen in the soil, potentially improving pasture biomass production (Sanford *et al.* 1995). Legumes and taller grasses can be more dominant at different times of the year (Sanford *et al.* 1995) and, in some cases, can complement each other. Lucerne (*Medicago sativa* L) has also been used as a legume in pastures to restore soil fertility and nitrogen status of soils in cropping and pastures (Davies *et al.* 2003, Ledgard *et al.* 1992).

Similarly, part of work undertaken by Garden *et al.* (2000) looking at grazing management on the botanical composition of native grass-based systems in southeast Australia demonstrated the varied botanical composition throughout the year at four sites in Southeast Australia that had been previously grazed by sheep and cattle (Garden *et al.* 2000). These examples (Figure 2) also demonstrate how the species composition mix can change composition throughout the year. One issue with having mixed species can be the effect of taller grasses shading other pastures (i.e., clover) at certain times of the year (Sanford *et al.* 1995), making it harder for these small plants to grow and possibly contributing to their reduction in density in a paddock. These taller pastures may be alive and still growing or senescing, but they provide shading that may reduce the performance of other grasses or clovers. Clover and pasture composition and make-up can also be influenced by defoliation caused by overgrazing (Sanford *et al.* 1995). Livestock can selectively graze certain plants/species, further stressing certain pastures.

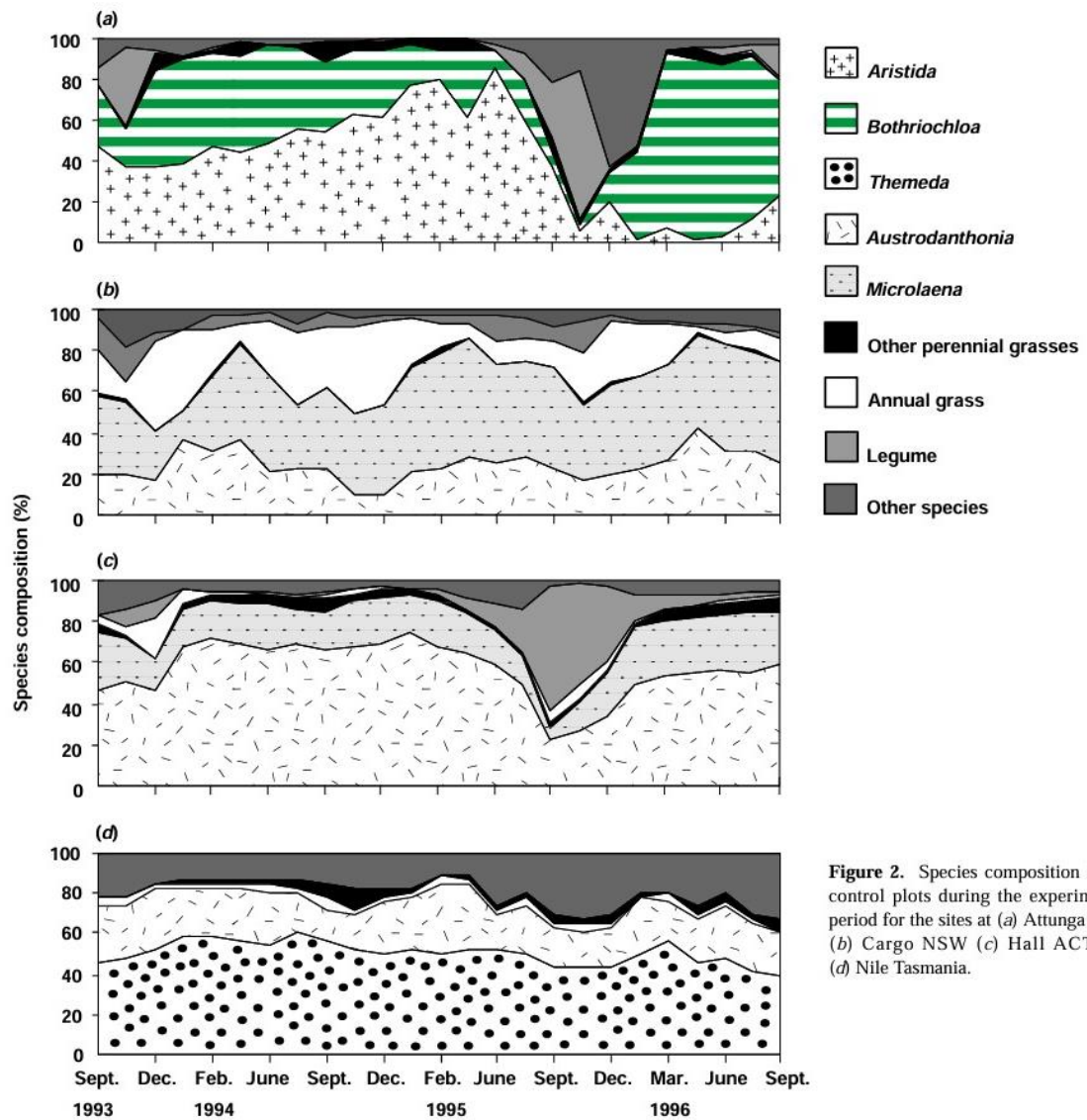


Figure 2. Species composition in the control plots during the experimental period for the sites at (a) Attunga NSW (b) Cargo NSW (c) Hall ACT and (d) Nile Tasmania.

FIGURE 2. THE VARIED SPECIES COMPOSITION AT FOUR SITES IN SOUTHEAST AUSTRALIA (A) ATTUNGA NSW, (B) CARGO NSW, (C) HALL ACT AND (D) NILE TASMANIA (GARDEN *ET AL.* 2000).

One of the major sources of variability in these production systems is the intra and inter annual variation in pasture production caused by climate variations (Chapman *et al.* 2009). Managing these risks is essential for profitable and sustainable grazing systems. Figure 3 presents the rainfall anomalies in the Murray Darling Basin going back to 1900, demonstrating the variability of rainfall, defined as deviations of annual rainfall from the long-run averages (Zaveri *et al.* 2020). The anomalies show how the rainfall can vary yearly and demonstrate the variability in rainfall farmers must manage. Southeast Australia has experienced three significant droughts since after the instrumental period: the Federation drought (1895-1902), the World War 2 drought (1937-1945) and the Millennium drought (1997-2009) (Dey *et al.* 2018) with the effects of reduced rainfall and elevated temperatures (Murphy *et al.* 2008). The variation in rainfall can change from year to year, decade to decade, as demonstrated by the drought periods in Figure 3.

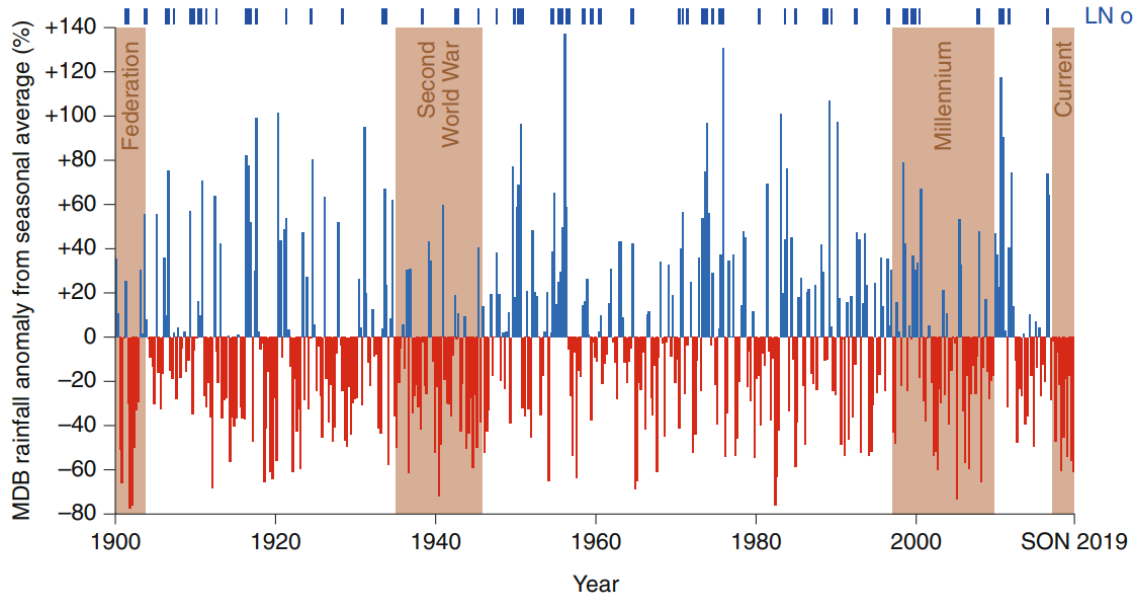


FIGURE 3. MAJOR DROUGHTS AND MDB (MURRAY DARLING BASIN) RAINFALL ANOMALY FROM SEASONAL AVERAGE %. (KING ET AL. 2020).

2.3 Climate in SE Australia.

The climate of Southeast Australia is characterised as a mixture of temperate and grassland (based on a modified Koeppen classification system) (Figure 4). Mean average annual rainfall for South East Australia can vary from 200 mm to 1500 mm (<http://www.bom.gov.au/climate/maps/averages/rainfall/>) High rainfall variability is a feature of the southeast Australian climate (Murphy & Timbal, 2008).

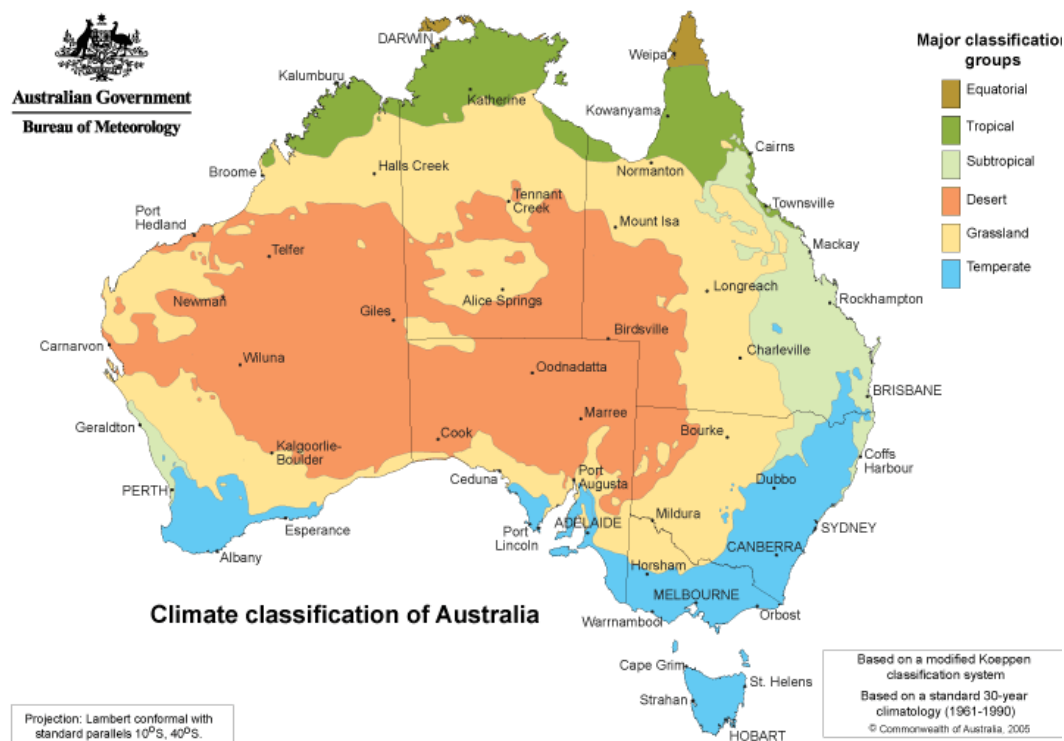


FIGURE 4. CLIMATE CLASSIFICATION OF AUSTRALIA (BUREAU OF METEOROLOGY)

Southeast Australian farmers typically rely on winter rains to restore the soil moisture levels leading into Spring, where most fodder is grown. However, this rainfall is highly variable and can change from season to season. Trends show that the April to October rainfall across southeastern Australia has declined, as shown in the rainfall anomaly Figure 5 (CSIRO State of the Climate 2020). Along with the year-to-year variability discussed above, there is also variability within a season shown below (figure 5), which can result in soil being unable to recharge fully before the next growing season.

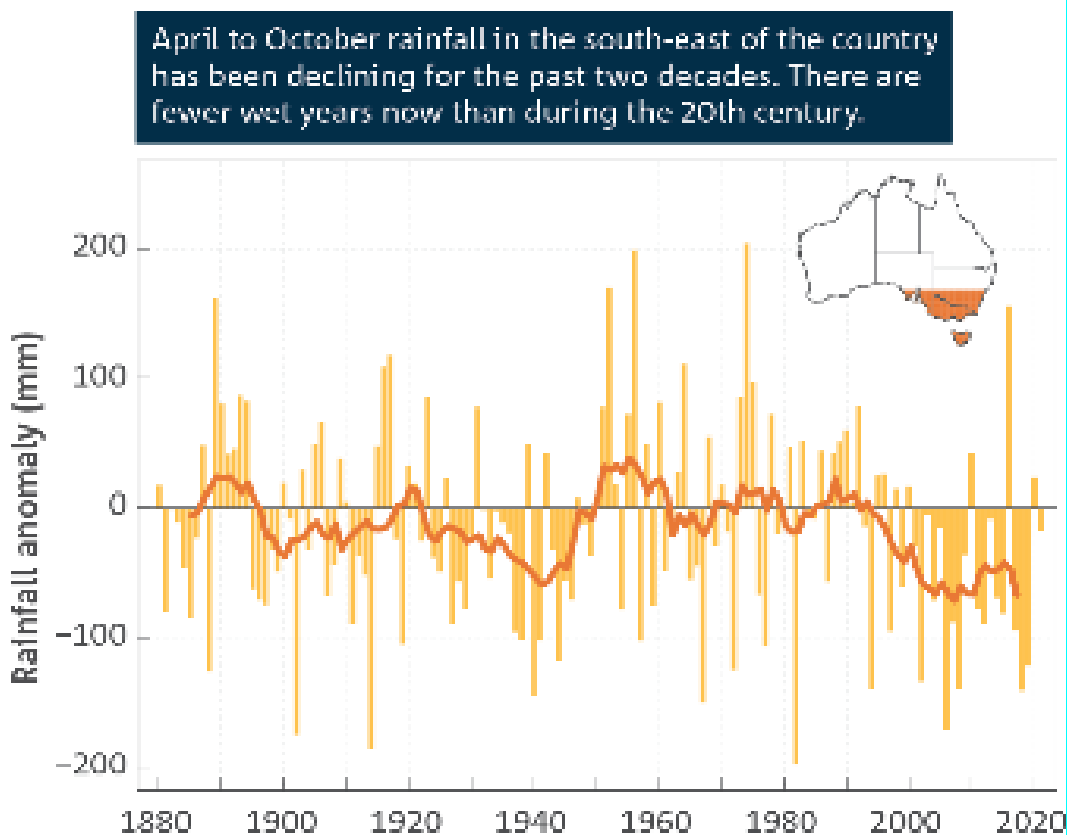


FIGURE 5. RAINFALL ANOMALY SOUTHEAST AUSTRALIA (APRIL – OCTOBER) (CSIRO STATE OF THE CLIMATE 2022).

Figure 6 presents the annual mean temperature anomaly for Victoria (1910-2022), demonstrating that during the 1970s, Victoria has changed from a negative mean temperature anomaly to a more consistent positive mean temperature anomaly, showing how climate change is starting to affect temperatures in Victoria (Australia).

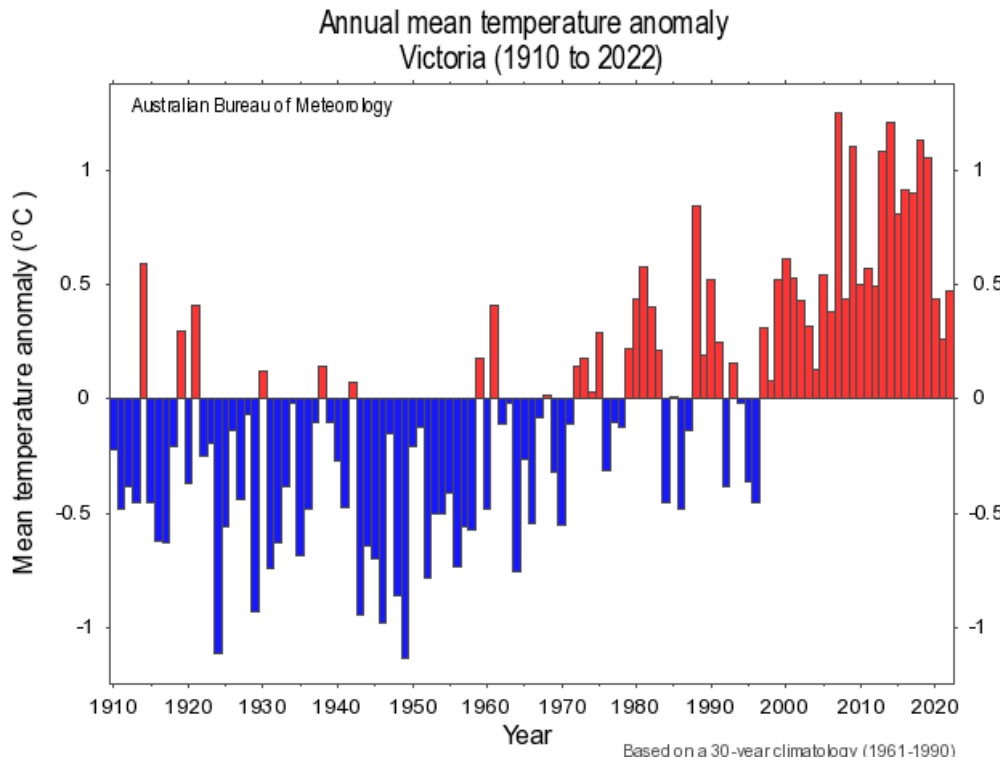


FIGURE 6. ANNUAL MEAN TEMPERATURE ANOMALY, VICTORIA. ([HTTP://WWW.BOM.GOV.AU/CGI-BIN/CLIMATE/CHANGE/TIMESERIES.CGI?GRAPH=SST&AREA=VIC&SEASON=0112&AVE_YR=T](http://WWW.BOM.GOV.AU/CGI-BIN/CLIMATE/CHANGE/TIMESERIES.CGI?GRAPH=SST&AREA=VIC&SEASON=0112&AVE_YR=T))

Australia's climate has warmed by just over 1°C since 1910, increasing the frequency of extreme weather heat events (CSIRO State of the Climate 2022). Eight of Australia's top ten warmest years on record have occurred since 2005, as shown in Figure 7 (CSIRO State of the Climate 2022), adding further complexity to the variability farmers are facing.

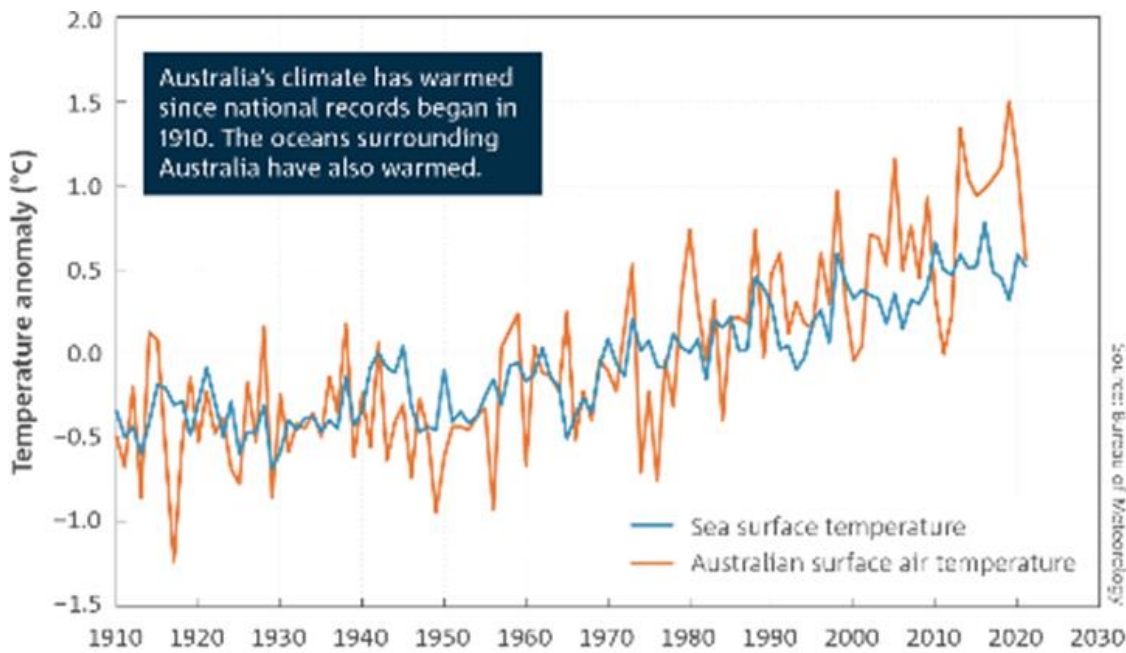


FIGURE 7. ANOMALIES IN ANNUAL TEMPERATURE OVER LAND IN THE AUSTRALIAN REGION (CSIRO STATE OF THE CLIMATE 2022).

2.3.1 Managing Variability

Globally and historically, farmers manage variability throughout a season and from one season to the next; however, with the additional variability created by climate change, farmers are learning to adapt more often and faster than in the past. The variability caused by climate change can affect the farmer's production numbers; farmers may have to potentially reduce their stocking numbers or result in purchasing, non-budgeted fodder to feed livestock. If not appropriately managed, this can affect the profitability of the enterprise (Mu *et al.* 2013; Beitnes *et al.* 2022). Therefore, the more suitable tools a farmer has to manage, monitor and oversee their farming operations, the more likely they can be nimble to make quick and critical decisions based on factual data as the season changes so they can generate profits whilst managing resources optimally (Chapman *et al.* 2013).

The literature shows that farmers need to adapt to increased climate variability. Following are some of the observations of changes in climate variability affecting agricultural production:

- Shorter Spring seasons in Southern Australia are increasing (Bell *et al.* 2011)
- Late autumn breaks in some locations have been observed (Bell *et al.* 2011)
- Increased winter and early spring pasture production (Cullen *et al.* 20012)
- Decreased late Spring and early Summer growth (Cullen *et al.* 20012)
- Future pasture production will be reduced, causing economic difficulties for farmers (Harrison *et al.* 2016)

The national livestock numbers (figure 8) fluctuate yearly, primarily dependent on pasture production, influenced by factors such as precipitation, flooding, and drought. Other factors, such as access to foreign markets and disease, can influence livestock numbers. Over the last five years, we have seen a drop in the beef, sheep, and lamb flocks, with a slight increase in 2020-2022 (Australian Bureau of Statistics, Agricultural Commodities, Australia 2021-2022).

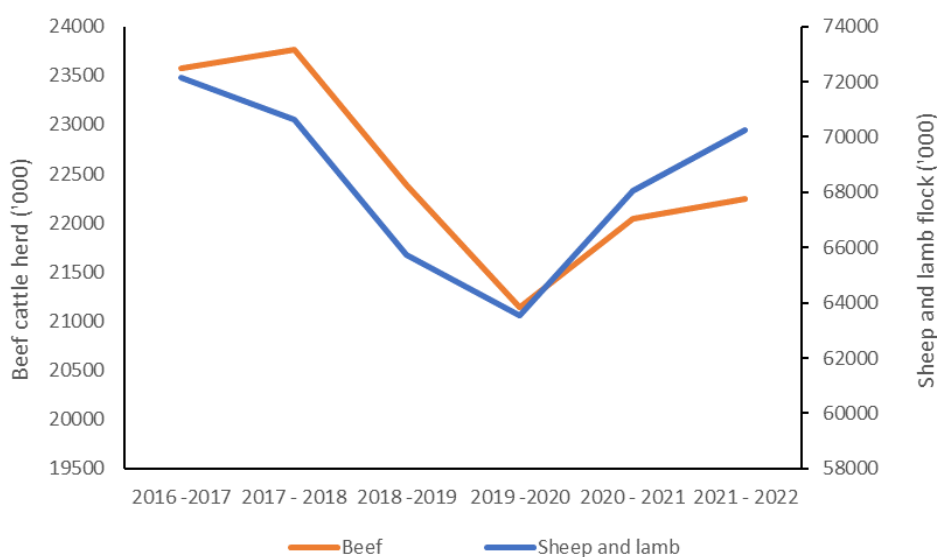


FIGURE 8. AUSTRALIAN BEEF, SHEEP AND LAMB FLOCK SIZE FLUCTUATIONS (SOURCE – ABS, AGRICULTURAL COMMODITIES, AUSTRALIA 2021-2022)

2.4 Use of biophysical models to understand climate variability impacts on agricultural production.

Farming is a complex occupation, with many variables influencing production from one season to the next. In the case of raising grazing stock on pastures in Southwest Victoria, the main complexities are around having enough grass in the paddocks to feed the livestock throughout the year, allowing for seasonal and annual climatic variations. Biophysical agricultural models, which can simulate biological systems, play a significant role in assisting farmers in predicting the pasture growth that they can expect in the weeks and months ahead. These models can utilise local historical data and current on-farm conditions to simulate a range of pasture growth possibilities ahead.

2.4.1 Agricultural Models History

Earl Heady and his students undertook some of the earliest agricultural systems modelling to optimise decision-making at the farm scale (Jones *et al.* 2016). Heady undertook experiments on the fertilisation of crops and feeding of hogs, broilers, turkeys, dairy cows, beef cows, etc., to predict yield per acre of crop, gain per bird or animal for chickens, turkeys, hogs and beef cattle and milk production per cow (Heady, 1957).

In 1972, the US government was surprised by a large order of wheat from the Soviet Union, causing price rises and shortages of wheat (Pinter *et al.* 2003). This prompted the US to fund research programs to create crop models to use with the US's recently available remote sensing equipment to predict the production of major crops globally (Jones *et al.* 2016). Figure 9 outlines the timeline of significant events that led to the models available today. Whilst the timeline stops around 2013, more recent models include data synthesis on greenhouse gases and the like. As our understanding of science, weather, and technological improvement (internet and personal computers) have progressed, the models have become more all-encompassing. These models are constantly evolving, with new agricultural models factoring in the emissions produced from farming.

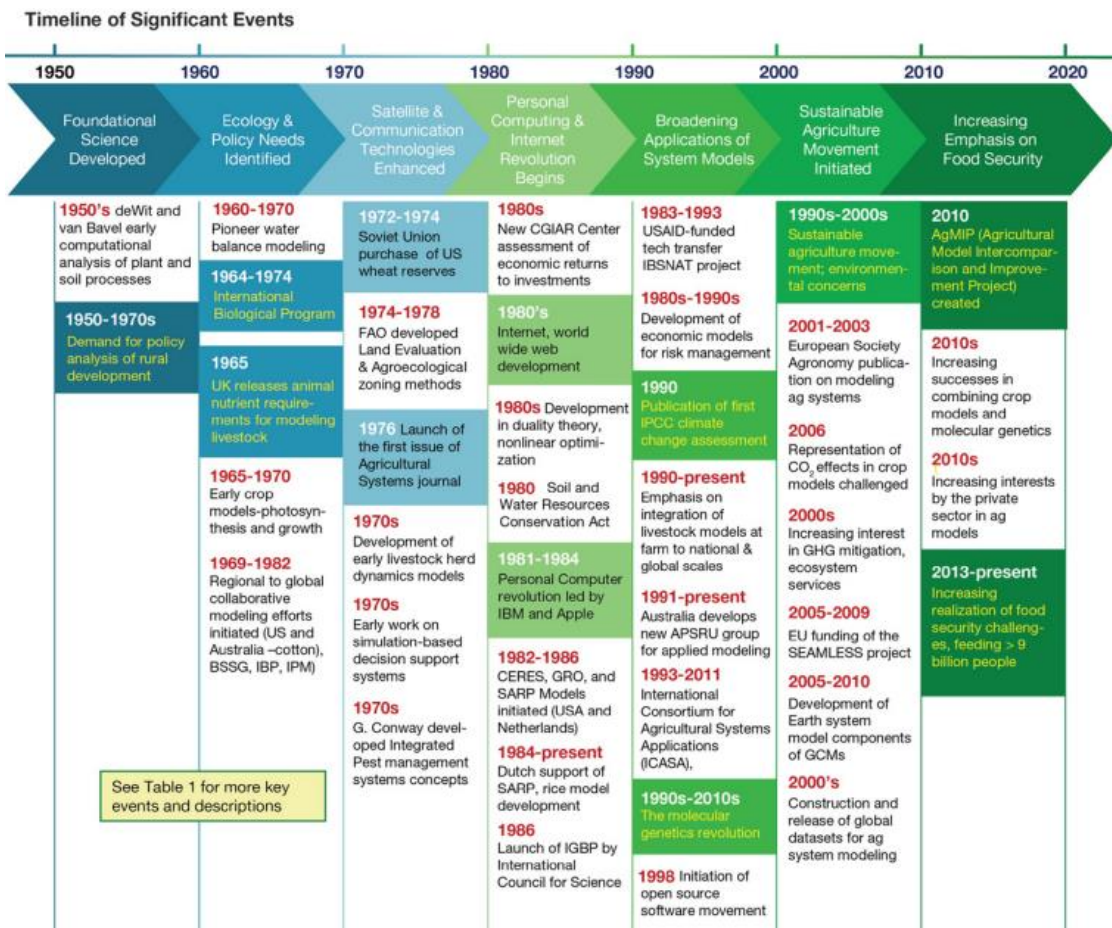


FIGURE 9. LOOKING BACK AT THE LAST 70 YEARS AND THE MAIN DRIVERS FOR DEVELOPING AGRICULTURAL SYSTEM MODELLING (SOURCE JONES ET AL. 2016).

2.4.2 Types of Agricultural Models

The scale of agricultural models can vary from the National / Global scale to the field scale as shown in Figure 10. This literature review concentrates on the field scale where individual farm production can be modelled to predict outputs at the operations scale.

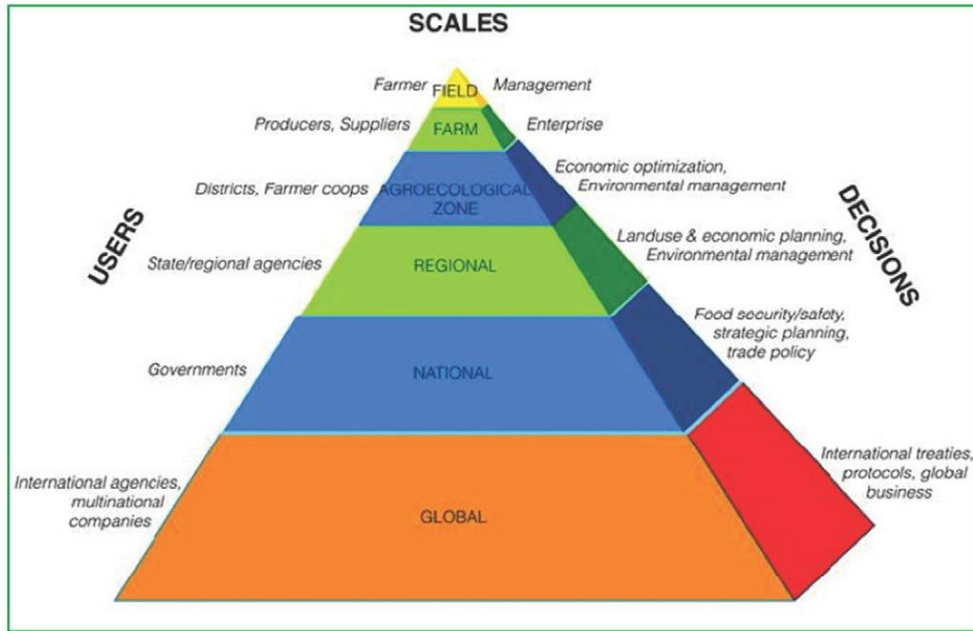


FIGURE 10. VARYING LEVELS AT WHICH AGRICULTURAL MODELS ARE DEVELOPED AND OPERATE AT. (JONES ET AL. 2016)

2.4.3 Australian Agricultural Models

Numerous agricultural models can be used to simulate biological systems in Australia, such as:

- The SGS (Sustainable Grazing Systems) Pasture Model, a multi-paddock, biophysical simulation model for livestock systems (Johnson *et al.* 2003),
- APSIM, an agricultural production systems simulator to simulate biophysical processes in agricultural systems as they relate to management practices' economic and ecological outcomes in the face of climate risk. (McCown *et al.* 1995)
- *Farmpredict (ABARES) – AUSTRALIA* (Hughes *et al.* 2019). A simulation model based on ABARES farm surveys. The model can simulate financial and physical outcomes for Australian farm businesses.
- DairyMod & EcoMod biophysical pasture-simulation models for Australia and New Zealand (Johnson *et al.* 2008)
- GRASP, a simulation model for soil water and pasture growth developed for northern Australia and rangeland pastures (Masoud, 2022).

The models typically rely on inputs such as the current and historical climate data from the Bureau of Meteorology (BOM), soil moisture /water content, fertiliser application rates and past applications, soil type, historical production figures (e.g. yield, tonnes/hectare. % protein), irrigation rates, etc.

The need for Agricultural models.

With the ever-increasing variability from season to season and throughout a season, it is critical that livestock managers can budget enough fodder for the stock they have at hand. Data-driven models using local inputs (i.e. current local weather data, historical local weather data, local soil moisture levels) can provide the livestock manager with potentially more accurate insights into the fodder availability (Jones *et al.* 2017) in the weeks and months ahead, resulting in better management decisions on farm and potentially improving the bottom line of the operations.

Agricultural models can also be used in the science industry to predict specific outcomes, such as the effect of climate change on production rates (Guerena *et al.* 2001). Similarly, the government can use the outputs of these models for planning and policy decisions (Holsworth *et al.* 2014).

Data collected from precision agriculture, such as rainfall quantities, evapotranspiration rates, soil moisture content, humidity, and other field data, can be imported into biophysical models such as the Sustainable Grazing Systems (SGS) Pasture Model, Agricultural Production Systems sIMulator (APSIM), Pasture for prophets and Yield Prophet. These biophysical models can be valuable tools to farm managers and scientists alike, as the models can be run to predict future scenarios, using different inputs into the model to see how this will affect the model's outputs/predictions. The data collected by remote sensing can also be used to measure plant canopy temperature and monitor plant water stress using the Crop Water Stress Index (CWSI) (Bellvert *et al.* 2014).

Agricultural models have several limitations. The data derived from the Agricultural models is only as good as the data quality used as the input and the operator's competency to question the results the model output provides. Studies undertaken by Silva *et al.* (2021) identified that although there have been significant advances in crop modelling, there are still knowledge gaps, with less attention paid to phosphorous and potassium limitations or yield production due to pests and disease. It was found that much focus has been put on the major cereal crops and less emphasis on root and tuber crops or tropical perennials (Donatelli *et al.* 2017). Agricultural models play a vital role in enhancing efficiency, sustainability, and resilience in agriculture. The models provide valuable insights that empower farmers, researchers, and policymakers with knowledge to make informed decisions in a rapidly changing agricultural landscape.

APSIM (Agricultural Production Systems sIMulator)

APSIM was developed by APSRU (Agricultural Production Systems Research Unit), a collaborative group comprising the CSIRO and the Queensland State Government, in 1991 (Keating *et al.* 2003). It was developed as there was a requirement for improved modelling to provide predictions of crop production in relation to climate, genotype, soil, and management factors whilst considering the long-term resource management issues in Australian farming (Keating *et al.* 2003). The

developers were influenced by overseas models such as CERES (Crop Environment Resource Synthesis). APSIM has been used extensively across numerous agricultural domains in Australia, such as crop management (Pembleton *et al.* 2016), climate change impact assessment (Wang *et al.* 2019), soil health and nutrient management (Wang *et al.* 2020), water management (Keating *et al.* 2002) and economic analysis (McCown *et al.* 1995).

Yield Prophet for grain growers.

One of the main models used in the grain-growing industry is Yield Prophet. In 2003, Yield Prophet started as a monthly fax to subscribers in the Wimmera – Mallee region of NW Victoria. In 2004, it became a web interface available for users, and in 2005, it expanded to all regions of Australia (Hunt *et al.* 2006). Yield Prophet is an example of an online, subscriber-based platform that provides grain growers and consultants with access to a crop production model presenting users with real-time information about their crops (Hunt *et al.* 2006). Yield Prophet utilises APSIM as the underlying model and runs simulations and delivers reports to assist farm managers in decision-making.

Yield Prophet provides a platform and model for users to;

- Forecast crop yields.
- Manage enterprise risks such as climate, soil, and water risks.
- Monitor inputs such as fertiliser rates with potential crop yield.
- Simulate the effect of changing sowing dates or trying new varieties.
- Assess the possible effects of climate change.

Figure 11 is a visual representation of the yield prophet simulation process as shown on their website, demonstrating how the underlying APSIM model aids in simulating yield production.

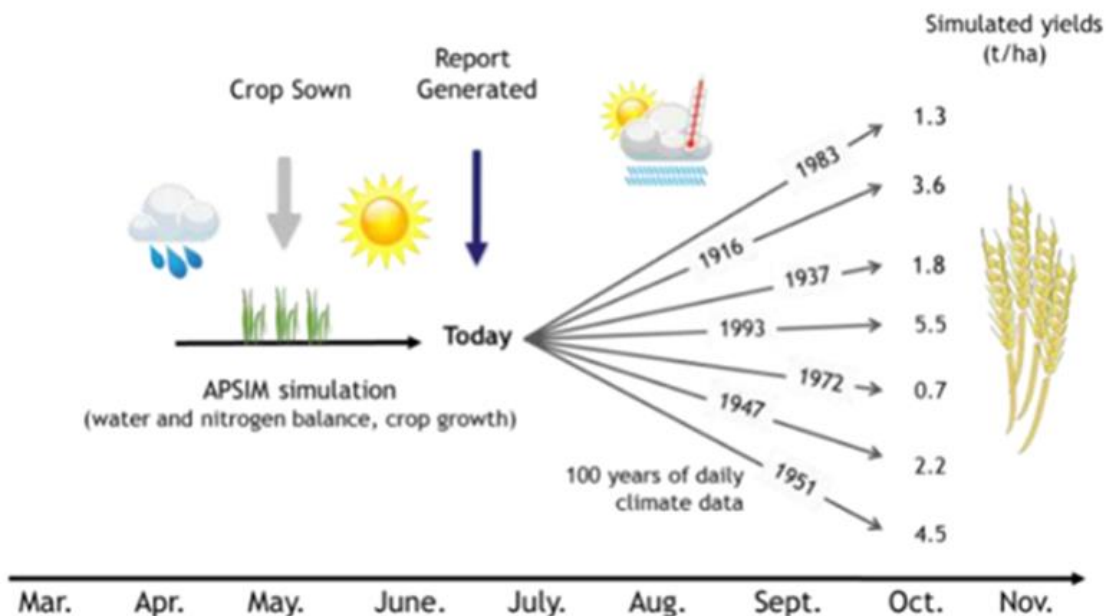


FIGURE 11. YIELD PROPHET SIMULATION OVERVIEW. (SOURCE – YIELD PROPHET WEBSITE)

ABARES (Australian Bureau of Agricultural and Resource Economics and Sciences) has developed a model called *farm-predict*, "which can simulate the effects of price and climate variability on the production and profitability of Australian broadacre farms" (Hughes *et al.* 2019). ABARES *farm-predict* simulates the production of outputs (e.g., wheat, beef cattle, wool, etc.), the use of inputs (fuel and fertilizer) and changes in farm livestock and grain at a farm level under selected conditions. An overview of 'farmpredict' is shown in Figure 12 giving an example of the range of inputs used in calculating the outputs.

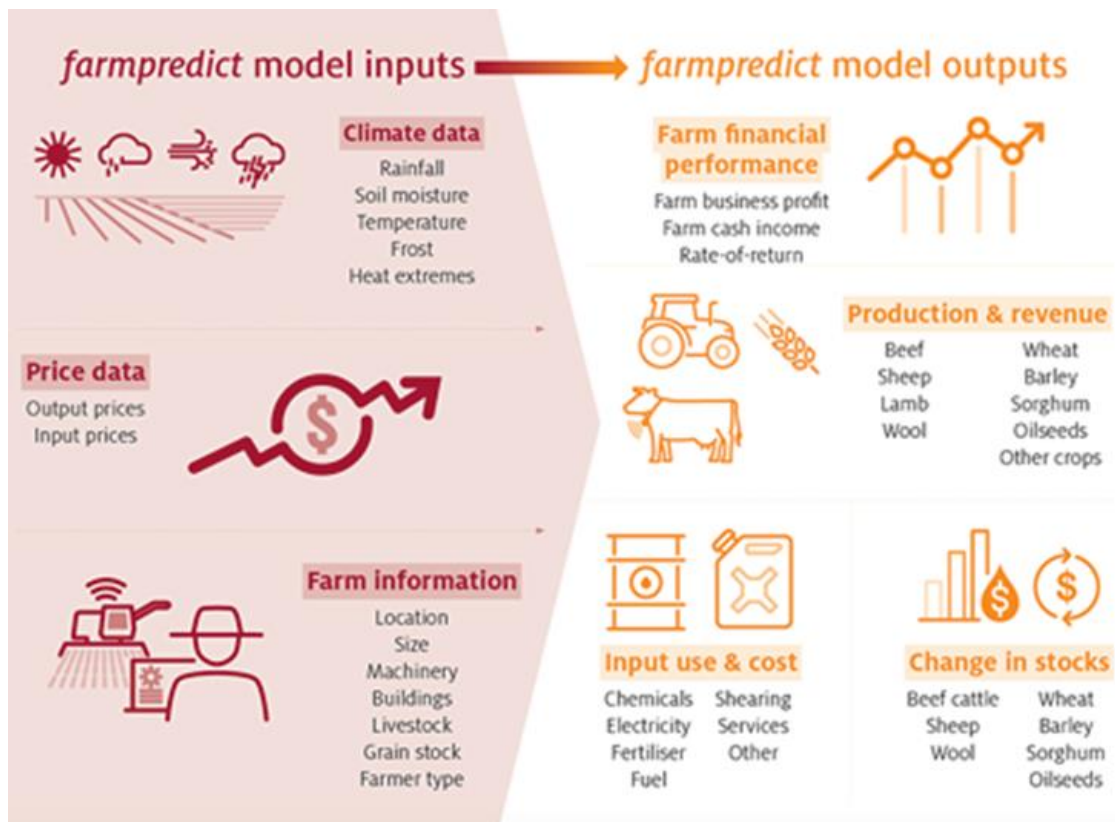


FIGURE 12. OVERVIEW OF THE FARM-PREDICT SYSTEM (SOURCE - WWW.AGRICULTURE.GOV.AU)

While *farmpredict* captures a lot of inputs and modelling outputs, at this stage, it does not appear to be using the models to produce short-term (3-12 month) forecasts of farm pasture production.

SGS Pasture Model

The SGS Pasture Model is a multi-paddock, biophysical simulation model for livestock systems. The SGS model can simulate pasture growth rates for grazing enterprises. The SGS Pasture Model was developed for Australian conditions by IMJ Consultants in collaboration with Meat and Livestock Australia (MLA), the University of Melbourne, and Dairy Australia. It was developed for researchers

(Johnson *et al.* 2003) to simulate grazing scenarios. The model can import the local weather data and use historical weather in certain simulations. The SGS model incorporates modules for water dynamics, herbage accumulation and utilisation, nutrient dynamics and animal intake and metabolism (Johnson *et al.* 2003). The interactions between these modules are crucial to understanding efficient pasture management (Johnson *et al.* 2003). Elements within the modules can be altered to see how changing certain variables can affect pasture production. The philosophy of model use is that all model outputs should be questioned. If the model's output agrees with the observed data, then the model should be interrogated to understand why this is so. Similarly, if the model output does not agree with the observed data, the model should be interrogated to see why (Johnson *et al.* 2003). The user of the model is encouraged to question the outputs of the model for accuracy and, in doing so, build up proficiency and competency in what to expect from the model (Johnson *et al.* 2003). Consideration needs to be considered when interrogating the output of the modelled versus actual data, as some variables are challenging to measure in the field, and errors can be derived from many sources, such as location error, calibration error and /or instrument error (Sinclair *et al.* 1979). The SGS model is typically used for academic research and is not widely available to the public.

2.4.4 Model and data output quality

Whilst agriculture models can add value, they are only as good as the data put into the model and the parameters the model runs on. Therefore, time must be taken to build the model, understand the model, and check the model against what is happening in the field to ensure a model runs as close to reality as possible. Beukes *et al.* (2008) conducted a three-year farm trial to evaluate the Whole-farm model (WFM) in New Zealand. Similarly, Barrett *et al.* (2004) evaluated four perennial ryegrass growth models to form the basis of a herbage growth model (HGM). Comparing the SGS biophysical simulation model against actual data, the model parameters can be refined to ensure the model simulates as close to reality as possible. Numerous variables within the SGS pasture model and other models must be 'calibrated' to local conditions. Variables include:

- Plant type (C3, C4, phalaris, fescue, clover, etc), annual or perennial, persistence coefficient.
- Plant composition (number of different species present in the paddock),
- Soil type(s) (soil profile depth, texture, saturated hydraulic conductivity),
- Soil compaction (soil texture),
- Nitrogen content. (Ability to alter soil nutrients and add fertiliser history/data),
- Grass management approach (set grazing, rotational grazing, cutting for hay, nitrogen replacement, etc).

2.4.5 Forecasting

Using forecasting available to farmers can potentially help manage the repercussions of climate variability that farmers are facing. Climate forecasts can

assist farmers with knowledge of future potential rainfall and temperatures, whereas pasture growth forecasts can assist farmers with feed budgeting in the weeks and months ahead. Using seasonal climate forecasts can assist farmers in making management decisions which may be one-way farmers can minimise losses in drought years and take advantage of favourable seasons (Ash *et al.* 2007).

The Bureau of Meteorology provides a wide range of rainfall forecasts to farmers across Australia with weekly, one and three-month forecasts, as shown in Figure 13 as an example. These types of forecasts can assist farmers with planning for future events.

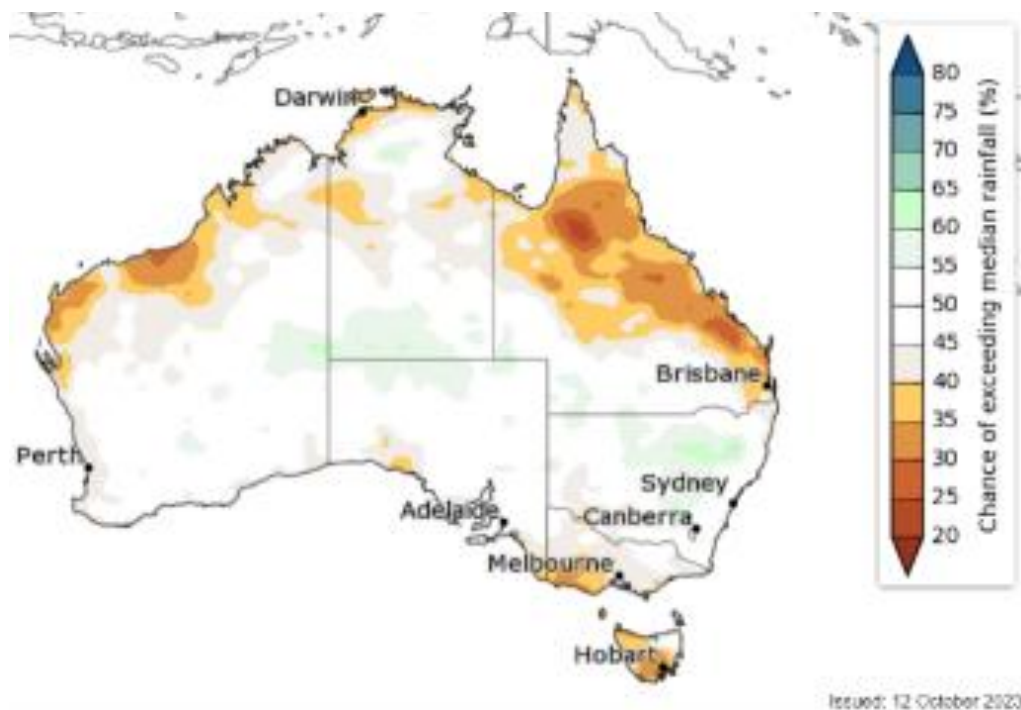
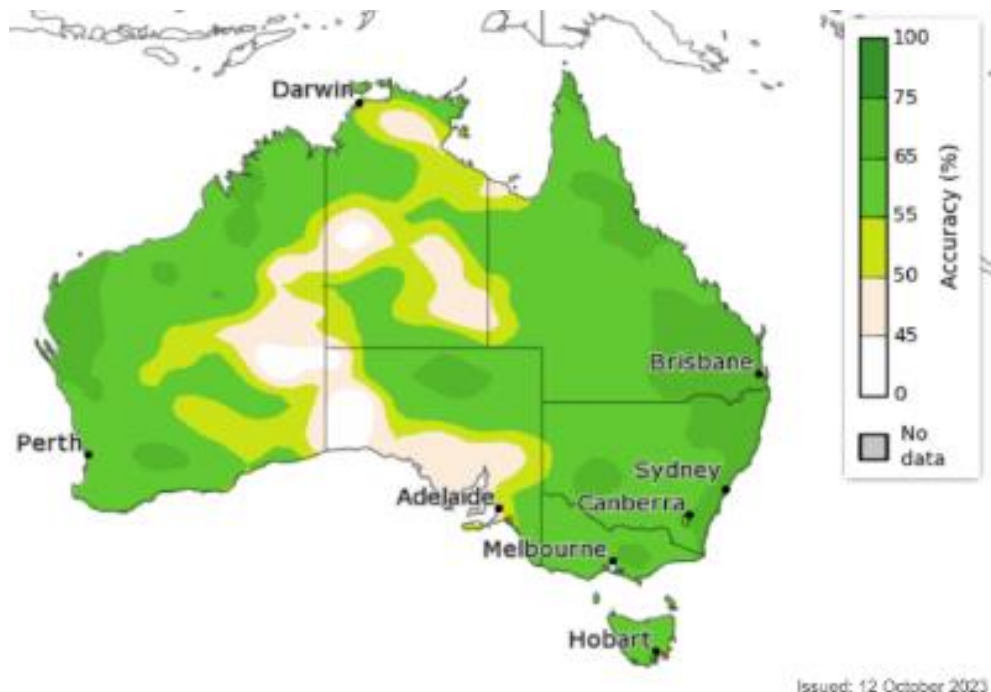


FIGURE 13. RAINFALL, THREE-MONTH OUTLOOK, DECEMBER TO FEBRUARY (2023-2024). THE CHANCE OF EXCEEDING MEDIAN RAINFALL (SOURCE - BUREAU OF METEOROLOGY).

The Bureau of Meteorology also provides past accuracies for their predictions, demonstrating that at some locations at certain times of the year, their forecast is accurate or inaccurate, as shown in Figure 14.



Issued: 12 October 2023

FIGURE 14. ACCURACY FOR CHANCE OF ABOVE MEDIAN RAINFALL, NOVEMBER-JANUARY (SOURCE BUREAU OF METEOROLOGY).

Like climate forecasts, forecasts of future pasture growth can provide farmers with important insights into pasture production in the weeks and months ahead. Knowing expected pasture production in the weeks and months ahead can assist farmers with facing the uncertainties around farming and be prepared for what is to come. Shown in Figure 15 is a forecast of projected green herbage available versus historic for the Riverina (NSW). Forecasts like these can assist farmers with knowing how this season is tracking compared to previous seasons and indicate how much pasture production can be generated in poor years versus excellent years (Mitchell *et al.* 2022).

Projected green herbage available relative to historic variation

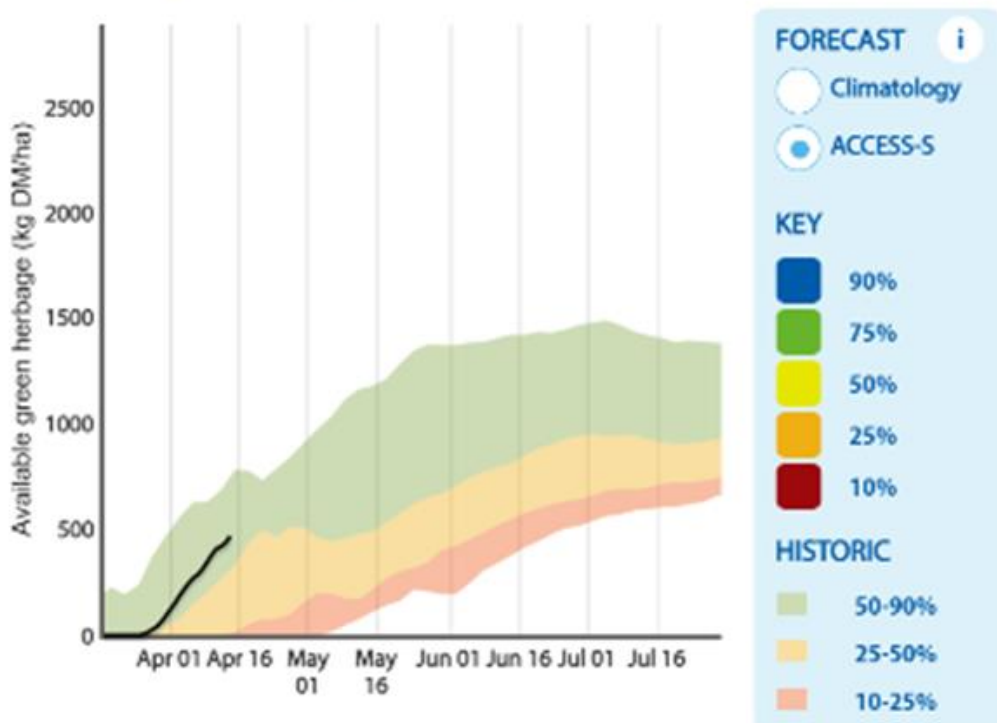


FIGURE 15. PROJECTED GREEN HERBAGE FORECAST AVAILABLE TO FARMERS USING THE CSIRO “FARMING FORECASTER.”

The skilfulness of the forecast is an issue. Ash *et al.* (2007) concluded from Ziervogel *et al.* (2005) that forecasts need to be 65-70% accurate to achieve long-term adoption and trust, which is similar to work undertaken by Jochec *et al.* (2001) and Leith (2006) that demonstrated that an accuracy of 70-80% is required and that forecasts have to be proven for a 4-5 year period before they would be adopted. Forecast skill varies over more extended periods, within seasons and spatially.

Predicting the most helpful variable to provide to farmers can be an issue. Forecasting rainfall and temperature for the three months ahead may be relevant to some, however, other farmers may want access to forecasts on crop/pasture growth rates and soil water storage (Ash *et al.* 2007). Whilst climate and fodder forecasts are available to farmers, they are not necessarily used by all farmers for various reasons. How forecasts are presented can cause confusion (Ash *et al.* 2007). Research undertaken by Keogh *et al.* (2005) demonstrated that only “20% of pastoralists correctly interpreted a forecast that stated there was a 70% probability of receiving above median rainfall”.

Farmers can act on forecasts if they have significant lead time and are willing to change. However, the implications of changing plans to short-term forecasts on long-term farm objectives must be considered. If a farmer knows they are going into a drier period, they may be able to purchase forage; however, if the lead time is short, extra forage may not be available or cost prohibitive. Similarly, if a farmer

knows they are heading into a drier period, it may not be practical to sell off a breeding herd (Stafford Smith *et al.* 2000) as this may affect long-term herd dynamics and profitability (Ash *et al.* 2007). The value of the forecast needs to be considered within the context of the whole farm and aligns with the manager's decision-making process (Stafford Smith *et al.* 2000). Overreacting to forecasts can result in losses of profits, whilst inappropriate responses can exceed the benefits of using forecasting (Smith *et al.* 2000).

2.4.6 Soil Moisture

Rainfall makes water available to the pastures as either in-season rainfall or stored soil water (Verburg *et al.* 2016). The amount of stored soil water, also known as Plant Available Water (PAW), is affected by pre-season and in-season rainfall, infiltration, evaporation, and crop/pasture water use (Verburg *et al.* 2016). The Plant available water capacity (PAWC) is the total amount of water that can be stored in a soil and released to a crop/pasture. The PAW is the amount of water stored within the soil and available to the plant (Figure 16) (Verburg *et al.* 2016).

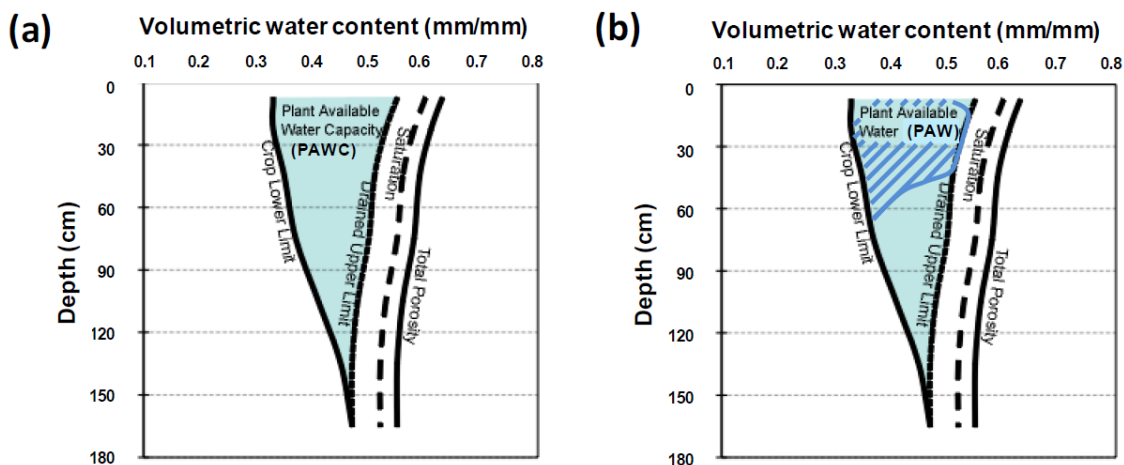


FIGURE 16. (A) PLANT AVAILABLE WATER CONTENT (PAWC) V (B) PLANT AVAILABLE WATER (PAW). SOURCE VERBURG *ET AL.* 2020.

Contributing to the PAWC is the soils texture. Particle size within the soil determines how much moisture can be stored and how tightly it is held in the soil (Verburg *et al.* 2016). The soil's structure, chemistry and mineralogy can all affect the PAWC (Verburg *et al.* 2016).

2.4.7 Summary

This section discussed the variability of the Australian climate and gives examples of agricultural models and how agricultural models are used in agriculture to assist in improving agricultural production. It also demonstrated the void and inaccessibility of agricultural models available for pasture forecasting in the weeks and months ahead in the Southeast region of Australia.

2.5 What is Precision Agriculture?

Precision agriculture can assist farmers in monitoring and managing their pastures. Precision agriculture intends to match agricultural inputs and practices to localised conditions within a field so user can do the “right thing in the right place, at the right time”, and in the right way (Banu, 2015).

A Lleida University Research Group lists 27 definitions from the scientific literature and the Internet (Lleida University, 2018). In 2019, the International Society of Precision Agriculture adopted the following definition: ‘Precision Agriculture is a management strategy that gathers, processes and analyses temporal, spatial and individual data and combines it with other information to support management decisions according to estimated variability for improved resource use efficiency, productivity, quality, profitability and sustainability of agricultural production.’

Source

(<https://www.ispag.org/about/definition#:~:text=%E2%80%9CPrecision%20Agriculture%20is%20a%20management,%2C%20productivity%2C%20quality%2C%20profitability%20d>). Another definition by Liaghat *et al.* (2010) is that “PA is an integrated, information and production-based farming system that is designed to increase long term, site-specific and whole farm production efficiency, productivity and profitability while avoiding the undesirable effects of excess chemical loading to the environment or productivity loss due to insufficient input application.”

2.5.1 Precision agriculture – tools and techniques

There is wide-scale adoption of precision agriculture technology (Castle *et al.* 2015), whilst the cost of precision agriculture technology has decreased since its introduction (Jochinke *et al.* 2007). Examples of pasture-related growth and monitoring technological tools include;

- Canopy temperature sensors,
- Nitrogen and moisture sensors,
- VRT. Variable Rate technologies, delivering desired rates to specific locations. (i.e. fertiliser application, sprays),
- Moisture probes with inbuilt communications (O'Shaughnessy *et al.* 2020),
- Local (farm) based weather stations (Conaty *et al.* 2012).

In the past, farmers would need to buy the individual components (sensors, data loggers, electronics boards, etc) of the required precision agriculture tools from different supplies and cobble together a system that works for their enterprise. Now, there are numerous off-the-shelf products that farmers can buy or subscribe to, to monitor individual parts of their enterprise (e.g., individual sensors) or packages that can monitor the whole farm, from their crops, soil moisture, humidity, temperature, salinity, dam heights, etc. (Rehman *et al.* 2014, Farooq *et al.* 2020).

2.5.2 Remote Sensing

Remote Sensing (RS) is defined as “the field of study associated with extracting information about an object without coming into physical contact with it” (Schott *et*

al. 2007). "Remote sensing applications in agriculture are based on the interaction of electromagnetic radiation with soil or plant material" (Mulla, 2013).

Remote sensing can utilise sensors in the paddock on vehicles capable of carrying measuring devices/sensors. Remote sensing can utilise drones, planes or satellites as vehicles to carry multispectral, hyperspectral and thermal Infrared cameras to capture images. Remote sensing also includes using a sensor or instrument mounted on a probe (Weiss *et al.* 2020) or pole. Remote sensing can virtually obtain measurements across a paddock in every location in time and space. Multispectral, hyperspectral and thermal Infrared cameras capture specific wavelength bands on the electromagnetic spectrum that humans cannot see. These bands can reveal information on vegetation that photos and the human eye cannot observe. The raw data captured from the multispectral and hyperspectral cameras must be converted to an output that farmers and others can utilise.

Applications of remote sensing across the agricultural environment include:

- Broadacre cropping picking up in-field variability (Jochinke *et al.* 2007).
- Citrus and silage yield mapping (Lee *et al.* 2005).
- Quality mapping in various crop types (Wahab *et al.* 2018).
- Variable rate technology (VRT) for spreading fertiliser efficiently (Han *et al.* 2019).
- Vegetation growth monitoring (Jung *et al.* 2018).
- Weed mapping and management (Bah *et al.* 2017).
- Irrigation management (Quebrajo *et al.* 2018, Albornoz *et al.* 2017).
- Crop spraying. (Xue *et al.* 2016, Garre *et al.* 2018).

Remote sensing uses non-contact measurements of radiation reflected or emitted from plants (Mulla, 2013) and can be used to detect issues such as plant water stress. Remote sensing has been used globally to monitor, measure and check plant water stress in numerous and diverse agricultural industry crops, such as; grains and seeds (Maise - *Zea mays* L, (Tsouros *et al.* 2019), Wheat - *Triticum durum* (Tsouros *et al.* 2019), Rice (Tsouros *et al.* 2019), Soya - *Glycme max* L Merr, (Tsouros *et al.* 2019), Sunflowers - *Hebanthus annuus* L (de Castro *et al.* 2018)), fruits and vegetables (Nectarines - *Prunus persica* (Park *et al.* 2017), Peaches - *Prunus persica* (Park *et al.* 2017), Grape vines - *Vitis vinifera* L.. (Knipper *et al.* 2019), Tomatoes (Hassler *et al.* 2019), Potato - *Solanum tuberosum* L. *Cilena*, (Gerhards *et al.* 2019), Cranberry - *V. macrocarpon*, (Sandler *et al.* 2018), Forestry and Fibres, (Conifers (Smigaj, *et al.* 2017), Forest characterisation (Michez *et al.* 2019), Cotton - *xinongmian 1008* (Bian *et al.* 2019)), Therapeutics, (Poppy crops (de Castro *et al.* 2018)), as well as invasive species mapping (Michez *et al.* 2019), wildlife census (Michez *et al.* 2019) and analysing commercial grass (Gerhards *et al.* 2018).

One area of remote sensing is the collection of leaf temperatures of crops/plants. Plants under water stress tend to close their stomata, and therefore, the plant's mechanism for self-cooling is decreased, increasing plant surface temperature (Gerhards *et al.* 2019). The water-stressed plant will have a higher leaf surface temperature than a well-watered plant nearby. The leaf temperature of crops can now be continuously monitored remotely with field canopy temperature sensors.

The leaf's temperature can also be collected by thermal infra-red (TIR) from drones, planes and satellites (Gonzalez-Dugo *et al.* 2019, Fisher *et al.* 2019). The remotely collected leaf temperature data can also be incorporated into the Crop Water Stress Index (CWSI), which farmers can also use to monitor water stress across their crops (Veysi *et al.* 2016).

2.5.3 Imaging technologies

Numerous imaging camera technologies exist and are used within agriculture. The imaging camera technologies utilised in agriculture fit into the following categories (Jin *et al.* 2020):

- Red, Green Blue (RGB) Camera.
- Multispectral Cameras, (Bands; blue 475 +/- 20 nm, green 560 +/- 20 nm, red 668 +/- 10 nm, near IR 840 +/- 40 nm, red edge 717 +/- 10 nm).
- Hyperspectral Cameras (narrower bands ((spectral range 400 - 1000 nm).
- Thermal infrared cameras (spectral range 7.5 – 13.5 nm)

The different imaging technologies concentrate on different bands of the electromagnet spectrum, some of which can be seen by the human eye and most of which cannot, as shown in Figure 17.

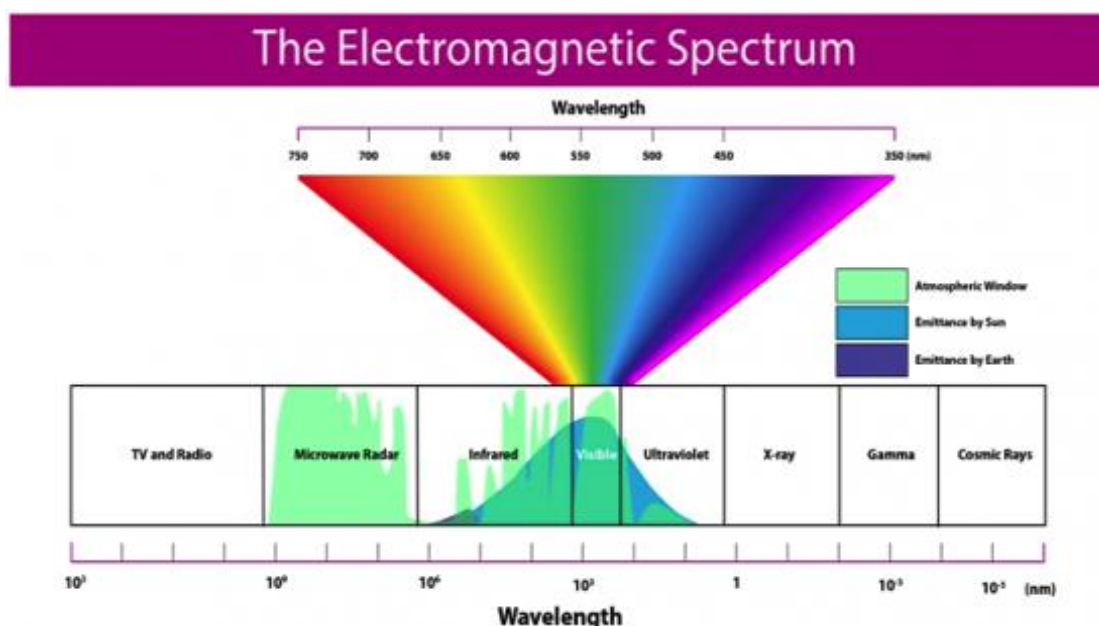


FIGURE 17. THE ELECTROMAGNETIC SPECTRUM. (SOURCE- [HTTPS://WWW.E-EDUCATION.PSU.EDU/GEOG160/NODE/1958](https://www.e-education.psu.edu/geog160/node/1958))

Plants interact with solar radiation differently from other materials. Plant components are expressed differently in the reflected optical spectrum from 400 nm to 2500 nm, as shown in Figure 18, with distinct reflectance behaviours, as can be seen by the different reflectance of leaf pigments, cell structure and protein and cellulose content. These variations within plants can be captured by the different remote imaging tools and used to assess varying crop health parameters.

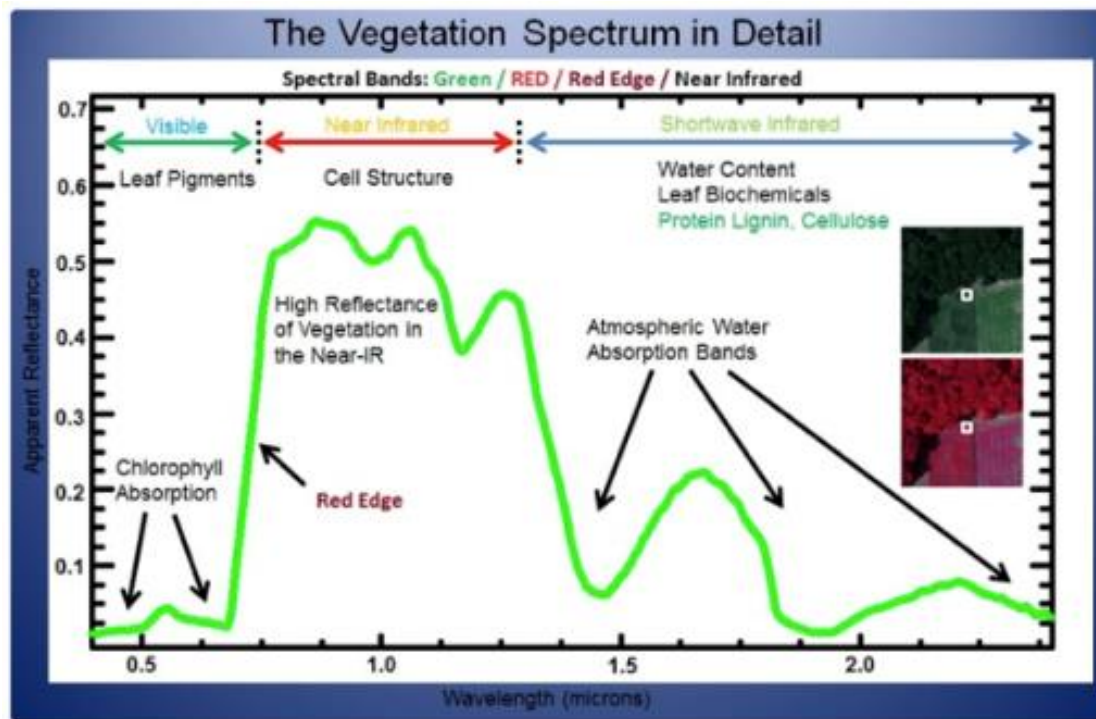


FIGURE 18. COMPONENTS OF PLANTS AND THE VEGETATION SPECTRUM. (SOURCE - WWW.DRONEZON.COM)

With regards to monitoring plant water stress, whilst the underlying technology may not be new, the availability, reduction in cost, size, and weight of the cameras, and access to and understanding of the outputs have undergone considerable improvement over the last two decades.

Thermal Infrared (TIR)

Thermal remote sensing involves acquiring, processing and interpreting data in the TIR range of the electromagnetic spectrum (EM) (Prakash, 2000). Sensors within a thermal camera pick up the infrared radiation emitted by a plant, displaying its temperature in a digital radiometric (Messina *et al.* 2020) or thermal image.

The thermal images can be taken with handheld thermal sensors, or sensors can be mounted on planes and satellites. The measurement of thermal temperature is a non-invasive, non-contact, and non-destructive technique (Ishimwe *et al.* 2014). Thermal remote sensing works as everything above absolute zero (0 k or -273.15°C) emits radiation within the infrared range on the electromagnetic spectrum (Prakash, 2000). The thermal properties of plant canopies are affected by the plant's structure and the amount of water per unit area (Ishimwe *et al.* 2014).

2.6 Monitoring Plant water stress using Remote Sensing

There are many methods for stress detection in plants. A number of the methods can be ineffective in early plant stress detection, time-consuming and require numerous measurements across a whole field to gain a true reflection of the field's

plants' water status (Conaty *et al.* 2014). Some of the methods for stress detection in plants are as follows:

- In the field, visual observation by a farmer looking for, wilting, soil moisture levels, etc.
- Scoring of plants for leaf rolling using a visual scale, i.e. scale 1-9 (1 correlates to no leaf rolling, and nine correlates to maximum leaf rolling. Baret *et al.* (2018)).
- The leaf wilting index (LWI) which is the ratio between the number of wilting leaves and the total number of leaves (Pungulani *et al.* 2013).
- Leaf water potential which provides data on the soil moisture content of a plant by measuring the amount of pressure the plant is exhibiting while pulling water from the soil (Bartell *et al.* 2021), typically measured using a pressure chamber.
- Stem water potential which directly measures the tree water status by measuring the water tension within the plant (Blanco *et al.* 2021).
- Plant water potential which provides data on the soil moisture content of a plant by measuring the amount of pressure the plant is exhibiting while pulling water from the soil (Bartell *et al.* 2021).
- Leaf relative water content which reflects the balance between water supply to the leaf tissue and transpiration rate (Lugojan *et al.* 2011).
- A leaf pyrometer which measures gas by placing the conductance of a leaf in series with two known conductance elements and comparing the humidity measurements between them to estimate water vapour flux (Batke *et al.* 2020).
- Gas exchange rate systems which measure the gas exchange based on a leaf cuvette connected to an infrared gas analyser. The cuvette is clamped over a single leaf, and the gas exchange of a small area of the leaf blade (typically 2-10 cm²) is measured (Kolling *et al.* 2015).
- CWSI (Crop water stress index) which uses the temperature comparisons of a leaf and an index to determine a stressed or non-stressed plant.

There are several ways to monitor plant water stress remotely. They range from soil moisture probes, Thermal Infrared (TIR) cameras, hyperspectral images, VNIR / SWIR (visible and near-infrared / Shortwave infrared) and the use of Fluorescence. Remote sensing methods are shown in Figure 19, demonstrating the relationship between stresses, plants response and applicable remote sensing techniques.

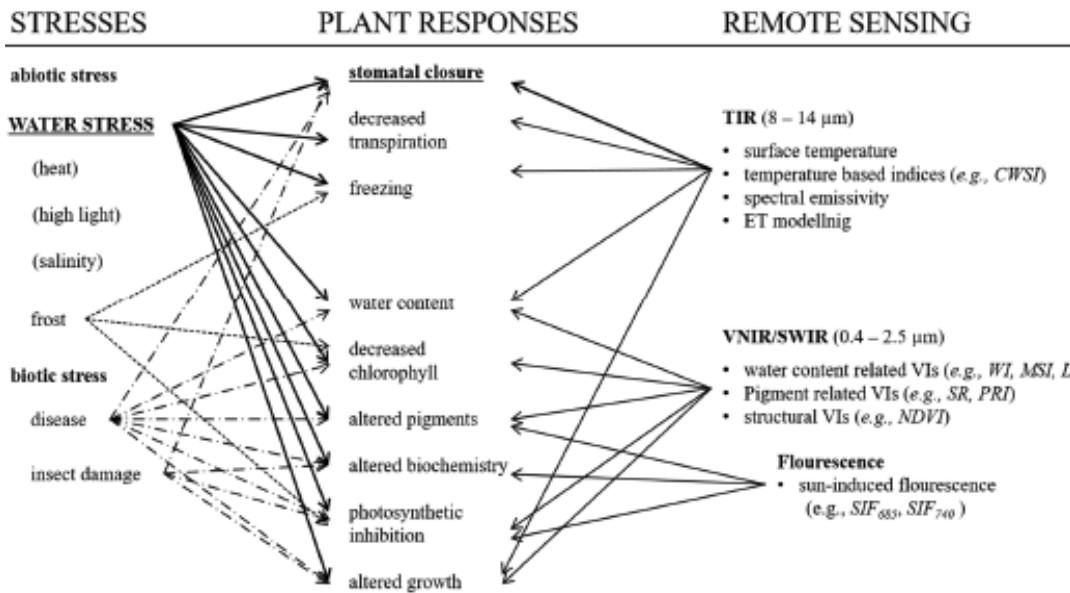


FIGURE 19. RELATIONSHIP BETWEEN THE STRESSES, PLANTS RESPONSE AND APPLICABLE REMOTE SENSING TECHNIQUE (SOURCE - JONES ET AL 2010).

A plant's performance is maximised when a plant is maintained within its optimum temperature range, which can be partially controlled through plant water availability. Guobin *et al.* (1992) found that the lack of water severely restricted plant growth and that tillers and stolons of clover and phalaris were reduced by 20% under water stress. Guobin *et al.* (1992) also found that phalaris and clover stomatal conductance declined by 80-90% with increasing water stress. They also found that soil moisture deficits reduced the pasture growth and survival and the fodder quality available for farm animals. By using the plant's canopy temperature as a guide to water stress, farmers can use a direct method to monitor plant water stress instead of using an indirect measurement of plant water stress, such as soil moisture conditions or evaporative demand (Conaty *et al.* 2012).

Declining stomatal conductance reduces transpiration and evaporative cooling, increasing canopy temperature (Struthers *et al.* 2015). Transpiration has the most influence in reducing leaf temperature to below the ambient temperature (Conaty *et al.* 2014). By the time wilting is observed in a pasture or crop, a proportion of the potential yield may have already been lost (Jones, 2004). If soil moisture is available, water flows through plants from the root system up the stem to the leaves to facilitate transpiration, as shown in Figure 20.

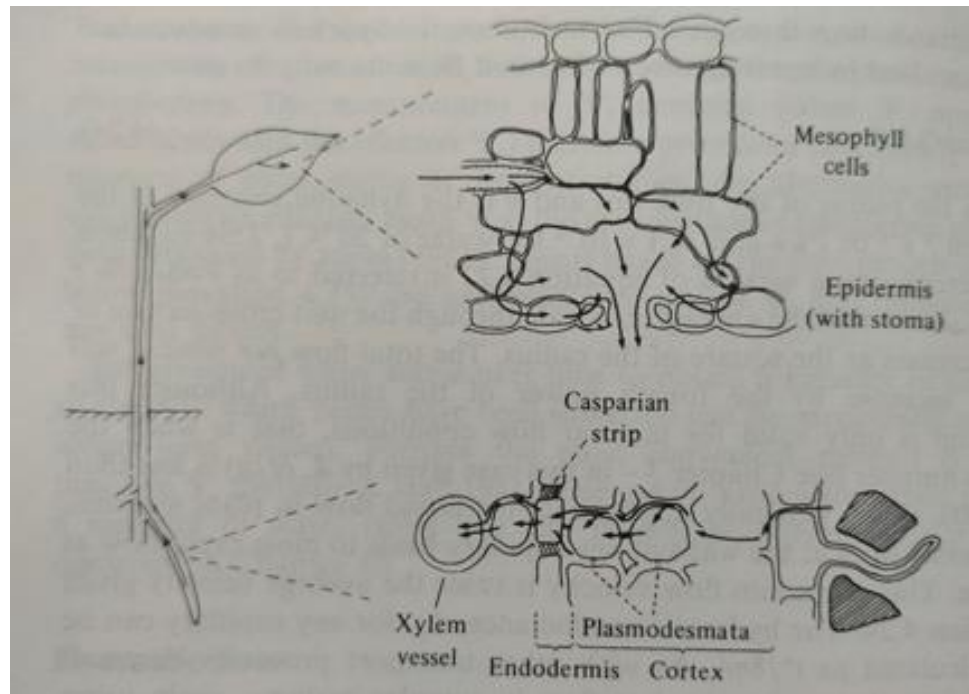


FIGURE 20. WATER FLOW THROUGH A PLANT (SOURCE - PLANTS AND MICROCLIMATE, JONES 1992)

During water stress, the stomata close, causing an increase in canopy temperature (Gerhards *et al.* 2019). Figure 21 shows an example of an open and closed stomata.

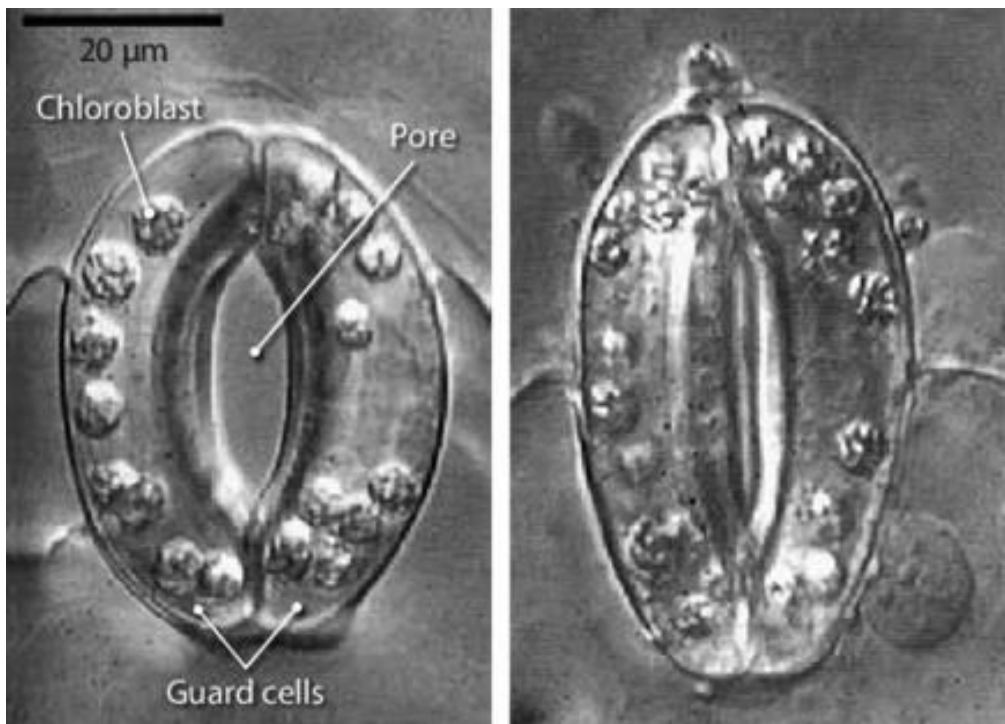


FIGURE 21. STOMATA OPEN AND CLOSED (SOURCE - PLANT PHYSIOLOGY, 2ND EDITION, P. 523, EDITED BY TAIZ AND ZEIGER.)

As a result, the crop canopy temperature (T_c), associated with transpiration, has been identified as a real-time, plant-based tool for crop water stress detection and

monitoring (Conaty *et al.* 2014). Figure 22 summarises the above points, demonstrating that a plant with access to soil moisture should have a lower leaf temperature as the stomata are open and the plants fully transpiring, compared to a plant in dry soil, where the stomata have closed and as a result the canopy temperature is higher.

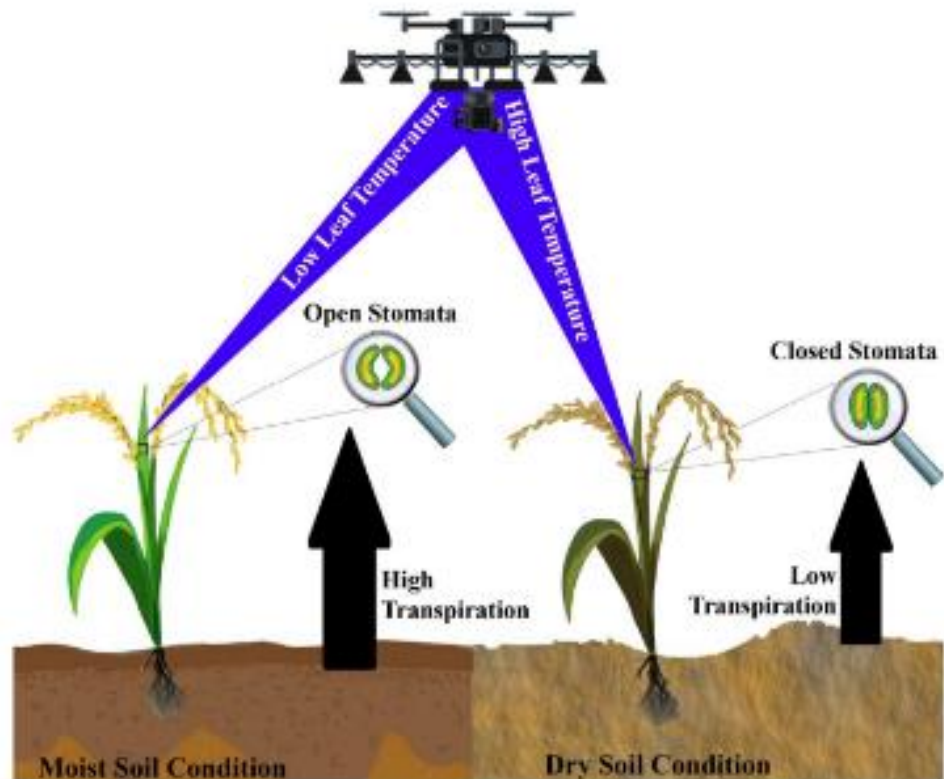


FIGURE 22. REMOTE MEASUREMENT OF CANOPY TEMPERATURE (SOURCE - AHMAD *ET AL.* 2021).

2.6.1 Monitoring soil moisture

Soil moisture probes are another form of remote sensor and come in different types. The capacitance sensor measures the amount of water in the soil through its capacity to transmit electromagnetic waves or pulses. Multi-depth capacitance sensors have become popular for real-time, continuous and non-destructive soil moisture profile measurements (Myeni *et al.* 2021). Soil moisture sensors can be used at individual sites to give the farmer an idea of their soil moisture, and these individual sites can be part of a larger network of soil sensors, as is used in Victoria (Figure 23). Here, a network of sensors is used for the cropping and pasture industries, with data available online. Some farmers use soil sensors when considering when to plant a crop. However, to get an accurate soil moisture measurement, the capacitance probes must be calibrated for different soil types (Myeni *et al.* 2021). Calibration undertaken on site factors in soil properties, such as soil texture, mineralogy, bulk density, salinity, temperature and organic matter (Myeni *et al.* 2021). Another issue in using soil moisture probes is the spatial

variability of soil moisture; the probe may give a relatively accurate result of the soil moisture at the probe; however, how much does the soil moisture vary as you move away from the probe?

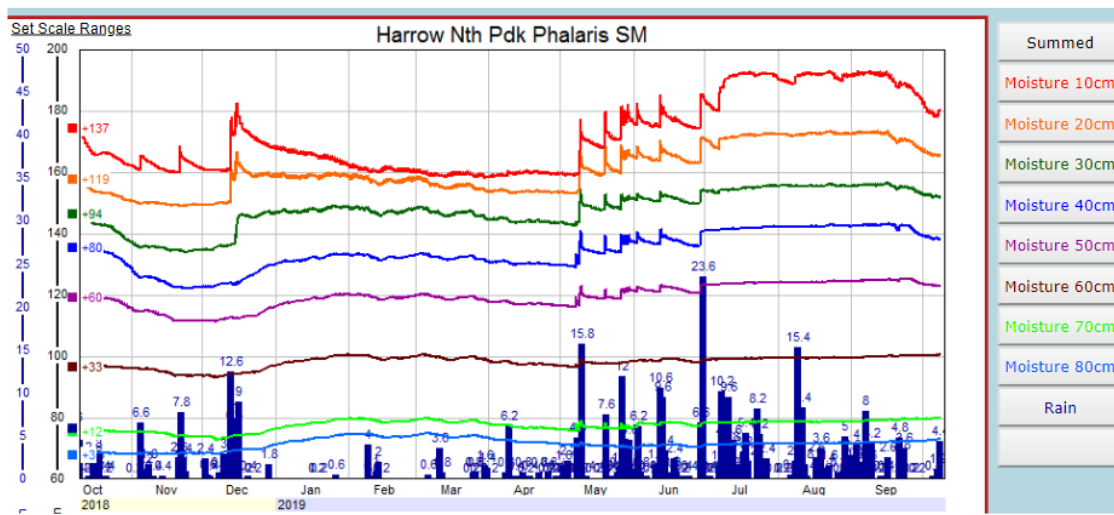


FIGURE 23. ANNUAL SOIL MOISTURE MEASURED AT DIFFERENT DEPTHS, INCLUDING ANNUAL RAINFALL FOR HARROW IN SOUTH-WEST VICTORIA. (SOURCE – [HTTPS://EXTENSIONAUS.COM.AU/SOILMOISTUREMONITORING/](https://extensionaus.com.au/soilmoisturemonitoring/))

2.6.2 Reliability, Interpretation, Cost

Thermal remote sensing makes it possible to quickly measure plant water stress in large areas with a thermal camera mounted on a drone, plane, or Satellite. This allows a farmer to identify areas of issue (stress) quickly and easily.

While using RS has many advantages, there are also numerous issues involved with collecting consistent and accurate data remotely in the field. Environmental conditions like wind and clouds can interfere with thermal measurements and cause errors. The presence of clouds, dust, snow, smoke, and high winds can also make the collection of data difficult in some parts of the globe (Akuraju *et al.* (2021), Nielsen (1990)). The cost of thermal sensors, planes, etc, can also be prohibitive for some technology users. Thermal images also tend to be recorded around thermal noon for most applications. Low-cost thermal cameras are not necessarily radiometrically calibrated and can only provide relative temperature differences (Messina *et al.* 2020). Field calibration is also required (Messina *et al.* 2020). The end users' ability to access, process and interpret the data can also be limiting. When measuring the canopy's temperature, errors can occur if the background (typically soil) influences the temperature recorded. The low resolution of some satellites means that the thermal data may not be used for gaining canopy temperature as the resolution is not small enough to pick up the temperatures of individual leaves and may also pick up a lot of background temperatures (i.e., soil) or 'mixed pixel values' which represent pixels that are a combination of leaf and background (Messina *et al.* 2020).

The data gathered is restricted to the sensor and platform capacities (viewing

direction and limited spatiotemporal information (Weiss *et al.* 2020). The sensor(s) need to be calibrated (Weiss *et al.* 2020), and atmospheric conditions (Weiss *et al.* 2020) and geometry of acquisition (Epiphanio *et al.* 1995), crop type, water status and phenological stages (Colombo *et al.* 2003) all need to be considered. Other uncertainties also include errors associated with the devices (Fernandes *et al.* 2005). With regard to using RS in the farming environment, the farmer needs to have access to the equipment, to be able to use the equipment and decipher the results.

The ability to collect the data using RS at the right time and place can be an issue, with clouds making it difficult to collect data remotely by plane, satellites, and, to a certain extent, drones. Similarly, the return times of satellites can make it challenging to monitor a crop constantly or daily if required. Using planes to monitor crops from the air constantly can be time-consuming and expensive. Hill *et al.* (2004) highlight how providing a 'pasture growth rate' is required in a timely and accurate manner as it is critical to assist livestock producers in developing grazing plans for their properties. Similarly, Handcock *et al.* (2016) highlight the 'irregular availability of suitable images' and the issue of generating an output useful for farmers. Banhazi (2012) highlights the abundance of information available to the farmer but how it is not generally structured in a way that can be applied readily". The issues of weather and return times need to be considered when choosing the right mix of PA and RS for specific crop monitoring.

Spatial resolution (Figure 24) is also a major consideration when choosing which type of RS to assist with data gathering. Many of the satellites may not have the spatial resolution to collect the data required (i.e., to collect plant water stress by collecting the thermal temperatures of individual leaves, resolution of a few centimetres are required, where some of the satellites resolutions can be 5m – 30m or more). Over time as satellite/technology improves we will see the spatial resolution continuing to reduce.

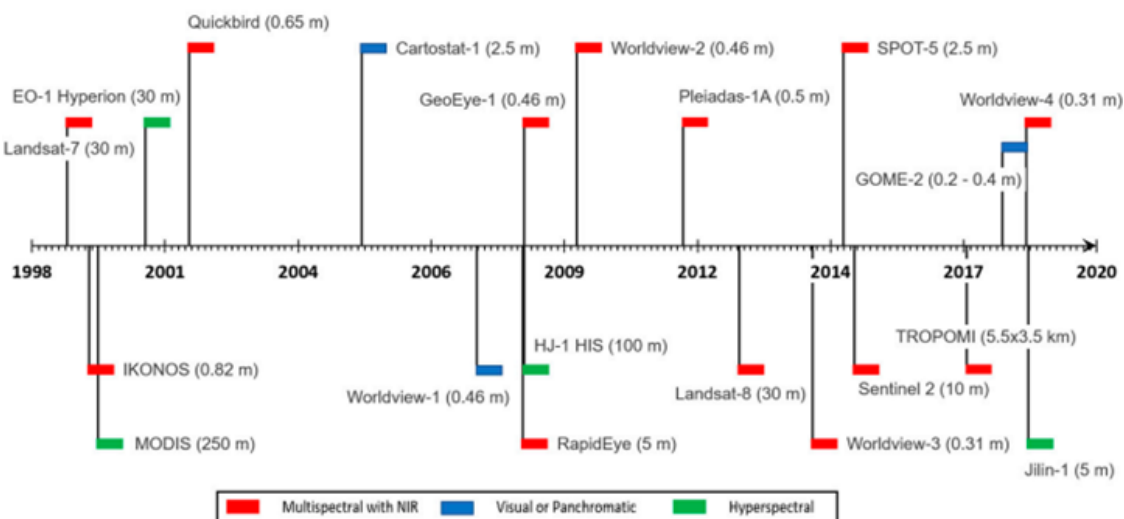


FIGURE 24. SATELLITES AND THEIR SPATIAL RESOLUTION SINCE 1999 (KHANAL *ET AL.* 2020).

RS is used more widely in some parts of the world, therefore more comparison studies are available to access. If limited studies are conducted in the area of interest, then more baseline data may be required to be gathered before using the RS method in the field. Figure 25 shows that Europe appears to be the leader in Satellite-based studies across multiple sensors, whilst Australia trails behind in both platforms and sensor types used in the field.

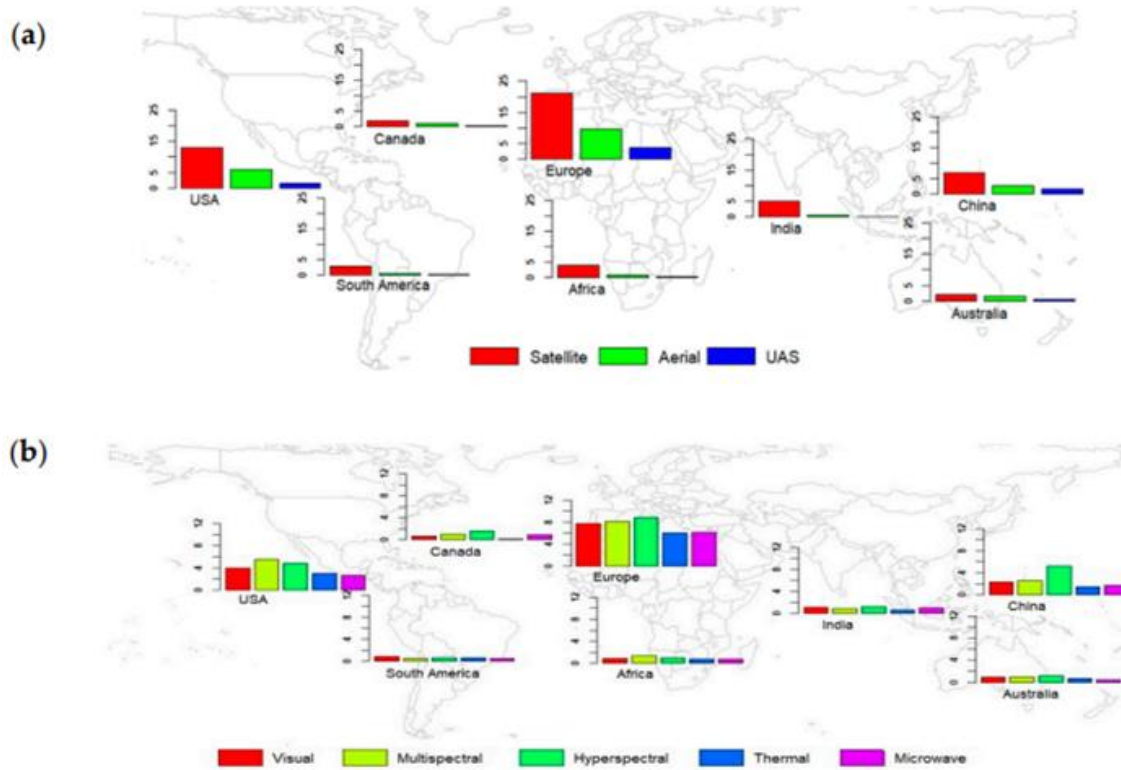


FIGURE 25. SUMMARY OF AGRICULTURE REMOTE STUDIES BY GEOGRAPHIC REGION BY (A) PLATFORM AND (B) SENSOR TYPE. (KHANAL ET AL. 2020).

When using satellites, planes and drones, the time of day the data is recorded must be considered. Certain data types must be collected at certain times (i.e., plant water stress thermal data should ideally be recorded around solar noon). If the data is not collected at the correct time, then the data may be less useful or completely useless. When the data is collected some filtering may need to be undertaken such as when monitoring plant water stress, any background soils temperatures need to be filtered.

With the increase in RS tools come other issues. What does the raw data mean? Can the farmers get the data on a timely basis? Is it a real-time or lagging indicator? Is the data measuring what the farmer needs? How accurate is the data? Is the data always available when the farmers need it? Do farmers need to calibrate new tools? Farmers do not necessarily have the time, knowledge, or skills to compute all this extra data to extrapolate specific insights that will improve their enterprise. Jones *et al.* (2017) state that "one issue is how to make data acquisition and analytical tools appropriate for and easy to use by farm-level decision-makers" (Jones *et al.* 2017). Shovelton *et al.* (2017) highlighted that "the correlations between NDVI and

feed on offer varied between sites and seasonality, and there was no consistent calibration to all situations". Higgins *et al.* (2018) also state the need for "high-quality ground truth data for cross-validation".

The cost of the RS equipment (i.e., thermal camera) and the vehicle it is mounted on can be cost-prohibitive for individual users. Calibration of the field equipment is also important, especially when collecting data using different pieces of equipment that then need to be combined for further calculation or interpretation. Having the time to collect and interpret the data is also time consuming. Other issues may involve special licence requirements (i.e., pilot license or drone licence) and maintenance of equipment (drones, planes, thermal cameras, etc).

2.6.3 Capturing plant canopy Temperature in the field.

Figure 26 demonstrates results from fieldwork undertaken by Bucks *et al.* (1985) that monitored the plant canopy temperature minus air temperature relative to irrigation treatments. Figure 26 demonstrates that the wet/irrigated guayule has a lower canopy temperature than an unwatered/dry plant. This variation in the canopy temperature of a wet vs. dry plant along with the VPD is used in developing the crop water stress index (CWSI).

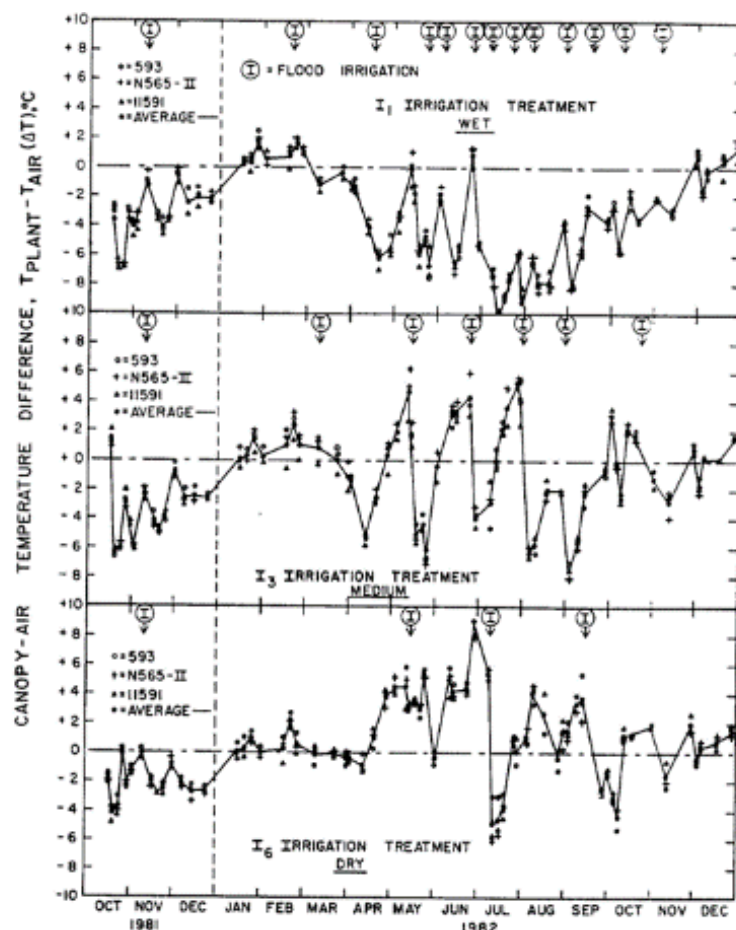


FIGURE 26. PLANT CANOPY MINUS AIR TEMPERATURE V'S TIME FOR THREE GUAYULE CULTIVARS UNDER WET (I₁), MEDIUM (I₃) AND DRY (I₆) IRRIGATION TREATMENTS. SOURCE – BUCKS *ET AL.* (1985)

2.6.4 Crop water stress index (CWSI)

The Crop Water Stress Index has been developed and is used in industry to measure the amount of plant water stress based on the canopy surface temperatures. The CWSI has been demonstrated to be closely related to water availability in the root zone of wheat crops (Jackson *et al.* 1981). The CWSI was calculated as proposed by Idso *et al.* (1981). The empirical CWSI formulae used are as follows in Figure 27.

$$CWSI = \frac{(Tc - Ta) - (Tc - Ta)_{LL}}{(Tc - Ta)_{UL} - (Tc - Ta)_{LL}}$$

FIGURE 27. CWSI FORMULAE

The $(Tc - Ta)$ represents the canopy temperature less air temperature of a canopy on the sampling day. The $(Tc - Ta)_{LL}$ represents the canopy temperature less air temperature of a canopy transpiring at its maximum rate. The $(Tc - Ta)_{UL}$ represents the canopy temperature less air temperature of a canopy when transpiration is halted due to lack of moisture. The temperature to develop the CWSI must be collected during daylight hours and clear skies.

To use the CWSI in the field, the user needs to know the canopy temperatures of a stressed and non-stressed plant to use the CWSI formula. However, having a stressed and non-stressed plant when using the CWSI is not always possible or practical. Alternatively, a number of crops have already been studied, and their stressed and non-stressed canopy temperatures have been recorded and turned into stressed and non-stressed baselines. The CWSI development requires two baselines specific for each site and crop (Idso, 1982; Gardner *et al.* 1992a; Nielsen, 1990). The upper baseline represents the canopy under full water stress with minimal to no transpiration. The lower baseline represents the non-stressed plants, where pastures/plants receive adequate water and are not limited in transpiration. By taking the air temperature from the temperature of the canopy $(Tc - Ta)$ and knowing the VPD, the CWSI can be calculated from the baseline, as demonstrated (Figure 28).

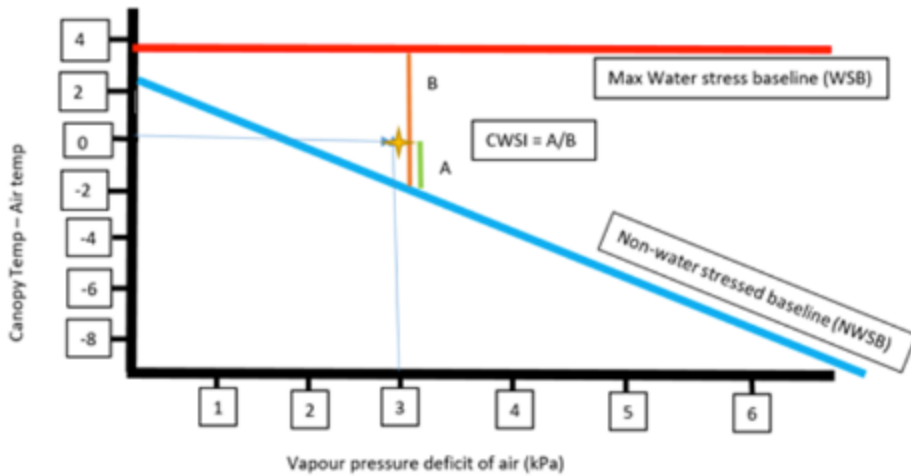


FIGURE 28. VISUAL REPRESENTATION OF HOW CWSI CAN BE CALCULATED FROM BASELINES.

Idso *et al.* (1982) conducted experiments on numerous crops, such as beans, alfalfa, lettuce, peas, squash, soybeans, etc., in varying locations (Kansas, Nebraska, Dakota, Arizona, etc) where they collected data to develop the baselines. Similarly, Maes *et al.* (2012) provide a long list of baselines developed by others over the years from many countries (Kansas, Iowa, California, Arizona, Turkey, Iran, Pakistan, Portugal, Argentina, France, Texas, etc.) for many crops and species; however, in these lists and other literature reviewed, there appear to be no references to annual ryegrass pastures or mixed species pastures baselines, especially in Southeast Australia.

The CWSI can be calculated empirically, as reported by Idos *et al.* (1981), and theoretically, as reported by Jackson *et al.* (1981). This work concentrates on the empirical approach, using field measurements to calculate the baselines and CWSI.

Collecting canopy thermal data to develop CWSI is typically undertaken using drones (UAV), planes and satellites. Figure 29 shows UAV sourced thermal data used to develop the CWSI for an olive grove.

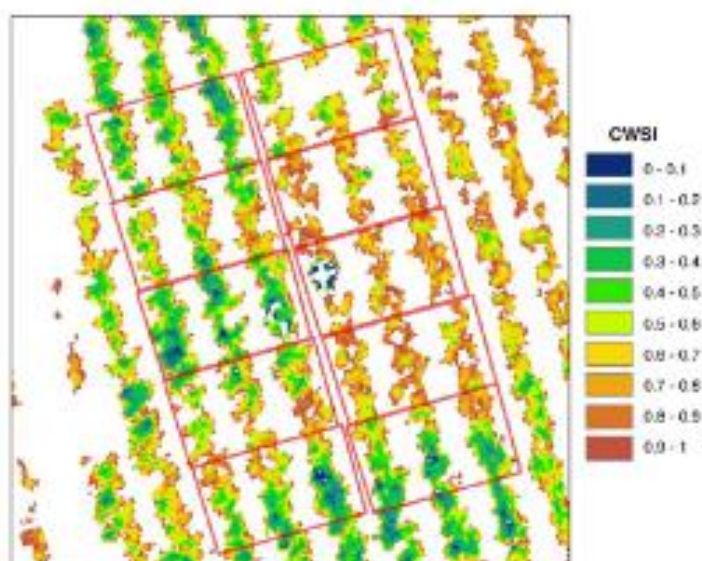


FIGURE 29. UAV SOURCED THERMAL DATA TO DEVELOP THE CWSI FOR AN OLIVE ORCHARD IN SPAIN (BERNI *ET AL.* 2009).

2.6.5 Issues Developing baselines.

While using CWSI and baselines can assist in identifying plant water stress in plants early, there are numerous issues in collecting the data. In the supplementary data in Maes *et al.* (2012) is an extensive list of non-water stressed baselines equations, similarly, in Idso's (1982) work there is a comprehensive list of baselines. Many early baselines were developed in more arid parts of the world (Arizona, California, Turkey, Iran, Texas, etc.) with limited work in the medium to high rainfall areas. A lot of the early work on developing the CWSI was done in the USA by Idso in Arizona, North Dakota, Nebraska, Kansas, etc, in arid environments with limited clouds. Similarly, other work on baselines since Idso's work has predominantly been in Turkey, Arizona, Iran, Texas, etc. (Maes *et al.* 2012), typically more arid areas. Idso (1981) mentions that his work was undertaken with clear skies with some thin cirrus conditions; he further mentions that for other types of cloudiness, the relationship begins to fall down, presumably due to changing illumination effects on stomates (Idso, 1981).

Similarly, O'Shaughnessy (2020) acknowledged the problem regarding irrigation scheduling by using instantaneous measurements taken over a short period near solar noon, which may be influenced by passing clouds, wind gusts or other micrometeorological incidents. Hipps (1985) discusses the small temporal variability of radiation and wind in the arid areas where much of the early work was undertaken and concludes that using the $T_f - T_a$ (Temperature foliage – Temperature air) has limited validity in regions with significant environmental variability. Consideration needs to be given to the usefulness of using the CWSI in non-arid regions.

Abdulelah *et al.* (2001). Stockle *et al.* (1992) found that the CWSI values for a non-stressed crop determined using the empirical CWSI baseline approach changed daily, especially under low VPD deficits. Abdulelah *et al.* (2001) also found that canopy temperature differences between stressed and non-stressed crops are usually small under low evaporative demand. Another finding by Jensen *et al.* (1989) was that the canopy temperature of either stressed or non-stressed wheat, barley, rape and perennial ryegrass crops could fluctuate up to 6°C within a few minutes to rapid changes in incident solar radiation. Environmental conditions (cloud cover and wind) can change canopy temperatures quickly.

The CWSI is an index that is measured between '0' (non-stressed plant) and '1' (stressed); however, using the data and baseline gathered from the plots, it was not possible to get all results to lie between these extremes. Abdulelah *et al.* (2001) also concluded that with their controlled environmental studies, there is strong evidence that there is no easy way to get the empirical CWSI results to consistently lie between 0 and 1. Similarly, the work by Wanjura *et al.* (1984) and Jalali-Farahani *et al.* (1993) experienced some negative CWSI values in their calculations.

Haghverdi *et al.* (2021) report that the reported CWSI baselines for Turfgrass vary widely in the literature and that specific baselines for each climatic region must be

developed. Jalail-Farahani, H *et al.* (1993) also discussed how baselines are site-specific. Adopting CWSI baselines derived from other countries, states, regions, or cultivars could be problematic as varying climatic conditions and microclimates exist, which can alter the CWSI from one place to another.

The CWSI can also be used as an irrigation trigger; when the CWSI reaches a specific level, it will trigger irrigation to start or stop. If the CWSI is not localised, then the CWSI trigger level may be wrong, and either over-watering or under-watering of a crop can occur, resulting potentially in plant damage from overwatering or reduction in production and plant death from under-watering, including the waste of natural resources (water).

Australia has experienced three La Nina weather patterns in a row (2020, 2021, 2022 – Source BOM). La Nina can be associated with above-average rainfalls and cooler days and nights in summer. With increasing variability in our climate, these changing weather patterns may influence where the CWSI works more optimally.

The process of senescence (change in colour and loss of leaves) and the plant dying may lead to changes in canopy temperature (Barbosa *et al.* 2005). Related to senescence is the reduction in canopy with the background soil influence on the infrared thermometer readings becoming more intensive. Barbosa *et al.* 2005 also mention that clouds were an operational issue, affecting the net radiation when collecting data, and that the field site is 60km from the Atlantic Ocean, which may be a reason behind the intermittent cloud cover.

Recording a range of VPDs can be difficult, especially if the fieldwork data collection time is short. Wanjura *et al.* (1984) highlighted that their VPD measurements did not exceed 4.0 kPa in their fieldwork. Wanjura *et al.* (1984) also mention the difficulty in recording canopy temperatures and how some of their plant canopies were not large enough to mask the soil background, and the TC included some contribution from the bare soil. Wanjura *et al.* (1984) also mention the possibility that early season stress caused by hail, wind and the seedling disease damaged the roots of many plants. Thus, their roots may be more resistant to water uptake than healthier plants.

Other issues include the sensors used to measure canopy temperatures and the weather stations used to derive the weather input data need to be evaluated and potentially calibrated to ensure accurate results for the CWSI (Gonzalez-Dugo, V *et al.* (2022). While the CWSI and associated baselines can be beneficial in monitoring plant water stress in the field, numerous issues are involved with data gathering to develop the baselines that can result in errors in the data gathered.

2.6.6 Baselines and their development

Figure 30 presents the results from experiments conducted by Idso *et al.* (1982) on (a) non-stressed (well-watered) Alfalfa to generate the non-stressed baseline for Alfalfa and (b) stressed soybeans to develop the stressed baseline for soybeans. To develop these baselines, he collected the canopy temperature, air temperature and VPD (Vapour pressure Deficit) over time.

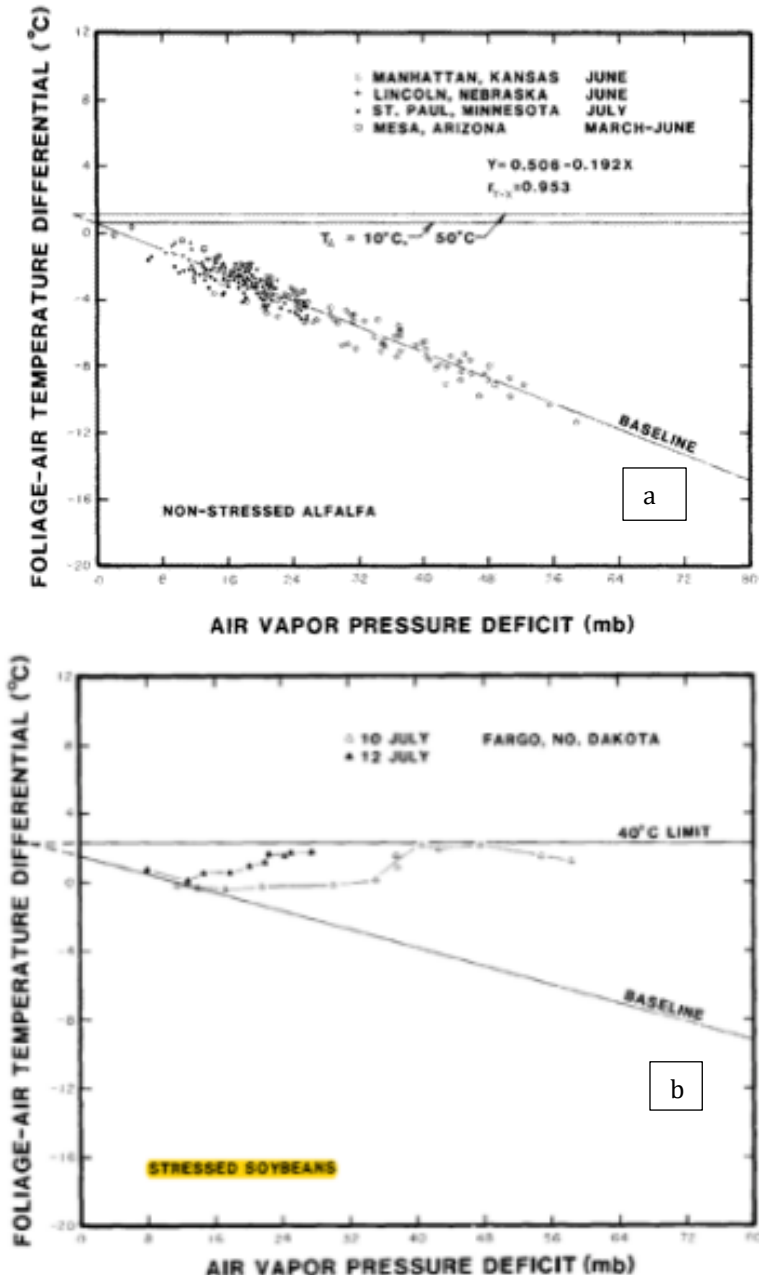


FIGURE 30. (A) NON-STRESSED ALFALFA (B) STRESSED SOYBEANS (SOURCE - IDSO *ET AL.* (1982))

2.6.7 Comparing baselines

Figure 31 is an example of comparing baselines of different plants, species, and varieties. It is noticeable how the different species have different stressed baselines and how some are similar (i.e., barley and wheat (Idso, 1982)), whilst others vary considerably, such as Bermuda Grass (Gonzalez-Dugo *et al.* 2022) and Turf grass (Gonzalez-Dugo *et al.* 2022) to wheat (Idso, 1982), and cowpeas (Idso, 1982). It is also noticeable how the growth stage can affect the baselines, such as in the wheat, pre- and post-heading (Figure 31).

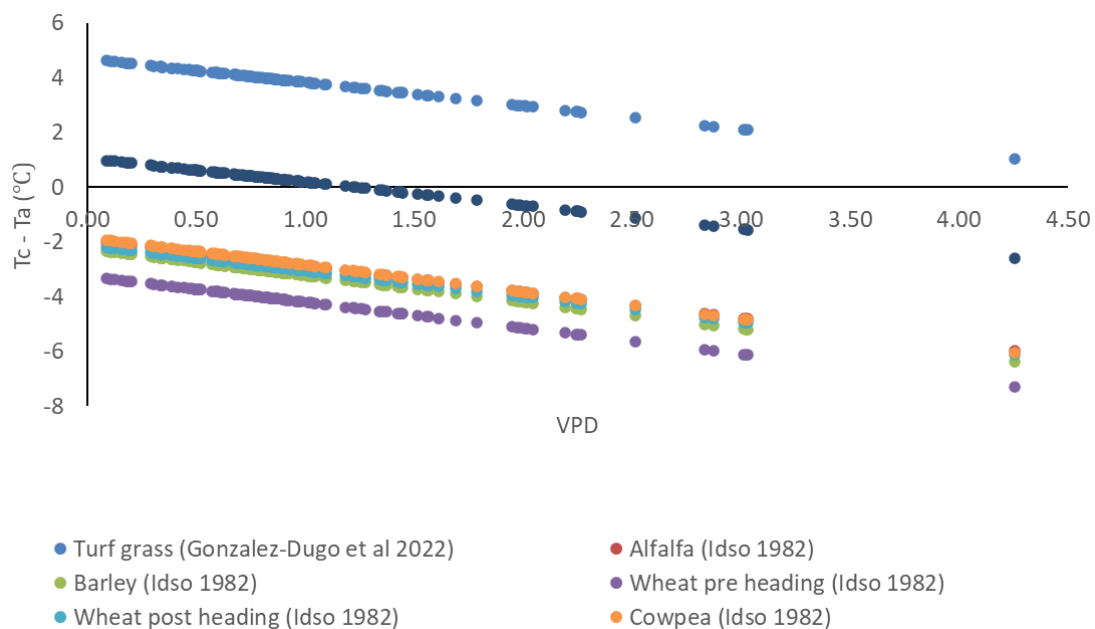


FIGURE 31. COMPARING BASELINES ACROSS A BROAD SELECTION OF SPECIES.

Figure 32 compares Tall fescue, Hybrid Bermuda grass and Turfgrass, comparing the $T_c - T_a$ versus VPD for the different species. Even for the same grass, the baselines can vary from one year to another as in the example in Figure 32 of the tall Fescue.

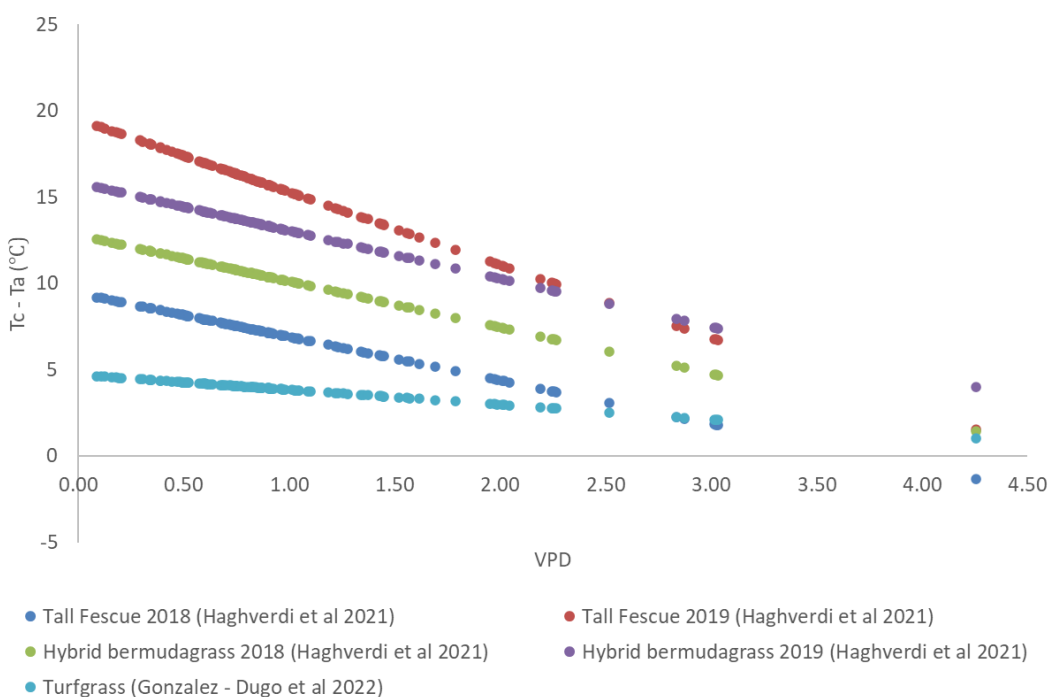


FIGURE 32. COMPARING BASELINES OF FESCUE, TURFGRASS AND BERMUDAGRASS.

Similarly, Payero *et al.* (2005) compiled Figure 33, demonstrating the different non stressed baselines that have been developed for Alfalfa, demonstrating how the baseline can vary for different locations and seasons.

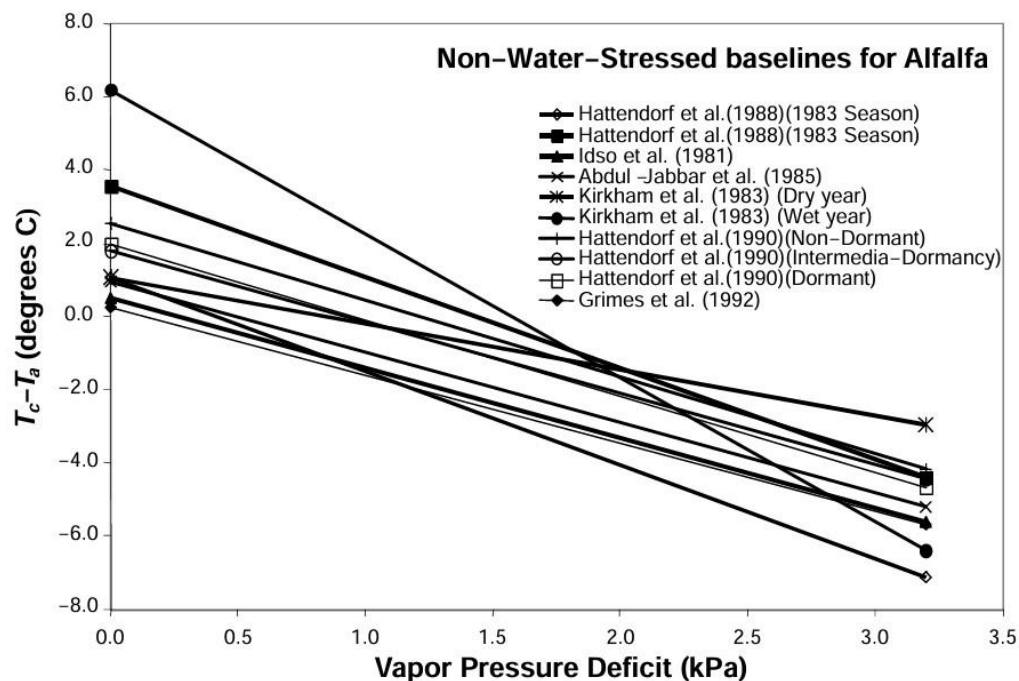


FIGURE 33. NON-WATER STRESSED BASELINES REPORTED BY VARIOUS RESEARCHERS FOR ALFALFA (PAYERO *ET AL.* (2005))

2.6.8 Use of CWSI to understand spatial variability in agriculture.

Using the point data provided by a soil moisture monitor in a paddock or from one or two plant canopy temperatures gives the farmer a good understanding of what is happening in part of their crop/pasture and the spatial variability in water status across the whole paddock/farm gives the farmer a more comprehensive idea of what is happening across their operations. Plant canopy temperatures obtained by thermal infrared cameras that may be plane or drone-mounted can provide a more extensive spatial data set to see what is happening across a field or farm. The collected plant canopy temperatures can be used to develop the CWSI of the farm, providing farm managers with a visual aid that tells them where any plant water stress is occurring across their operations and allowing them to rectify the issue where possible by applying irrigation in areas demonstrating high plant water stress.

The use of thermal remote sensing uses have been undertaken and implemented in other industries, assisting with identifying issues over a larger spatial area. Thermal remote sensing has been widely used overseas and in Australia, but mainly for 'high value' crops such as,

- Almonds (Garcia-Tejero *et al.* 2018)
- Maise (Dar *et al.* 2016),

- Wheat (Banerjee *et al.* 2020),
- Grape vines (Knipper *et al.* 2019),
- Nectarines (Park *et al.* 2017),
- Peaches (Park *et al.* 2017),
- Cotton (Bian *et al.* 2019, Conaty *et al.* 2012, Conaty *et al.* 2014)
- Conifers (Smigaj *et al.* 2017)
- Lentils (Biju *et al.* 2018)
- Potatoes (Rud *et al.* 2011)

2.7 Knowledge Gaps

The literature review critically evaluated the scientific literature on what biophysical models are used in agriculture, the use of the CWSI and the development of baselines (stressed and non-stressed) to evaluate plant water stress and how and where it has been applied.

With the climate variability faced by farms and the changes that climate change will bring, the earlier farmers can detect changes in their pasture status, giving them more time to react. Whether it is predicting how much pasture they can produce in the months ahead or the plant water status of their pastures, the more farmers are forewarned, the more time they have to plan.

Pasture growth forecasting.

Regarding biophysical modelling, limited tools are available for modelling pasture production compared to biophysical models available in horticultural and cropping industries. Limited work had also been undertaken on biophysical models and using soil water content (SWC) to project pasture production in the following weeks and months.

- * Knowledge gap – limited research has been conducted to date linking field soil water content to biophysical models to improve pasture growth predictions for the month(s) ahead.

CWSI

The literature review highlighted the extensive global use of precision agriculture in homogenous, high-value crops. However, it also showed that limited research has been conducted on heterogeneous pastures and annual rye grass-based grazing pastures, predominantly used by Australian farmers in SW Victoria. Minimal examples in the literature could be found where CWSI of pastures had been used, and no baselines could be found for annual ryegrass or mixed pastures in the Australian context. Most of the CWSI work appeared to be in arid zones, with limited work being undertaken in medium to high rainfall zones.

The use of precision agriculture to record the canopy temperatures of pastures in Australia was limited. Numerous studies have been conducted using planes or drones to remotely collect the thermal temperatures of horticultural crops in Europe and the United States, with minimal reference to using these methods in Australia on pastures. Similarly, there was minimal literature on using plant water

stress and the CWSI to scale point data to the paddock or farm scale, enabling farmers to monitor plant water stress of their pastures over broader areas.

- * Knowledge gap - A lack of work has been undertaken using remote precision agriculture to monitor plant water stress in single and multi-species pastures in Southeast Australia.
- * Knowledge gap - The literature review showed a lack of use of adaptive CWSI to measure variability in pastures in Southeast Australia.

If some of these knowledge gaps can be filled with new insights and the results from field trials, then the farmers of tomorrow should be able to more accurately predict the pasture produced in their fields and be able to monitor the plant water status of their pastures, identifying a stressed pasture prior to visual identification of wilting and senescence. These new insights should result in improved pasture prediction and use.

3 Utilising soil water content to predict pasture growth rates in Victoria, Australia.

3.1 Introduction

One of the major sources of variability in pasture-based livestock production systems is the intra- and inter-annual variation in pasture production caused by climate variations (Chapman *et al.* 2009). The variation in rainfall can have a marked impact on the quantity and quality of pasture available to livestock from season to season, and this variation impacts management decisions made at the farm level such as stocking rate adjustments (Chapman *et al.* 2009) and purchasing of supplementary feed (Clark *et al.* 2003). Managing these risks is important for profitable and sustainable grazing systems. There is emerging evidence that variability in pasture production in southern Australia has increased in recent decades (Perera *et al.* 2020). The changes in seasonal pasture growth patterns include increasing pasture growth rates in winter and early spring (Cullen *et al.* 2012; Perera *et al.* 2020) and increased frequency of short spring growing seasons (Bell *et al.* 2011; Perera *et al.* 2020). This increasing variability, together with expectations that climate variability will continue to increase into the future (Collins *et al.* 2021), places an increased emphasis on developing approaches to understand climate variability and predict pasture growth rates in coming months to manage climate risks in pasture-based livestock production systems.

In rain-fed cropping systems, SWC or Plant Available Water (PAW) is well established as a useful indicator of future yield potential (Carberry *et al.* 2002, Foale *et al.* 2004), and systems have been developed to store soil moisture prior to planting in order to minimise climate risk (Hunt *et al.* 2011). Tools such as 'Yield Prophet' have been developed to improve the understanding of seasonal climate risk in cropping systems (Hochman *et al.* 2009) and to evaluate management input decisions (such as nitrogen fertiliser rates) to improve decision making for grain growers (Hunt *et al.* 2006). However, there has been much less research on the value of SWC for managing climate risk in pasture-based livestock production systems. Pasture systems have important differences from crop systems because they are often based on perennial plants rather than annual species and generally aim to supply year-round feed to meet the demands from livestock rather than a single crop harvest.

Biophysical farm systems models of pasture-based livestock systems provide useful tools for simulating the impacts of climate variability on pasture production using long-term climate records. These tools simulate pasture production based on daily climate, soil characteristics, pasture species and management (such as soil fertility and grazing). Tools such as Grassgro (Moore *et al.* 1997) and the SGS Pasture model

(Johnson *et al.* 2008) have been applied in southern Australia to simulate impacts of climate variability, but there has not been any systematic assessment of the usefulness of using SWC to predict pasture growth in the region. Simulation modelling of the climate impacts will not be able to predict a single future outcome, but it can guide in quantifying an uncertain future (Hayman *et al.* 2008). Presenting probabilistic information as percentage chance of the outcome being in the lowest, middle or highest third of possible outcomes has been shown to be an effective way to communicate results of seasonal forecasting studies (McIntosh *et al.* 2005, Ash *et al.* 2007).

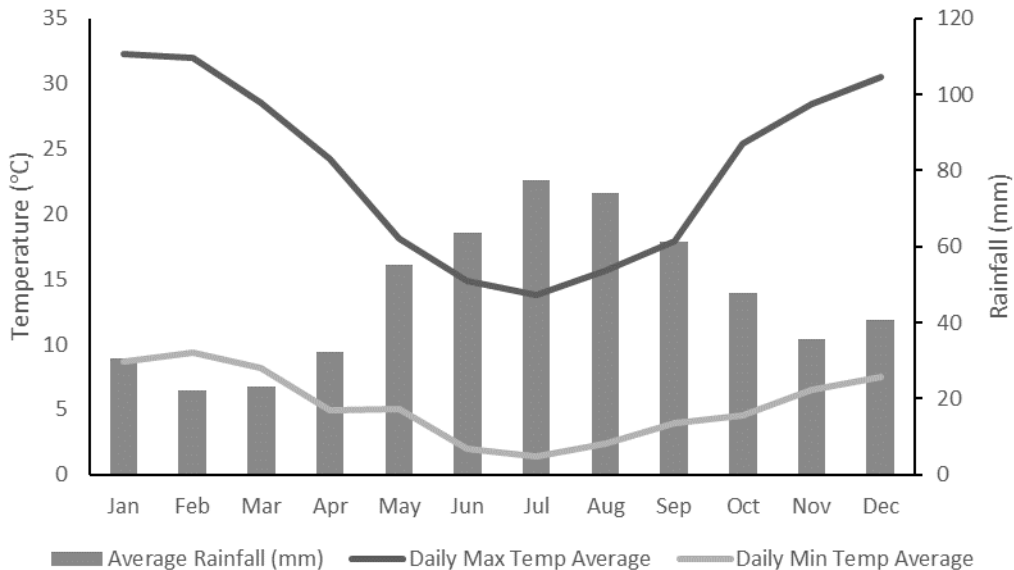
The aim of the study was to assess the usefulness of SWC to predict pasture growth in the following one to three months ahead using the SGS Pasture Model at three sites across central and south-west Victoria, Australia. The study consisted of two main components, first to validate the simulated SWC against measured data in the field, and second to predict monthly pasture growth rates based on historically dry (10th percentile), moderate (50th percentile) or wet (90th percentile) SWC on the first day of each month.

3.2 Materials and Methods

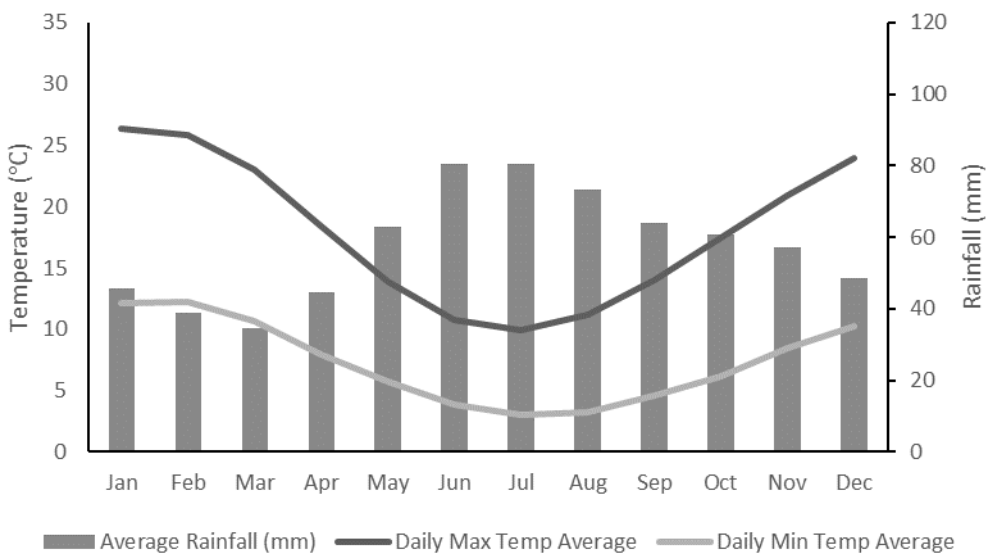
3.2.1 Site Descriptions

Three sites were selected in central and south-west Victoria, Australia, to present the range of climatic conditions in the region: Baynton (Lat -37.12, long 144.61); Pigeon Ponds (Lat -37.29, long 141.67); and Dartmoor (-37.92, Long 141.27). The sites all have a winter dominant rainfall pattern typical of temperate climates in southern Australia (34). Pigeon Ponds was the lowest rainfall site (564 mm annual average rainfall from 1990-2019, range 329-856 mm), Baynton was intermediate (690 mm average annual rainfall, range 408-1153 mm) and Dartmoor was the highest (754, range 482-977 mm). Monthly rainfall and temperatures are shown in Figure 34.

(a)



(b)



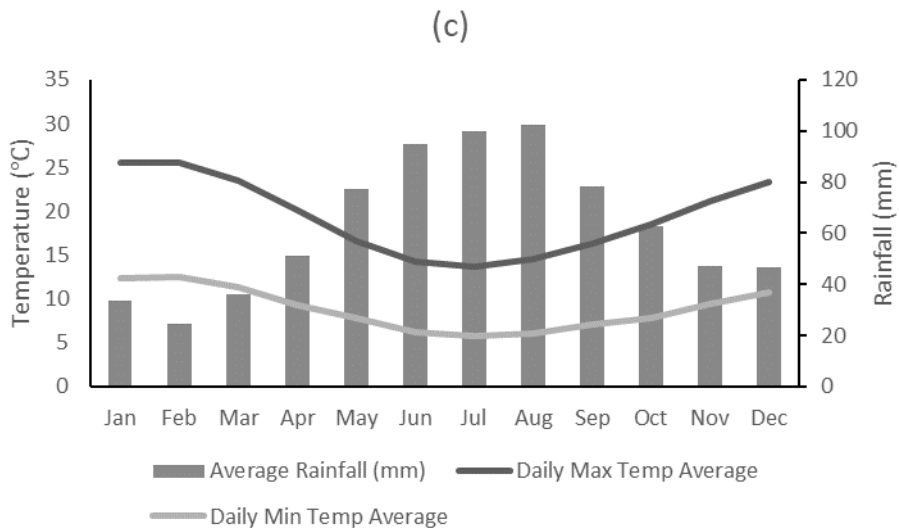


FIGURE 34. CLIMATE SUMMARY WITH AVERAGE MONTHLY RAINFALL (GREY BARS), AND AVERAGE MONTHLY MAXIMUM (BOLD LINE) AND MINIMUM TEMPERATURES (LIGHTER LINE) AT (A) PIGEON PONDS, (B) BAYNTON, (C) DARTMOOR FROM 1990-2021.

The pastures consisted of phalaris (*Phalaris aquatica* L.) and sub-clover (*Trifolium subterraneum*) at Baynton (also a small proportion of annual weeds) and Pigeon Ponds, while at Dartmoor the pasture species were phalaris, lucerne (*Medicago sativa* L.) and perennial ryegrass (*Lolium perenne*). The soil physical characteristics and water holding capacities used in the simulation study for each site are summarised in Table 1. Soil moisture probes (Enviropro capacitance probe – 80cm, connected with MAIT logger and telemetry) were installed in February 2018 in the paddocks. The probes measure and collect SWC up to 80cm deep every hour. The sensor data was sourced from Agriculture Victoria online (source – <https://extensionaus.com.au/soilmoisturemonitoring>).

TABLE 1. PHYSICAL CHARACTERISTICS AND SOIL WATER HOLDING PARAMETERS, INCLUDING SATURATED WATER CONTENT, FIELD CAPACITY AND WILTING POINT (ALL % VOLUMETRIC) AT THE THREE SITES.

	<i>Pigeon Ponds</i>				<i>Baynton</i>		<i>Dartmoor</i>	
Soil Profile Depth (cm)	0 – 5	5 – 30	30 – 80	80 – 140	0 – 50	50 – 150	0 – 50	50 – 150
Soil Texture	<i>Loam</i>	<i>Clay</i>	<i>Clay</i>	<i>Clay</i>	<i>Sandy loam</i>	<i>Clay</i>	<i>Sandy loam</i>	<i>Sandy clay</i>
Saturated hydraulic conductivity (cm/day)	31	10	14	6	6.2	3.6	32.4	6.7
Saturated water content (% volumetric)	50	41	44	48	40	50	42	48
Field Capacity (% volumetric)	31	27	34	36	29	46	27	40
Wilting Point (% volumetric)	11	15	29	32	17	28	11	19

3.2.2 Validation of predicted SWC

At each of the three sites the daily SGS Pasture model predicted volumetric SWC was compared to the SWC measured by the in-field sensors for the period 1 June 2019 to 31 December 2021. The simulations used the SGS Pasture model (Johnson *et al.* 2003, 2008). The soil type and pasture species were defined in the model as described in Table 1. Climate data for each site was obtained through the closest Bureau of Meteorology site accessed through the SILO website (<https://www.longpaddock.qld.gov.au/silo/>, Jeffrey *et al.* 2001) Baynton (Station 88073), Pigeon Ponds (Station 89003) and Dartmoor (Station 90032).

The measured relative SWC from in-field moisture probes and the modelled SWC (from SGS pasture model) were used to determine if the SGS Pasture model could realistically simulate the measured patterns of SWC change over time. The in-field sensors were not calibrated (e.g., to field capacity and wilting point) so provided a relative SWC, but on a different scale to the modelled volumetric SWC. To express the in-field sensor SWC on the same scale as the SGS pasture model predicted volumetric SWC, the following procedure was used:

1. The range of the in-field sensor relative SWC was calculated for the period, using the 95th percentile as the upper limit and 5th percentile as the lower limit,
2. The in-field sensor daily measured relative SWC minus the lower limit was calculated as a proportion of the range,
3. The range of the SGS Pasture volumetric SWC was calculated for the period, using the 95th percentile as the upper limit and 5th percentile as the lower limit,
4. The daily in-field sensor proportion (point 2) was multiplied by the range of SGS volumetric SWC (point 3) plus the lower limit to give the equivalent volumetric soil water content.

For example, at Baynton on 1 June 2019,

- the range of the in-field sensor relative SWC was 23-61%.
- on the date of 1st June 2019, the in-field sensor measured relative SWC was 48% and the range of data which is 0.66 of the range $\{[48-23]/[61-23]=0.66\}$.
- the range of the SGS Pasture model volumetric SWC was 16.5-33.4%
- the proportion (point 2) was multiplied by the range from the SGS model data and the lower limit was added $\{[0.66*(33.4-16.5)]+16.5 = 27.7\}$.

This calculation was completed daily for all three sites. The daily measured and modelled SWC were compared, with linear trendline and coefficient of determination computed using Microsoft Excel.

3.2.3 Modelling the effect of SWC on pasture growth rate

At each of the sites the effects of historically 'dry', 'moderate' and 'wet' SWC on the first day of each month on pasture growth rates over the following 4 months was simulated, and results expressed relative to the historical distribution of pasture growth using 'low', 'mid' and 'high' terciles. The first step in the modelling process was to run long-term simulations at each site to predict the historical variation in SWC and pasture growth rates. The SGS Pasture model was used to simulate each site using climate data from 1990-2020. A cut trial was implemented in the model, with pasture cut to 1 t DM/ha on the last day of each month, and soil fertility was assumed to be unlimited so that the predicted pasture growth rates reflected the climate variation and not other management factors.

To determine the historically 'dry', 'moderate' and 'wet' SWC on the first day of each month, the plant available water (PAW) was calculated from the SGS pasture model predicted SWC for the soil depth from 0-50 cm. The PAW calculation was the SWC – Wilting point (WP) multiplied for the depth for intervals from surface to 50cm depth. Depths were 0-2cm, 2cm – 5cm, 5cm- 10cm, 10cm -15cm, 15cm -20cm, 20cm -30cm, 30cm – 40 cm and 40cm -50cm. The PAW on the first day of each month from each year (1990-2020) was used to determine historically 'dry' (0.1 percentile), 'moderate' (0.5 percentile) and 'wet' (0.9 percentile) conditions. The individual years representing 'dry', 'moderate' and 'wet' conditions were identified and the modelled SWC on that day was used to initialise the model. The 'dry', 'moderate' and 'wet' PAW for each month is shown in Figure 35.

The effect of 'dry', 'moderate' and 'wet' SWC on the first day each month on pasture growth rates over the following four months was simulated using the 'soil water reset' function in the SGS Pasture model. The simulations were run using climate data for 1990-2020 with the SWC in the model reset to the appropriate SWC on the date in each year. The simulations were conducted as a cut trial with no soil nutrient limitation, using the same modelling approach described above. A total of 108 simulations were completed (3 sites x 3 SWC x 12 months). The daily 'net positive growth rate' simulated by the SGS Pasture model was averaged for each month, and then categorised into the 'low', 'mid' or 'high' terciles of pasture growth according

to the categories described above. Results are presented as the percentage chance of the simulated pasture growth rate being in each tercile, similar to the 'chocolate wheel' approach described by McIntosh *et al.* (2005).

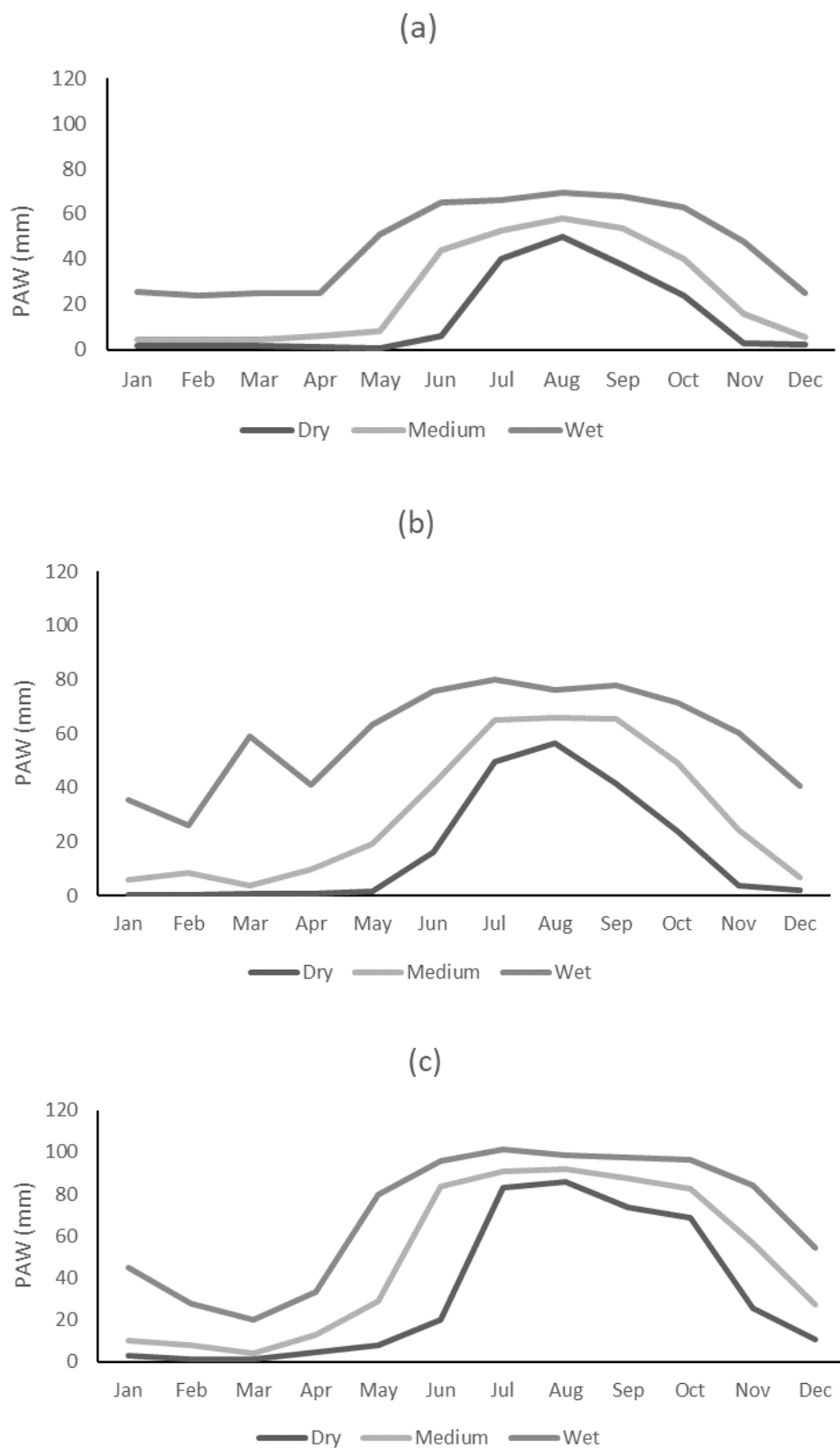


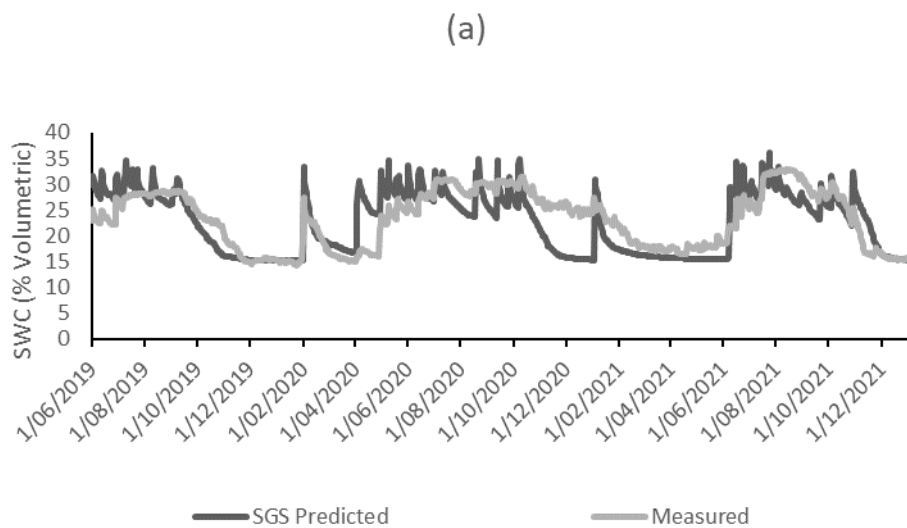
FIGURE 35. PLANT AVAILABLE WATER FOR THREE PERCENTILES "DRY" (0.1 PERCENTILE), 'MODERATE' (0.5 PERCENTILE), 'WET' (0.9 PERCENTILE) ON THE FIRST DAY OF EACH MONTH AT (A) PIGEON PONDS, (B) BAYNTON, AND (C) DARTMOOR.

In this study, a 30% increase in the chance of the predicted pasture growth rate being in a tercile was used as an indicator of when the forecast would be useful to a land manager (i.e. without knowing the SWC there is a 33% chance of the predicted pasture growth rate being in the each of the terciles, but when this increases to 43% or greater the forecast was considered useful). This threshold was based on the conclusion of Ash *et al.* (2007) who found that a seasonal climate forecast of above or below median rainfall needed to be at least 65% accurate (i.e. a 30% increase in the chance of above or below the median) to achieve adoption by farmers.

3.3 Results

3.3.1 Validation of predicted SWC

The time series of measured relative SWC and predicted SWC from the SGS pasture model at 20 cm soil depth is presented in Figure 36. Visual inspection of the figure indicates that there was overall good agreement in the timing of wetting up and drying down between the measured and predicted data, however there were some points that were not well simulated. The regression equations for the daily data plotted as measured vs. predicted were at Baynton ($Y = 0.89x + 1.87$, $R^2 = 0.73$), Pigeon Ponds ($Y = 0.81x + 3.8$, $R^2 = 0.55$) and Dartmoor ($Y = 0.97x + 1.1$, $R^2 = 0.85$). The SWC validation data for other soil depths is provided as supplementary information to this chapter.



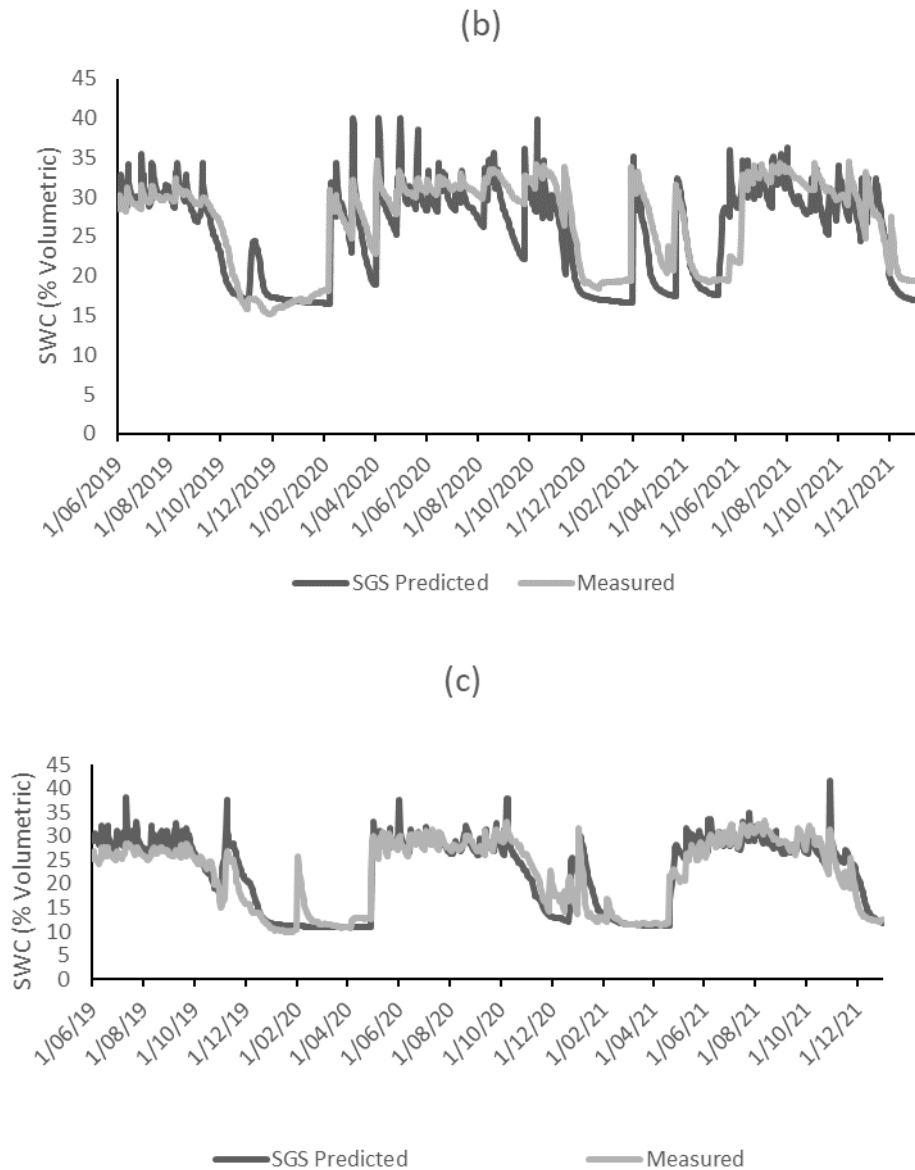


FIGURE 36. DAILY MEASURED RELATIVE SWC AND PREDICTED SWC FROM THE SGS PASTURE MODEL AT 20 CM AT (A) PIGEON PONDS, (B) BAYNTON, (C) DARTMOOR.

3.3.2 Pasture Growth Rates

The long-term simulated pasture growth rates for Baynton, Pigeon Ponds and Dartmoor are shown in Figure 37. The terciles are indicated on the Figures as the areas below the 33rd percentile line (low tercile), between the 33rd and 66th percentile (mid tercile), and greater than 66th percentile (high tercile). The time of highest variability in pasture growth rates in autumn and spring at Baynton and Pigeon Ponds, and spring and summer at Dartmoor (Figure 37). Pasture growth rates in the winter months had low variability. For example, pasture growth rates varied from 20-120 kg DM/ha.day at Baynton in late spring whereas during winter the variation only ranged between 10 – 20 kg DM/ha.day. Similarly, at Pigeon Ponds during late spring the pasture growth rates varied from 0- 120 kg DM/ha.day depending on the season, whilst in late summer pasture growth rates were low. At

the Dartmoor site, lucerne-based pasture growth rates in summer varied from 15–100 kg DM/ha.day compared to 10 – 20 kg DM/ha.day in winter.

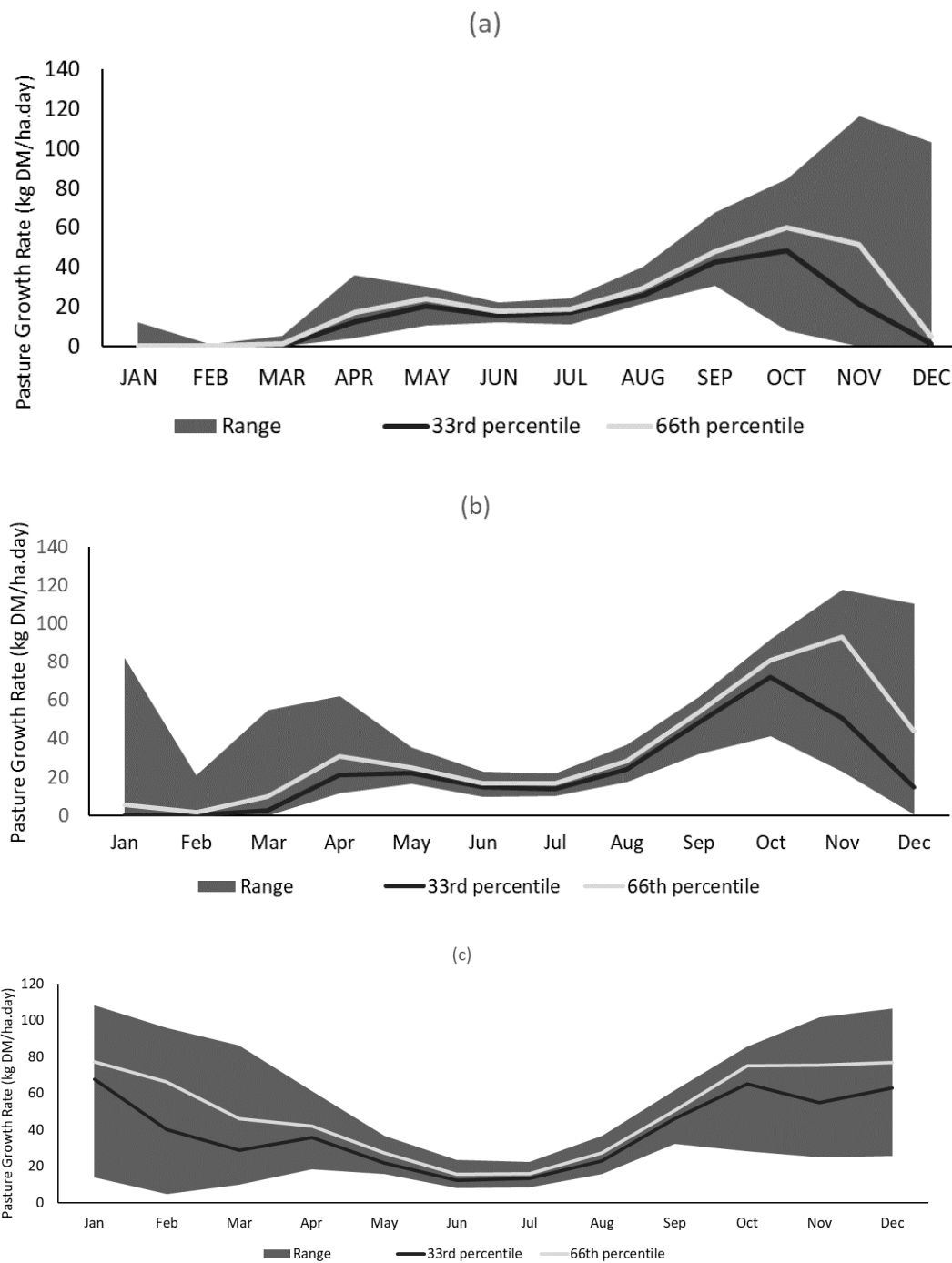


FIGURE 37. SIMULATED MONTHLY AVERAGE PASTURE GROWTH RATES (KG DM/HA.DAY) AT (A) PIGEON PONDS, (B) BAYNTON, (C) DARTMOOR. THE SHADeD AREA SHOWS THE RANGE OF PASTURE GROWTH RATES, THE DARK LINE THE 33RD PERCENTILE AND LIGHT LINE THE 66TH PERCENTILE. SHADeD AREAS BELOW THE 33RD PERCENTILE LINE REPRESENTS THE LOW TERCILE, BETWEEN THE 33RD AND 66TH PERCENTILE LINE THE MID TERCILE), AND ABOVE THE 66TH PERCENTILE THE HIGH TERCILE.

3.3.3 Pasture growth predictions using SWC

The results for the three sites showing the percent chance of predicted pasture growth being in the Low, Mid and Upper tercile are shown in Tables 2-4. The SGS simulation model results showed that SWC at the start of each month influenced the pasture growth rates, notably during the Australian spring and autumn for phalaris based pastures but had minimal effect during winter and summer for phalaris based pastures. There were some differences between the sites, reflecting the different patterns of SWC (Figure 36) and pasture growth (Figure 37) variability at the sites.

For Baynton (Table 3) in Spring, the data demonstrates that if it is dry in September and October there is an increased chance of growth being in the mid to low tercile over the following two months. For Pigeon Ponds (Table 2) the data demonstrates that if it is dry in November, there is an increased chance of being in the low tercile growth, whereas a wet SWC in November increases the chance of high tercile growth. For Dartmoor (Table 4) the effects of SWC are more pronounced in the late spring and summer than at other times of year.

For Baynton the results show SWC in Autumn has an impact on pasture production in the following months. A dry SWC in March indicated growth being in the lower tercile throughout Autumn, where a wet SWC increased the chance of growth being in the high tercile in April and May. For Pigeon Ponds with a wet SWC, the results show increased chance of growth in the high tercile in Autumn. For Dartmoor with a wet SWC the results show growth being in the higher tercile in early Autumn (March).

The majority of the results for the three sites when calculating the percent chance of predicted pasture growth being in the Low, Mid and Upper tercile appear with higher pasture production predicted when there was higher SWC, however there are some cases that do not fit with what would have been expected (Tables 2-4). The February Pigeon Ponds result seems inconsistent with the rest of the results because all three initial SWCs predicted an increased chance of low tercile growth in the prediction months, and increased chance of high tercile in +2 and +3 months. February does have the lowest pasture growth rate, so very small differences in predicted growth rates can result in different tercile being predicted. Similarly at Dartmoor, the dry SWC in April predicted a 43% chance of High tercile where one would expect a lower tercile, as the lucerne growing season is coming to an end. Different subsoil moisture content may explain this result.

TABLE 2. SUMMARISED RESULTS FOR PIGEON PONDS SHOWING PERCENT CHANCE OF PREDICTED PASTURE GROWTH BEING IN THE LOW, MID AND UPPER TERCILE. UPPER TERCILE ABOVE 43 SHADED IN GREEN, MID TERCILE ABOVE 43 SHADED IN GREY AND LOWER TERCILE ABOVE 43 SHADED IN ORANGE.

Pigeon Ponds		Prediction month	+ 1 month	+ 2 months	+ 3 months
	SWC	% chance predicted pasture growth rate in each tercile			
		Low, Mid, High	Low, Mid, High	Low, Mid, High	Low, Mid, High
January	Dry	35,32,32	38,27,35	27,32,41	27,32,41
January	Med	38,27,35	35,24,41	27,30,43	27,32,41
January	Wet	38,27,35	35,24,41	24,32,43	22,35,43
February	Dry	43,27,30	30,32,38	19,38,43	16,27,57
February	Med	43,27,30	30,30,41	19,30,51	11,30,59
February	Wet	43,27,30	30,30,41	19,32,49	11,30,59
March	Dry	30,38,32	41,35,24	46,30,24	38,38,24
March	Med	32,32,35	38,32,30	38,35,27	35,41,24
March	Wet	35,30,35	22,27,51	8,32,59	19,38,43
April	Dry	32,27,41	32,27,41	24,41,35	27,24,49
April	Med	32,27,41	19,41,41	22,38,41	27,22,51
April	Wet	22,30,49	8,32,59	19,43,38	30,27,43
May	Dry	32,32,35	27,35,38	30,24,46	30,32,38
May	Med	24,35,41	27,38,35	30,32,38	32,32,35
May	Wet	16,32,51	30,46,24	32,35,32	35,30,35
June	Dry	32,35,32	35,30,35	30,35,35	32,32,35
June	Med	27,38,35	35,27,38	35,30,35	30,35,35
June	Wet	32,35,32	35,30,35	35,30,35	30,35,35
July	Dry	32,30,38	32,32,35	32,32,35	35,30,35
July	Med	38,27,35	32,32,35	30,35,35	35,30,35
July	Wet	38,27,35	35,30,35	30,35,35	35,30,35
August	Dry	32,32,35	30,35,35	35,30,35	32,32,35
August	Med	32,32,35	30,35,35	35,30,35	32,32,35
August	Wet	35,30,35	30,35,35	35,30,35	32,32,35
September	Dry	32,32,35	41,27,32	38,27,35	38,27,35
September	Med	30,35,35	32,27,41	32,32,35	32,32,35
September	Wet	35,32,32	32,27,41	32,32,35	32,32,35
October	Dry	38,27,35	41,30,30	43,27,30	32,35,32
October	Med	27,24,49	32,30,38	30,35,35	32,35,32
October	Wet	24,24,51	32,30,38	30,35,35	32,35,32
November	Dry	46,41,14	49,24,27	32,35,32	30,24,46
November	Med	41,35,24	46,27,27	35,32,32	30,32,38
November	Wet	24,24,51	30,30,41	35,35,30	35,30,35
December	Dry	35,35,30	35,32,32	35,24,41	30,32,38
December	Med	30,32,38	43,24,32	35,27,38	30,32,38
December	Wet	27,32,41	46,19,35	35,24,41	32,27,41

TABLE 3. SUMMARISED RESULTS FOR BAYNTON SHOWING THE PERCENT CHANCE OF PREDICTED PASTURE GROWTH BEING IN THE LOW, MID AND UPPER TERCILE. UPPER TERCILE ABOVE 43 SHADED IN GREEN, MID TERCILE ABOVE 43 SHADED IN GREY AND LOWER TERCILE ABOVE 43 SHADED IN ORANGE.

Baynton		Prediction month	+ 1 month	+ 2 months	+ 3 months
	SWC	% chance predicted pasture growth rate in each tercile			
		Low, Mid, High	Low, Mid, High	Low, Mid, High	Low, Mid, High
January	Dry	32,38,30	32,41,27	38,35,27	51, 24,24
January	Med	30,38,32	35,38,27	35,32,32	35,38,27
January	Wet	32,22,46	30,35,35	32,30,38	24,41,35
February	Dry	30,41,30	38,46,16	68,11,22	65,16,19
February	Med	30,32,38	32,30,38	22,30,49	14,30,57
February	Wet	35,27,38	32,27,41	16,24,59	8,19,73
March	Dry	41,43,16	76,5,19	73,11,16	73,14,14
March	Med	32,30,38	22,38,41	16,32,51	22,35,43
March	Wet	32,30,38	14,27,59	8,19,73	24,22,54
April	Dry	73,16,11	65,22,14	65,27,8	41,43,16
April	Med	43,43,14	49,32,19	41,43,16	32,38,30
April	Wet	14,27,59	11,24,65	32,32,35	32,32,35
May	Dry	86,14,0	70,19,11	49,32,19	38,38,24
May	Med	24,30,46	32,27,41	32,30,38	32,32,35
May	Wet	22,32,46	32,41,27	38,30,32	38,30,32
June	Dry	32,32,35	35,27,38	32,35,32	35,32,32
June	Med	32,32,35	32,30,38	32,30,38	35,32,32
June	Wet	32,35,32	38,27,35	32,35,32	35,32,32
July	Dry	32,35,32	30,35,35	32,38,30	38,27,35
July	Med	30,30,41	30,38,32	35,30,35	35,30,35
July	Wet	35,27,38	32,35,32	35,32,32	32,32,35
August	Dry	27,41,32	35,32,32	32,32,35	32,32,35
August	Med	27,41,32	32,35,32	32,32,35	32,32,35
August	Wet	27,41,32	35,32,32	32,32,35	32,32,35
September	Dry	32,43,24	43,27,30	40,27,32	37,29,32
September	Med	32,32,35	32,24,43	30,35,35	32,32,35
September	Wet	32,35,32	32,27,41	32,32,35	32,32,35
October	Dry	54,24,22	43,35,22	46,24,30	38,30,32
October	Med	24,32,43	30,38,32	38,30,32	35,30,35
October	Wet	24,32,43	19,49,32	32,35,32	35,30,35
November	Dry	27,54,19	35,35,30	32,30,38	35,35,30
November	Med	16,43,41	24,38,38	32,30,38	32,38,30
November	Wet	16,43,41	24,38,38	32,30,38	32,38,30
December	Dry	27,35,38	35,24,41	35,30,35	32,30,35
December	Med	22,38,41	32,27,41	32,32,35	32,30,38
December	Wet	22,38,41	32,27,41	35,30,35	32,30,38

TABLE 4. SUMMARISED RESULTS FOR DARTMOOR SHOWING THE PERCENT CHANCE OF PREDICTED PASTURE GROWTH BEING IN THE LOW, MID AND UPPER TERCILE. UPPER TERCILE ABOVE 43 SHADED IN GREEN, MID TERCILE ABOVE 43 SHADED IN GREY AND LOWER TERCILE ABOVE 43 SHADED IN ORANGE.

Dartmoor		Prediction month	+ 1 month	+ 2 months	+ 3 months
	SWC	% chance predicted pasture growth rate in each tercile			
		Low, Mid, High	Low, Mid, High	Low, Mid, High	Low, Mid, High
January	Dry	89,5,5	73,22,5	59,32,8	65,16,19
January	Med	51,24,24	49,43,8	46,43,11	49,30,22
January	Wet	3,11,86	0,35,65	5,41,54	30,14,57
February	Dry	51,46,3	43,41,16	49,19,32	35,38,27
February	Med	0,0,100	0,11,89	8,27,65	16,32,51
February	Wet	0,3,97	0,32,68	22,27,51	22,35,43
March	Dry	11,59,30	38,19,43	30,35,35	30,35,35
March	Med	3,62,35	30,19,51	27,35,38	27,38,35
March	Wet	0,46,54	27,27,46	24,38,38	30,35,35
April	Dry	14,38,49	22,35,43	24,41,35	38,27,35
April	Med	14,30,57	27,27,46	24,38,38	38,30,32
April	Wet	11,19,70	22,27,51	22,38,41	38,27,35
May	Dry	27,38,35	24,38,38	32,32,35	32,32,35
May	Med	27,38,35	27,35,38	32,32,35	32,32,35
May	Wet	27,35,38	24,38,38	35,30,35	35,32,32
June	Dry	27,35,38	32,32,35	32,32,35	30,32,38
June	Med	32,32,35	32,32,35	32,32,35	30,35,35
June	Wet	32,32,35	32,32,35	32,32,35	32,32,35
July	Dry	32,32,35	35,30,35	30,35,35	30,35,35
July	Med	32,32,35	32,32,35	27,38,35	30,35,35
July	Wet	35,30,35	38,30,32	35,32,32	30,38,32
August	Dry	35,30,35	35,32,32	30,35,35	32,35,32
August	Med	35,30,35	35,32,32	32,32,35	32,35,32
August	Wet	35,30,35	35,30,35	32,32,35	32,32,35
September	Dry	32,32,35	32,35,32	32,32,35	27,38,35
September	Med	32,30,38	30,35,35	32,32,35	24,41,35
September	Wet	32,32,35	32,32,35	32,32,35	27,38,35
October	Dry	35,27,38	32,32,35	32,38,30	41,30,30
October	Med	30,32,38	32,32,35	32,35,32	35,32,32
October	Wet	30,38,32	30,35,35	24,41,35	27,35,38
November	Dry	32,43,24	35,32,32	51,16,32	27,59,14
November	Med	30,32,38	38,30,32	49,19,32	27,59,14
November	Wet	27,32,41	24,35,41	11,38,51	16,41,43
December	Dry	57,22,22	70,14,16	57,38,5	46,43,11
December	Med	27,41,32	62,14,24	41,54,5	46,41,14
December	Wet	27,35,38	8,24,68	5,46,49	8,49,43

3.4 Discussion

This study examined the role of SWC in predicting pasture growth in the months ahead at three sites across Victoria, Australia. The spring and autumn period is typically when SWC can limit pasture growth. This research demonstrates that SWC can be used to improve the prediction of pasture growth rates at these times. For Baynton the main growth periods were October to January with some growth occurring in March to April. For Pigeon Ponds the main growth periods was October to December. Dartmoor also demonstrated that the predictions for lucerne demonstrate a large variation in October through to March/April depending on the starting SWC.

In the Dartmoor scenario (Table 4) the December, wet, at one month gave a 68% of “High” chance of predicted pasture growth, where at the +2month and +3month it gave a 49% and 43% chance respectively. The higher percentage in this example would indicate a more reliable prediction at the one month than the later months (Harrison *et al.* 2017). One observation was that in a ‘dry’ start to a month, that month’s pasture production may be in the lower tercile due to the dry SWC, however it did not mean the following months would remain in the lower tercile. Whilst a low SWC may affect that month’s pasture production there can still be a possibility of a rainfall event(s) occurring that will lift a ‘dry’ SWC to a ‘medium’ or ‘high’ SWC which can lead to an increase in pasture production. An example of this is in Dartmoor in a dry January, if sufficient rains are received, the following month can still be in the positive growth tercile (i.e. 68%).

The predicted impact of SWC on pasture growth over successive months can be estimated using a weighted average approach from the data provided in Tables 2-4 and the tercile growth rates in Figures 37. For example, at Pigeon Ponds in October, if the SWC is dry (20mm) then there is a 38,27,35% chance of low medium and high terciles compared to 24,24,51% if the SWC is wet (60mm). This leads to a weighted average predicted growth rate of 52kg DM/ha.day if the SWC is dry, compared to a 56kg DM/ha if the SWC is wet. Over a 4-month period (Oct to Jan) this would translate to an average 3,596kg DM/ha for a wet SWC and 2,750kg DM/ha for a dry SWC. Similarly for Baynton in April, if the SWC is dry (40 mm) then this could lead to 21kg DM/ha, compared to a 33kg DM/ha if the SWC is wet. Over a 4-month period (April to July) this would translate to an average 2,735kg DM/ha for a wet SWC and 2,272kg DM/ha for a dry SWC. In Dartmoor in December, if the SWC is dry it would lead to 69kg DM/ha.day, compared to a 75kg DM/ha.day if the SWC is wet. Over a 4-month period (Dec to Mar) this would translate to an average 8,512kg DM/ha for a wet SWC and 6,463kg DM/ha for a dry SWC. These predictions in pasture growth production could assist farmers in managing and planning their fodder budgets.

The results are largely expected as the literature highlighted the increase in pasture growth in spring and autumn with limited growth in winter and summer as the pastures are either limited by temperature or SWC (Rawnsley *et al.* (2013), Clark *et al.* (2003), Perera *et al.* (2020)). The ability of the model to predict ahead two - three months and give a tercile prediction dependent on a starting SWC whilst partially could provide valuable information to a farmer who is making decisions such as to change stocking rates (Ash *et al.* 2007). One issue with relying on SWC as a predictor

of pasture growth rates is the limited amount of lead time the results give the farmer to make a decision and then act on that decision for example, by decreasing stock or buying hay.

Other studies have also demonstrated similar findings to the data presented here. Cullen *et al.* (2012) used soil water to predict pasture growth rates and noted that the knowledge of SWC can be valuable when looking at pasture growth rates in autumn and spring, when variability is high. They also noted that SWC in the winter and summer months did not impact on future pasture growth rate. Chapman *et al.* (2009) also highlighted the variability in pasture growth outcomes is driven by the interannual variability in rainfall (and its availability to the plant in soil water) and of the variability of pasture growth within a year (seasonal variation) and between years (interannual variation). Brown *et al.* (2019) acknowledged the year-to-year fluctuations in rainfall and how this affects pasture growth and as a result the difficulties in aligning stock numbers and forage supply. Brown *et al.* (2019) also discusses the issue of knowing potential pasture growth ahead of time could lead to more proactive approach in fodder management. If the farmer knew now that the next three months are looking poor for pasture growth, they can make decisions earlier. Knowing if the next two/three months is tending towards the upper or lower tercile can allow farmers to manage the risks of over or under stocking, of having adequate supplementary feeding available if required. Rawnsley *et al.* (2013) also had similar findings of a strong seasonality and high inter annual variation in feed supply. Ash *et al.* (2007) highlights the need to receive the information in a timely manner, where the farmer has time to act on the data.

In other industries such as annual cropping, modelling approaches utilising historical climate records in combination with seasonal forecast data to predict potential crop yield (Hunt *et al.* 2006) are undertaken. Similarly, Brown *et al.* (2018) looked at the use of integrating dynamic seasonal climate models when forecasting crop yield predictions in the Australian cropping zone and found that seasonal climate forecasts provide more definitive and accurate crop yield predictions than when seasonal climate forecasts were not used. Combining seasonal forecasts into the SGS pasture model instead of relying on historical climate data may improve the pasture predictions further, similar to work undertaken by Harrison *et al.* (2017).

The validation demonstrated that the modelled SWC from the SGS model was very similar to the actual SWC for the three sites. Whilst there are some variations between the two data sets, they tend to follow a similar drying down and wetting up sequence (Figure 36). This validation work is important to ensure the modelled data is an accurate representation of what is happening in the ground. Having confidence in the modelled data increases confidence for the modelling of SWC to predict the pasture growth at the three sites (Baynton, Dartmoor, Pigeon Ponds) in Victoria.

3.5 Conclusion

The spring and autumn period is typically when SWC can limit pasture growth. This research demonstrates that SWC can be used to improve the prediction of pasture growth rates at these times. The predicted pasture output tables were able to

display tercile probabilities for the month of prediction and the following three months given a dry, medium, or wet SWC at the start of the month. One issue with relying on SWC as a predictor of pasture growth rates is the limited amount of lead time the results give the farmer to make a decision and then act on that decision by decreasing stock, buying hay or the like. Some locations appear to have an extremely short lead time (Pigeon Ponds) whilst other sites with longer growing season (Dartmoor), give the farmer a lot more time to react to the forecast.

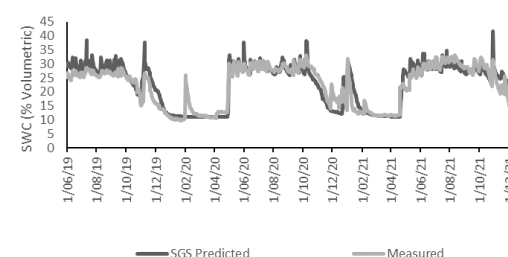
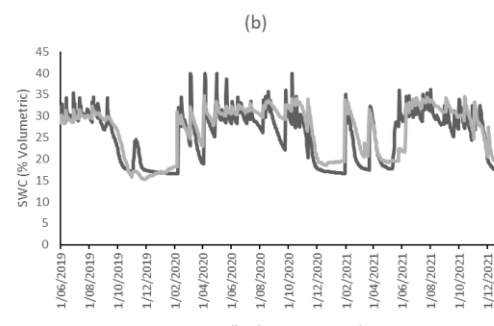
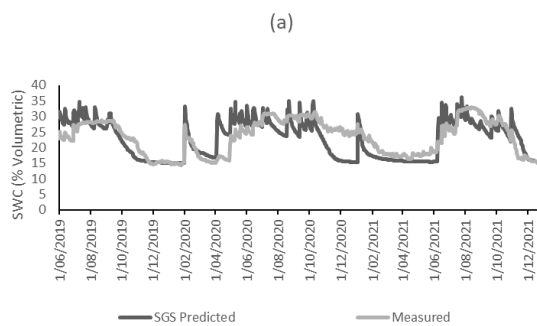
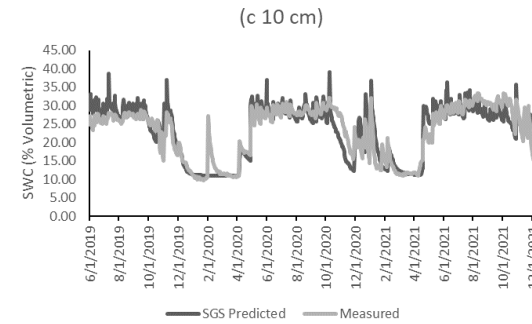
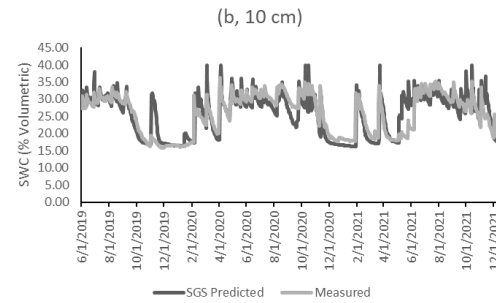
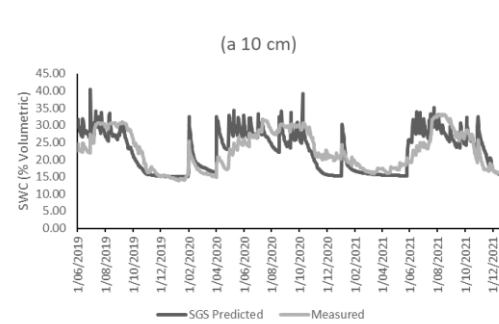
Conflicts of Interest

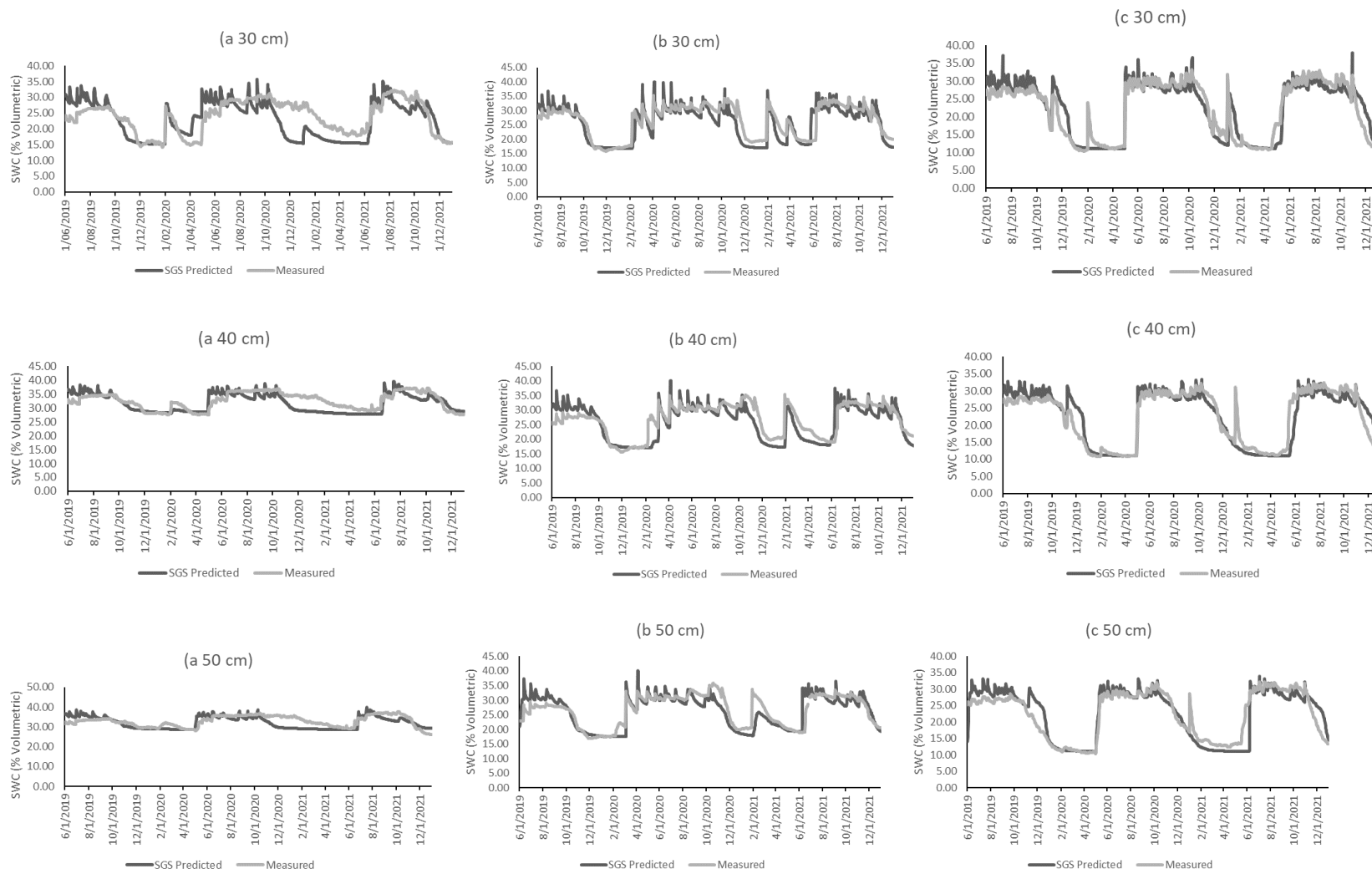
No conflicts of interest

3.6 Supplementary Material

Validation of predicted Soil Water Content (SWC).

The time series of measured relative SWC and predicted SWC from the SGS pasture model at 10, 20, 30, 40 and 50 cm soil depth is presented below for (a) Pigeon Ponds, (b) Baynton, (c) Dartmoor.





SOIL WATER CONTENT VALIDATION, MODELLED V'S MEASURED SOIL WATER CONTENT (A) PIGEON PONDS, (B) BAYNTON, (C) DARTMOOR.

4 A Crop Water Stress Index for a phalaris (*Phalaris aquatica L*) and subterranean clover (*Trifolium subterraneum L*) pasture in southeastern Australia.

4.1 Introduction

Field-grown pasture is the main and cheapest form of feedstock for cattle and sheep in southern Australia (Perera *et al.* 2020; Chapman *et al.* 2009) and many other regions around the world. Climate, particularly rainfall variability, is one of the significant sources of intra- and inter-annual variation in pasture growth (Chapman *et al.* 2009). In the temperate and Mediterranean climates of southern Australia, pasture growth is primarily limited by water availability from mid-late spring to the time of the opening rains in autumn, while appropriate spring and autumn temperatures, nutrients, disease and other management practices (overgrazing) can also affect pasture growth. As soil moisture reduces, plant transpiration declines and the leaf's temperature increases along with a reduction in photosynthesis (Idso *et al.* 1981). Water deficits occur in plants when evaporative demand exceeds the water supply in the soil (Slatyer, 1967). Where there is inadequate water for the plant, the water stress causes partial or complete stomatal closure and reduction in transpiration rates, and the reduced evaporative cooling raises the canopy temperature in relation to the ambient temperature (Jones, 1998).

Canopy temperature is generally accepted as an indirect, rapid, accurate and large-scale indicator of crop water stress (Gonzalez-Dugo. *et al.* 2022). Canopy temperature is considered a reliable proxy for plant water stress monitoring and irrigation scheduling (Tanner, 1963; Idso *et al.* 1984; Steele *et al.* 1994). Different plants and species respond differently to water stress as they can have different transpiration rates (Gonzalez-Dugo, V *et al.* 2022) and, as a result, have a different crop water stress index (CWSI). For example, different turfgrass species (Turfgrass Tifway Bermuda (*Cynodon dactylon* x *C. transvaalensis*), Meyer zoysia (*Zoysia japonica*), Common Centipede (*Eremochloa ophiuroides*), Common Bermuda (*Cynodon dactylon*), all have different CWSI as result of how they react to plant water stress (Gonzalez-Dugo *et al.* 2022). Different transpiration rates can also occur at different stages in a plant's growth stages, which Idso (1982) found in his work on barley (*Hordeum vulgare*) and wheat (*Triticum*). The use of a thermal infrared thermometer to assess water stress was initially proposed by Jackson *et al.* (1977). In the absence of biotic stress such as from fungi, bacteria, or viruses, the restrictions in canopy growth under sub-optimal water levels is generally related to stomatal closure (Jones, 1998) and chlorosis (Shimshi, 1967), resulting in both water and nutrient stress due to limited uptake from the roots (Zarco-Tejada, 2021).

Changes in plant canopy temperatures due to water availability have been studied extensively in other crops such as alfalfa (*Medicago sativa*), tomatoes (*Lycopersicum esculentum*), sunflowers (*Helianthus annus*), turnips (*Brassica rapa*), potatoes

(*Solanum tuberosum*), lettuce (*Lactuca scariola*), beet (*Beta vulgaris*), cotton (*Gossypium hirsutum*), cowpeas (*Vigna catjang Walp*)), soybeans (*Glycine max*), peas (*Pisum sativum*), etc. (Idso, 1982). However, none has been undertaken on pastures. Non-water stressed baselines (NWSB) can be developed by conducting experiments to measure canopy temperatures, air temperature and Vapour Pressure Deficit (VPD) of a well-watered plant transpiring at its potential rate over time (Idso, 1982). In developing the baselines, clear sky conditions (Idso, 1982) are required, as well as consideration of the plant's growth stage (i.e., for grain crops pre-heading or post-heading, Idso 1982). The NWSB for different plants and species generate different slopes, which have an effect on the CWSI calculations (Gonzalez-Dugo, V *et al.* 2022). Many NWSBs have been developed and reported by Idso (1982) and Maes *et al.* (2012).

The $T_c - T_a$ values for the upper stressed baseline can be manually calculated similar to the stressed baselines calculated by Irmak *et al.* (2000), where they averaged their upper baseline values for T_c-T_a and drew the stressed baselines parallel to the VPD for this point.

The CWSI has been predominantly used to monitor the CWSI spatially across homogeneous crops/orchards globally (Gonzalez-Dugo *et al.* 2022) and across different orchard tree species; however, these different orchard tree species are typically located where a particular species is planted together, with different species planted in different sections. Some work has been undertaken on attempting to use the CWSI in non-homogeneous areas such as a wetland as has been attempted by Ciezkowski *et al.* (2020), and Liu *et al.* (2020) undertook work measuring CWSI in 'non-managed' ecosystems (Australian bush context).

The baselines can vary depending on which type of plant, the cultivar, the stage of growth, and the prevailing environmental conditions (Gonzalez-Dugo, V *et al.* 2022) and can change from month to month. In developing the baselines, consideration needs to be given to the weather conditions at the time of temperature data gathering, such as solar radiation and wind speed (Gonzalez-Dugo, V *et al.* 2022), as these can affect the thermal temperatures of the canopy being measured.

Most work to date developing baselines has been undertaken on horticultural crops, with limited work to date undertaken on pastures. This study aimed to develop the stressed and non-stressed baselines and the CWSI for pastures in Southeast Australia.

Hypothesis

The pasture canopy temperatures from the treatment plots, along with climate data, can be used to develop stressed and non-stressed baselines that can then be used to develop a CWSI for pasture. Remotely gathered thermal infrared data can be used to develop the CWSI on a broader scale across a paddock(s).

4.2 Material and Methods

4.2.1 Experimental design and plot management

Study Area, Agricultural practices, and pasture growth.

The field experiment was set up on a commercial farm in Murroon, in the Otway's (38°27'S. 143°50'S, 273m alt.) in southwest Victoria and ran from October 2020 to January 2022. Two treatment plots were set up in the paddock: a well-watered (non-stressed) and a rainfall-only (stressed) plot. The pastures were predominantly *Phalaris (Phalaris aquatica L)* with a small amount of Clover (*Trifolium subterraneum L*) and Dandelion (*Taraxacum officinalis*) weeds. A permanent thermal canopy sensor was installed in each plot, along with soil moisture probes and a weather station. The property has been a beef production enterprise for over 20 years.

Yearlings are typically bought at the local Colac market, held for approximately 12 months and then sold back into the local market. The cattle rely on pastures that are solely dependent on rainfall. Animal numbers are managed to align with fodder availability, with a higher stocking rate during the Spring and a reduced stocking rate throughout the Winter. Minimal extra fodder (hay) is brought onto the property, and hay/silage is not cut. Pastures are maintained with routine spraying of woody weeds and annual applications of fertilizer. A loose form of rotational grazing is practised. The farm has a mixture of flat areas and several hills and gullies with small creeks and dams (Figure 38). The soil type is a Sandy Loam (Colac Map sheet). Geological maps indicate the pasture covers a range of Cretaceous age, Eumeralla Formation, which is part of the Otway Group of soils (Geovic). The field trials were undertaken in a relatively flat area of the farm, as shown in Figure 38. To the east, a small creek and rolling hills can be observed from the topographic map below.



FIGURE 38. TOPOGRAPHIC MAP OF THE PROPERTY WITH A BLACK CIRCLE INDICATING THE LOCATION OF STRESSED AND NON-STRESSED FIELD PLOTS. (SOURCE - [HTTPS://MAPSHARE.VIC.GOV.AU/VICPLAN](https://mapshare.vic.gov.au/vicplan))

The active pasture growth periods are typically Autumn and Spring when most pasture is produced. Pasture growth is typically restricted in Winter when it is too cold and in summer when it can be too hot and dry. Usually, late spring and summer are characterized by increasing soil water deficit. As a result, the pastures die off (or become dormant) until Autumn rains occur and the pasture begins to grow again. Season-to-season pasture growth can vary considerably due to variability in climate, particularly rainfall. In the period after the autumn break and through to mid-spring, soil water availability is not usually limiting because regular rainfall events 'top up' the soil moisture profiles. Typically, throughout these periods, the ambient temperatures are not high enough to induce plant water stress.

Experimental Design

A soil moisture probe (depth 80 cm) and a thermal infrared camera (Goanna Ag, 'GoField" package G4FLDC11) were used to measure soil moisture and canopy temperatures continuously, respectively. The soil moisture probe was placed in the centre of each plot, and the thermal infrared camera was located within one metre of the soil moisture probe. The pasture canopy temperature of the stressed and non-stressed plots was continuously measured throughout the field trials. The canopy temperature sensor was positioned 50cm above the ground at an angle of 30 degrees to ensure that the camera captured the thermal temperature of the pasture and not any background soil. The canopy temperature was recorded every 15 minutes. A meteorological weather station, "GoWeather" from Goanna Ag, was located approximately 15 m away to collect metrological data, including temperature, wind speed, rainfall, humidity, barometric pressure and soil temperature. The field plot site was flat and received full sunlight throughout the day.

The stressed plot was not watered and received only rainfall, whilst the non-stressed plot was watered throughout the experiment to provide enough water, so the pasture was not limited by water. Watering was undertaken by hand and involved using watering cans to disperse the water across the non-stressed plot area evenly. The amount of water was recorded after each watering event. The soil moisture probe and thermal infrared cameras were placed within each 6m by 6 m-fenced field plot to prohibit grazing by livestock and wildlife (Kangaroos). The plots were within 6 metres of each other. As part of the study, spatial variation in canopy temperature was also assessed with a FLIR thermal infrared camera mounted on an aeroplane.

4.2.2 Meteorological Conditions throughout the experiment

The climate is classified as warm and temperate. The area (Barwon Downs) receives, on average, 824mm of precipitation per year (1980-2022). Barwon Downs is the closest weather station (approximately 6 km from the field trial's location) from the site with long-term weather data; this data was sourced from the 'Long Paddock' website (<https://www.longpaddock.com.au>) and used for the following graphs. From the annual total rainfall (Figure 39), we can see the last two years

(2021 and 2022) exceeded 900mm of rain, which has been reached only one other time (2010) since 2001.

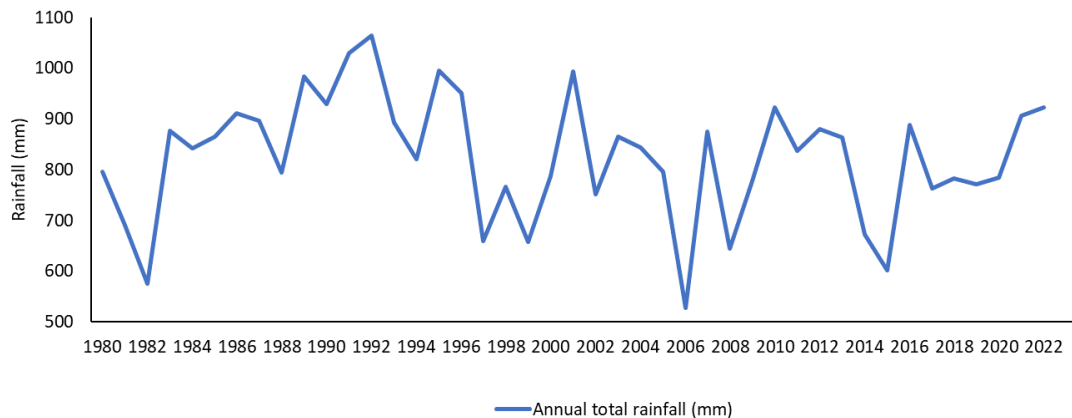


FIGURE 39. ANNUAL TOTAL RAINFALL (MM) FROM 1980 TO 2022.

Figure 40 plots the long-term monthly rainfall (1980-2022) together with the monthly rainfall for 2021 and 2022. 2021 and 2022 had higher-than-average rainfall in October, November and January.

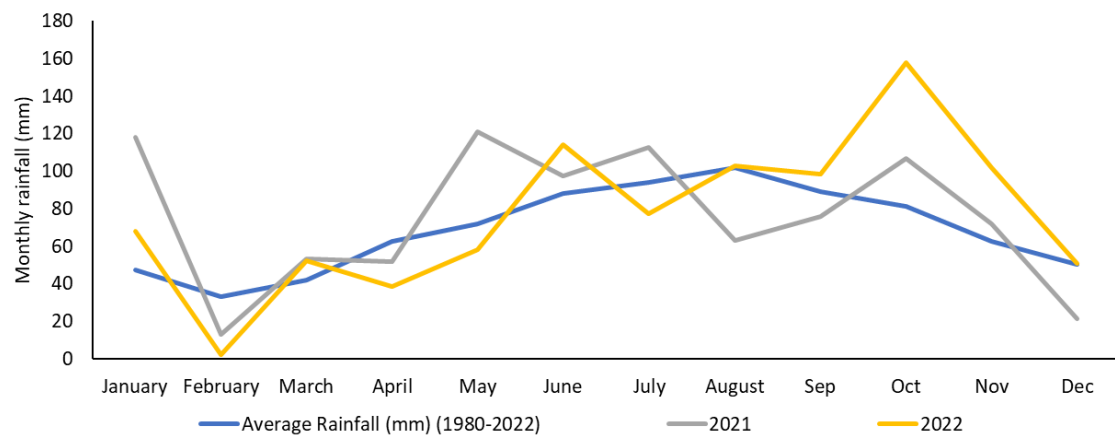


FIGURE 40. MONTHLY RAINFALL (MM) AVERAGED BETWEEN 1980 AND 2022, AND 2021 AND 2022 AS A COMPARISON.

From the maximum monthly temperatures (1980-2022), Figure 41 shows that the monthly average temperatures in 2021 and 2022 were lower than the long-term average, particularly from September through March. These cooler temperatures mean the high temperatures were not experienced for a month or two later than usual, and the historical maximum temperatures were not experienced at all through 2021 and 2022.

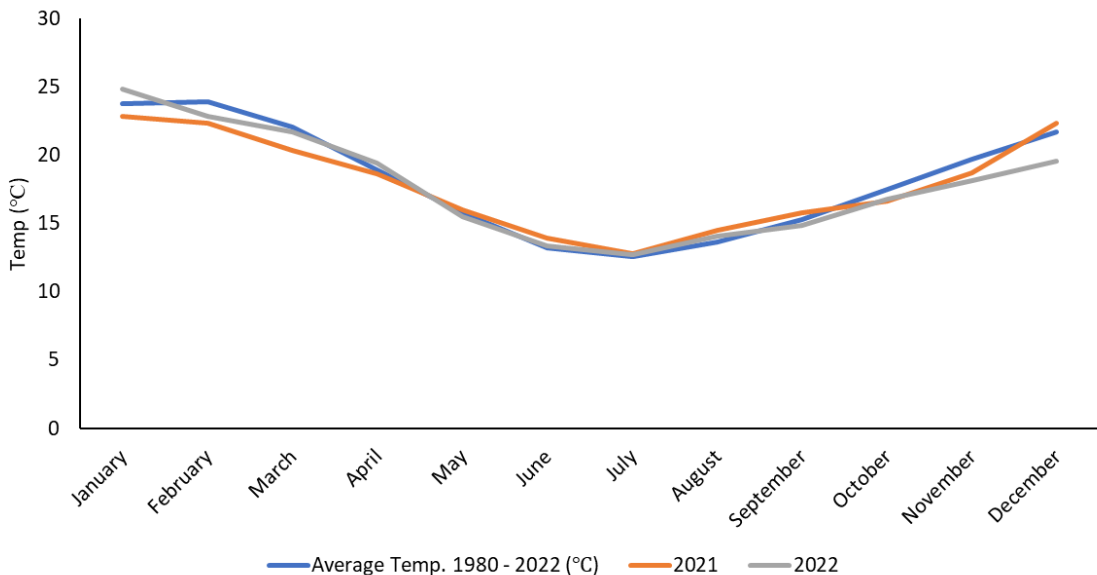


FIGURE 41. MAXIMUM MONTHLY TEMPERATURES (°C) AVERAGED BETWEEN 1980 AND 2022, INCLUDING 2021 AND 2022 AS A COMPARISON.

4.2.3 Air Temperature during the Monitoring Period

The air temperature was recorded during the experiment with the 12.00 am-1.00 pm average temperature presented in Figure 42, with dates of the flights also shown (red arrows). Seasonal variation in air temperature can be observed from the temperatures in Figure 41 and Figure 42.

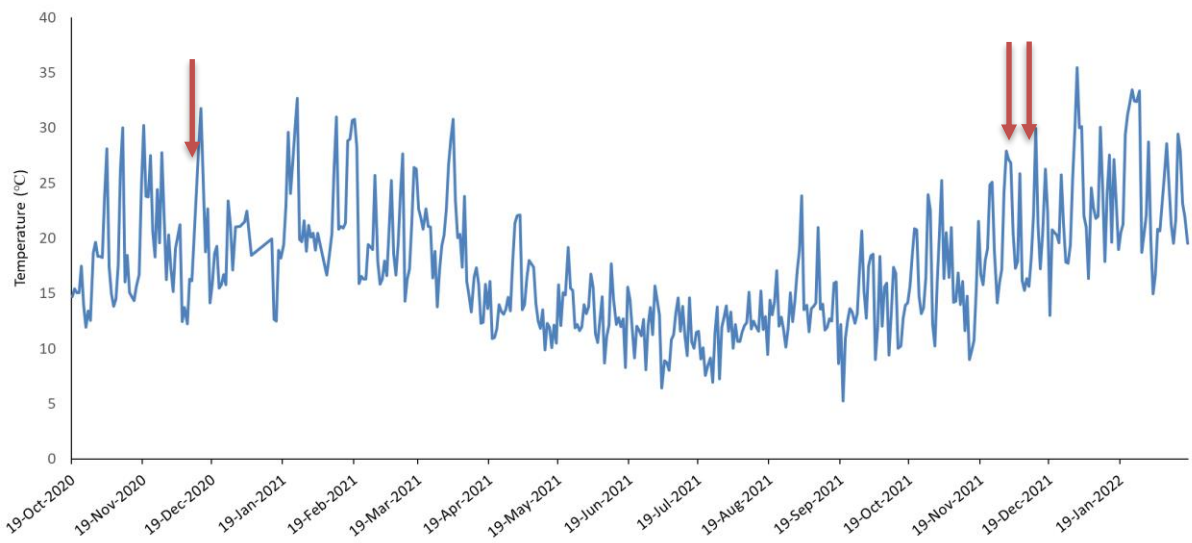


FIGURE 42. AIR TEMPERATURES (°C, 12.00 NOON – 1.00 PM) THROUGHOUT PERIOD OF THE FIELD EXPERIMENTS WITH FLIGHT DATES (RED ARROWS).

Figure 43 shows the rainfall experienced on-site throughout the field study period. This rainfall fell on both plots (stressed and non-stressed), as a rainout shelter was

not used for the stressed plot. Figure 43 also includes the dates and quantities of waterings for the non-stressed field plot throughout the experiment. During the Winter, watering ceased as the plants received enough water from rainfall, with watering commencing again in Spring. Waterings were undertaken using a watering can, evenly spreading the water around the non-stressed plot to ensure all pasture in the plots was evenly watered. The specific watering amounts are shown in Figure 43 and range from 2.5mm to 11mm.

The soil moisture levels for the stressed and non-stressed plots fluctuated as expected throughout the field trials. From Figure 43, it can be seen how the watering affects the soil moisture of the non-stressed field plot. Figure 43 shows how the soil moisture profile increases during the winter months and starts to be drawn down during spring and summer as pasture growth increases and rainfall declines.

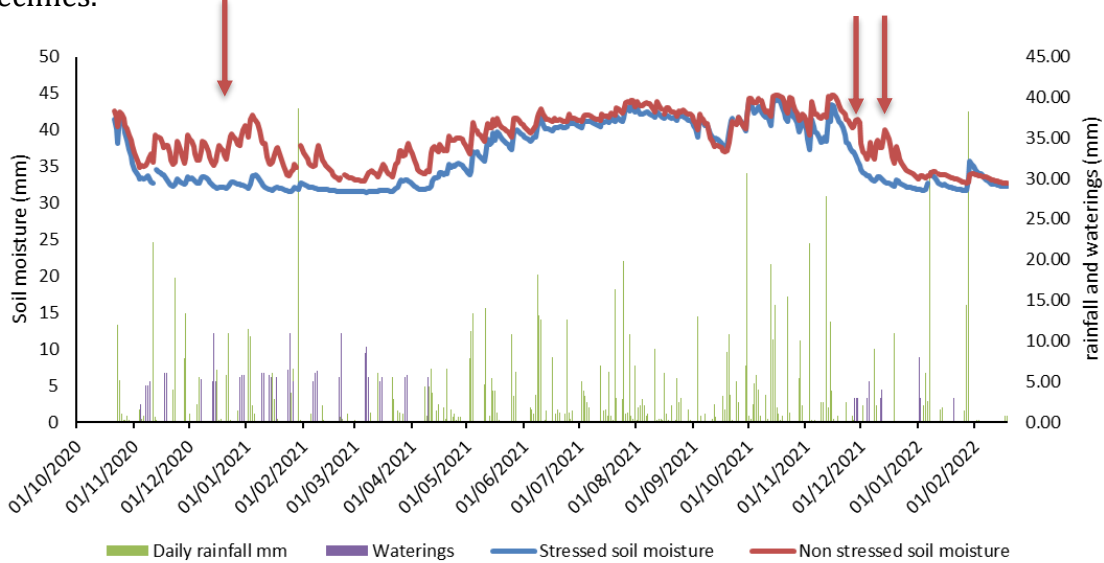


FIGURE 43. SOIL MOISTURE, RAINFALL AND WATERING THROUGHOUT THE FIELD EXPERIMENTS. RED ARROWS INDICATE THE TIME OF THE FLIGHTS.

The Vapor Pressure Deficit (VPD) ranged from 0-4.25 kPa throughout the study period, typically being lower during Winter and rising in late Spring to Summer period. VPD was calculated using the method of the FAO Irrigation and Drainage Paper, No.56, Crop Evapotranspiration (Allen *et al.* 1998). The calculated VPD was compared to a sensor (HT.w Sensor, SensorPush) placed in the field, with the two methods showing similar results (Figure 44).

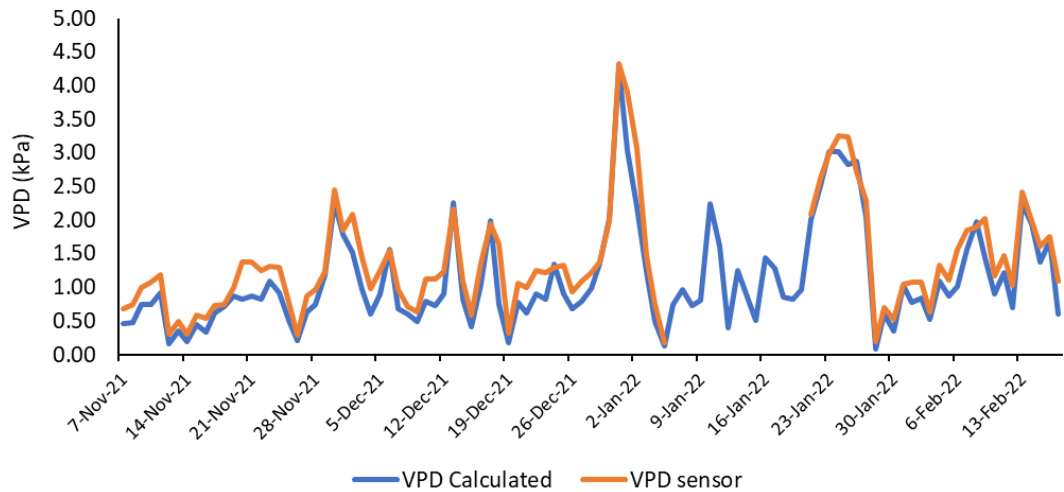


FIGURE 44. VPD COMPARISON BETWEEN CALCULATED AND COLLECTED FROM THE SENSOR (HT.w SENSOR, SENSORPUSH).

Figure 45 shows the setup of one of the field plots and an aerial view of the field trial plots. Fencing was used to prevent stock and kangaroos from grazing the area and to protect the monitoring equipment.

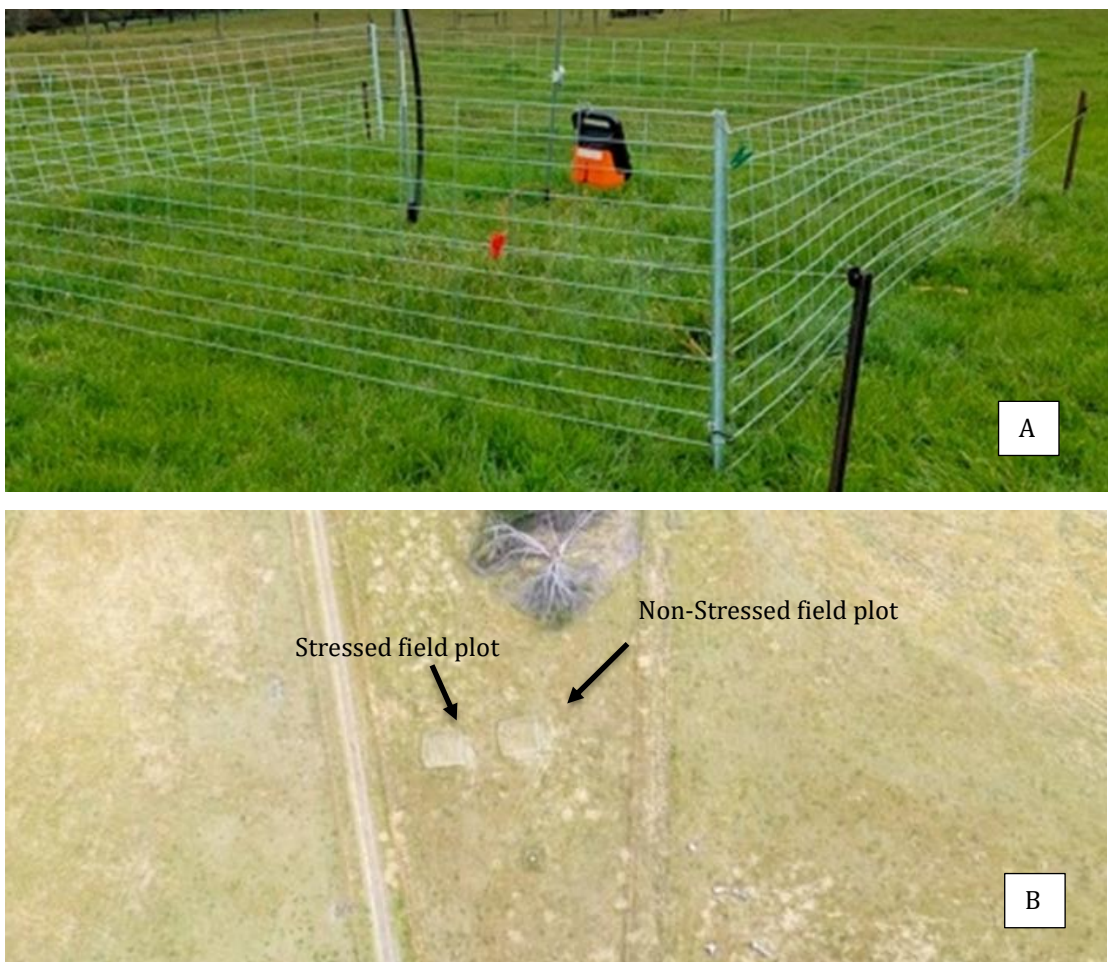


FIGURE 45. (A) FIELD PLOT SET UP, SHOWING SOIL MOISTURE PROBE AND THERMAL CAMERA, FENCED OFF TO RESTRICT STOCK AND WILDLIFE. (B) AERIAL VIEW OF TWO FIELD PLOTS WITHIN THE PADDOCK.

Figure 46 shows the species composition of pastures within the field plots (non-stressed and stressed) on 11/9/2021. Three sites were selected within each field plot, and a steel quadrant (30cm by 30cm) was used to define the boundaries for the sample. Pasture within the quadrant was cut, collected, dried (48 hours at 80°C), sorted into species, and weighed. The species composition changed slightly throughout the field experiment due to the seasonal growth patterns of the species mix.

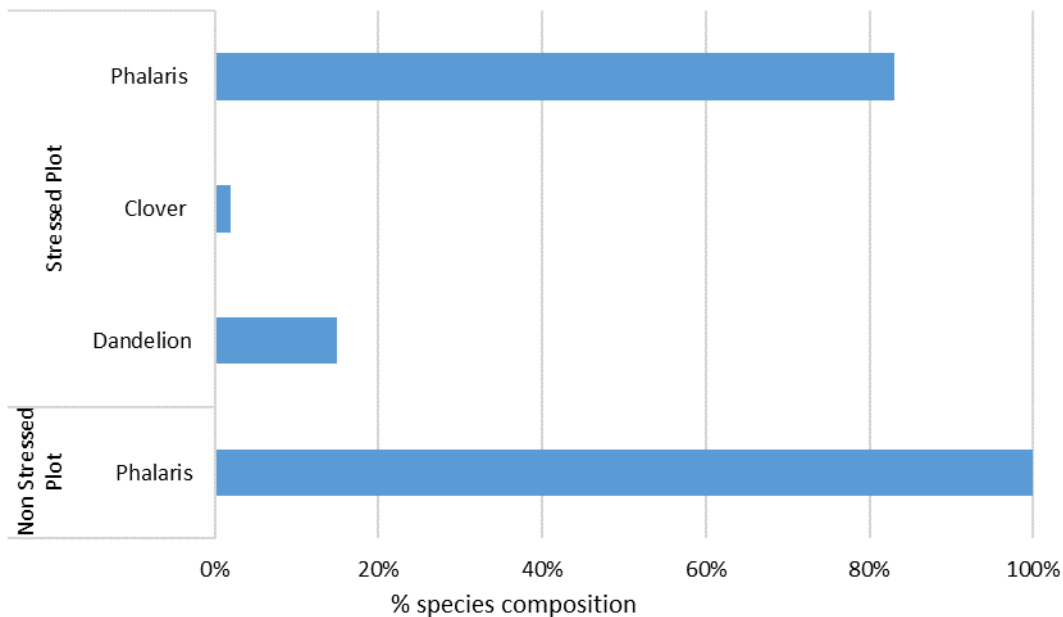


FIGURE 46. PASTURE COMPOSITION (% DM) WITHIN THE PLOTS ON THE 11/9/2021.

4.2.4 Validation of canopy temperature sensors

Diurnal sampling, measuring the canopy temperatures throughout a day, was undertaken, comparing the canopy temperatures between the Goanna ag sensors and the handheld sensor to validate the accuracy of the Goanna ag permanent field sensors in both the stressed and non-stressed plots. Diurnal sampling was undertaken on 12/10/2021, 26/10/2021, 8/11/2021, 13/12/2021, 2/1/2022, and 21/1/2022. The method for recording the canopy temperature for the diurnal sampling was to record five canopy temperatures with a handheld device (Optis MS, non-contact infrared thermometer) from the one field plot to calculate an average. The five samples were all taken within 2 minutes of each other, approximately 30 centimetres apart. The averaged results were then compared against the Goanna ag sensor data for that specific time and date.

4.2.5 Calculation of baselines

The stressed and non-stressed baselines were calculated using the approach of Idso (1981). The stressed and non-stressed baselines were calculated by plotting the $T_c - T_a$ versus the VPD between 12-1 pm from the 19/10/2020 – 17/2/2022 for the separate plots (stressed and non-stressed), removing any periods that were wet or

windy and then calculating the line of best fit. These baseline equations were used to develop a CWSI plot to determine which plants are under plant water stress and which plants are not under plant water stress. The CWSI ranges from '0' to '1', '0' being a well-watered, non-stressed plant and '1' being a fully stressed plant with transpiration halted. The non stressed baseline excluded wet days and where solar radiation was under 1,100 W/m², this data was removed from the spreadsheet prior to baseline calculations.

4.2.6 CWSI Calculations

The CWSI of pastures were calculated using the method of Idso *et al.* (1981). The CWSI formula used was:

$$\text{CWSI} = ((T_c - T_a) - (T_c - T_a)_{LL}) / ((T_c - T_a)_{UL} - (T_c - T_a)_{LL})$$

The $(T_c - T_a)$ represents the canopy temperature less air temperature of a canopy on the sampling day. The $(T_c - T_a)_{LL}$ represents the canopy temperature less air temperature of a canopy transpiring at its maximum rate. The $(T_c - T_a)_{UL}$ represents the canopy temperature less air temperature of a canopy when transpiration is halted due to stomata closure. The temperature to develop the CWSI must be collected during daylight hours and under clear skies.

4.2.7 Airborne thermal imagery acquisition

The airborne thermal flight plan shown in Figure 47 was conducted with a Cessna aircraft flying approximately 500m above the site with a heading on the solar plane. Airborne thermal acquisition was conducted on 14/12/2020, 29/11/2021 and 14/12/2021. The plane took approximately one hour to fly over the property to record the canopy's thermal temperature remotely. The aircraft recorded canopy temperature with a thermal camera (SC655 model, FLIR Systems, Wilsonville, OR, USA) with a resolution of 640 × 480 pixels, 16-bit radiometric resolution, 13.1-mm focal length, and 45 × 33.7 ° FOV (Field of view) yielding a spatial resolution of 0.25 m.

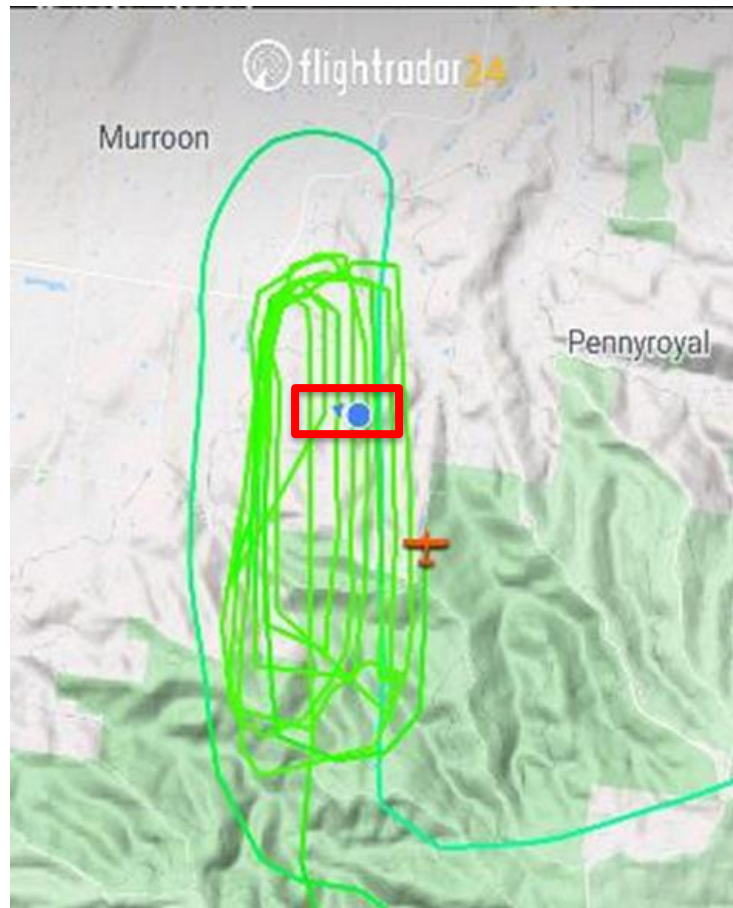


FIGURE 47. FLIGHT PATH TAKEN TO COLLECT AERIAL CANOPY DATA, THE RED BOX INDICATES THE FARM BOUNDARY WHERE FIELD EXPERIMENTS WERE CONDUCTED (14/12/2020). RED BOX INDICATES AREA OF FARM.

4.2.8 Processing of Thermal Images

The thermal images were processed as in Calderon *et al.* (2015) and Hornero *et al.* (2021). The thermal imagery data obtained from the flights recorded the pasture's canopy temperatures, and the ambient air temperature from the on-site weather station combined with the baselines was used to calculate the CWSI for the treatment plots and broader area. Data processing was undertaken using ENVI Classic 4 image processing and analysis software.

4.2.9 Ground Truthing sites Species Composition – broader farm area

Figure 48 shows where the species composition and pasture mass (kg DM/ha) were collected. A 'rising plate meter' was used at each site to measure the pasture mass present (kg DM/ha). At each site, a steel quadrant (30cm by 30cm) was used to define the boundaries for the sample. Pasture within the quadrant was cut, collected, sorted into species, and weighed. These samples were then dried in an oven for 48 hours at 80°C and weighed. The results of the species composition are presented as a percentage in Figure 49. Canopy temperature was also recorded at these sites on flight days (29/11/2020 and 14/12/2021) using a handheld sensor (Figure 48).



FIGURE 48. LOCATIONS WHERE SPECIES COMPOSITION AND PASTURE MASS (KG DM/HA) WERE COLLECTED.

The species composition was not conducted during the first flight (14/12/2020). However, it was undertaken for the subsequent two flights (Figure 49). Phalaris was the dominant species in the paddocks, with clover and dandelions also present in different amounts at different times of the year. The pasture mass also varied across the paddock and farm, from the bare ground (location 3) to areas of short pasture where intermittent partial grazing may have occurred, and to areas of higher pasture mass.

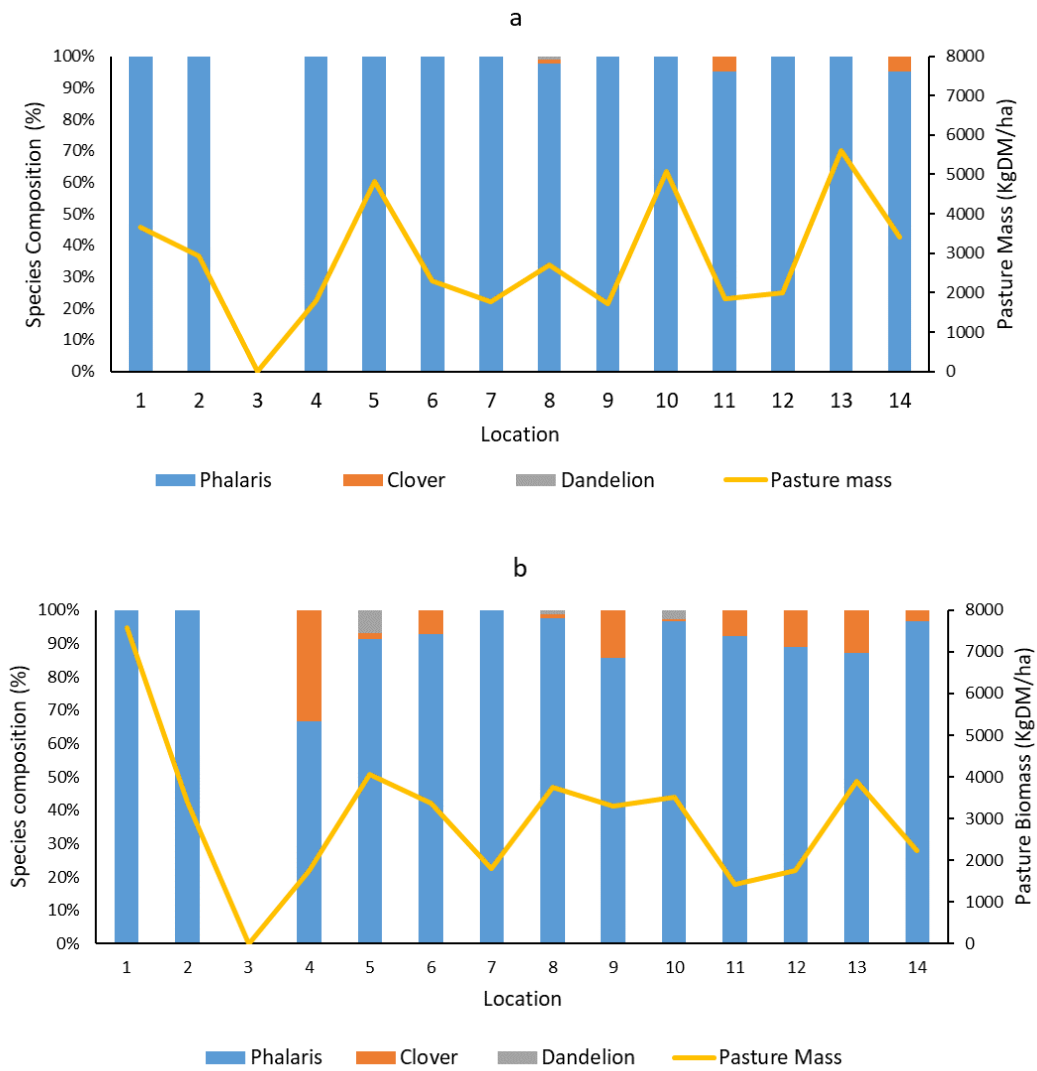


FIGURE 49. SPECIES COMPOSITION AND PASTURE MASS (KG DM/HA). (A) 29/11/2021 (B) 14/12/2021.

4.2.10 Calculating CWSI of the paddocks

Figure 50 is the outline of two paddocks (approx. 9.5 hectares) with Phalaris pasture used for the CWSI calculations that follow. The clump of trees was removed from the CWSI calculations, and the dam and farm tracks have been excluded. The CWSI was calculated from the flight area using the aerially sourced pasture canopy temperatures and the baselines (non-stressed $y = -2.9289x + 7.286$. Stressed = 16)

and then plotted using the software package ENVI Classic 4. Calculation of the average CWSI in the images was undertaken and presented in Figure 50.



FIGURE 50. OUTLINE (IN BLACK) OF THE TWO PADDOCKS USED FOR THE FOLLOWING CWSI CALCULATIONS.

4.3 Results

4.3.1 Diurnal Sampling

The diurnal sampling shows the variation in canopy temperature throughout the day, as shown in Figure 51. A clear distinction can be seen between the stressed and non-stressed pastures' canopy temperatures throughout the day, with the stressed pastures' canopy temperature being higher than the non-stressed pastures' canopy temperature for the sampling period.

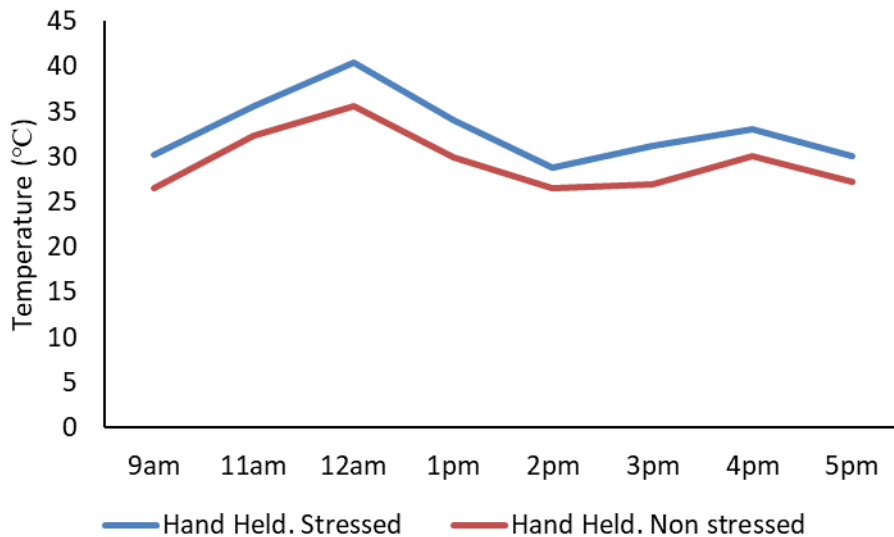


FIGURE 51. DIURNAL SAMPLING CANOPY TEMPERATURE (°C) UNDERTAKEN ON STRESSED AND NON-STRESSED PLOTS ON 1/1/2022.

In Figure 52, the canopy temperatures have been plotted, including the five individual measurements for each time interval and the average temperature for each time interval during the diurnal cycle taken on 21/1/2022. Interestingly, there were higher fluctuations in canopy temperature in the mid to early afternoon, as opposed to the cooler mornings, with a wider variety of canopy temperatures being recorded for the stressed plot. It would be expected to see the stressed canopy temperature results higher than the non-stressed canopy temperatures. However, as shown in Figure 52 there is one interval (at 13.00) where the non-stressed canopy temperature was higher than the stressed canopy temperature. This could be due to several reasons, such as a different ambient temperature from when the stressed sample was taken to when the non-stressed was taken, and environmental factors such as a gust of wind or cloud influencing the canopy temperature.

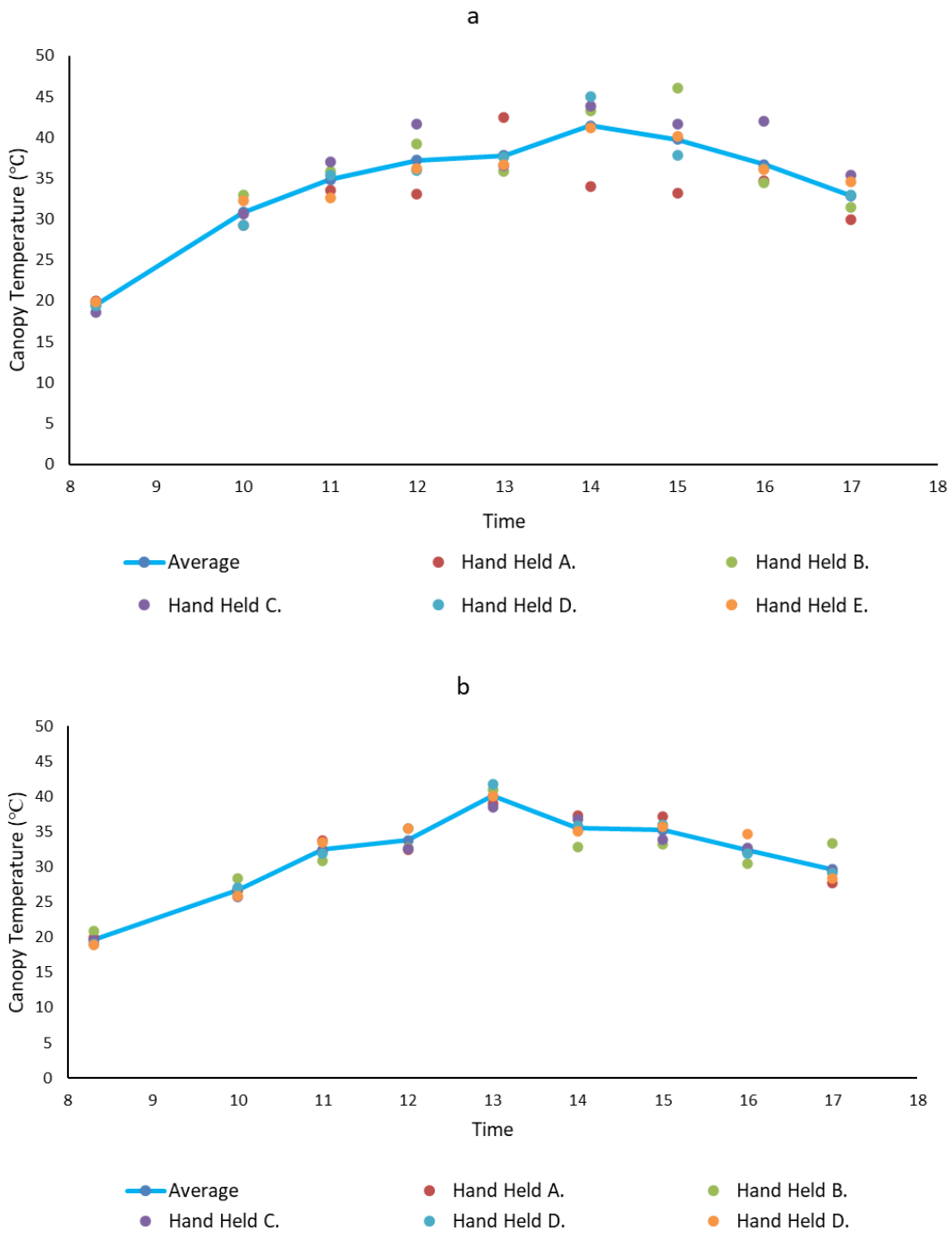


FIGURE 52. CANOPY TEMPERATURE (DEG C) SPREAD RECORDED BY HANDHELD THERMAL SENSOR (A) STRESSED PASTURE (B) NON-STRESSED PASTURE ON 21/1/2022.

There was a strong correlation between canopy temperatures measured with the Goanna Ag sensor and the canopy temperatures measured with the handheld sensor (Figure 53). The data are close to the one-to-one line with R^2 values of 0.85 and 0.86. This data was from the diurnal sampling, comparing all the handheld thermal sensor temperature data against the Goanna Ag canopy sensor data.

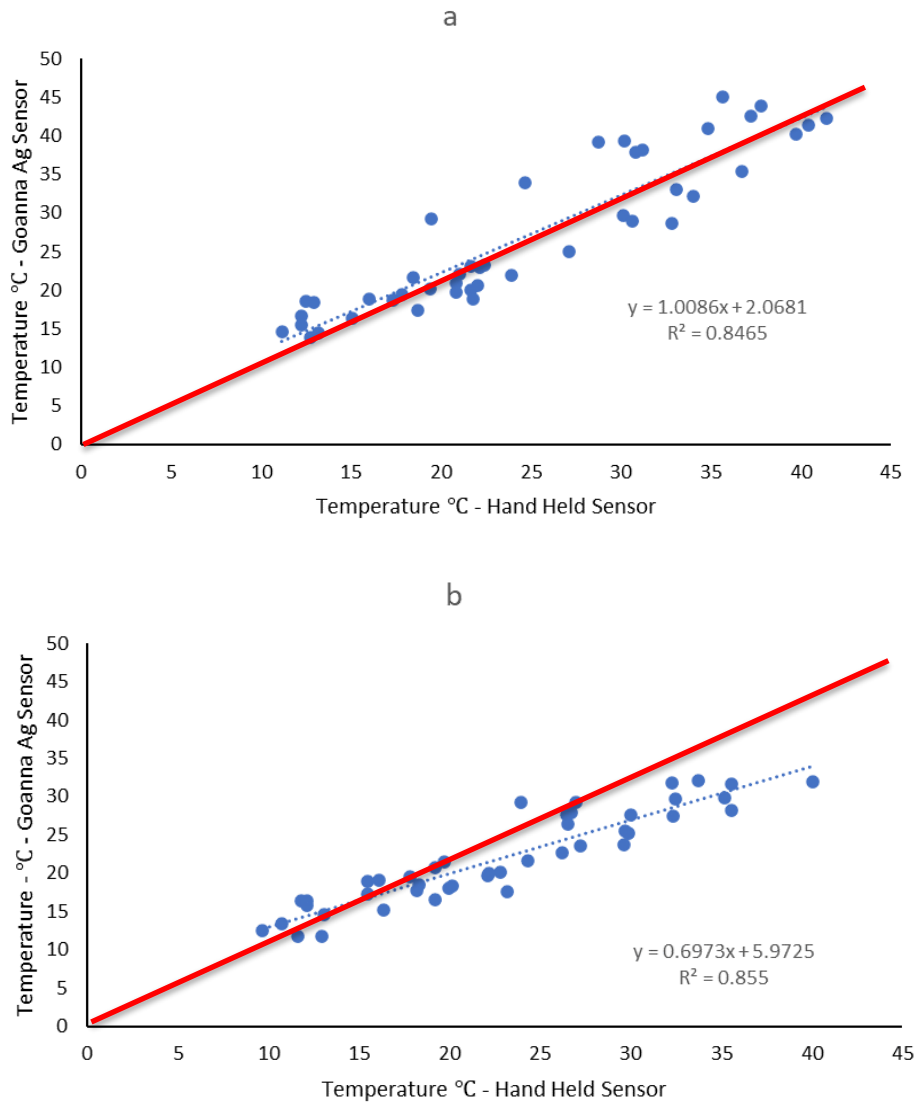


FIGURE 53. VALIDATION OF CANOPY TEMPERATURE COMPARING HANDHELD THERMAL SENSOR TO GOANNA AG FIELD SENSOR (A, STRESSED FIELD PLOT, B, NON-STRESSED FIELD PLOT)

4.3.2 Validation of canopy temperature measurements using ground-truthing sites.

Handheld sensor Vs Airborne image

Figure 54 is a scatter plot comparison of the canopy thermal temperatures measured with the handheld sensor at ground level versus the flight canopy data at numerous (13) sites around the farm. The data does not fit the 1-to-1 line exactly. However, the data shows a strong, positive, linear association between the two measurement techniques and has an R^2 of 0.92 and 0.78 for the flights in November and December 2021, respectively.

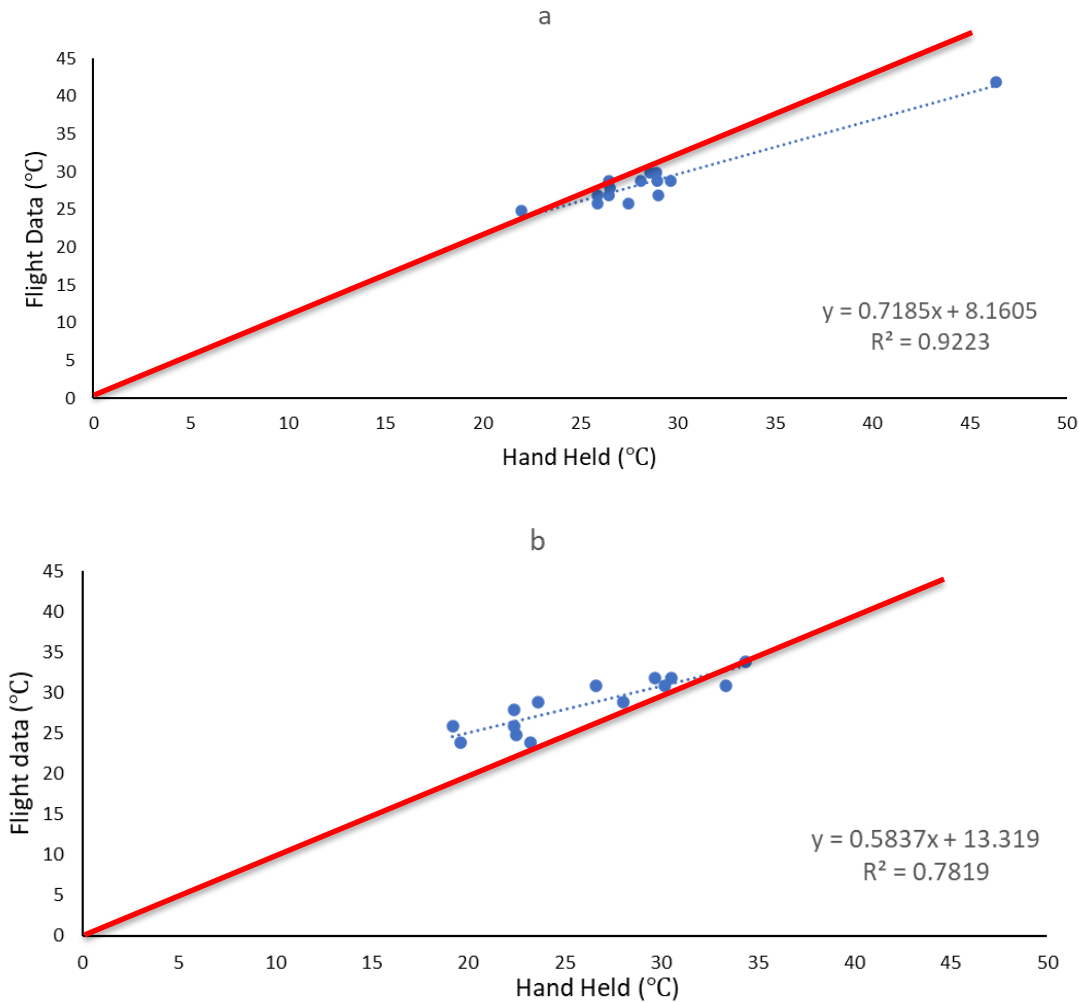


FIGURE 54. COMPARISON OF HANDHELD TEMPERATURES (13 SITES AROUND THE FARM) AND FLIGHT DATA (A) 29/11/2021, (B) 14/12/2021.

4.3.3 Time series of Canopy Temperatures

In Figure 55, (a) and (b) are the canopy temperatures (T_c) and the $T_c - T_a$ for the stressed and non-stressed plots recorded from the ground-based sensors, showing that the stressed plots' temperatures were typically higher than the non-stressed plots' temperatures, primarily through the 'hotter' months. During January/February, the stressed canopy temperatures were up to 14°C hotter than the non-stressed canopy, with all days in January and February having higher temperatures for the stressed compared to the non-stressed canopy. The average temperature difference between the stressed and non-stressed canopies in January- February was 6.13°C , whereas in June- July, the difference was 0.55°C .

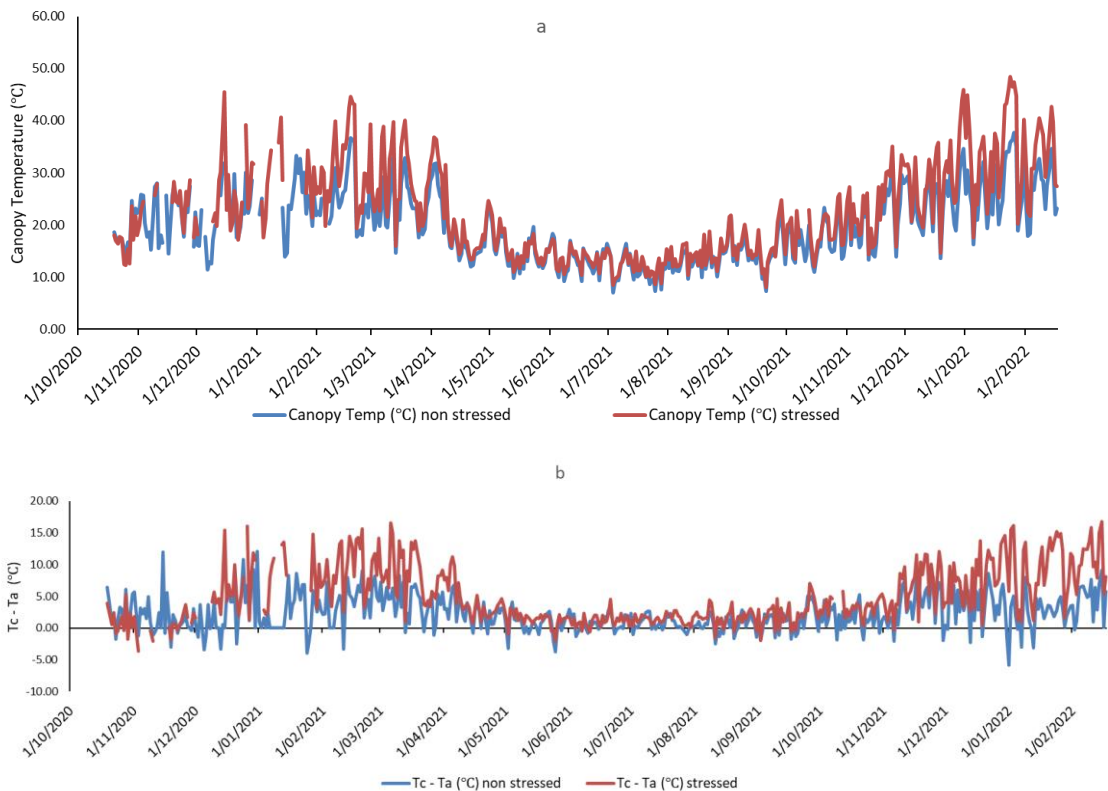


FIGURE 55. (A) DAILY CANOPY TEMPERATURES (Tc) OF THE STRESSED AND NON-STRESSED PASTURE. (B) DAILY Tc – Ta OF STRESSED AND NON-STRESSED PASTURES BETWEEN 1-2 PM.

4.3.4 Baselines

Non-stressed baseline

Figure 56 presents the baselines developed for the non-stressed field plot. A number of baselines were developed using different screening parameters to determine the most appropriate baseline. Wet days (>0 mm) were taken out of the data before developing the baselines, and then different solar radiation (W/m^2) intensities were used to screen the data further. Different 'screening' parameters (i.e., using different solar radiation intensity cutoffs) resulted in slight differences between the non-stressed baselines, but all baselines had similar fitted linear trendlines. Baseline 'c' (figure 56) was chosen as the final baseline because it had the highest R^2 .

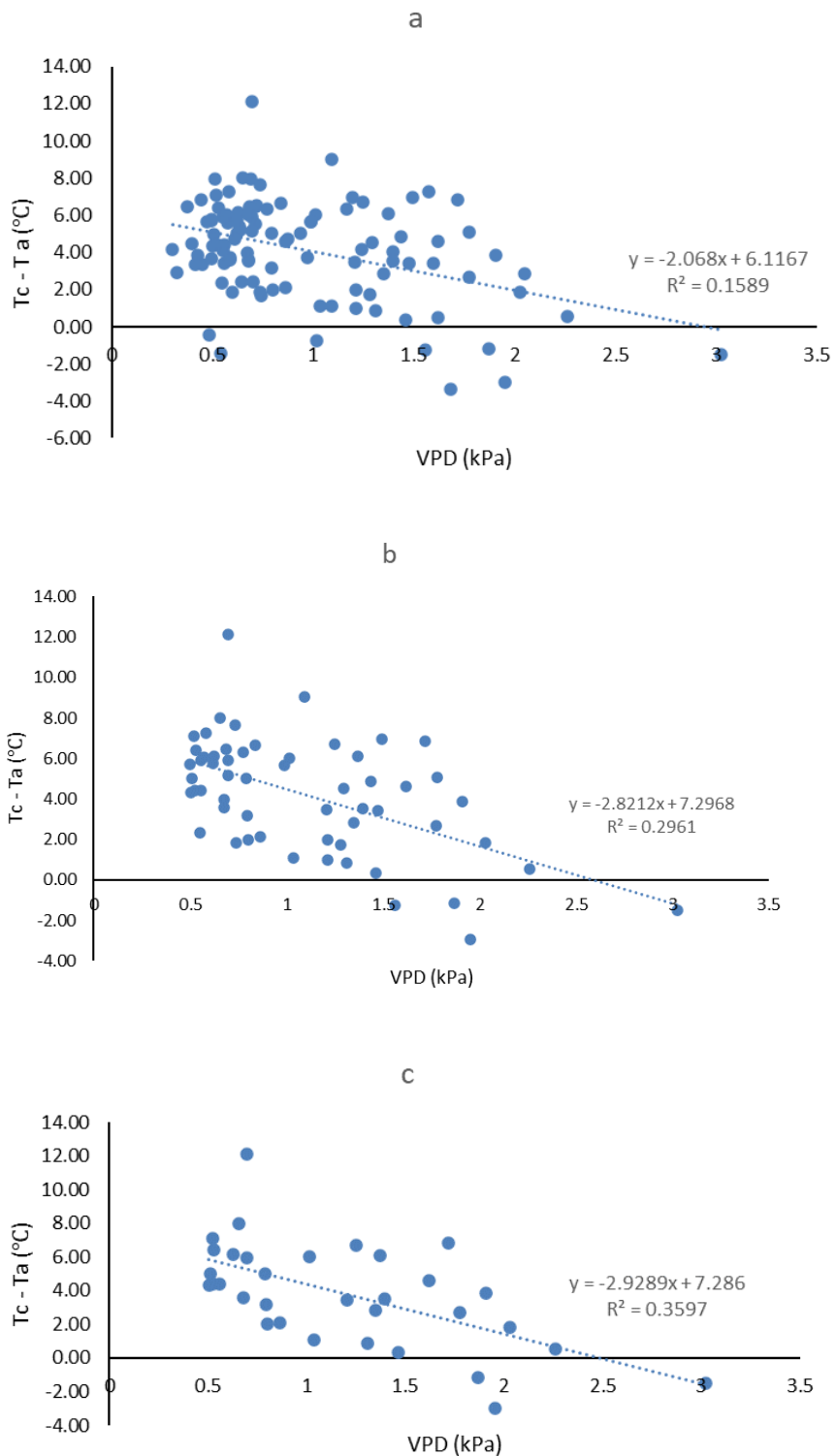


FIGURE 56. NON-STRESSED BASELINE DEVELOPMENT, (A) EXCLUDING WET DAYS AND SOLAR RADIATION UNDER 700 W/M², (B) EXCLUDING WET DAYS AND SOLAR RADIATION UNDER 1,000 W/M², (C) EXCLUDING WET DAYS AND SOLAR RADIATION UNDER 1,100 W/M².

Stressed baseline development

Two of the stressed baselines resulting from different screening for wet days and intensities of solar radiation are shown in Figure 57 (a). The baselines were developed initially using all the recorded data and then screening out unsuitable

days (i.e. wet and cloudy days). The stressed baseline was set at a $T_c - Ta$ of 16°C because this was the highest $T_c - Ta$. This indicated maximum stress in the stressed field plot. The chosen stressed baseline of 16°C is shown in red in Figure 57 (b).

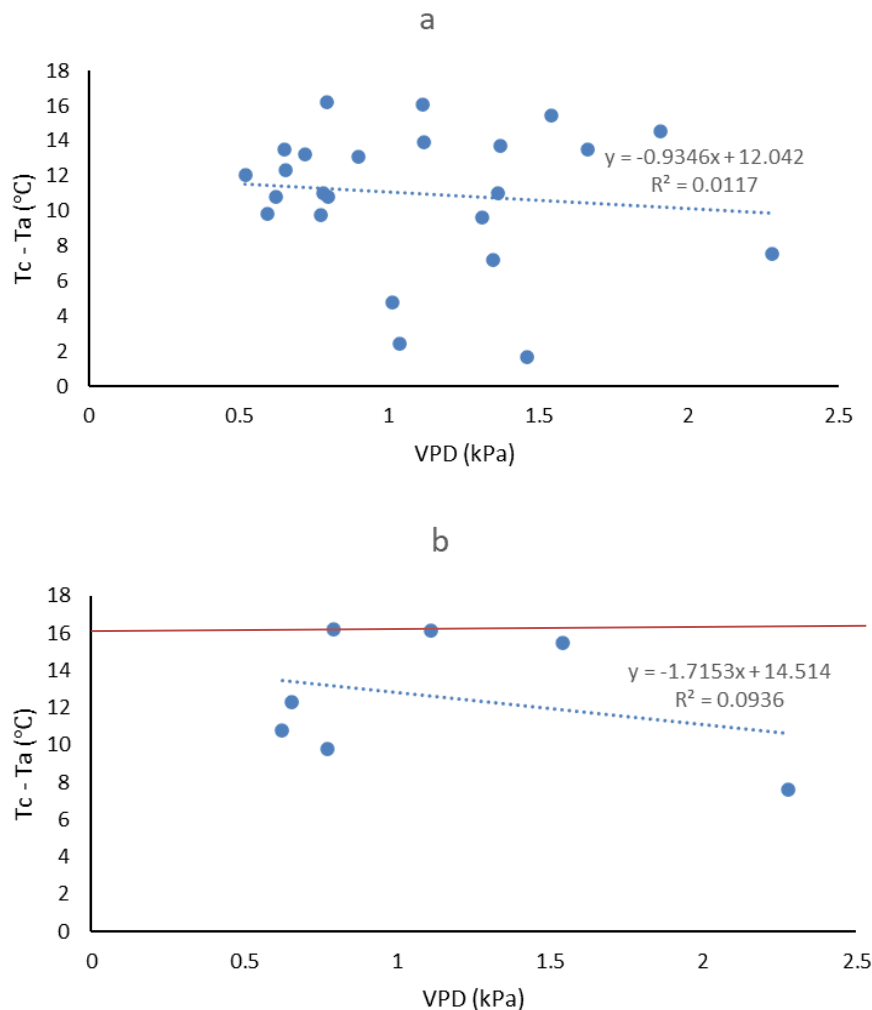


FIGURE 57. STRESSED BASELINE DEVELOPMENT (A) $T_c - Ta$, LESS RAIN AND SOLAR RADIATION UNDER 1200 W/m^2 . (B) $T_c - Ta$, LESS RAIN AND SOLAR RADIATION UNDER 1250 W/m^2 .

The daily CWSI results calculated from the stressed and non-stressed plots are shown in Figure 58. Figure 58 shows the majority of the stressed plants having a high CWSI and many of the non stressed plants having a lower CWSI as expected.

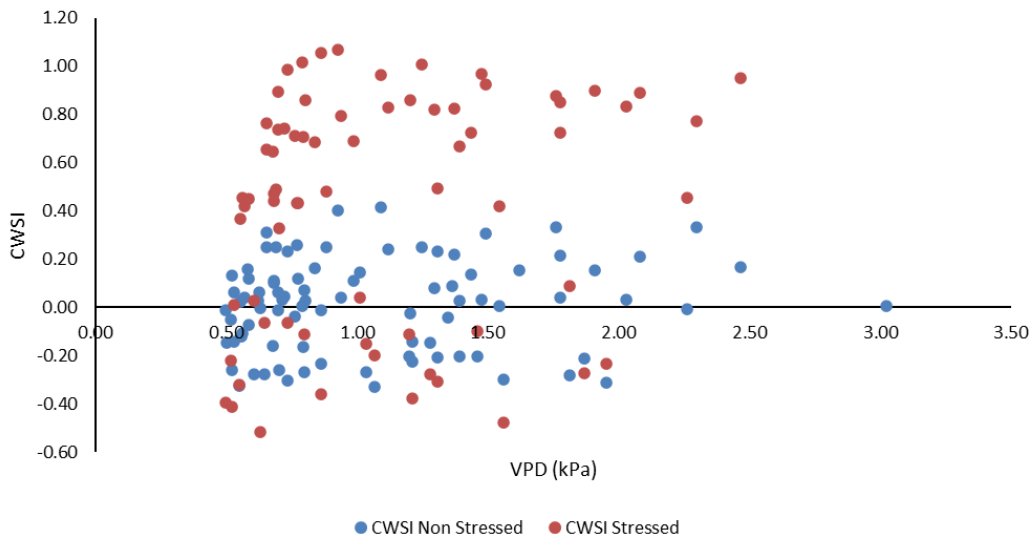


FIGURE 58. CWSI CALCULATED FROM THE GROUND CANOPY SENSORS SCREENING FOR WET DAYS AND SOLAR RADIATION UNDER 900 W/M²

Figure 59 demonstrates further examples of the CWSI results calculated from the field plots data; however, more data has been screened out as the solar radiation up to 1,200 W/m² have also been removed. Seventy-one (71) percent of CWSI results are within the CWSI range (0-1) when using the higher stressed baseline of 16°C and the 1,200 W/m² than the 62 percent when using the higher stressed baseline of '16' and the 900 W/m² as shown in Figure 59.

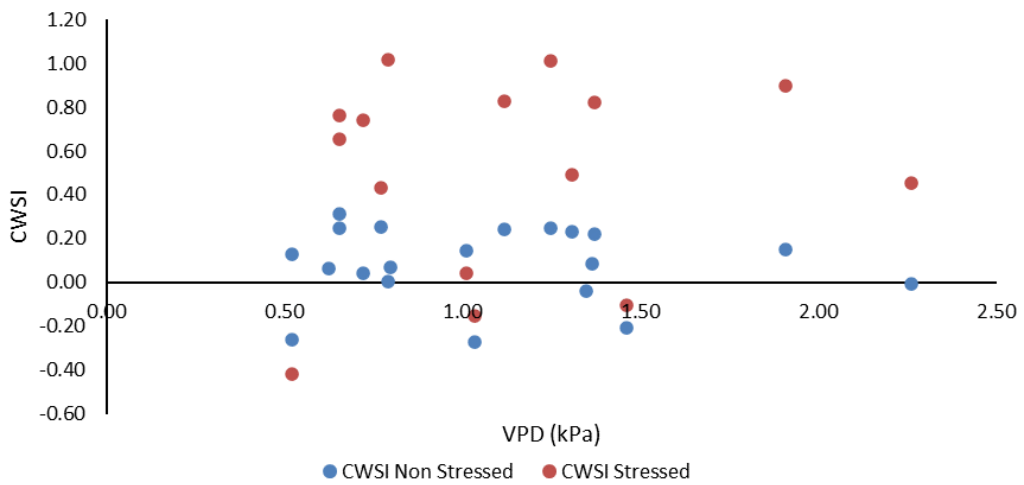


FIGURE 59. CWSI WAS CALCULATED FROM THE GROUND CANOPY SENSORS, EXCLUDING WET WEATHER AND SOLAR RADIATION UNDER 1200 W/M² USING 16 DEG C AS THE STRESSED BASELINE ($Y = -2.9289x + 7.286$).

4.3.5 Canopy temperature of field plots from flights

Figure 60 is a close-up image showing the canopy temperature variation across the field plots on 14/12/2020. The temperature of the stressed plot ranges from 38.85-41.85°C with the majority at 40.85°C, while the non-stressed plot ranges from

35.85-39.85°C with the majority at 38.15°C. With the range of canopy temperatures across the non-stressed plot, there may be some edge effects where watered-pastured areas are close to non-watered pastures.

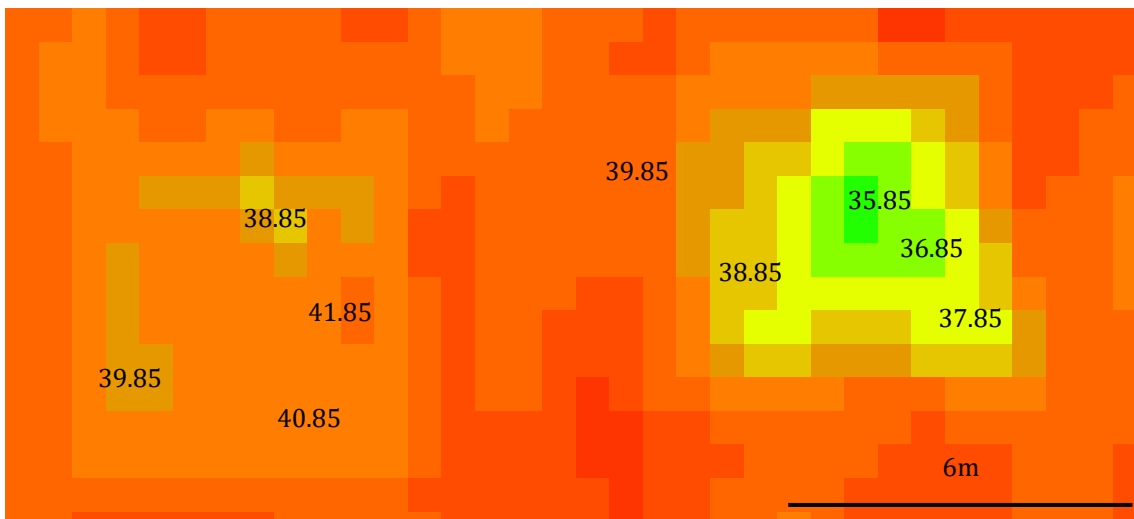


FIGURE 60. CANOPY TEMPERATURE (DEG C) VARIATION ACROSS NON-STRESSED AND STRESSED PLOTS FROM AERIAL FLIGHT (14/12/2020). THE AVERAGE TEMPERATURE OF THE STRESSED PLOT WAS 40.88 °C, AND THE NON-STRESSED PLOT WAS 38.15 °C.

Figure 61 is a broader view of pasture canopy temperatures (°C) recorded during the flight from the FLIR camera, showing canopy temperature variation over a broader scale, over several paddocks.

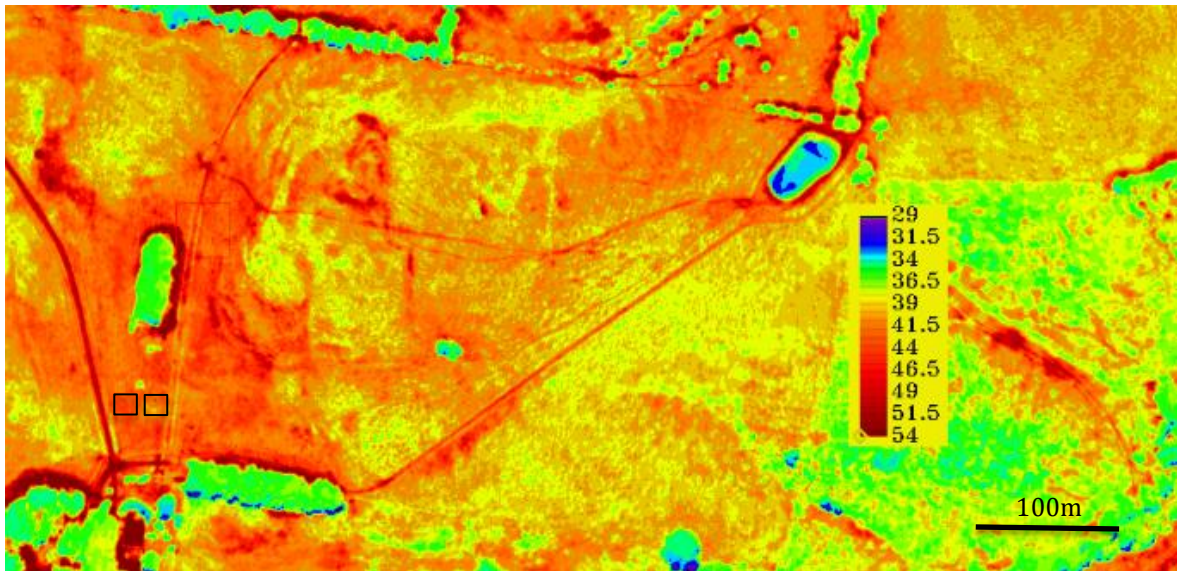


FIGURE 61. A BROADER VIEW OF PASTURE CANOPY TEMPERATURES (DEG C) RECORDED DURING THE FLIGHT (14/12/2020) FROM THE FLIR CAMERA. FIELD TRIAL PLOTS IN SQUARE BOXES (CANOPY TEMPERATURES).

4.3.6 CWSI from flights

In Figure 62. the CWSI has been calculated for the flight area using the aerially sourced pasture canopy temperatures and the baselines (non-stressed $y=-2.9289x+7.286$. Stressed = 16).

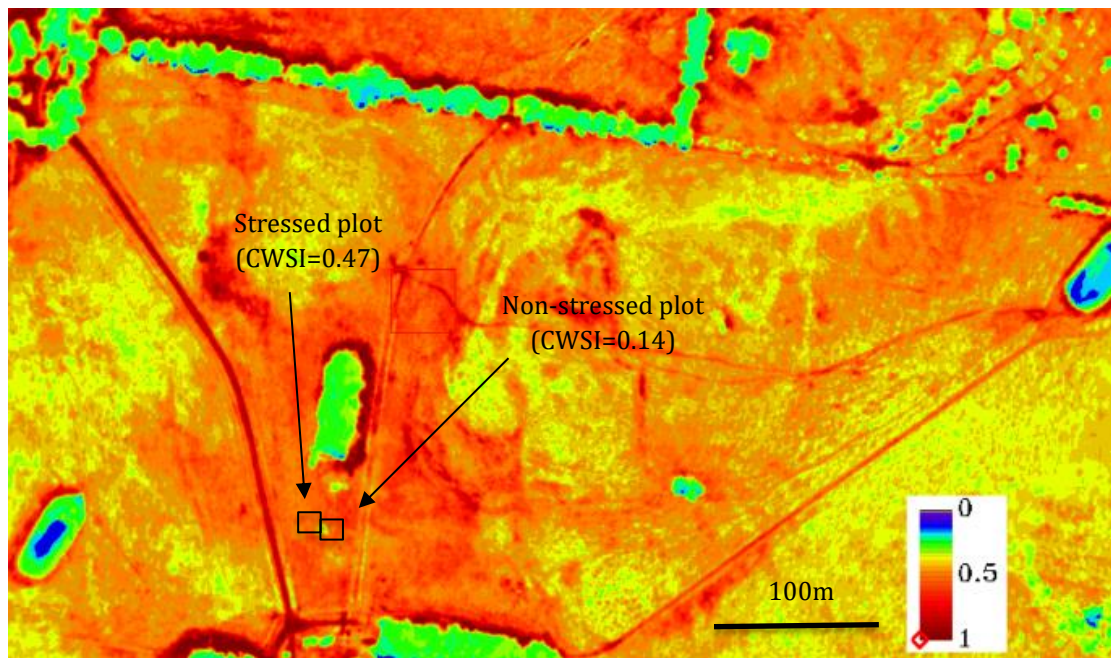


FIGURE 62. CWSI WAS DERIVED FROM FLIGHT 1 (14/12/2020). FIELD TRIAL AREAS IN BLACK SQUARES. NON-STRESSED COMPOUND CWSI = 0.15 STRESSED COMPOUND CWSI=0.48.

4.3.7 Comparison of canopy temperature and CWSI

A comparison of the canopy temperatures over the three flights is shown in Table 4. The second and third flights occurred on cooler days compared to flight 1; hence, the plants may not have been under as much water stress. In Table 5, the CWSI values have been plotted for the field plots, with the non-stressed plots showing a lower CWSI than the stressed plots, which is to be expected.

TABLE 4. TEMPERATURES AND CWSI OF STRESSED AND NON-STRESSED FIELD PLOTS USING FLIGHT CANOPY TEMPERATURES AND BASELINES (NON-STRESSED $y=-2.8212x+7.2968$. STRESSED = 16) DURING THE THREE FLIGHTS.

	Date of Flight	Air Temperature °C	Canopy Temperature Stressed °C	Canopy Temperature Non-Stressed °C	VPD	CWSI Stressed	CWSI Non-Stressed
Flight 1	14/12/2020	32.99	40.85	35.85	2.26	0.48	0.15
Flight 2	29/11/2021	22.36	29.85	26.85	1.24	0.32	0.08
Flight 3	14/12/2021	20.36	26.85	25.85	1.06	0.21	0.12

Figure 63 shows the CWSI calculated from the baselines (non-stressed $y=2.9289x+7.286$. Stressed = 16) for each of the three flights. The figures show the CWSI values for the pasture paddock (outlined in black), including the field plots.

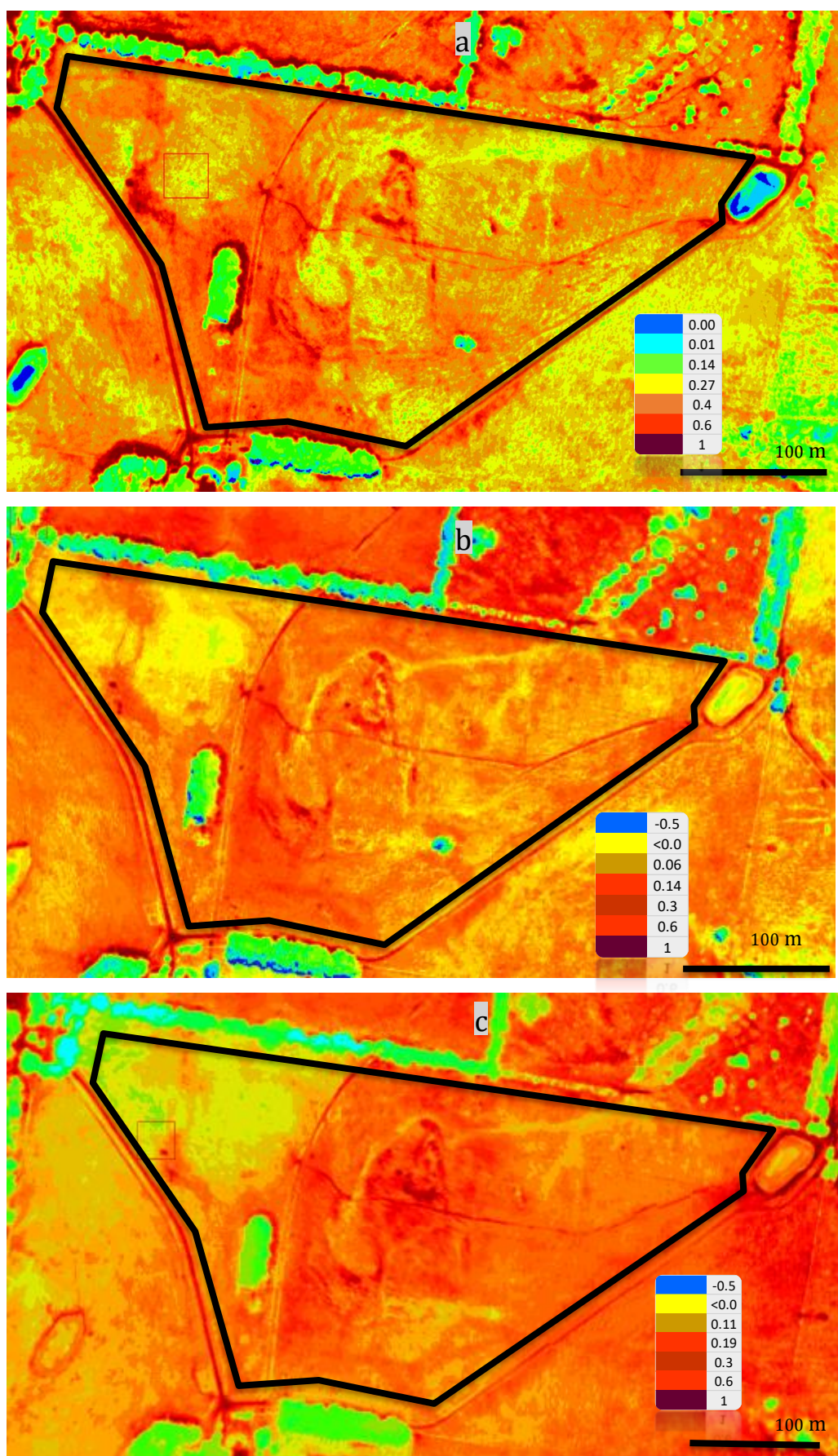


FIGURE 63. CWSI OF FLIGHTS (A) FLIGHT 1. 14/12/2020, (B) FLIGHT 2. 29/11/2021, (C) FLIGHT 3. 14/12/2021. USING THE BASELINES (NON-STRESSED $Y = -2.9289x + 7.286$. STRESSED = 16).

Figure 64 is an analysis of the % per CWSI range across the paddocks for flights 1, 2 and 3 as per the areas in Figure 63.

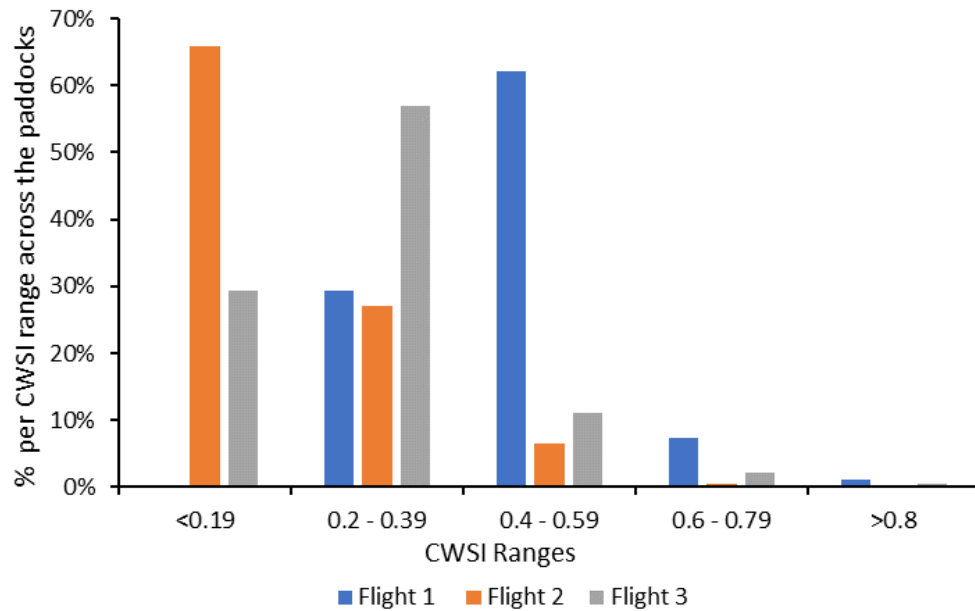


FIGURE 64. ANALYSIS OF THE % PER CWSI RANGE ACROSS THE PADDOCKS FOR FLIGHTS 1, 2 AND 3. THE AVERAGE CWSI RANGE FOR FLIGHT 1 WAS 0.45, FOR FLIGHT 2, IT WAS 0.18 AND FOR FLIGHT 3, IT WAS 0.27.

4.4 Discussion

This study created CWSI baselines for phalaris - sub clover pastures in southeastern Australia, demonstrating that the approach developed largely for individual species could be applied to pastures. The results show that the temperature difference between the stressed and non-stressed pastures could be recorded on the ground and remotely, with canopy temperatures of the stressed plot typically hotter than the non-stressed plot. Viewing the spatial CWSI also provides insight into water stress across paddocks and the larger area (farm).

The non-stressed baseline was developed using all the field data collected during the field studies and screening out wet days and solar radiation intensities. Screening for solar radiation was used to screen out days where clouds may be present. Numerous baselines were developed using different solar radiation cutoffs to ascertain the most accurate baseline. A cutoff of 700 W/m², 1000 W/m², and 1,100 W/m² radons gave a similar non-stressed baseline (see Figure 56). Numerous other variations were applied in an attempt to calculate the non-stressed baseline.

Unfortunately, in the literature, there is minimal work on developing baselines for pastures, so we are unable to compare our results directly with other peer-

reviewed work. The pasture baselines developed from these field experiments were compared against previously designed non-stressed baselines undertaken by Idso *et al.* (1981) and compiled in the supplementary data by Gonzalez-Dugo *et al.* (2022), for other plants and a selection is shown in Figure 65. Figure 65 also shows the non-stressed baselines for a variety of species and stages of growth, such as Barley, Wheat, Turfgrass, and Alfalfa. Figure 65 also shows that the baseline developed for pasture has a slope similar to that of some other species.

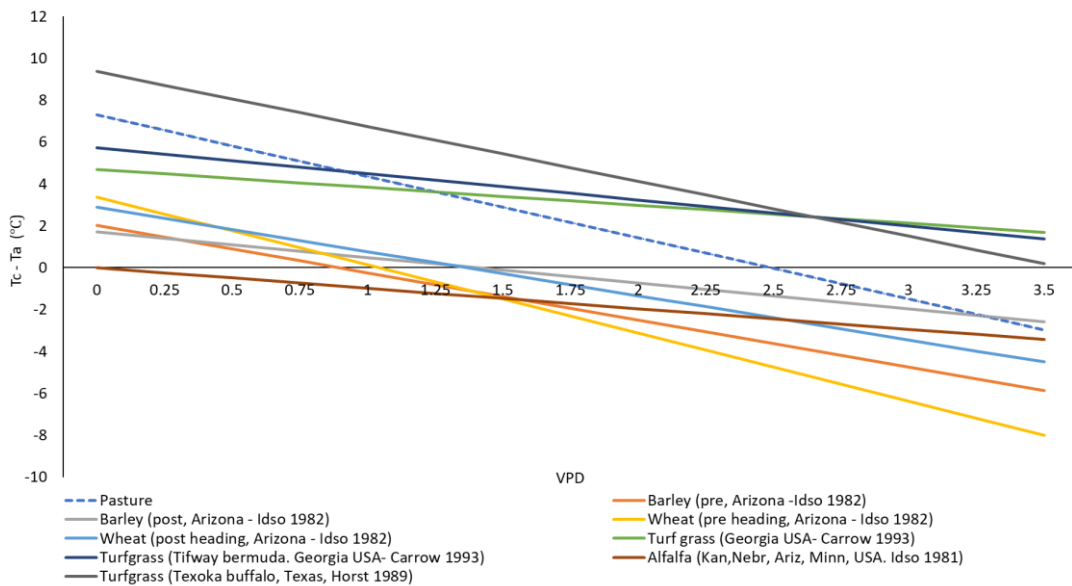


FIGURE 65. PASTURE NON-STRESSED BASELINE COMPARED AGAINST OTHER BASELINES DEVELOPED BY IDSO *ET AL.* (1981).

The stressed baseline was developed using all the data screening for rain and taking out days where solar radiation was under 1250 W/m^2 (figure 57). Numerous other variations were applied in attempting to calculate the stressed baseline. Trials were also undertaken to manipulate the stressed baselines for other values such as $T_c - T_a$ equalling 11°C and 16°C . Figure 57 shows the stressed baseline development, with a $T_c - T_a$ of 16°C chosen as the final stressed baseline. It is difficult to obtain a stressed baseline from plants in the field given that the plants are 'just holding on' before plant death when the plants are under the most stress. The stressed field plots were rainfed (not rain excluded), and therefore, it was not possible to create a highly stressed pasture. It is difficult to accurately record stressed baseline in the field as the measurement attempts to measure the plant under maximum stress, effectively just before the plant senesces.

Three flights were undertaken (14/12/2020, 29/11/2021, 14/12/2021). The higher ambient temperature during flight 1 would most likely have contributed to the increase in CWSI in flight 1 compared to the other two flights. Flight 1 was undertaken on 14/12/2020 with an air temperature of 33 degrees Celsius. Flight 2 (29/11/2021) and flight 3 (14/12/2021) were undertaken on days when the temperature was 22 degrees Celsius and 20 degrees Celsius respectively.

The CWSI was plotted for the field pastures using the generated baselines. Figures 58 and 59 demonstrate a range of CWSI values spread between -0.6 to just under

1.2. Figure 66 is the CWSI viewed over time, excluding wet days and days where solar radiation is below 600 W/m^2 . The results demonstrate a clear increase in CWSI during the hotter periods, where the stressed CWSI exceeds the non-stressed CWSI. There are gaps in the data because during Winter and other periods there were numerous cloudy days, and these have been screened out by taking out all the wet days and days below 600 W/m^2 solar radiation (Idso *et al.* 1981). Due to the cooler winters, the pastures were not under water stress for the whole year but only for periods in summer when the air temperatures increased. Similar to results from Haghverdi *et al.* (2021), Al-Faraj *et al.* (2001) and Jalali-Farahani (1993), it was not possible for all the CWSI results to be within the 0 - 1 range, with some results exceeding the one and below zero. Whilst we developed stressed and non-stressed baselines from the field experiments undertaken, it is essential to remember that baselines are localized and may not be appropriate for use in the next valley, region or other parts of Australia (Jalali-Farahani (1993).

One issue not thoroughly studied in this field experiment is the phenological stage of the plant versus the canopy temperature. Bellvert *et al.* (2015) found that the non-stressed baseline differed with grapevines depending on variety and phenological stage. Similarly, Kar *et al.* (2010) found that regarding winter maize irrigation, the CWSI varied at different plant growth phases. Further work should look at creating baselines at different stages of the pasture's growth to see how this may change throughout a season and from year to year.

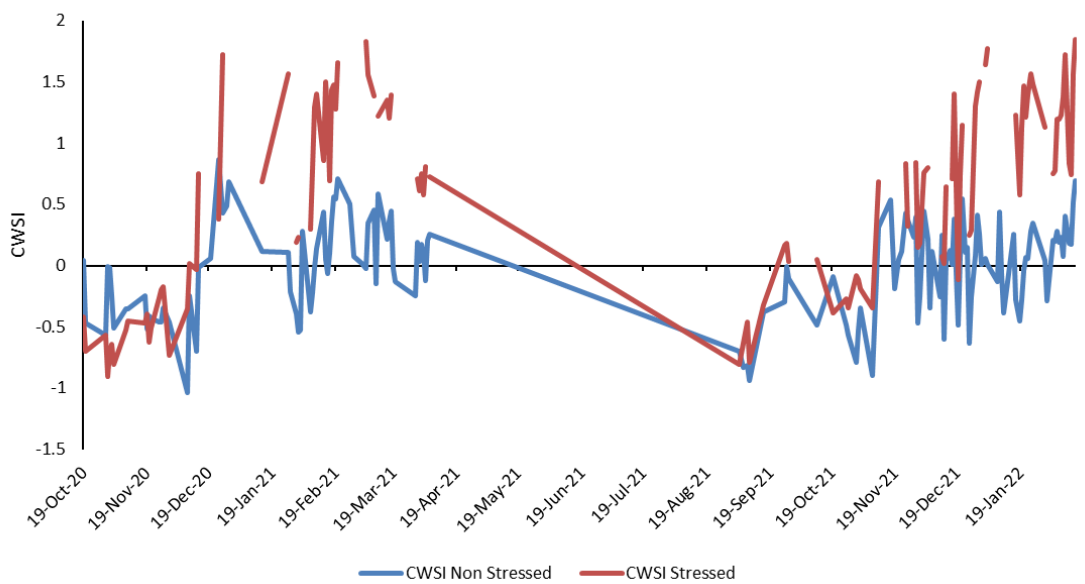


FIGURE 66. CWSI OVER TIME, LESS WET DAYS AND DAYS WHERE SOLAR RADIATION ARE BELOW 600 W/m^2 .

4.4.1 CWSI vs Pasture mass comparison

A comparison was undertaken comparing the CWSI and pasture mass (figure 67) with no correlation being found. The minimum pasture mass was around 1,500 kg

/DM/ha, demonstrating that most of the paddock had adequate pasture cover and that soil temperatures were not affecting the pasture CWSI.

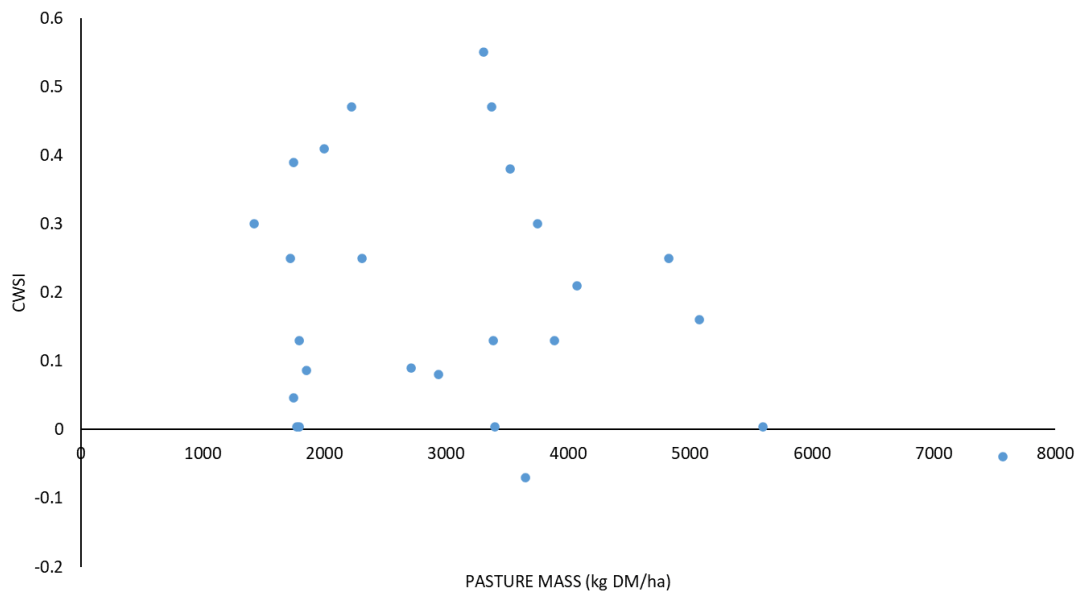


FIGURE 67. COMPARISON COMPARING THE CWSI AND PASTURE MASS (KG DM/HA).

4.4.2 Spatial CWSI Discussion

Looking at the temperature, $T_c - T_a$ and CWSI images at the paddock scale, there is a significant variation in canopy temperatures and CWSI, especially during the first flight (14/12/2020) when the ambient temperature was high. This is due to several effects. Some of the temperature differences are the difference in stresses between the pastures in certain parts of the paddock, where some paddocks may be holding more or less water or have a slightly different orientation or soil type. Other variations may be caused by a mix of species and seasonal variations in species mix. This is somewhat similar to an orchard/vineyard environment where different species of trees or vines may be present that have different canopy temperatures and result in a different CWSI or where different soil types across an orchard/vineyard will have different moisture-holding capacities, which may affect the stress of a plant (Horst *et al.* 1989).

For this study, we had to exclude or remove any non-pasture temperatures, such as roads and trees (Figure 68). When a farmer looks at the canopy temperature or CWSI over a broader scale than the paddock, non-pasture-related temperatures (bare ground, roofs, tree canopy, etc.) can affect the CWSI. However, if the farmer/user is familiar with the location. In that case, the CWSI can be calculated by selectively using the canopy temperature of the stressed and non-stressed pastures, avoiding the potential error of selecting a higher or lower temperature that is not pasture-related, which would result in a skewed CWSI. This is similar to using CWSI in an orchard-type environment, where the user or AI (Artificial Intelligence) needs to preferentially ensure that data is related to the canopy and screens out background data (Berni *et al.* 2009). Similarly, in an orchard/vineyard

scenario, there may be other infrastructure (water tanks, dams, tractors, sheds, etc) that, if not screened out correctly, can affect the CWSI results.

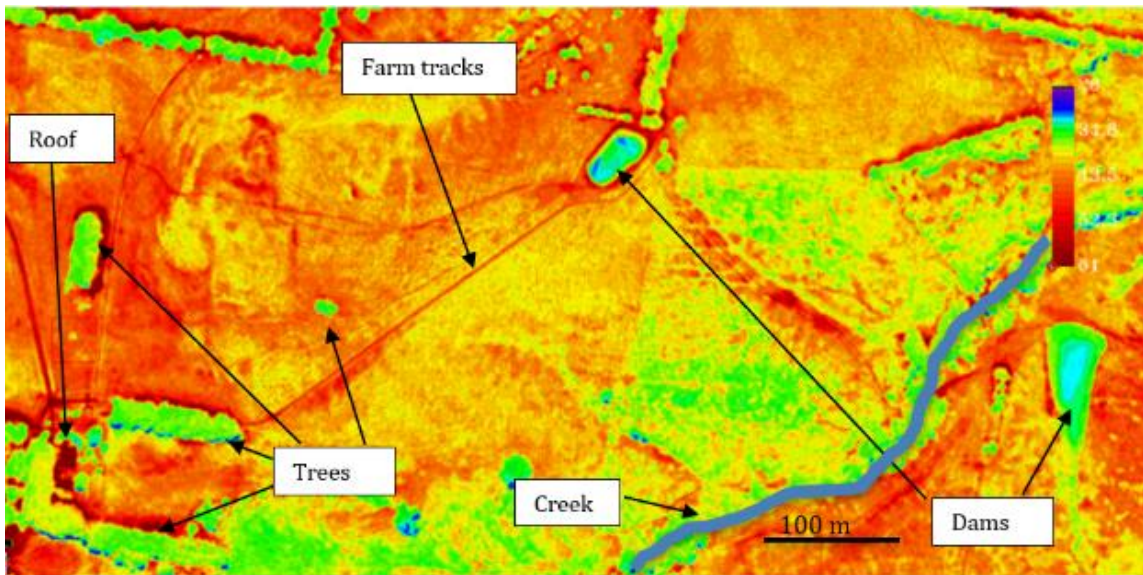


FIGURE 68. THERMAL TEMPERATURE ISSUES. PASTURE AND NON-PASTURE-BASED THERMAL TEMPERATURES WERE RECORDED WITH A FLIR CAMERA DURING FLIGHT DATA ACQUISITION.

4.4.3 Comparing Flight data to ground data.

There was a difference between the canopy temperature data gathered aerially from the plane and the ground-sourced canopy temperature data (goanna ag and handheld). The plane flies 'lines' (Figure 47) in the sky to record the flight data over the broader area and can take an hour to collect all the filed data, as in the case of these field experiments. The canopy temperature data gathered with the handheld thermal sensor is collected over a few minutes, as temperatures are recorded and written down and then the recorder moves to the following location whilst the flights are being undertaken. Therefore, the three sources of canopy temperature are not all taken at the same time, meaning there can be a variation between the canopy temperatures gathered. The canopy temperatures are all recorded within an hour of each other with no significant changes in climate occurring (i.e., storm); therefore, the temperatures represent what is happening in the field. Going forward, improvements could include installing canopy thermal sensors in the field plots (stressed and non-stressed) and across the broader paddock, all recording the canopy temperature simultaneously. The data collection could be improved if the actual time the flight image is taken over certain parts of the farm is known and timed with the ground recorded data.

4.4.4 Cloud Cover

Cloud cover has been an issue with the on-ground remote sensors and the aerial data collection. The on-ground sensors collect data continuously, and as a result, there are many instances where cloud cover is an issue, and these need to be screened out when developing the baselines. Similarly, the presence of clouds made it difficult to time flights, as days, when there was cloud cover, meant the plane

could not fly to collect the thermal canopy data. Days of intermittent cloud made it difficult to schedule flights for breaks in the clouds.

The cloud cover maps from the Bureau of Meteorology (Figure 69) show that the field experiments were undertaken in a high total cloud amount (oktas – unit of measurement of clouds) area. As discussed in the previous chapter, the use of the CWSI is restricted by clouds, and therefore, using the CWSI in the southern parts of Australia will increase complications with data sourcing due to cloud cover. However, using the CWSI in lower cloud areas, which corresponds to central parts of Australia, would be more advantageous and could cause fewer issues with calculating the CWSI due to less cloud cover.

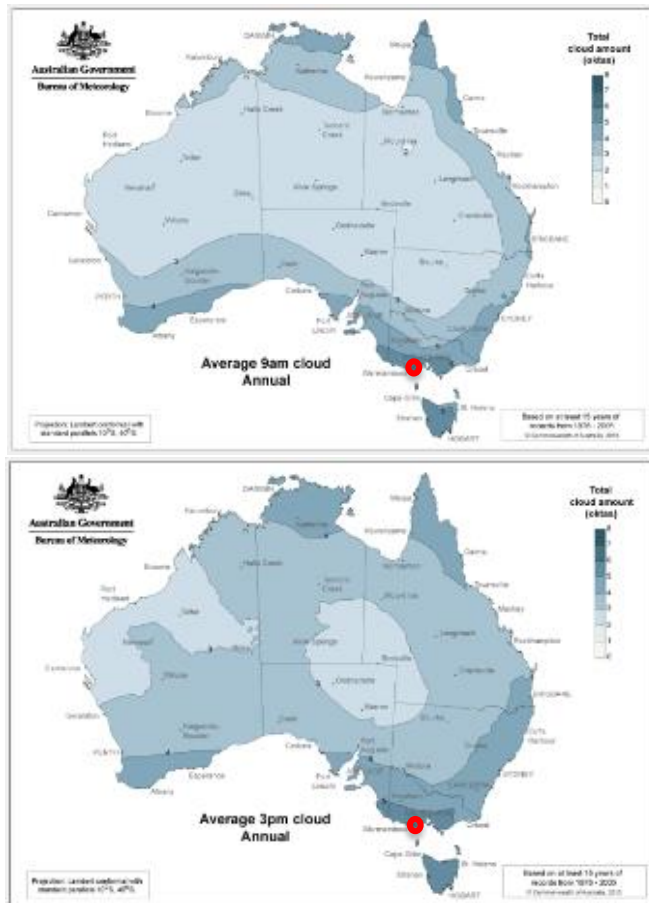


FIGURE 69. AVERAGE CLOUD COVER BETWEEN 9 AM AND 3 PM FOR AUSTRALIA (SOURCE BOM). RED CIRCLE INDICATES LOCATION OF FIELD SITE.

4.4.5 Further Research

Throughout the field experiment, the pastures develop through stages of growth and are consumed and senescing as the seasons change, influenced by rainfall, grazing, and temperature. It would be worthwhile investigating a month-by-month comparison as different species progress through different growth stages; for example, in spring, the pastures will typically crowd out the clover, and then as the pastures progress, the clovers may come back.

The development of these baselines allowed for the CWSI to be generated from the aerial data, which could be used for automated irrigation control. Using the spatial CWSI image over a couple of paddocks (Figure 62) can assist with selecting areas that may need irrigation and areas within a paddock that may not. Limits could be set for initiating irrigation, i.e., when the CWSI is over 0.65, irrigation is turned on, similar to work undertaken by Golgul *et al.* 2022 where they postulated that a CWSI between 0.13-0.22 could be used to initiate irrigation for mung beans.

4.5 Conclusions

The baselines and CWSI derived from the thermal canopy data collected at ground level and aerial flights were suitable indicators for water stress monitoring of pastures. This study demonstrated that the thermal canopy data collected at ground level throughout a season could be used to develop the stressed and non-stressed baselines. The thermal canopy data collected aerially could also be used to develop the CWSI over the paddock and farm scale. The applicability of these results showed that using the CWSI in pastures is a valuable tool for assessing the variability of crop water stress over pasture paddocks.

Declaration of Competing Interests

None

Acknowledgements

Thanks to Tomas Poblete Cisterna for flight coordination and thermal data collection.

5 A Crop water stress index of annual ryegrass pastures in southern Australia.

5.1 Introduction

Farmers typically rely on homegrown pastures to provide fodder for their livestock. Australia's climate is highly variable which affects the productivity and profitability of the farms they manage (Waha et al. 2022). Monitoring plant water stress of pastures can assist Australian farmers to manage in a variable climate, thus improving fodder management and assisting enterprises to be profitable in a changing climate.

The crop water stress index (CWSI) relates canopy temperature to water stress, as water-stressed plants reduce transpiration due to partial or complete closure of their stomata, and as a result, the plant's canopy temperature increases (Idso et al. 1981; Jones, 1999). This difference in canopy temperature between stressed and non-stressed plants can be measured and used to produce the CWSI. The CWSI has been developed for a range of crops; however, to date, work has yet to be undertaken to examine the use of Crop Water Stress Indices (CWSI) on annual ryegrass pastures in southeastern Australia.

This work aimed to develop the CWSI for an annual ryegrass pasture in Southeast Australia.

5.2 Materials and Methods

5.2.1 Experimental design and plot management

Study Area, Agricultural practices and pasture growth.

The field experiments were undertaken at Murroon, in the Otway Range's (38°27'S. 143°50'S, 273m alt.) in Southwest Victoria, Australia. The property is approximately 147 km southwest of Melbourne and has flat areas and rolling hills. Field experiments were primarily conducted on the flat areas. Further details can be found in chapter 4.

5.2.2 Meteorological Conditions throughout the experiment

The climate is classified as warm and temperate. The area receives, on average, 640mm of precipitation a year, with May and October being the wetter months. Waterings conducted on the annual rye pasture in the non stressed field plot and rainfall that occurred during the trials are shown in Figure 70.

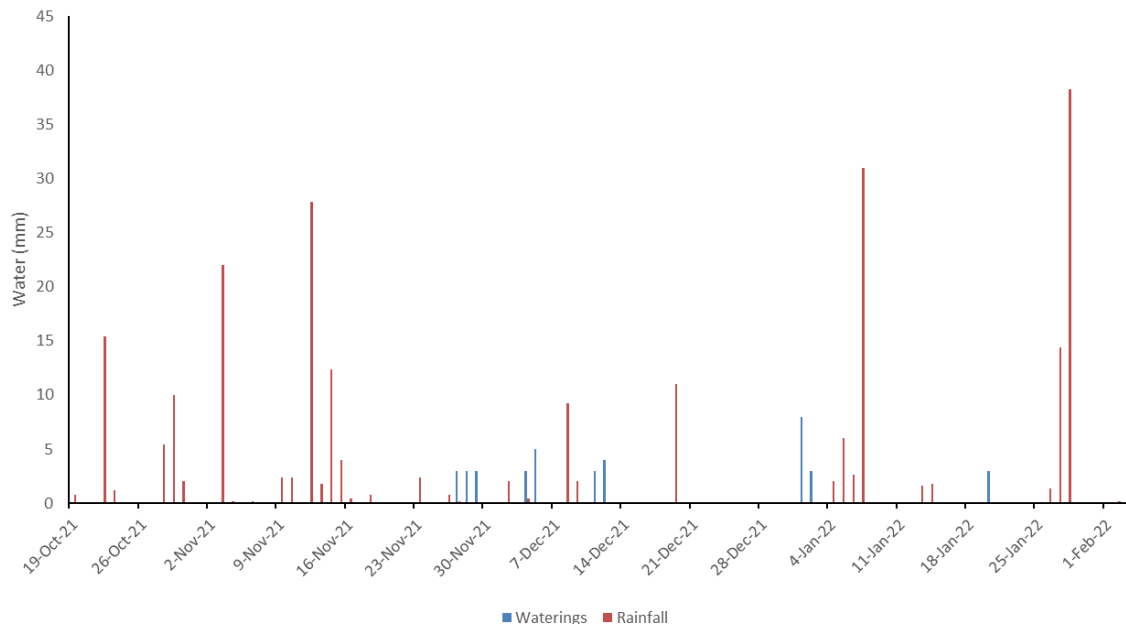


FIGURE 70. WATERINGS (MM) AND RAINFALL (MM) THROUGHOUT THE EXPERIMENT.

Further information on the Materials, methods and experiment design are included in the previous chapter (chapter 4).

PowerPak sprinter (blend of Ascend and Astro tetraploid annual ryegrasses), was sown on 7/5/2021 at a rate of 25kg/ha with DAP (Di-Ammonium Phosphate) fertiliser applied at 72kg/ha. The newly planted annual ryegrass pasture within the field plots was not cut during the field trial, and it did not experience grazing pressure from any livestock or wildlife (Kangaroos). Measurements for the stressed and non stressed field plots were undertaken from 18/10/2021 – 1/2/2022. The soil moisture probe was placed in the centre of each plot, whilst the thermal infrared camera was located within one metre of the soil moisture probe. The equipment was installed on the 18/10/2021.

5.2.3 Baseline Calculations

The baselines are derived by recording the temperature of the canopy, air temperature and VPD between 12-1. The T_c (Temperature Canopy) – T_a (Temperature air) V's VPD (Vapour Pressure deficit) calculations were undertaken on the stressed and non-stressed canopy temperature to determine the stressed and non-stressed baselines. The baseline data was then filtered to remove days where rain occurred (stressed plot) and cloudy days. This data was then used to develop the stressed and non-stressed baseline equations used to develop a CWSI plot to determine which plants are under plant water stress and which plants are not under plant water stress. The CWSI ranges from '0' to '1', '0' being a well-watered non-stressed plant and '1' being a fully stressed plant.

5.2.4 CWSI Calculations

The CWSI was calculated as proposed by Idso *et al.* (1981). The CWSI was calculated for the pastures in the stressed and non-stressed plots. The empirical CWSI formulae used are as follows in Figure 71.

$$CWSI = \frac{(Tc - Ta) - (Tc - Ta)_{LL}}{(Tc - Ta)_{UL} - (Tc - Ta)_{LL}}$$

FIGURE 71. CWSI FORMULAE

The $(Tc - Ta)$ represents the canopy temperature less air temperature of a canopy on the sampling day. The $(Tc - Ta)_{LL}$ represents the canopy temperature less air temperature of a canopy transpiring at its maximum rate. The $(Tc - Ta)_{UL}$ represents the canopy temperature less air temperature of a canopy when transpiration is halted due to lack of moisture. The temperature to develop the CWSI needs to be collected during daylight hours and clear skies. The development of the CWSI requires two baselines that are specific for each site and each crop (Idso, 1982). The upper baseline represents the canopy under full water stress with minimal transpiration. The lower baseline represents the non-stressed plants, where pastures/plants receive adequate water and are not limited in transpiration.

5.3 Results

5.3.1 Temperature

The pasture canopy temperature between the stressed and non-stressed plots throughout the experiment is shown in Figure 72. The temperature increased to over 30 °C in early January, putting the pasture under water stress and differentiating the stressed and non-stressed plants' canopy temperature. Prior to the early January increase in temperature, the temperatures had not increased significantly, and the pastures were receiving intermittent rainfall during November and December and were therefore not experiencing extreme plant water stress.

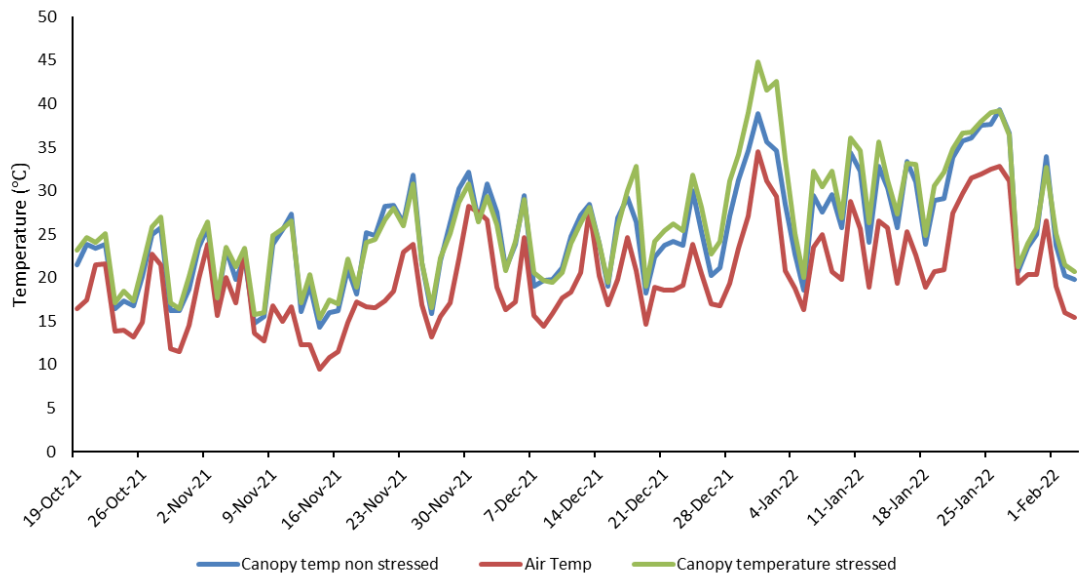


FIGURE 72. CANOPY TEMPERATURE OF STRESSED AND NON-STRESSED PLANTS, INCLUDING AIR TEMPERATURE.

5.3.2 Diurnal Sampling

The diurnal sampling shows the variation in canopy temperature throughout the day, as shown in Figure 73. A clear distinction can be seen between the stressed and non-stressed pastures' canopy temperatures throughout the day, with the stressed pastures' canopy temperature being higher than the non-stressed pastures' canopy temperature for the sampling period.

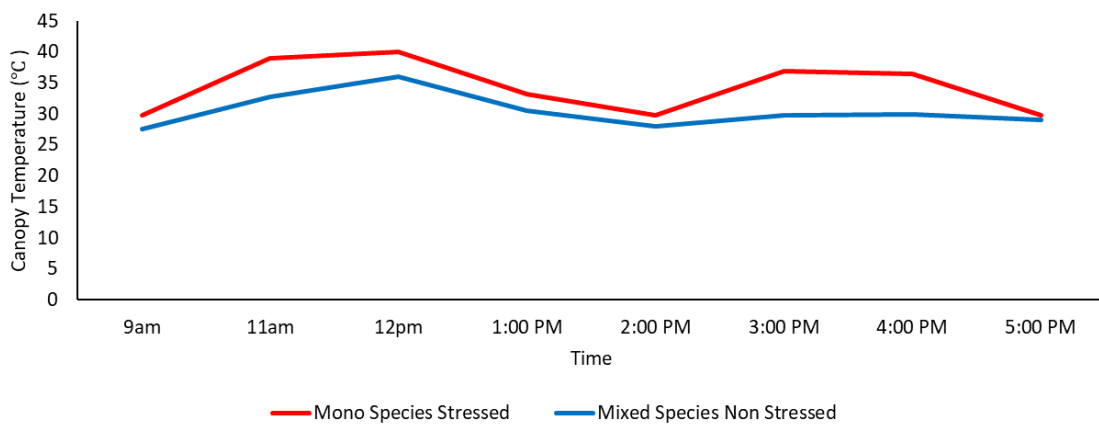


FIGURE 73. DIURNAL SAMPLING OF RYEGRASS 2/1/2022

In Figure 74, the canopy temperatures have been plotted, including the five individual measurements for each time interval and the average temperature for each time interval during the diurnal cycle taken on 2/1/2022. This sampling shows that the canopy temperature of similar plants under similar conditions can vary over a range.

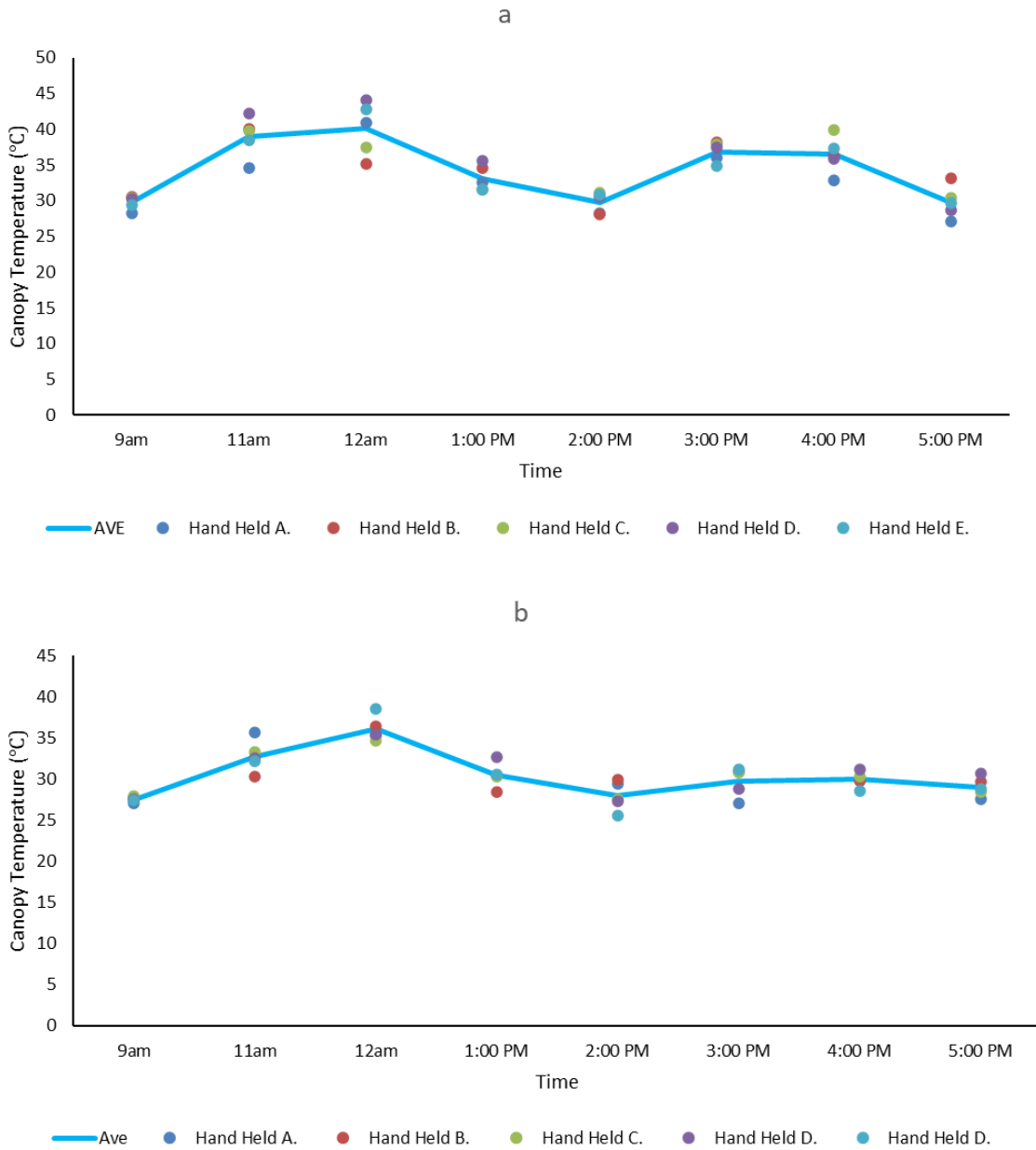


FIGURE 74. CANOPY TEMPERATURE (DEG C) SPREAD RECORDED BY HANDHELD THERMAL SENSOR (A) STRESSED PASTURE (B) NON-STRESSED PASTURE ON 2/1/2022.

5.3.3 Soil Moisture

The soil moisture levels between the stressed and non stressed field plots were relatively equal until late November, when there was some separation between the soil moisture levels (75). The stressed soil moisture level decreased consistently, whilst the non-stressed soil moisture level did not reduce as quickly. The soil moisture for the non-stressed plot temporarily increased at intervals as a response to the watering.

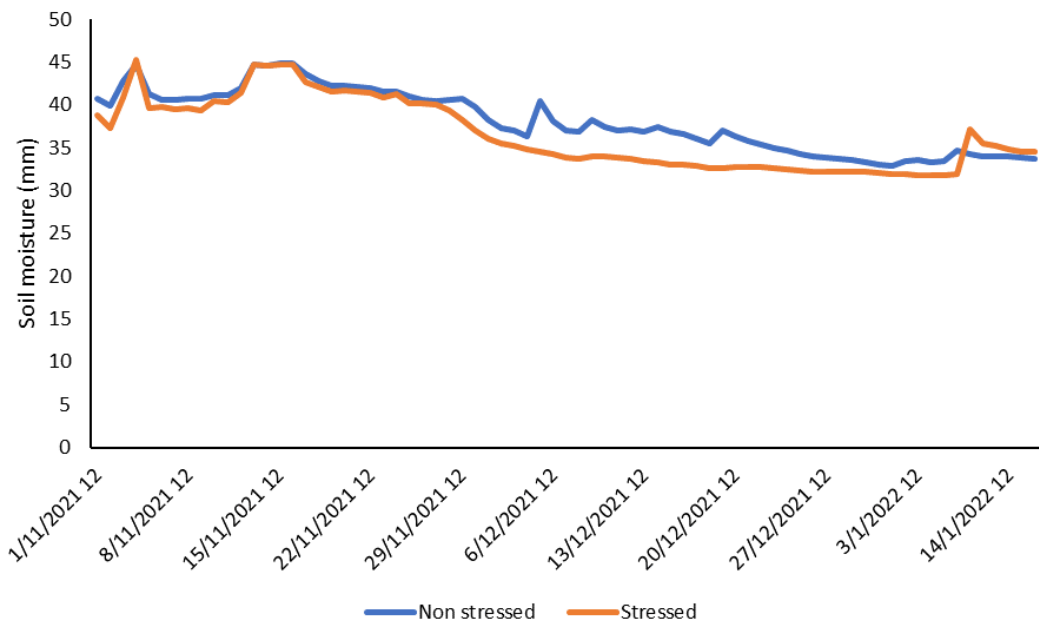


FIGURE 75. SOIL MOISTURE (MM) OF THE STRESSED AND NON-STRESSED PLOT AREAS.

5.3.4 Baselines

The stressed and non-stressed baselines developed for the annual ryegrass are shown in Figure 76. The stressed data points representing the $T_c - T_a$ of the stressed pastures were averaged to determine the water-stressed baseline (10.2°C).

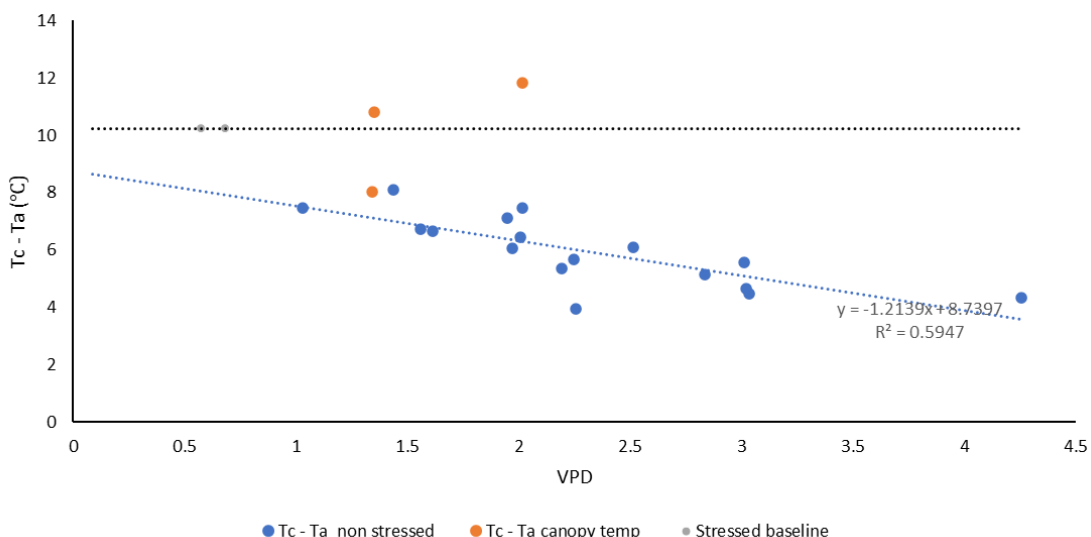


FIGURE 76. BASELINES (STRESSED AND NON-STRESSED) WITH MANUALLY ADJUSTED STRESSED BASELINE.

5.3.5 Resulting CWSI

Figure 77 shows the CWSI results for the period throughout the field trials when the plants were under the most water stress due to an increase in temperatures in late December 2021 and early January 2022.

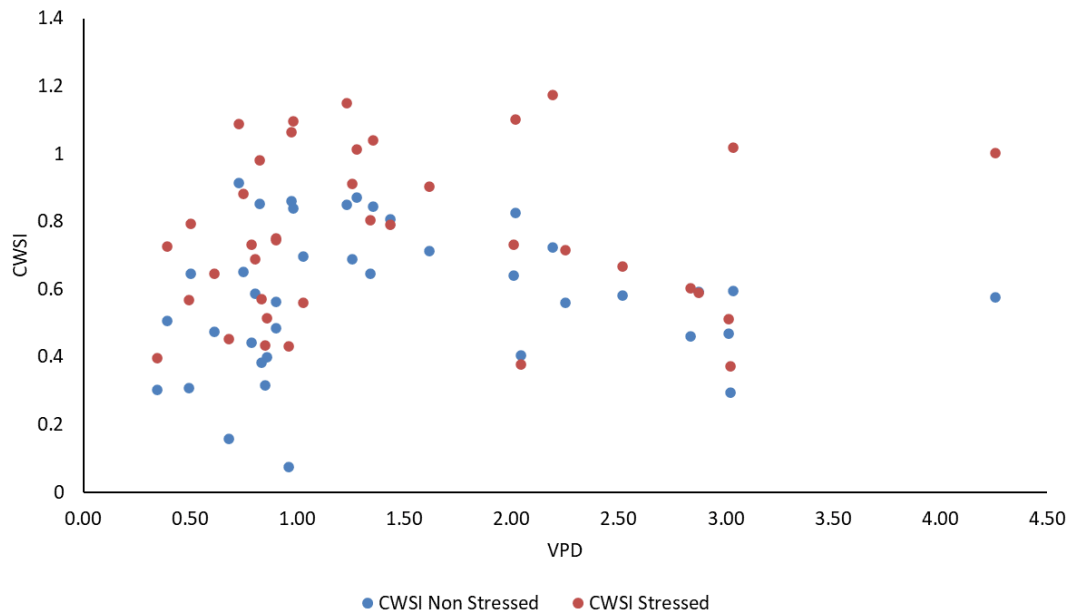


FIGURE 77. CWSI DURING PERIODS OF HIGHER AMBIENT TEMPERATURE, EXPERIENCED IN LATE DECEMBER AND JANUARY (21/12/2021)

The CWSI over time (21/12/2021 and 31/1/2022) shows that the stressed pasture had a higher CWSI than the non-stressed pasture on certain days when the ambient air temperature increases (Figure 78).

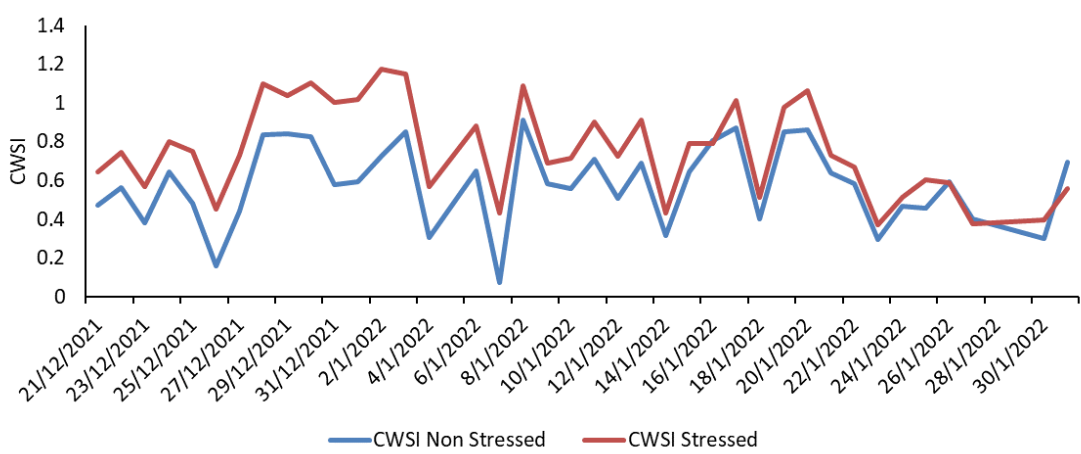


FIGURE 78. CWSI BETWEEN 21/12/2021 AND 31/1/2022 DURING HOTTER PERIODS OF YEAR, PUTTING THE PLANTS UNDER WATER STRESS.

5.4 Discussion

The stressed and non-stressed CWSI baselines for annual ryegrass developed in this study were similar to what Idso *et al.* (1982) and others (Maes *et al.* 2012) achieved for other plant species. The baselines were difficult to generate if we used all the data collected; however, by screening the data and removing days that were cloudy, wet or conditions where the pasture was not under plant water stress, we were able to develop baselines.

There is limited literature on other ryegrass or annual ryegrass baselines to compare our data. Our non-stressed baselines sits higher than most other crop types compared to Idso's (1980's) work and the numerous other baselines in the supplementary data (Maes *et al.* 2012). Some of the closest baselines are in turf, tall fescue, and hybrid Bermudagrass, as shown in figure 10; however, there are no direct comparisons for annual Ryegrass. In Figure 79, the non-stressed baseline for the annual Ryegrass has been plotted against some field-derived baselines for Tall fescue and Hybrid Bermudagrass undertaken by Haghverdi *et al.* (2021) in central California in 2018 and 2019. The Tall fescue and Hybrid Bermudagrass are from a climate where evapotranspiration is approximately five times the precipitation received in the area of this study (Haghverdi *et al.* (2021)). The work undertaken on Tall Fescue was conducted over 2018 and 2019, and the baselines have been plotted separately.

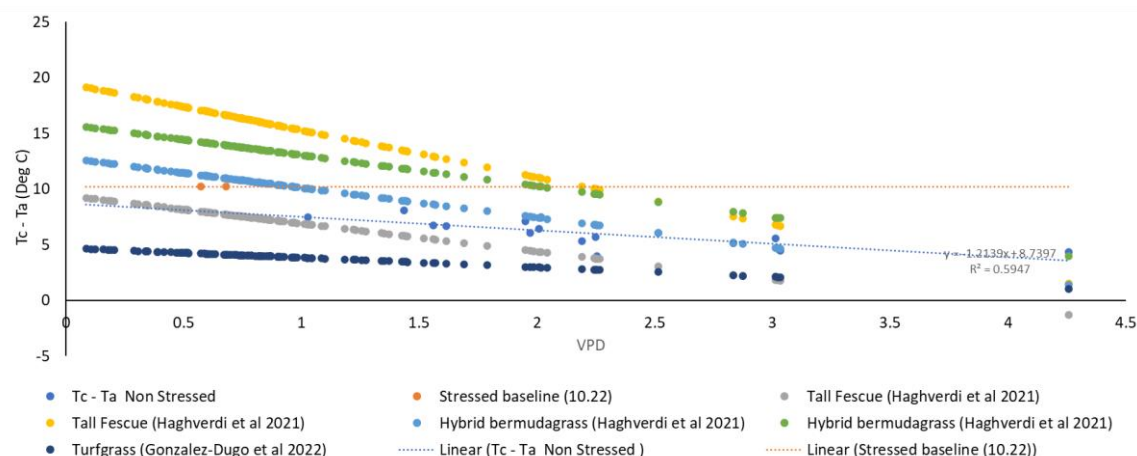


FIGURE 79. COMPARISON OF ANNUAL RYEGRASS BASELINE TO TALL FESCUE (HAGHVERDI ET AL 2021), HYBRID BERMUDA (HAGHVERDI ET AL 2021) AND TURFGRASS (GONZALEZ-DUGO ET AL 2022).

The supplementary data in Maes *et al.* (2012) is an extensive list of non-water-stressed baseline equations. Many early baselines have been developed in more arid parts of the world (Arizona, California, Turkey, Iran, Texas, etc). Alderfasi *et al.* (2001) Stockle *et al.* (1992) found that the CWSI values for a non-stressed crop determined using the empirical CWSI baseline approach changed daily, especially under low VPD deficits. Alderfasi *et al.* (2001) also found that canopy temperature differences between stressed and non-stressed crops are usually small under low evaporative demand. This was also found in our field trials. During the periods

before mid-December, when plants had soil moisture and ambient temperatures were not excessive (above 30 °C) it was difficult to determine plant water stress between the two field plots. However, this changed as the ambient temperature increased in mid to late December and early January and the soil moisture levels between the two plots started to differ. Another finding by Jensen *et al.* (1990) was that either stressed or non-stressed wheat, barley, rape and perennial ryegrass crops could fluctuate up to 6 deg C within a few minutes to rapid changes in incident solar radiation. With the high amount of cloud cover during the winter and spring when the canopy temperature measurements were taken for the field trials, we could expect a rapid change in canopy temperatures in our field plots. This was experienced when taking canopy temperature checks with a handheld thermometer (Optris MS, non-contact infrared thermometer). Taking five canopy temperature measurements within one metre over one minute gave a range of canopy temperatures for a similar pasture (figure 5).

The CWSI relies on clear skies, and therefore, while it is useful in areas outside arid environments, its use is limited to non-cloudy days or periods of no clouds during the day (O'Shaughnessy *et al.* 2012). O'Shaughnessy *et al.* (2012) also points out that wind gusts and other micrometeorological incidents influence the CWSI. Barbosa *et al.* (2005) also mention that clouds were an operational issue, affecting the net radiation when collecting data and that the field site being 60km from the Atlantic Ocean may explain the intermittent cloud cover. Similarly, our site was only 15km from the ocean, which may have increased the occurrence of cloud cover.

One implication of using the CWSI in this region (South of the Great Dividing Range) is the occurrence of clouds throughout the year, making it challenging to collect data to develop the baselines and test the CWSI. Much of the early work on developing the CWSI was undertaken in the USA by Idso, (1981) in Arizona, North Dakota, Nebraska and Kansas, that is in arid environments with limited clouds. Similarly, other work on baselines since Idso's work has predominantly been in Turkey, Arizona, Iran, Texas, etc. (Maes *et al.* 2012), typically more arid areas. Idso (1981) mentions that his work was undertaken under clear skies with some thin cirrus conditions; he further mentions that the relationship begins to decline for other types of cloudiness, presumably due to changing illumination effects on stomates (Idso, 1981). Similarly, O'Shaughnessy (2012) acknowledged the problem regarding irrigation scheduling by using instantaneous measurements taken over a short period near solar noon, which may be influenced by passing clouds, wind gusts or other micrometeorological incidents. Consideration needs to be given to the usefulness of using the CWSI in non-arid regions, especially if used for irrigation scheduling.

The CWSI values are meant to vary between 0 and 1 (representing no transpiration and maximum transpiration, respectively); however, from our results, we had several CWSI values exceeding one and less than zero. It was possible to 'clean' this data by taking out days with obvious cloud cover or recent rainfall events; however, even allowing for this screening, keeping all our results within the CWSI 0 to 1 range was not possible. Haghverdi *et al.* (2021) found that their CWSI values ranged from -0.34 – 0.56. Similarly, work undertaken on Tall Fescue by Al-Faraj *et al.* (2001) and

Alderfasi *et al.* (2001) within a controlled environment found that it was not possible to consistently get the empirical CWSI results to lie between 0 and 1. Similarly, the work by Wanjura *et al.* (1984) and Jalali-Farahani *et al.* (1993) experienced some negative CWSI values in their calculations.

Australia has experienced three La Nina weather patterns in a row (2020, 2021, 2022 – Source BOM). La Nina can be associated with above-average rainfall, cooler days, and cooler nights in summer. With the wetter-than-normal periods (refer chapter 4) and cooler conditions (refer chapter 4), pasture was still growing in January, which in 'normal' times would have ceased growing. Further work could be undertaken in developing baselines in non-La Nina years and comparing to these results.

Haghverdi *et al.* (2021) report that the reported CWSI baselines for turfgrass vary widely in the literature and that specific baselines for each climatic region should be developed. Jalail-Farahani, *et al.* (1993) also discussed how baselines are site-specific. Adopting CWSI baselines derived from other countries, states, regions, or cultivars could be problematic as varying climatic conditions and microclimates can alter the CWSI from one place to another. Using Haghverdi *et al.* (2021) premise and other comments in the literature about site-specific baselines, further work needs to be undertaken on developing further baselines for annual Ryegrass across southeast Australia to compare this study to.

Due to the process of senescence (change in colour and loss of leaves), the senescence changes may lead to changes in canopy temperature (Barbosa *et al.* 2005). As pastures change from growth to senescence the pasture can become stalky, as seen in this study. This change could have effects on the canopy temperature, as stalky material may influence the canopy temperature. Further work on developing baselines at different stages of pasture growth could demonstrate if senescence influences canopy temperature.

When collecting the data, recording a range of VPDs can be quite difficult, especially if the fieldwork data collection time is limited. Wanjura D *et al.* (1984) highlighted that their VPD measurements did not exceed 4.0 kPa in their fieldwork whereas work undertaken by Idso (1982) demonstrated a wider range of VPD's such as a VPD of up to 7kPa for field measurements for tomatoes. The VPD collected during these field trials ranged from close to zero to about 4 kPa. Similar to Haghverdi *et al.* (2021) studies throughout 2018 and 2019, where their VPD was restricted between 1 – 5 kPa. Undertaking similar field trials in different locations across Victoria and Australia may assist in obtaining results over a wider VPD range.

Wanjura *et al.* (1984) also mention the difficulty in recording canopy temperatures, noting that some of their plant canopies were not large enough to mask the soil background, and that the Tc included some contribution from the bare soil. Wanjura *et al.* (1984) also mention the possibility that early season stress caused by hail, wind and seedling disease damaged the roots of many plants, and thus, their roots may be more resistant to water uptake than healthier plants. Jackson *et al.* (1981) mention that wheat took 5-7 days to resume transpiring normally after a stress period. Whilst during these field trial, the presence of hail, excessive wind and disease was not identified as an issue, it does demonstrate further issues that need

to be considered when relying on CWSI in the field. Further work could involve trialling how quickly annual Ryegrass takes to resume full transpiration after a stress period.

Whilst the CWSI and associated baselines can be of benefit in monitoring for plant water stress in the field, there are numerous potential issues involved with data gathering to develop the baselines that can result in errors in the data gathered. Further work must be undertaken to verify this study's baselines and resulting CWSI, especially in non-arid regions.

5.5 Conclusion

The canopy temperature difference between the stressed and non-stressed annual ryegrass pastures was able to be detected using a thermal sensor in the field, with the stressed pastures typically recording higher canopy temperatures than the non-stressed pasture canopies during the hotter periods of the year. From the canopy temperature differences, the stressed and non-stressed baselines for the stressed and non-stressed rye grass pastures were developed during periods of plant stress and over a range of VPD. CWSI values for stressed and non-stressed rye grass pastures were able to be determined when the plants were under water-stressed conditions (increase in ambient temperature) but did not work well, as expected, during times when the plant was not under water stress (cooler ambient temperatures or when the plant had adequate soil moisture). The stressed and non stressed baselines developed as part of this field work could be used in the agriculture environment to monitor plant water stress across a paddock or farm, and also could be used as a tool to set irrigation limits if irrigation water is available.

Declaration of Competing Interests

None

Acknowledgements

Thanks to Tomas Poblete Cisterna for flight coordination and thermal data collection.

6 Comparison of empirical, adaptive, and baseline-derived Crop Water Stress Index (CWSI) methods to assess plant water stress in pastures in Southeast Australia.

6.1 Introduction

Field-grown pasture is the main and cheapest feedstock for cattle and sheep in southern Australia (Perera *et al.* 2020; Chapman *et al.* 2009) and many other regions worldwide. Climate, particularly rainfall variability, is one of the significant sources of intra - and inter-annual variation in pasture growth (Chapman *et al.* 2009). In southern Australia's temperate and Mediterranean climates, pasture growth is primarily limited by water availability from mid-late spring to the opening rains in autumn. In contrast, appropriate spring and autumn temperatures with nutrients, disease, and other management practices (overgrazing) can also affect pasture growth. As soil moisture reduces, plant transpiration declines and the canopy temperature increases along with a reduction in photosynthesis (Idso *et al.* 1981). Water deficits occur in plants when evaporative demand exceeds the water supply in the soil (Slatyer, 1967). Where there is inadequate water for the plant, the water stress causes partial stomatal closure and reduction in transpiration rates, and the reduced evaporative cooling raises the canopy temperature in relation to the ambient temperature (Jones, 1999).

Canopy temperature is considered a reliable proxy for plant water stress monitoring and irrigation scheduling (Idso *et al.* 1984; Steele *et al.* 1994). Canopy temperature is accepted as an indirect, rapid, accurate, and large-scale crop water stress indicator (Gonzalez-Dugo *et al.* 2022). Using a Thermal infra-red thermometer to assess plant canopy temperatures of water-stressed plants was initially put forward by Jackson *et al.* (1977). In the absence of biotic stress from fungi, bacteria, and viruses, the restrictions in canopy growth under sub-optimal water or nutrient levels are generally related to stomatal closure (Jones, 1998) and chlorosis (Shimshi. 1967), resulting in both water and nutrient stress due to limited uptake from the roots (Zarco-Tejada, 2021). The Crop Water Stress Index (CWSI) is an efficient indicator of crop water status and is based on the difference between foliage and air temperature (Idso *et al.* 1981; Jackson *et al.* 1981) of stressed and non-stressed plants normalised by the vapour pressure deficit (VPD).

To measure the CWSI empirically, an alternative method requires a stressed and non-stressed plant to normalise the results. The canopy temperature measurements from the stressed and non-stressed canopies and the canopy temperature from the plant of interest are used to develop the CWSI. The requirement for having a non-stressed and stressed plant present to measure the CWSI in the field has made it difficult to use the CWSI extensively in the Agricultural setting. Alternatively, if a stressed and non-stressed plant is unavailable, it is possible to utilise baselines if they have been developed for that species at that location. Idso initially undertook numerous baselines for various crops in the (1980's). One limiting factor of using already developed baselines is that the

baselines are site, species and variety specific (Idso, 1982) and may not work that well when used in the next valley or in a different region, country, continent or time of year.

One method to avoid the requirement for having a stressed and non-stressed plant available to normalise the results is the use of reference leaves, using materials that may imitate the stressed and non-stressed leaf's canopy temperatures in the field (Jones *et al.* 2002). Alternative methods include cloth knitted around a solid frame (Maes, 2016), cellulose paper (Apolo – Apolo 2020), leaves sprayed with water or covered in petroleum gelly (Leinonen, 2004), a small quantity of detergent on the leaf (Jones *et al.* 2002), filter paper (Jones *et al.* 2002) and a wet artificial reference surface (WARS).

Park *et al.* (2017) used an adaptive derived T_{wet} (non-stressed) and T_{dry} (stressed) to calculate the CWSI as part of one of their studies on nectarine and peaches under different irrigation treatments. They used a temperature histogram derived from a TIR (thermal infrared) image to generate the stressed and non-stressed values for CWSI. They used T_{wet} (non-stressed), the histogram's coldest part, and T_{dry} , the hottest part. They excluded any pixels with a mixture of canopy and background (such as soil). Their experiment-imposed deficit plots, where irrigation was withheld for five days before the field trials (Park *et al.* 2017). The other plots were irrigated and were the control plots. Park *et al.* (2017) collected the canopy's thermal temperatures remotely using a thermal camera. This allowed the quick recording of the thermal temperatures over a larger area (paddock/farm scale) than would be possible if taking point measurements on the ground. By using the remote collection method, they assessed the spatial variability of plant water stress over larger areas quickly and efficiently.

This work compares the baseline calculated CWSI against the CWSI developed empirically and uses an adaptive CWSI method similar to Park *et al.* (2017) on pasture species in Southeast Australia. The baseline approach relies on CWSI baselines having been developed for the particular species, at the same location to then calculate the CWSI of the plant from using the canopy temperature and VPD (Vapor Pressure Deficit) at the time. The empirical CWSI approach uses two canopy temperatures on the day of sampling, one from a stressed plant and one from a non-stressed plant. These stressed and non stressed temperatures are then used in the CWSI formulae to calculate the CWSI. The adaptive approach uses a temperature histogram derived from a thermal infrared image to generate the stressed and non-stressed values for the CWSI.

6.2 Materials and Methods

6.2.1 Experimental design and plot management

Study Area, Agricultural practices and pasture growth

The field experiments were undertaken at Murroon, in the Otway's (38°27'S. 143°50'S, 273m alt.) in Southwest Victoria, Australia. The property is approximately 147 km southwest of Melbourne and has flat areas and rolling hills. Field experiments were primarily conducted on the flat areas. Further details on the property and pasture can be found in Chapter 4.

6.2.2 Meteorological Conditions throughout the experiment

The climate is classified as warm and temperate. The area receives, on average, 824mm of precipitation (Average 1980-2022 Barwon Downs) a year, with May and October being the wetter months. Further details can be found in Chapter 4.

6.2.3 Field Plots

The field experiment was set up in Murroon, in south-west Victoria and ran from October 2020 to January 2022. Two treatment plots were set up in the paddock, a well-watered (non-stressed) and a rainfall only (stressed) plot. The pastures were predominantly Phalaris (*Phalaris aquatica L*) with a small amount of Clover (*Trifolium subterraneum L*) and Dandelion (*Taraxacum officinalis*) weeds. A permanent thermal canopy sensor was installed in each plot along with soil moisture probes and a weather station. The pasture canopy temperature of the stressed and non-stressed plots was continuously measured throughout the field trials. As part of the study, spatial variation in canopy temperature was also assessed with a Flir thermal infrared camera mounted on an aeroplane. Further information can be found in Chapter 4.

Figure 80 shows the rainfall experienced on-site throughout the field study period. This rainfall fell on both plots (stressed and non-stressed), as a rainout shelter was not used for the stressed plot. Whilst a rainout shelter was considered, introducing a rainout shelter introduces other variables that can affect the microclimate and, therefore the plants water stressed state. The rainout shelter would also have added complications for aerial data gathering, effectively blocking the pasture from the FLIR camera mounted to the plane.

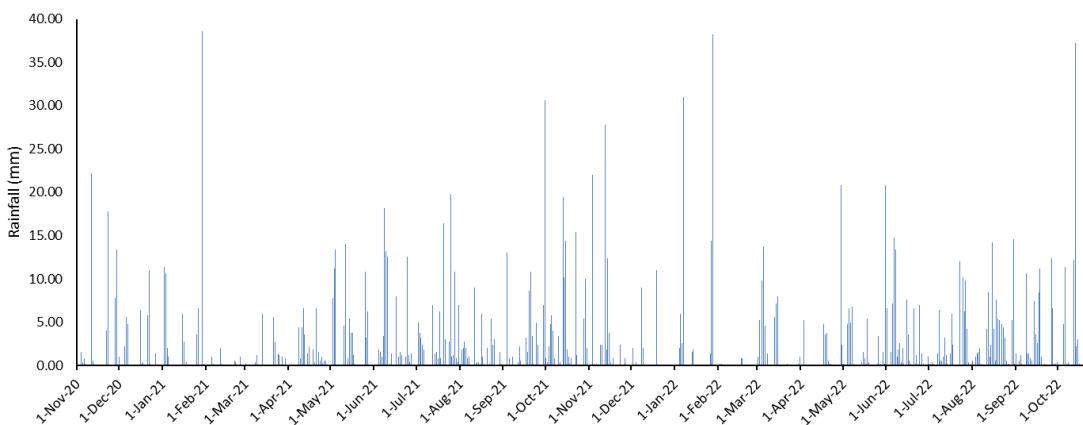


FIGURE 80. RAINFALL (MM) COLLECTED FROM AN ON-SITE WEATHER STATION.

In Figure 81 are the dates and quantities of waterings for the non-stressed field plot throughout the experiment. During the winter, watering ceased as the plants received enough water from rainfall, with watering continuing again in spring. Waterings were undertaken using a watering can, evenly spreading the water around the non-stressed plot to ensure all pasture within the plot was evenly watered.

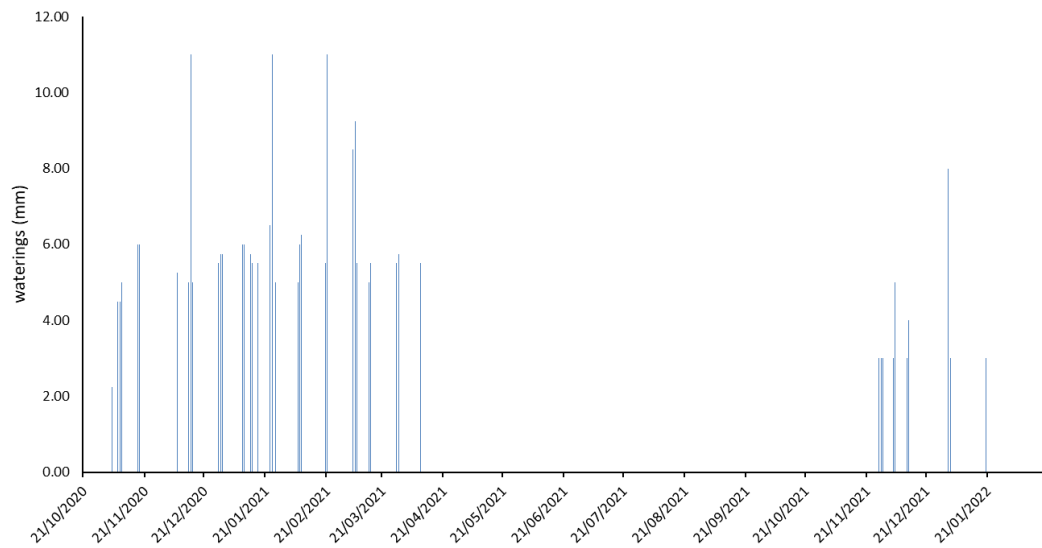


FIGURE 81. DATES AND AMOUNTS (MM) OF WATER ADDED TO NON-STRESSED PLOT DURING FIELD TRIALS.

6.2.4 Study Area

The field plots are shown in Figure 82, including the area used to develop the histogram (Area A), which covers approximately 5.8 hectares and excludes the stressed and non-stressed field plot areas.



FIGURE 82. FIELD PLOTS (BLUE SQUARES) AND AREA A USED TO DEVELOP THE HISTOGRAM.

6.2.5 Thermal Image Acquisition Remote

The airborne thermal imagery was collected with a Cessna aircraft flying 500m above the site on 14/12/2020 (figure 9), 29/11/2021 (figure 10) and 14/12/2021 (figure 11) heading on the solar plane. The aircraft recorded canopy temperature with a thermal camera (SC655 model, FLIR Systems, Wilsonville, OR, USA) with a resolution of 640×480 pixels, 16-bit radiometric resolution, 13.1-mm focal length, and 45×33.7 °FOV yielding a spatial resolution of 0.25 m.

6.2.6 Processing of Thermal Images

The thermal images were processed as in Calderon *et al.* (2015) and Hornero *et al.* (2021). The thermal imagery map obtained from the flight was then used to calculate the CWSI for the treatment plots and the wider area (across the paddocks or farm).

6.2.7 CWSI Calculations

Three different methods to calculate the CWSI were used, they included,

1. Baselines – using the previously calculated (Chapter 4) pasture baseline ($y = 2.9289x + 7.286$. and 16) to generate the CWSI (Idso, 1982).
2. Empirically using the stressed and non-stressed plants' canopy temperatures to calculate the CWSI (Gonzalez-Dugo *et al* 2018) using the $CWSI = ((T_c - T_a) - (T_c - T_a)_{LL}) / ((T_c - T_a)_{UL} - (T_c - T_a)_{LL})$ (The $(T_c - T_a)_{LL}$ represents the canopy temperature less air temperature of a canopy transpiring at its maximum rate, the non stressed plot. The $(T_c - T_a)_{UL}$ represents the canopy temperature less air temperature of a canopy when transpiration is halted due to stomata closure, the stressed plot.)
3. Adaptive - using a temperature histogram derived from a thermal infrared image to generate the stressed and non-stressed values for the CWSI (Park *et al* 2017) using the $CWSI = ((T_c - T_a) - (T_c - T_a)_{LL}) / ((T_c - T_a)_{UL} - (T_c - T_a)_{LL})$ (The $(T_c - T_a)_{LL}$ represents the canopy temperature less air temperature of a canopy transpiring at its maximum rate, in this scenario the lower temperature on the histogram. The $(T_c - T_a)_{UL}$ represents the canopy temperature less air temperature of a canopy when transpiration is halted due to stomata closure, in this scenario, the upper temperature on the histogram.

6.2.8 Data analysis

Describe the data was analysed – eg temperature histograms, and CWSI – average and spatial distribution.

The thermal temperatures from the flight were analysed and the temperature occurrences were put in the histogram (figure 83). The temperatures were then used to develop the CWSI for the field plots (figure 84) for each flight using each method

(baseline, empirical and adaptive). The data was then used to display the spatial canopy temperature across the farm (figures 85-87) and for the CWSI across the paddock (figure 88).

6.3 Results

From the aerial pasture canopy temperature data the CWSI were generated from the baselines, empirically and using the adaptive approach.

6.3.1 Baseline approach

The baselines were generated as part of the fieldwork, with full details in Chapter 5. The CWSIs generated for each flight using the baselines approach are shown in Table 6. These baselines were developed from the canopy temperatures from the stressed and non stressed field plots.

TABLE 5. CWSI GENERATED USING BASELINES

	Flight 1	Flight 2	Flight 3
CWSI Non Stressed	0.15	0.08	0.12
CWSI Stressed	0.48	0.32	0.21

6.3.2 Empirical Approach

The maximum and minimum canopy temperatures could be measured for the stressed and non-stressed plots for the three flights. The canopy temperature from the stressed plot (maximum temperature) and the canopy temperature from the non-stressed plot (minimum temperature) were used to develop the empirical CWSI for each flight, and the CWSI results are shown in Table 7. The CWSI index ranges from 0 (stressed) to 1 (non stressed) (Jackson et al. 1981), which can be seen in the stressed and non stressed results obtained (Table 2). As the stressed and non stressed canopy temperatures from each flight are used to develop the empirical CWSI, these canopy temperatures represent the highest and lowest canopy temperatures and therefore calculate into the maximum and minimum CWSI. For the canopy temperatures between the maximum and minimum canopy temperatures, these will range between 0 and 1 on the CWSI.

TABLE 6. MAXIMUM AND MINIMUM CANOPY TEMPERATURES FOR THE STRESSED AND NON-STRESSED PLOTS AND EMPIRICALLY DEVELOPED CWSI.

	Non Stressed canopy temperature °C	Stressed canopy temperature °C	Non-Stressed CWSI	Stressed CWSI
Flight 1 (14/12/2020)	35.85	40.85	0	1
Flight 2 (29/11/2021)	26.85	29.85	0	1
Flight 3 (14/12/2021)	25.85	26.85	0	1

6.3.3 Adaptive Approach

In Figure 82, “Area A”, shows the area used to determine the canopy temperature for the CWSI histogram method. The histogram results for “Area A” for each flight are shown in Figure 83.

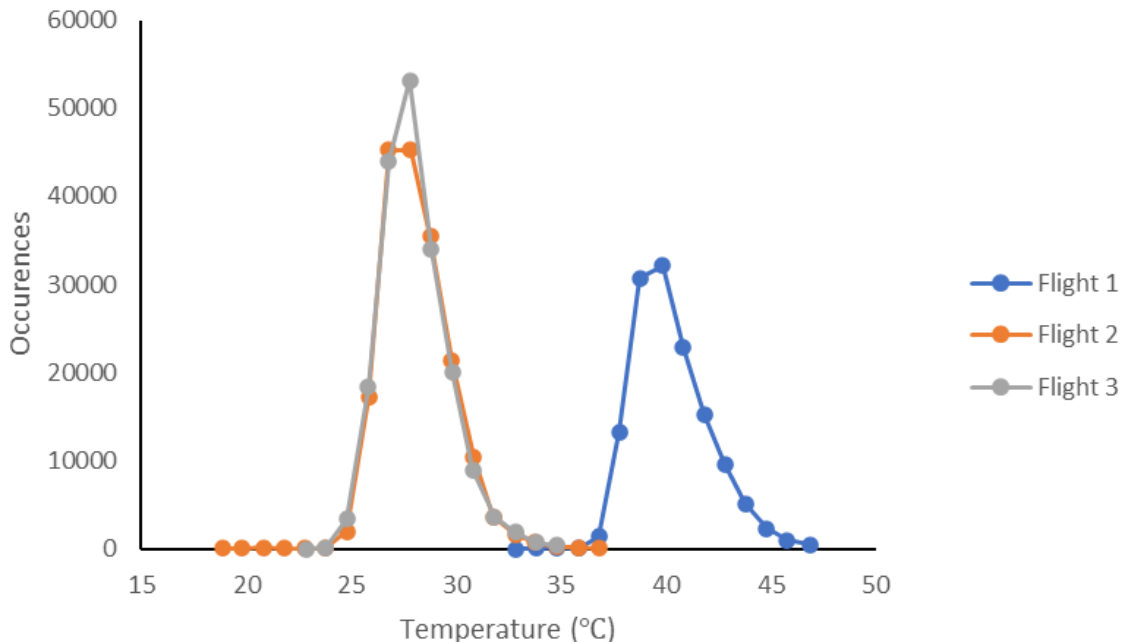


FIGURE 83. FREQUENCY DISTRIBUTION HISTOGRAM OF FIELD CANOPY TEMPERATURES (°C) OF AREA IN FIGURE 6 FOR EACH FLIGHT.

In Table 8 are the CWSI results for the adaptive approach. The maximum (stressed) and minimum (non stressed) temperatures (°C) used for the CWSI were obtained from the histograms (Figure 83) for each flight and then the CWSI was calculated for the stressed and non-stressed field plots.

TABLE 7. CWSI RESULTS FOR THE ADAPTIVE APPROACH

	Non Stressed canopy temperature °C (from histogram)	Stressed canopy temperature °C (from Histogram)	Non-Stressed CWSI	Stressed CWSI
Flight 1 (14/12/2020)	32.85	46.85	0.21	0.57
Flight 2 (29/11/2021)	18.85	36.80	0.45	0.61
Flight 3 (14/12/2021)	22.85	34.83	0.25	0.33

6.3.4 Comparison of the CWSI's generated

The CWSIs could be developed for all the methods (baseline, empirical and adaptive). Figure 84 presents the results using the different methods to derive the

CWSI on the field trial plots (stressed and non-stressed). The CWSI results differ for the differing approaches for the two areas (stressed and non-stressed plots); however, the CWSI results still demonstrate areas of high to low water stress. The empirical results are always going to have a CWSI upper and lower limits of 1 – 0 and rely on the canopy temperature of the stressed and non stressed plot on the day. The adaptive approach will differ, depending on the pasture canopy temperatures and the variation in the pastures water stress status across the paddock on the day. For flight 1 the ambient temperature was significantly higher than for flight 2 and flight 3, and this is seen in the data with the CWSI higher for flight 1 than for flights 2 and 3.

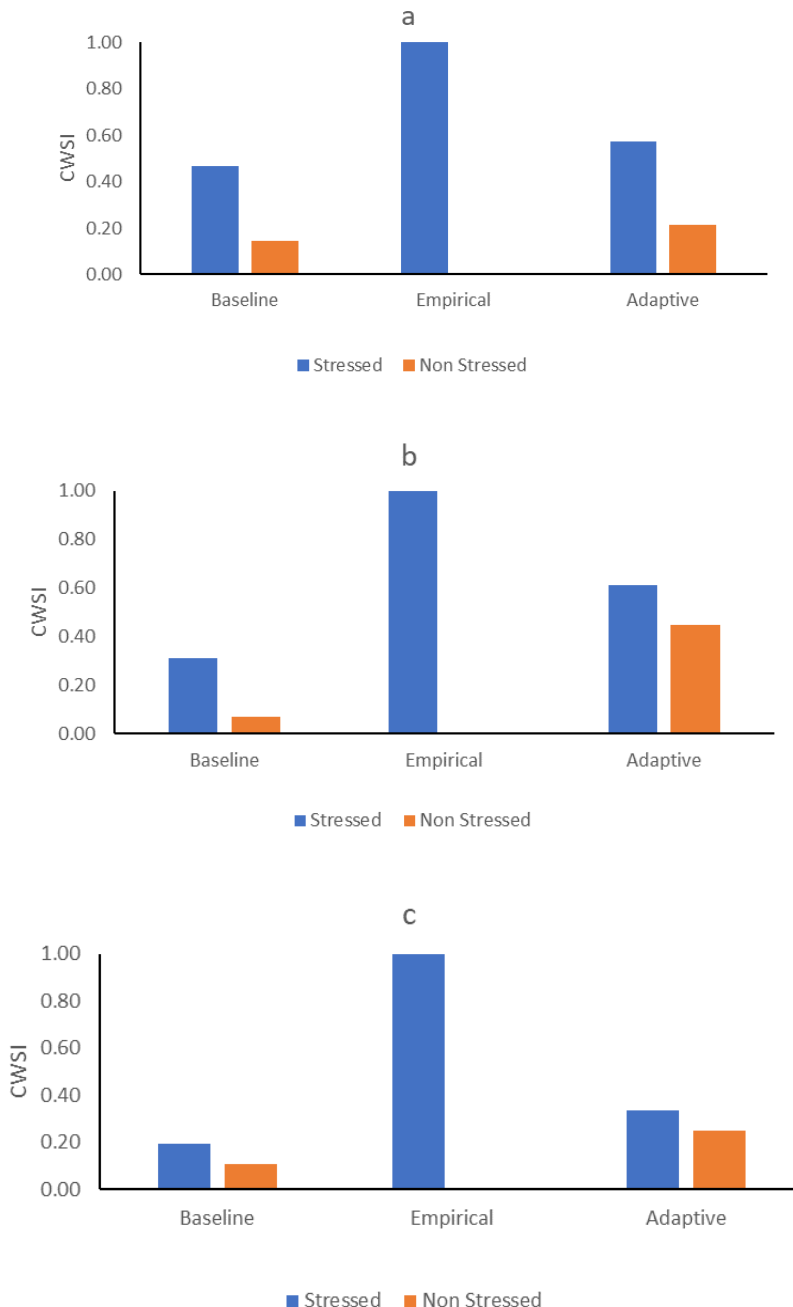


FIGURE 84. COMPARING THE THREE FLIGHTS' (BASELINE, EMPIRICAL AND ADAPTIVE) GENERATED CWSI RESULTS. (A) FLIGHT 1, (B) FLIGHT 2, (C) FLIGHT 3 OF THE FIELD PLOTS. (NOTE: EMPIRICAL WILL ALWAYS RESULT IN A CWSI OF 0 TO 1.)

6.3.5 CWSI of paddocks

Figures 85-87 shows the canopy temperatures collected remotely during the flights, showing the variation in canopy temperature across the paddocks.

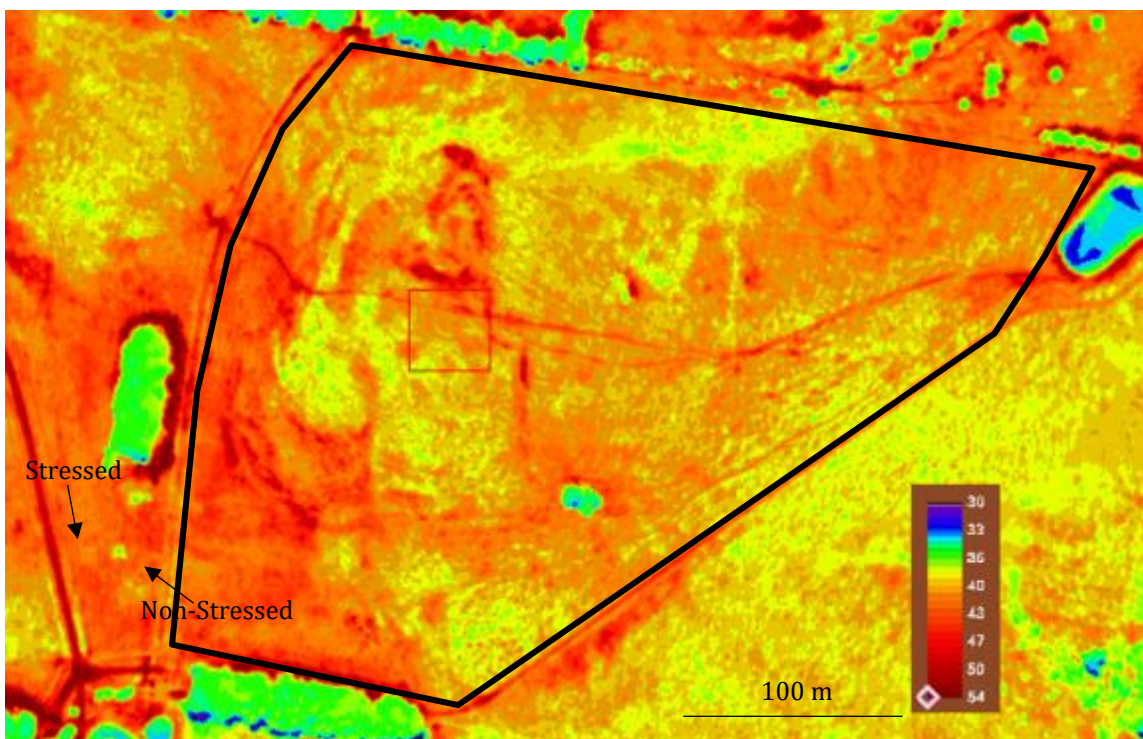


FIGURE 85. PASTURE CANOPY TEMPERATURES (°C) WERE OBTAINED REMOTELY (BY PLANE) ON 14/12/2020. STRESSED AND NON-STRESSED FIELD PLOTS AND A BROADER AREA (PADDOCKS) ARE SHOWN. AREA WITHIN BLACK OUTLINE IS THE PADDOCK BOUNDARY.

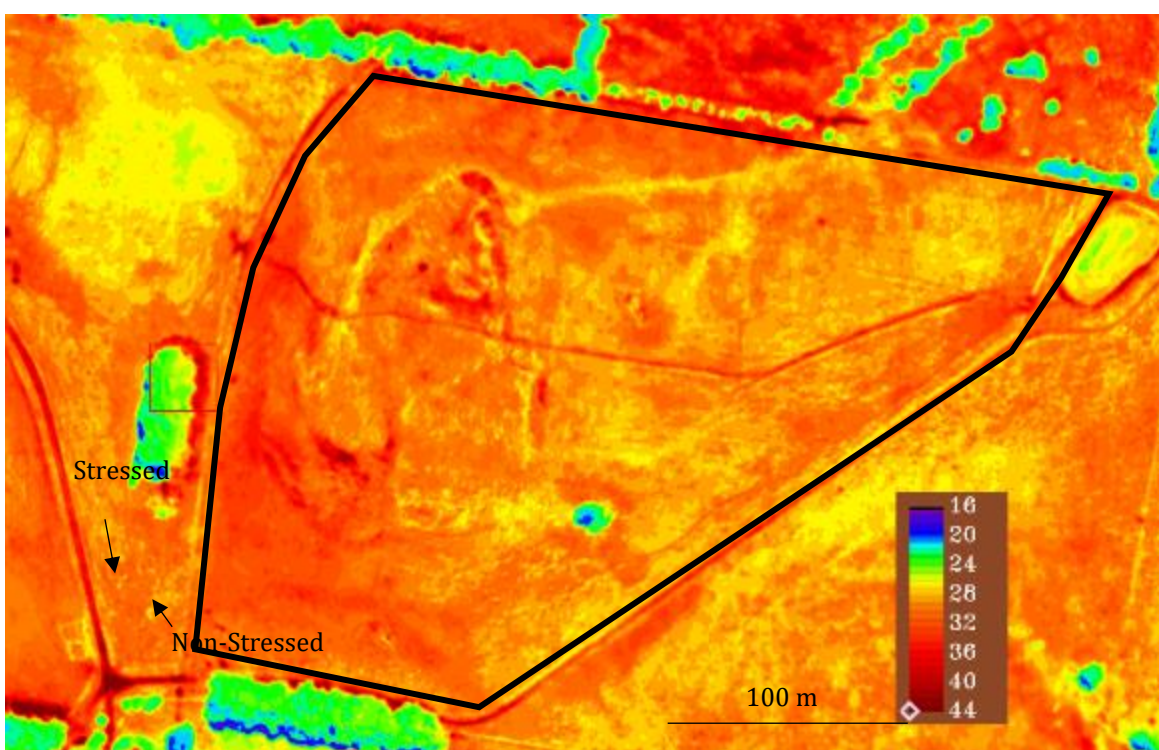


FIGURE 86. PASTURE CANOPY TEMPERATURES (DEG C) WERE OBTAINED REMOTELY (BY PLANE) ON 29/11/2021. STRESSED AND NON-STRESSED FIELD PLOTS AND A BROADER AREA (PADDOCKS) ARE SHOWN. AREA WITHIN BLACK OUTLINE IS THE PADDOCK BOUNDARY.

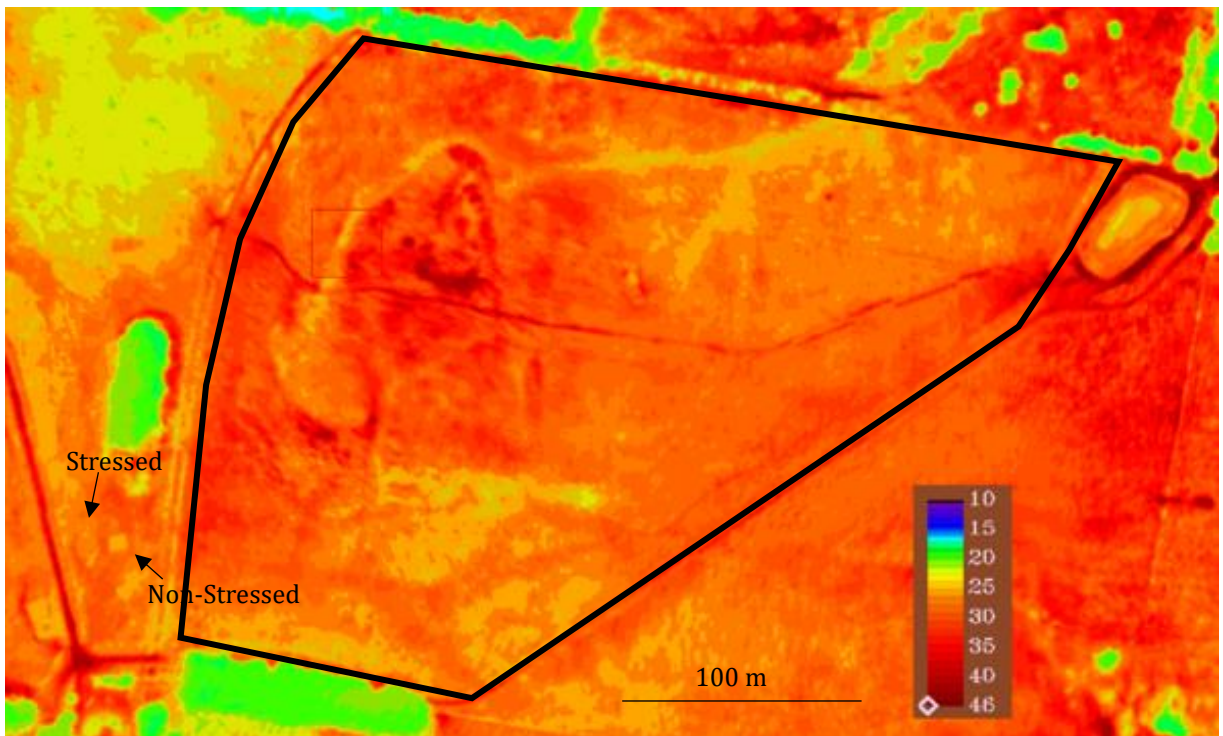
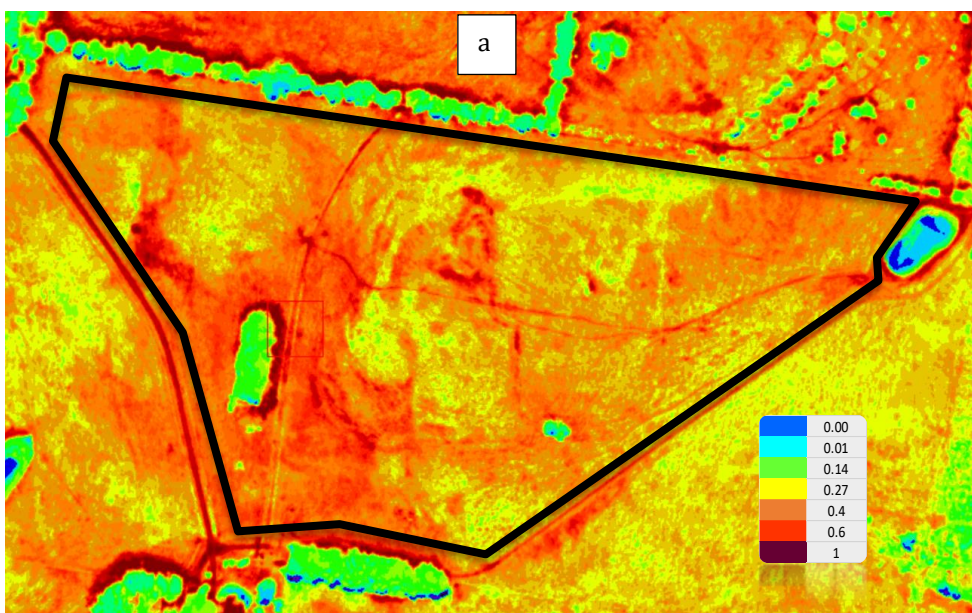


FIGURE 87. PASTURE CANOPY TEMPERATURES (DEG C) WERE OBTAINED REMOTELY (BY PLANE) ON 14/12/2021. STRESSED AND NON-STRESSED FIELD PLOTS AND A BROADER AREA (PADDOCKS) ARE SHOWN. AREA WITHIN BLACK OUTLINE IS THE PADDOCK BOUNDARY.

Figure 88 shows the CWSI calculated by the different approaches spatially for the data for the first flight (14/12/2020).



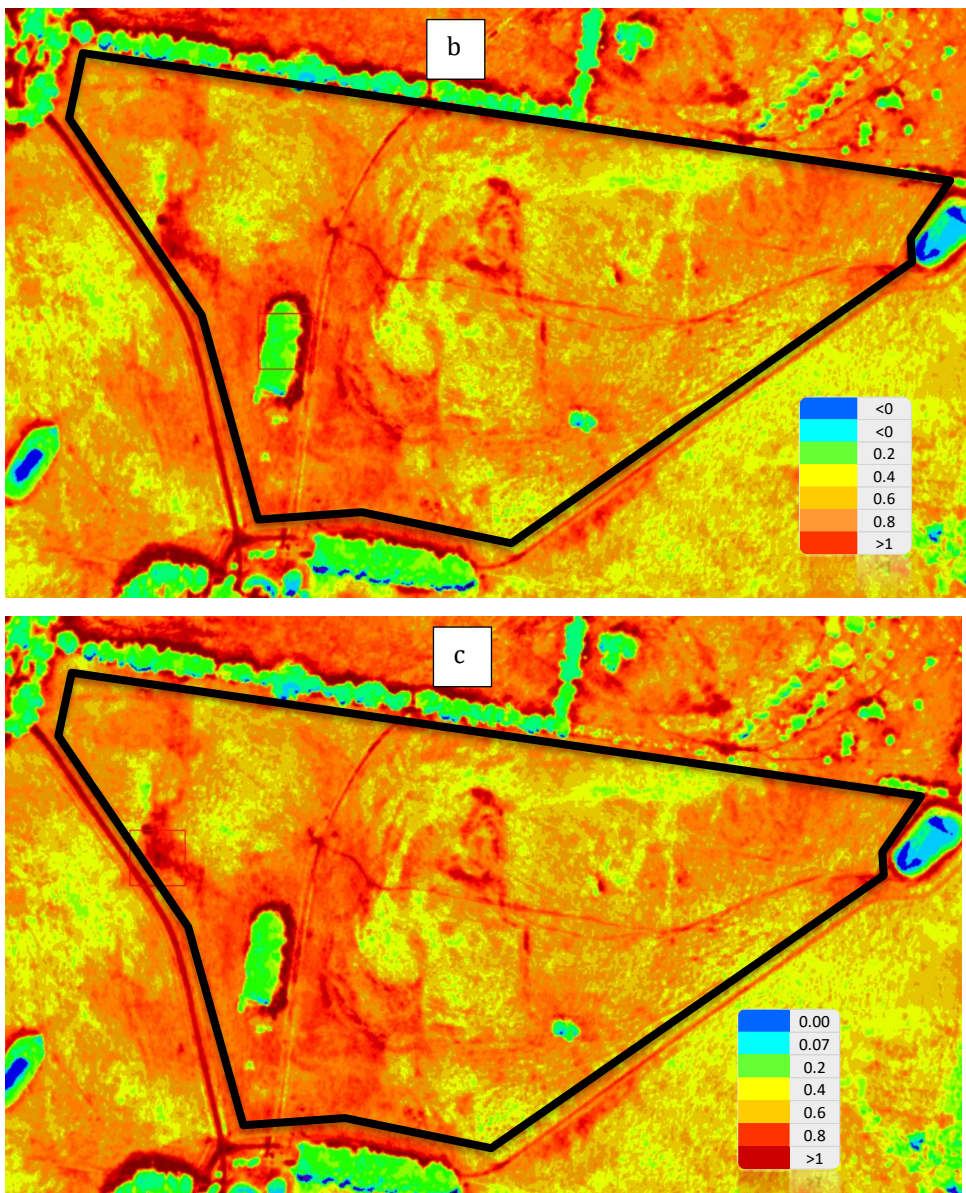


FIGURE 88. ANALYSIS OF THE CWSI RANGE FOR FLIGHT 1 OVER SEVERAL PADDOCKS, USING THE (A) BASELINE, (B) EMPIRICAL AND (C) ADAPTIVE CWSI METHODS.

Analysis of the % CWSI range for (a) flight 1 (14/12/2020) and (b) flight 2 (29/11/2021) using the baseline, empirical and adaptive CWSI methods (Figure 88). The ambient temperature on the day of flight 1 was 33 °C compared to 22 °C for flight 2. As a result of the higher ambient temperatures during flight 1 the pasture canopy temperatures were higher and as seen in figure 88 the resultant CWSI's were higher than flight 2. Examining the average CWSI's for each method (figure 89), the empirical and baseline method showed a clearly higher average CWSI for flight 1 than flight 2. The average CWSI using the adaptive approach was similar for flight 1 and flight 2.

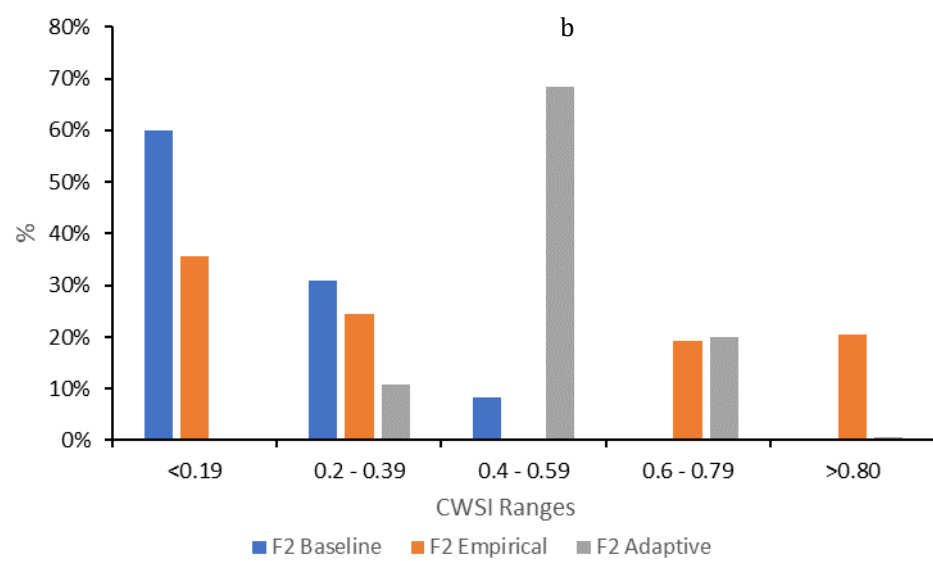
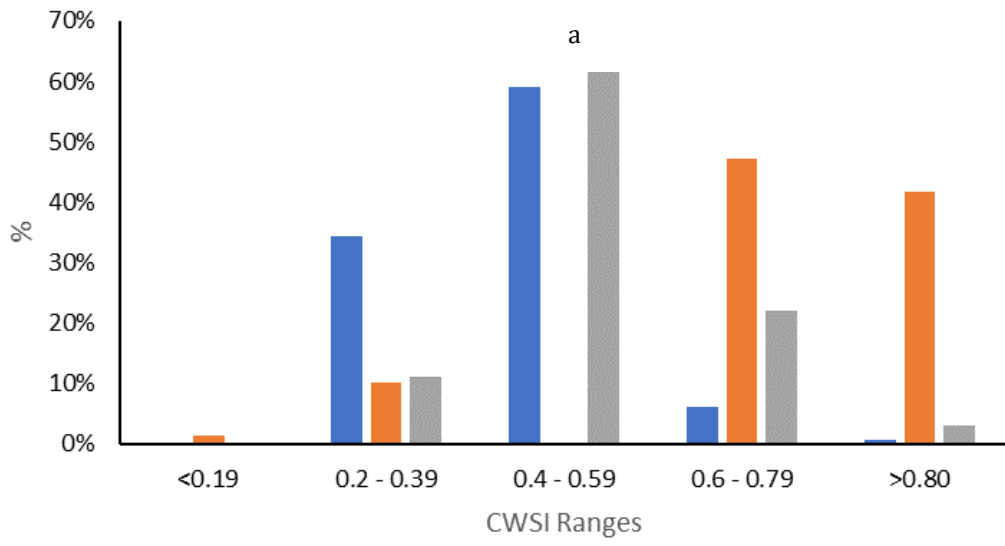


FIGURE 89. ANALYSIS OF THE % CWSI RANGE FOR (A) FLIGHT 1 (14/12/2020) AND (B) FLIGHT 2 (29/11/2021) USING THE BASELINE, EMPIRICAL AND ADAPTIVE CWSI METHODS.

The area average CWSI for flight 1 (14/12/2020) and flight 2 (29/11/2021) for the baseline, empirical and adaptive CWSI methods is shown in Figure 90.

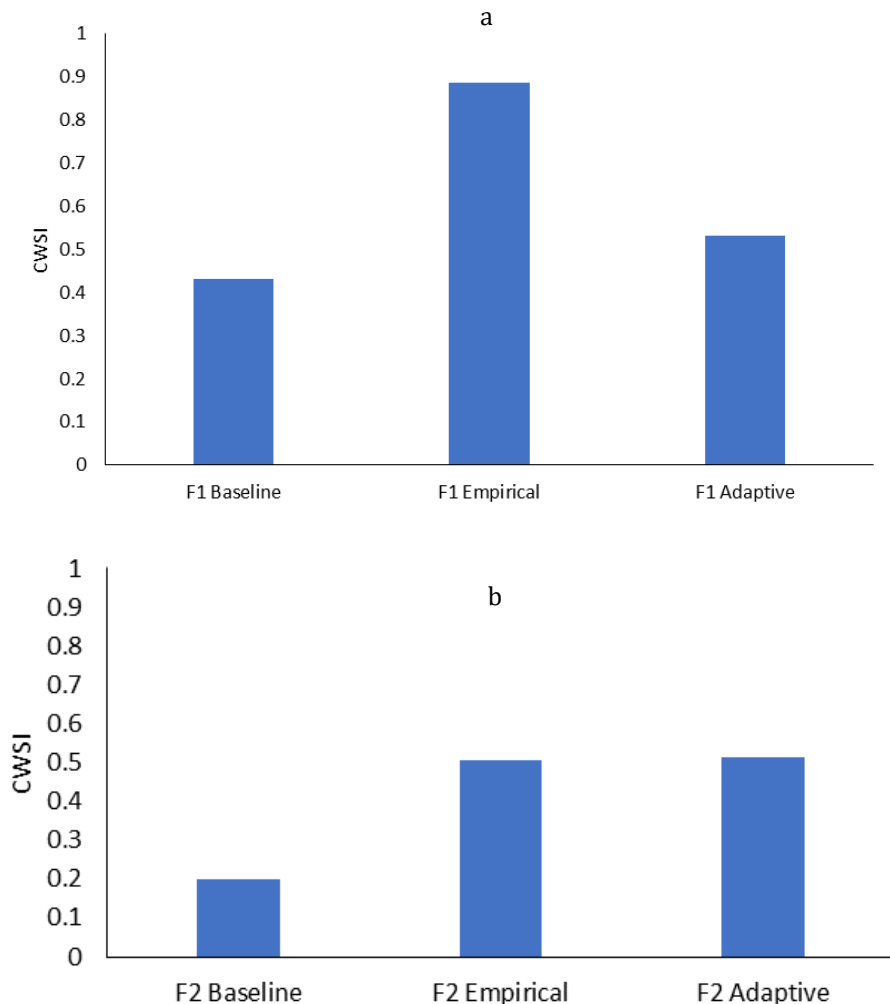


FIGURE 90. AVERAGE CWSI FOR (A) FLIGHT 1 (B) FLIGHT 2, USING THE DIFFERENT CWSI CALCULATION METHODS.

6.4 Discussion

Using the CWSI calculation methods (baseline-derived, empirical, and adaptive), the CWSI for the plot areas and spatially across the paddocks were calculated. All methods used a form of stressed and non-stressed plant canopy temperature to calculate the CWSI but these temperatures were derived in different ways. The baseline approach was derived from collecting canopy temperatures of stressed and non-stressed plants over time to develop the baselines as undertaken in chapter 4 and 5. The empirical CWSI approach only uses two canopy temperatures on the day of sampling, one from a stressed plant and one from a non-stressed plant. In using the empirical approach, we must ensure the two points selected for the CWSI accurately reflect an example of a stressed and a non-stressed pasture. The adaptive CWSI approach uses more data points (pixels) from a larger area to determine the maximum and minimum pasture canopy temperatures across the target areas. Before calculating the adaptive CWSI non pasture canopy temperatures need to be removed (bare ground, roads, trees, water bodies, etc) as temperatures from these areas can vary considerably from pasture canopy

temperatures and so affect the CWSI considerably. For the adaptive CWSI to work well, there needs to be a representative stressed and non-stressed plant in the field of view to produce an accurate CWSI, which may not always be possible.

In the data collected on 14/12/2020, due to the time of year (early summer) and nature of the season, there was a lot of canopy temperature variation across the paddock, due to some pasture experiencing water stress, other pastures starting to undertake senescence, whilst other pastures were still growing. As a result, there was a large amount of canopy temperature variation across the paddocks. The ambient temperature was 33°C on the day (14/12/2020). However in the data collected in the second (29/11/2021) and third (14/12/2021) flights, the ambient temperature on the day of the flights was lower, 22°C and 20°C respectively, and the field conditions leading up to the flight had not been as dry, resulting in more plants that were not under water stress and therefore resulted in lower canopy temperatures than the first flight which can be seen in figure 87. The average CWSI temperatures for flight 1 were higher than the average temperatures for flight 2 (Figure 90). Similarly, looking at the % CWSI ranges (Figure 89), flight 2 had more of the results in the lower % CWSI ranges.

The baseline and empirical CWSI (using a fully stressed plant) will give a more accurate result for plant water stress, and the adaptive CWSI will be less accurate; however, the adaptive CWSI will still highlight areas of plant water stress in the field over a broad area (farm scale). The adaptive CWSI can provide a faster (although less accurate) way to identify plant water stress in the field, although the extent of the water stress will not be known as the CWSI calculation does not necessarily include a stressed and non-stressed canopy temperature like the baseline and empirical CWSI approach. The adaptive approach may not be accurate enough to set irrigation limits. However, it may assist users in identifying which parts of their paddocks are under stress compared to the pastures around them, which could then be visually inspected in the field. The adaptive approach would be suitable for using for irrigation controls if a stressed and non stressed plant was within the area where the data is collected for the histogram.

The baseline and empirical CWSI method could be used in the field for irrigation control. The baseline approach relies on many months of collecting field temperature data to generate the baselines, incorporating a range of temperatures and seasons in the final baseline whereas the other two methods (empirical and adaptive) rely only on collecting plant canopy temperatures on the day of analysis. Whilst the empirical approach relies on having a stressed and non stressed plant for the calcultion, its not always possible in the field to have a fully stressed plant. In this study we chose not to use a rain out shelter as introducing a rainout shelter introduces other variables that can affect the microclimate and therefore the plants water stressed state and would also have added complications for aerial data gathering, effectively blocking the pasture from the FLIR camera mounted to the plane. As a result, our stressed plant although stressed, may not have been fully stressed.

The main finding was that the CWSI can be generated using the baseline, empirical and adaptive approaches. If the adaptive CWSI is undertaken when there is a range

of plant water stress occurring in a paddock, then the resultant adaptive CWSI is closer to the baseline and empirical CWSI.

This work expands on the work by Park *et al.* (2017) and demonstrates that an adaptive CWSI could be developed. Using the adaptive approach with pastures was different to how Park *et al.* (2017) initially used the adaptive approach. This work, using the adaptive approach demonstrated that the adaptive approach can add value in identifying plant water stress spatially, however it is not always accurate enough to use for irrigation controls if stressed and non stressed plants are not used.

The shortcomings of using the adaptive CWSI is that the accuracy can be an issue if no stressed or non-stressed plant is present. Although it can be quicker than developing baselines, the process of data gathering and analyse takes time. The user needs access to a current thermal image area of the area in question. They then need access to geospatial software, and then they need to sort the canopy temperatures and develop the histogram. The shortcomings are that a stressed and non-stressed plant is still required to generate an accurate empirical and adaptive CWSI. The stressed plant can be similar to the ones in this experiment, where they were not watered, or similar to other studies (Park *et al.* 2017), where irrigation is stopped for several days before measuring the CWSI. Similarly, a well-watered plant also needs to be used, which could be undertaken similarly to this experiment where it receives specific watering in the field or similar to Park *et al.* (2017), where the plants receive 100% irrigation treatment.

There is minimal literature using an adaptive CWSI. Previous work using a form of adaptive CWSI was undertaken by Park *et al.* (2017, 2021) on nectarines and peaches. The method used to develop the baseline is similar to what has been documented by Idso and used extensively since the 1980's. The adaptive CWSI approach is relatively new, with Park *et al.* (2017) recently completing work on a similar approach.

One implication of using the CWSI in this region (South of the Great Dividing Range) is the occurrence of clouds throughout the year, making it challenging to collect data to develop and test the CWSI. A lot of the early work on developing the CWSI was done in the USA by Idso in Arizona, North Dakota, Nebraska, Kansas, etc, in arid environments with limited clouds. Idso (1981) mentions that his work was undertaken with clear skies and some thin cirrus conditions. He further mentions that the relationship begins to fall down for other types of cloudiness, presumably due to changing illumination effects on stomates (Idso, 1981). Consideration needs to be given to the usefulness of using the empirical and adaptive CWSI in non-arid regions.

Another difficulty in using the CWSI in grazed pastures is the variability introduced by cattle grazing practices, where a pasture may be long one day and shorter a few days after grazing.

Relying solely on spatial images, such as Figure 88, can make it challenging to quickly identify the differences visually between the CWSI methods. However, sorting the data into CWSI ranges and averages, such as in Figures 89 and 90, can

aid in evaluating the spatial data and make it easier to make management decisions from the data.

6.5 Conclusion

Developing the CWSI using the baseline, empirical and adaptive approach was carried out and assessed. The three approaches identified areas across the paddock that ranged from stressed to non-stressed. Whilst more confidence is given to the baseline and empirical CWSI approach as it inherently includes stressed and non-stressed pasture canopy temperatures within the formulae calculation, using the adaptive CWSI approach was still able to identify a range of stressed to non-stressed plants across the field. Once the baselines are developed, calculating the CWSI using the baseline approach is quick, only needing the plant canopy and air temperatures. Using the empirical and adaptive approach in the field requires a lot more data collection, synthesis and calculation.

7 General Discussion

7.1 Introduction

With improved approaches to monitor plant water stress in pastures together with improved pasture forecasting, primary producers can manage the risks associated with climate variability better. This work examined the use of the SGS biophysical model to assist farmers in looking ahead at pasture forecasts in the weeks and months ahead and at how the CWSI can assist farmers in monitoring the water stress of their pastures in the field. This study involved a combination of modelling and field work in pasture systems in medium-high rainfall zones of Southeast Australia.

7.2 Aims

This research aimed to assess the usefulness of soil water content (SWC) as a predictor of pasture growth at three sites in Victoria, Australia, across different climatic conditions and pasture types. This was done using The Sustainable Grazing Systems (SGS) pasture model to predict monthly pasture growth rates based on historically dry (10th percentile), moderate (50th percentile) or wet (90th percentile) Soil Water Content (SWC), simulated using local climate data from 1990-2020. Results were presented as the probability that pasture growth will be in the lowest, middle, or top tercile (third) of expected monthly growth rates.

Another aim was to develop the CWSI for two pasture types (phalaris-based and annual ryegrass) in Southeast Australia by measuring the canopy temperature differentials between the stressed and non-stressed pastures to develop their baselines and the CWSI. Another aim was to compare methods for calculating the CWSI, using an adaptive, empirical and baseline approach.

7.3 Key findings and original contributions

Chapter 3 assessed the usefulness of SWC to predict pasture growth for a one-to-three-month period, using the SGS Pasture Model at three sites across central and southwest Victoria, Australia. The study consisted of two main components: to validate the simulated SWC against measured data in the field and to predict monthly pasture growth rates based on historically dry (10th percentile), moderate (50th percentile) or wet (90th percentile) SWC on the first day of each month. The validation demonstrated that the modelled SWC from the SGS model was very similar to the actual SWC for the three sites. Whilst there are some variations between the two data sets, they tend to follow a similar drying down and wetting up sequence. The key questions were: Is soil water content (SWC) a useful predictor of pasture growth? If so, what are its strengths and weaknesses?

The findings demonstrated that pasture growth is most variable in Autumn and Spring but less variable in Winter when pasture growth is typically limited by temperature. The key findings of this study are that during the main growth periods, predictions of SWC are most useful where variation in pasture growth is high and affected by the initial soil water content. Predictions for lucerne showed a large variation in summer pasture growth predictions, depending on the starting

SWC. For Baynton, the forecasting skill was in October (Spring) and April and May (Autumn), at Pigeon Ponds it was in October and November (Spring) and April and May (Autumn) whilst at Dartmoor the forecasting skill was January through to April (Summer and Autumn). For example, considering Baynton in April, if the SWC is dry (40 mm) then this could lead to 21kg DM/ha, compared to a 33kg DM/ha if the SWC is wet. Over a 4-month period (April to July) this would translate to an average 2,735kg DM/ha for a wet SWC and 2,272kg DM/ha for a dry SWC. This varying pasture production as a result of the initial SWC can be large over a broad farm, and especially useful where stock is relying on only field grown pasture fodder for growth.

The more forewarning a farmer has, the more time is available to react and plan for a changing environment. If the farmer has site-specific tools that utilise historical local data, then they may have more confidence in the output being more relevant for their scenario. This modelling exercise using historical weather data and the farmer's soil moisture level at the start of each month means that predictions of pasture growth rates in the months ahead are more tailored and site-specific than modelling that is more generic and regional. These site-specific 'heads up' pasture growth forecasts can give the farmer more time to prepare for the upcoming season and give them more time to align the fodder budget with the expected pasture growth forecast, assisting farmers manage the risks of a variable climate. The results show that skill in forecasting pasture growth is highest in the first month of prediction and then declines over time (+1month, +2 month, +3 month), therefore more emphasis should be put on the short term predictions (Prediction month) and less emphasis should be on the longer term predictions, where intervening weather events may influence these longer term predictions.

This research also expanded on pasture growth predictions using the SGS model (Cullen *et al.* 2012) and compared different SWC at the start of each month to calculate pasture growth predictions for three sites around regional Victoria. The work demonstrates that SWC can be used to improve the prediction of pasture growth rates at these times of the year. The predicted pasture output tables could display tercile probabilities for the month of prediction and the following three months, given a dry, medium, or wet SWC at the start of the month. Modelling tools that can assist with predicting how much pasture is available to farmers can assist in managing risk in their agricultural business. Knowing how much fodder is available in the months ahead can affect livestock numbers and a business's economics. With increasing climate variability and global warming occurring, it would be interesting to see if and, if so, how much the winter pasture growth patterns may change over time.

Whilst the SGS model is a tool that can be used to predict future pasture production, one limitation is that setting up and running the SGS model is time-consuming and would be difficult for first-time users. Another limitation is that the output data from the SGS model also requires interpretation to understand what it is predicting.

Chapter 4 involved establishing water stressed (rainfed) and non-stressed (irrigated) pasture field plots and recording the pasture canopy temperature and VPD to develop the baselines so the CWSI could be calculated. Once the CWSI was

established, three flights were also undertaken to capture the pasture's canopy temperature remotely across the paddocks to see if the CWSI could be recorded spatially. The key questions were: Can the CWSI and baselines be developed for a pasture species in southeast Australia? If so, what are the limitations of using the CWSI and baselines on mixed pastures in southeast Australia? Can the CWSI and baselines be developed by gathering canopy temperatures remotely by plane? Can this data be used spatially to project the CWSI across a paddock or property?

The findings and new contributions to science demonstrated that the field experiment enabled the capturing of the pasture's canopy temperatures for the stressed and non-stressed plots, which could then be used to develop the baselines for pastures (figure 91). It was possible to project the CWSI baselines across the paddock/farm spatially. This adds to the work on developing baselines for alfalfa, tomato, sunflower, cotton, cowpeas, etc undertaken by Idso *et al.* (1982) and others, compiled by Maes *et al.* (2012). The phalaris and annual ryegrass non stressed baselines (figure 91) are somewhat similar and different. There is a pronounced difference between the stressed baselines, with the stressed baseline for the phalaris pasture higher than the annual rye grass. The differences in the baselines are due to two different species being measured, which can differ in transpiration response to environmental constraints (Gonzalez – Dugo *et al* 2022). The data to develop the pasture baselines was collected over a longer time interval (October 2020 - January 2022) than the data to collect the annual rye grass baseline (18/10/2021 – 1/2/2022) which may also affect the baselines. Future work gathering data over a longer time period would be an interesting addition to this work, to determine if the longer data gathering time frame would affect the baselines.

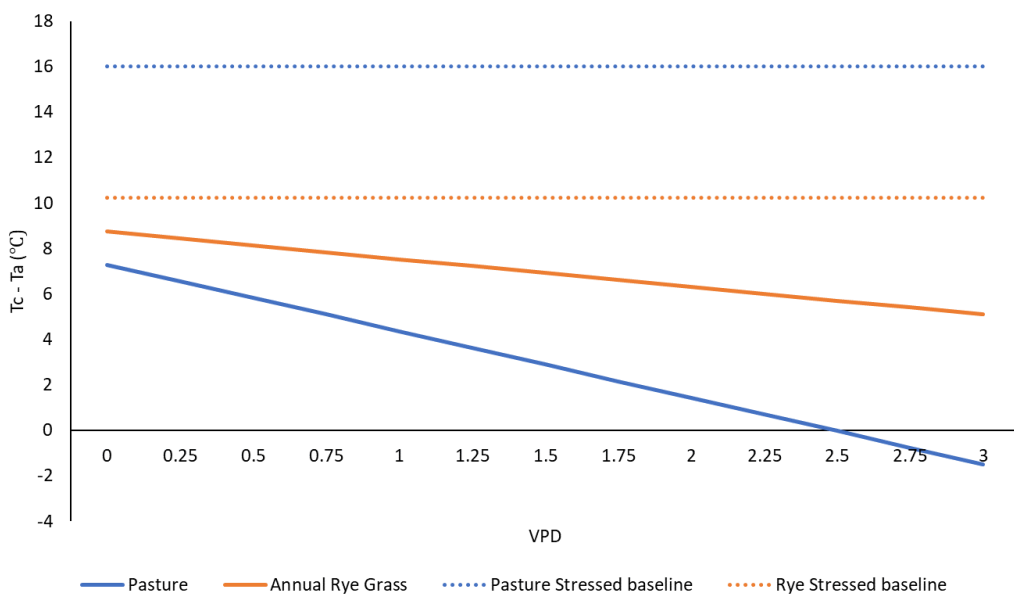


FIGURE 91. COMPARING PASTURE AND ANNUAL RYEGRASS STRESSED AND NON-STRESSED BASELINES DEVELOPED IN SE AUSTRALIA AS PART OF THE FIELD WORK UNDERTAKEN FOR THIS THESIS.

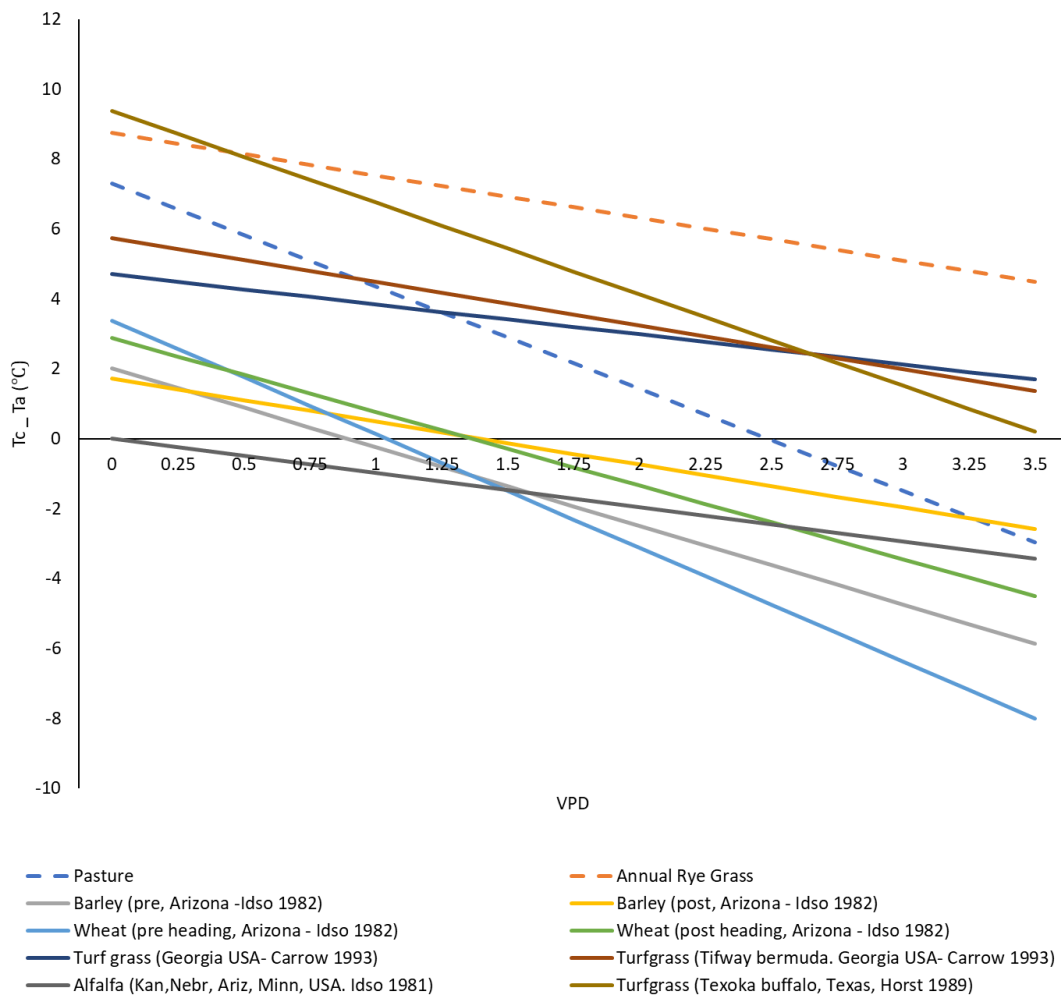


FIGURE 92. COMPARING THE PASTURE AND ANNUAL RYEGRASS NON-STRESSED BASELINES DEVELOPED AS PART OF THIS THESIS AGAINST A NUMBER OF OTHER PLANTS.

The thermal canopy data collected aerially could also be used to develop the CWSI over the paddock and farm scale. The applicability of these results showed that using the CWSI in pastures is a valuable tool for assessing the variability of crop water stress over pasture paddocks. Areas of stressed to non stressed pastures could be observed in the spatial images, clearly identifying the variance in plant water stress across the paddock.

Chapter 5, like Chapter 4, involved setting up stressed and non-stressed field plots and recording the annual ryegrasses canopy temperature and VPD over time to develop the baselines (Figure 91) so the CWSI for annual ryegrass could be calculated. The baselines vary from one plant to another as demonstrated in Figure 92, due to a number of factors including varying leaf stomatal densities between species (Costa *et al.* 2012), different hormonal regulation of stomata (Schultz 2003), the size of the canopy leading to different velocities in dehydration (Rogiers *et al.* 2009), etc.

It was possible to remotely record canopy temperature differences between stressed and non-stressed annual ryegrass plants in the field. From the temperature differentials in the canopy temperatures of the stressed and non-stressed annual

ryegrass pastures, it was possible to develop the stressed and non-stressed baselines and resulting CWSI. The result was the development of baselines for annual ryegrass pastures.

Using the CWSI results can potentially assist farmers in managing fodder production. Knowing the state of the pasture's water stress at any one time gives managers time to react to changes in pasture growth. If a pasture is getting increasingly stressed and no irrigation is possible, farmers may preferentially graze it before it deteriorates further or cut it for fodder to conserve some of the quality. Better monitoring of the plant's water stress would improve pasture utilisation and resource management.

It was possible, although difficult, to use the CWSI in a non-arid region. Using the CWSI with a drone to collect the canopy's thermal temperatures would help the farmer be quick and nimble to collect the thermal temperatures when clouds are absent. With drones becoming cheaper and easier to use, as well as the thermal cameras coming down in cost, collecting actual data at the farm level is more realistic than ever.

As these field trials were conducted in the field, without a rainout shelter, it was not possible to fully limit rainfall falling on the stressed field plot, therefore the stressed plants may not have been fully stressed. A rainout shelter could be used, however this addition may affect the pastures growth by altering the microclimate and therefore add other variables. Not having a 'fully' stressed plant could affect the CWSI calculations by potentially having a lower stressed baseline than a fully stressed pasture.

This research contributes towards the remote gathering and use of the CWSI in pastures in Southeast Australia. The resulting baselines for annual ryegrass and mixed species have been developed, and further work in this field could result in further baselines for pastures in different climates and micro climates. This work demonstrates that the CWSI can work on pastures, giving farmers a new tool to monitor their pastures. The earlier a farmer knows the condition of their pasture is deteriorating, the more time they have to react. If the farmers first notice that there is water stress in their pastures by the visible presence of senescence or wilting, then the window is small to react to the situation by cutting hay, irrigating, grazing, etc. However, using the CWSI, farmers can see the deterioration of their pastures prior to senescing. The CWSI also allows the farmer to see which plants are more stressed than others, therefore giving the farmer the ability to target any remedial action they take to the affected pastures.

Prior to this work, no research was found using the CWSI in the Australian grazing pasture context. As access to drones and thermal cameras increases, farmers can undertake their analyses, developing the CWSI for their pastures. Similarly, as the number of satellites increases (O'Reilly *et al.* 2021), with more satellites with thermal infra red cameras attached (Stavros *et al.* 2017), farmers can access the satellites to retrieve the thermal data. Along with the increasing number of satellites, the return time of satellites is being reduced, so instead of waiting a week for a satellite to return to an area, the return times are getting smaller and smaller. Being able to compare the CWSI of the pasture more regularly allows the farmers

to pick up changes quicker than if they must wait for a week to get the subsequent data from a satellite, by which time the pasture may have deteriorated significantly.

Chapter 6 compares the 'baseline' calculated CWSI (refer chapter 4) against the CWSI developed 'empirically' and an 'adaptive' CWSI method similar to the one Park *et al.* (2017) used on pasture species in Southeast Australia. The key questions were: How comparable are the three CWSI methods (baseline, empirical, and adaptive), and how comparable is the adaptive method as a method that does not use a stressed and non-stressed plant to the other two methods? Are they interchangeable? What are the advantages and disadvantages of each method?

While each method gave a resultant CWSI, the baseline approach has been calculated by collecting data over a more extended period to generate the pasture's response to different climatic conditions. The adaptive approach gave insight into relative stress across a paddock; however, as it is unknown if a stressed or non-stressed plant is in the area used to develop the CWSI, it is unreliable as an accurate measure of the CWSI. Whilst the baseline method could be considered more robust, the other methods can provide insights to the farmer without additional information. For example, using the adaptive approach can still assist in developing a spatial image of the pasture, which gives the farmer an idea of the relative stress variation across a paddock or area, with the ability to pinpoint the farmer to areas of high stress. If the farmer wanted to use the CWSI results to set their irrigation, then the baseline approach, if developed for the local environment, should be suitable, whereas the adaptive approach would be unsuitable.

This work also shows the application of the CWSI in pastures of mixed species in mid to high-rainfall zones. Prior to this research, most work has been undertaken using the CWSI in more arable areas on crops and orchards. However, this work involved the use of the CWSI in a wetter environment and applied to pastures, demonstrating that the CWSI could be used as a new tool for Australian farms with regards to identifying plant water stress in pastures. Using CWSI in medium to high rainfall zones can present issues with data handling and gathering. Due to the increased amount of cloud compared to arid zones which results in extra data sorting before calculating baselines and the CWSI. The collecting, analysing and developing of the CWSI is also time-consuming, limiting its use in the present format for easy use on the farm.

This research examined gathering the CWSI data remotely using planes and infield canopy sensors. The use of planes and satellites is not always practical and cost-effective for primary producers, furthermore, there are limitations related to the need to collect flight/satellite data on a clear day (minimal cloud cover). Collecting the data remotely by satellite and plane or using the canopy sensors generates a lot of data, which must be filtered and sorted to meet the required output.

7.4 Future Research

7.4.1 Pasture Growth Forecasting

Further work to improve the pasture predictions could also involve combining seasonal forecasts into the SGS pasture model instead of relying on historical climate data. Seasonal forecasts can provide long range forecasts on rainfall and temperatures expected in the next 1 to 3 months. Farming forecaster is one tool that is starting to use current soil moisture to provide nowcasts (real time conditions) forecasts from 1 – 4 months (Mitchell *et al.* 2022). McDonnell *et al.* 2019 has used short term weather forecasts (up to ten days in advance) to predict short term grass growth in Ireland. Further work also needs to be conducted to investigate if farmers regard this work and the form it is presented as helpful in improving their risk management on their farms.

7.4.2 CWSI/Baselines

A broad range of different pasture species and combinations are used across SE Australia. This research highlights that different pasture species will respond differently and have different baselines. There is a need to develop baselines for different pasture types and regions. Future work could be undertaken on developing baselines for pastures, clover dominant pastures, annual and perennial ryegrass pastures at different locations and throughout the year, including examining baselines at different stages of growth throughout the season – (Vegetative, elongation and reproductive). Bellvert *et al.* (2015) and Idso (1982) found that non water stressed baselines differed depending on phenological stage and variety. How do these growth stages affect the pasture's canopy temperatures and resulting baselines?

Further work could also examine the use of the baselines in developing irrigation scheduling, similar to work undertaken by Kumar *et al.* (2019) on using the CWSI for scheduling irrigation for Indian Mustard, where they “postulate that irrigation should be provided when the CWSI value exceeds 0.4”. Finding a CWSI value whereby irrigation could be initiated would assist farmers who have access to irrigation, although considerations would need to be considered that the baseline used is suitable for the location. Alternatively, a baseline could be calculated for the particular location and tests undertaken to determine the appropriate CWSI to initiate irrigation for the particular location.

Further work could also involve the use of rainout shelter to limit any rainfall falling on the stressed plot in order to determine how no rainfall water affects the stressed baseline. This work would also need to consider if the use of a rainout shelter introduces other variables that influence the canopy temperature when calculating the stressed baseline, such as creating a microclimate limiting wind and solar radiation. Alternatively, a drone could be used to collect the thermal data, avoiding the long delay in getting the plane in the air. The drone would add a nimbleness, allowing canopy temperatures to quickly be measured on days of intermittent cloud cover.

Further work may combine the above-mentioned approaches for a more automated and accurate forecast. There is potential to test the use of canopy temperature sensors permanently set up in the field, with an algorithm that only computes data between 12-1 daily and filters for clouds, wind, rain, and other environmental

factors affecting the CWSI could be tested. Mohammed *et al* 2022 discusses using neural networks and the CWSI to develop an ‘intelligent and automatic’ system for irrigation. This canopy data could be fed into the SGS model to validate and improve the modelling pasture forecasts in real time.

7.5 Conclusions

In conclusion, the findings from this research can assist farmers with managing risks associated with climate variability by assisting them to improve pasture growth predictions in the months ahead using local, current and historical data. The predicted pasture output tables were able to display tercile probabilities for the month of prediction and the following three months given a dry, medium, or wet SWC at the start of the month, with the ability to give farmers a predicted pasture growth rate determined by their actual SWC, assisting farmers in estimating future fodder production and therefore stock health.

The findings from the research also demonstrates that the CWSI can be used on pastures, with stressed and non-stressed baselines being developed for pastures and annual ryegrass in Southeast Australia and also how the CWSI could be used spatially, across a paddock, on pastures in Southeast Australia. These results showed that using the CWSI in pastures is a valuable tool for assessing the variability of crop water stress over pasture paddocks/farms. The research also showed that there are several ways for using the CWSI, with the empirical approach being more reliable than the adaptive approach in this scenario. Using the CWSI on pastures in the Australian farming context could aid in increasing fodder production if irrigation water is available to water stressed pastures, applying irrigation at a predetermined CWSI threshold.

8 References

- Ahmad, U., Alvino, A., & Marino, S. (2021). A review of crop water stress assessment using remote sensing. *Remote Sensing*, 13, 4155.
- Akuraju, V. R., Ryu, D., & George, B. (2021). Estimation of root-zone soil moisture using crop water stress index (CWSI) in agricultural fields. *GIScience & Remote Sensing*, 58(3), 340-353.
- Albornoz, C., & Giraldo, L. F. (2017, October). Trajectory design for efficient crop irrigation with a UAV. In 2017 IEEE 3rd Colombian Conference on Automatic Control (CCAC) (pp. 1-6). IEEE.
- Alderfasi, A., & Nielson, D. (2001). Use of crop water stress index for monitoring water status and scheduling irrigation in wheat. *Agricultural Water Management*, 47(1), 69-75.
- Al-Faraj, A., Meyer, G. E., & Horst, G. L. (2001). A crop water stress index for tall fescue (*Festuca arundinacea* Schreb.) irrigation decision-making—A traditional method. *Computers and Electronics in Agriculture*, 31(2), 107-124.
- Anderson, M. W., Cunningham, P. J., Reed, K. F. M., & Byron, A. (1999). Perennial grasses of Mediterranean origin offer advantages for central western Victorian sheep pasture. *Australian Journal of Experimental Agriculture*, 39(3), 275-284.
- Apolo-Apolo, O. E., Martínez-Guanter, J., Pérez-Ruiz, M., & Egea, G. (2020). Design and assessment of new artificial reference surfaces for real time monitoring of crop water stress index in maize. *Agricultural Water Management*, 240, 106304. experimental Agriculture, 39(3), 275-284.
- Ash, A., O'Reagain, P., McKeon, G., & Smith, M. S. (2000). Managing climate variability in grazing enterprises: a case study of Dalrymple Shire, north-eastern Australia. *Applications of seasonal climate forecasting in agricultural and natural ecosystems*, 253-270.
- Ash, A., McIntosh, P., Cullen, B., Carberry, P., & Stafford Smith, M. (2007). Constraints and opportunities in applying seasonal climate forecasts in rural industries. *Australian Journal of Agricultural Research*, 58, 952-965.
- ASCE-EWRI. (2005). The ASCE standardized reference evapotranspiration equation. In 'Reported by the American Society of Civil Engineers (ASCE) Task Committee on Standardization of Reference Evapotranspiration'.
- Bah, M. D., Hafiane, A., & Canals, R. (2017, November). Weeds detection in UAV imagery using SLIC and the hough transform. In 2017 Seventh International Conference on Image Processing Theory, Tools and Applications (IPTA) (pp. 1-6). IEEE.
- Banerjee, K., & Krishnan, P. (2020). Normalized Sunlit Shaded Index (NSSI) for characterizing the moisture stress in wheat crop using classified thermal and visible images. *Ecological Indicators*, 110, 105947.

- Banhazi, T. M., Lehr, H., Black, J. L., Crabtree, H., Schofield, P., Tscharke, M., & Berckmans, D. (2012). Precision livestock farming: an international review of scientific and commercial aspects. *International Journal of Agricultural and Biological Engineering*, 5(3), 1-9.
- Banu, S. (2015). Precision agriculture: tomorrow's technology for today's farmer. *Journal of Food Processing & Technology*, 6(8), 1.
- Barbosa da Silva, B., & Ramana Rao, T. (2005). The CWSI variations of cotton crop in a semi-arid regional of Northeast Brazil. *Journal of Arid Environments*, 649-659.
- Baret, F., Madec, S., Irfan, K., Lopez, J., Comar, A., Hemmerle, M., Dutare, D., Praud, S., & Tixier, M. (2018). Leaf-rolling in maize crops: from leaf scoring to canopy-level measurements for phenotyping. *Journal of Botany*, 69, 2705-2716.
- Barrett, P. D., Laidlaw, A. S., & Mayne, C. S. (2004). An evaluation of selected perennial ryegrass growth models for development and integration into a pasture management decision support system. *The Journal of Agricultural Science*, 142(3), 327-334.
- Bartell, C., Bayabil, H. K., Schaffer, B., Tilahun, F., & Getachew, F. (2021). Measuring Leaf Water Potential: AE563/AE563, 10/2021. *EDIS*, 2021(5).
- Batke, S., Yiotis, C., Elliot-Kingston, C., Holohan, A., & McElwain, J. (2020). Plant responses to decadal scale increments in atmospheric CO₂ concentration: comparing two stomatal conductance sampling methods. *Planta*, 251, 52.
- Beitnes, S., Kopainsky, B., & Potthoff, K. (2022). Climate change adaptation processes seen through a resilience lens: Norwegian farmers' handling of the dry summer in 2018. *Environmental Science and Policy*, 133, 146-154.
- Bell, M. J., Cullen, B. R., Christie, K. M., Rawnsley, R., & Eckard, R. J. (2011). Is the variability of seasonal pasture growth patterns changing? 2nd Annual Conference of the Grassland Society of Southern Australia Inc., 2011 Hamilton, Victoria, 113-116.
- Bellvert, J., Zarco-Tejada, P. J., Girona, J., & Fereres, E. J. P. A. (2014). Mapping crop water stress index in a 'Pinot-noir' vineyard: comparing ground measurements with thermal remote sensing imagery from an unmanned aerial vehicle. *Precision agriculture*, 15, 361-376.
- Bellvert, J., Marsal, J., Girona, J., Zarco-Tejada, P. (2015) Seasonal evolution of crop water stress index in grapevine varieties determined with high – resolution remote sensing thermal imagery. *Irrigation Science* DOI 10.1007/s00271-014-0456-y.
- Berni, J., Zarco-Tejada, P., Sepulcre-Canto, G., & Fereres, E., & Villalobos, F. (2009). Mapping Canopy conductance and CWSI in olive orchards using high-resolution thermal remote sensing imagery. *Remote Sensing of Environment*, 2380-2388.
- Beukes, P. C., Palliser, C. C., Macdonald, K. A., Lancaster, J. A. S., Levy, G., Thorrold, B. S., & Wastney, M. E. (2008). Evaluation of a whole-farm model for pasture-based dairy systems. *Journal of Dairy Science*, 91(6), 2353-2360.

- Bian, J., Zhang, Z., Chen, J., Chen, H., Cui, C., Li, X., ... & Fu, Q. (2019). Simplified evaluation of cotton water stress using high resolution unmanned aerial vehicle thermal imagery. *Remote Sensing*, 11(3), 267.
- Biju, S., Fuentes, S., & Gupta, D. (2018). The use of infrared thermal imaging as a non-destructive screening tool for identifying drought-tolerant lentil genotypes. *Plant physiology and biochemistry*, 127, 11-24.
- Blanco, V., & Kalcsits, L. (2021). Microtensiometers accurately measure stem water potential in woody perennials. *Plants*, 10(12), 2780.
- Brown, J. N., Hochman, Z., Holzwirth, D., & Horan, H. (2018). Seasonal climate forecasts provide more definitive and accurate crop yield predictions. *Agricultural and Forest Meteorology*, 260, 247-254.
- Brown, J. N., Ash, A., MacLeod, N., & McIntosh, P. (2019). Diagnosing the weather and climate features that influence pasture growth in Northern Australia. *Climate Risk Management*, 24, 1-12.
- Bucks, D. A., Nakayama, F. S., French, O. F., Legard, W. W., & Alexander, W. L. (1985). Irrigated guayule—evapotranspiration and plant water stress. *Agricultural water management*, 10(1), 61-79.
- Calderon, R., Navas-Cortes, J.A., Zarco-Tejada, P.J., (2015) Early detection and quantification of Verticillium wilt in olive using Hyperspectral and thermal imagery over large areas. *Remote Sens.* 7, 5584–5610. <https://doi.org/10.3390/rs70505584>
- Carberry, P. S., Hochman, Z., McCown, R. L., Dalgliesh, N. P., Foale, M. A., Poulton, P. L., & Robertson, M. J. (2002). The FARMSCAPE approach to decision support: farmers', advisers', researchers' monitoring, simulation, communication and performance evaluation. *Agricultural systems*, 74(1), 141-177.
- Castle, M., Lubben, B. D., & Luck, J. (2015). Precision agriculture usage and big agriculture data.
- Chapman, D. F., Cullen, B. R., Johnson, I. R., & Beca, D. (2009). Inter-annual variation in pasture growth rate in Australian and New Zealand dairy regions and its consequences for system management. *Animal Production Science*, 49, 1071-1079.
- Chapman, D., Rawnsley, R., Cullen, B., & Clark, D. (2013). Inter-annual variability in pasture herbage accumulation in temperate dairy regions: causes, consequences, and management tools. 2013 Proceedings of the 22nd international grassland conference.
- Ciezkowski, W., Szporak-Wasilewska, S., Kleniewska, M., Jozwiak, J., Gnatowski, T., Dabrowski, P., Goraj, M., Szatylowicz, J., Ignar, S., Chormanski, J. (2020) Remotely sensed land surface temperature -based water stress index for wetland habitats. MDPI, *Remote Sensing*. DOI: 10.3390/rs12040631
- Clark, S. G., Austen, E. A., Prance, T., & Ball, P. D. (2003). Climate variability effects on simulated pasture and animal production in the perennial pasture zone of south-eastern Australia. 1. Between year variability in pasture and animal production. *Australian Journal of Experimental Agriculture*, 43(10), 1211-1219.

- Collins, B., & Chenu, K. (2021). Improving productivity of Australian wheat by adapting sowing date and genotype phenology to future climate. *Climate Risk Management*, 32, 100300
- Colombo, R., Bellingeri, D., Fasolini, D., & Marino, C. M. (2003). Retrieval of leaf area index in different vegetation types using high resolution satellite data. *Remote sensing of environment*, 86(1), 120-131.
- Conaty, W. C., Burke, J. J., Mahan, J. R., Neilsen, J. E., & Sutton, B. G. (2012). Determining the optimum plant temperature of cotton physiology and yield to improve plant - based irrigation scheduling. *Crop Science*, 52(4), 1828-1836.
- Conaty, W. C., Mahan, J. R., Neilsen, J. E., & Constable, G. A. (2014). Vapour pressure deficit aids the interpretation of cotton canopy temperature response to water deficit. *Functional Plant Biology*, 41(5), 535-546.
- Costa, J. M., Ortuño, M. F., Lopes, C. M., & Chaves, M. M. (2012). Grapevine varieties exhibiting differences in stomatal response to water deficit. *Functional Plant Biology*, 39(3), 179-189.
- Cullen, B. R., Johnson, I. R., Eckard, R. J., Lodge, G. M., Walker, R. G., Rawnsley, R. P., & McCaskill, M. R. (2009). Climate change effects on pasture systems in south-eastern Australia. *Crop and Pasture Science*, 60, 933.
- Cullen, B. R., Eckard, R. J., Callow, M. N., Johnson, I. R., Chapman, D. F., Rawnsley, R. P., ... & Snow, V. O. (2008). Simulating pasture growth rates in Australian and New Zealand grazing systems. *Australian Journal of Agricultural Research*, 59(8), 761-768.
- Cullen, B. R., & Johnson, I. R. (2012, October). Using soil water content to predict pasture growth rates. In Capturing Opportunities and Overcoming Obstacles in Australian Agronomy' (Ed I Yunusa) Proceedings of the 16th Australian Agronomy Conference.
- Cullen, B., Eckard, R., D., & Rawnsley, R. (2012). Resistance of pasture production to projected climate changes in south-eastern Australia. *Crop and Pasture Science*, 63, 77-86.
- Culvenor, R., Boschma, S., & Reed, K. (2007). Persistence of winter-active phalaris breeding populations, cultivars, and other temperate grasses in diverse environments of south-east Australia. *Australian Journal of Experimental Agriculture*, 47, 136-148.
- Culvenor, R. A. (2009). Breeding and use of summer - dormant grasses in southern Australia, with special reference to phalaris. *Crop Science*, 49(6), 2335-2346.
- Culvenor, R., Simpson, R. (2014). Persistence traits in perennial pasture grasses: the case of phalaris (*Phalaris aquatica* L.). *Crop and Pasture Science*, 65, 1165-1176.
- Culvenor, R., Clark, S., Harris, C., Hayes, R., Li, G., Nie, Z., Norton, M., & Partington, D. (2016). Field evaluation of cocksfoot, tall fescue, and phalaris for dry marginal environments of south-eastern Australia. 2. Persistence. *Journal of Agronomy and Crop Science*, 202, 355-371.

- Dar, Z. A., Sheshsayee, M. S., Ajaz, A., Pratibha, M. D., Khan, J. A., & Biradar, J. (2016). Thermal induction response (TIR) in temperate maize Inbred lines. *Ecol. Environ. Conserv.*, 22, 387-393.
- Davies, S., & Peoples, M. (2003). Identifying potential approaches to improve the reliability of terminating a lucerne pasture before cropping: a review. *Australian Journal of Experimental Agriculture*, 43, 429-447.
- De Castro, A. I., Torres-Sánchez, J., Peña, J. M., Jiménez-Brenes, F. M., Csillik, O., & López-Granados, F. (2018). An automatic random forest-OBIA algorithm for early weed mapping between and within crop rows using UAV imagery. *Remote Sensing*, 10(2), 285.
- Donatelli, M., Magarey, R., Bregaglio, S., Willocquet, L., Whish, J., & Savary, S. (2017). Modelling the impacts of pests and disease on agricultural systems. *Agricultural Systems*, 155, 213-224.
- Epiphanio, J. N., & Huete, A. R. (1995). Dependence of NDVI and SAVI on sun/sensor geometry and its effect on fAPAR relationships in Alfalfa. *Remote Sensing of Environment*, 51(3), 351-360.
- Farooq, M., Riaz, S., Abid, A., Umer, T., & Zikria, Y. (2020). Role of IOT Technology in Agriculture: A systematic Literature Review. *Electronics*, 9,319.
- Fernandes, R., & Leblanc, S. G. (2005). Parametric (modified least squares) and non-parametric (Theil-Sen) linear regressions for predicting biophysical parameters in the presence of measurement errors. *Remote Sensing of Environment*, 95(3), 303-316.
- Fisher, J. B., Lee, B., Purdy, A. J., Halverson, G. H., Dohlen, M. B., Cawse - Nicholson, K., & Hook, S. (2020). ECOSTRESS: NASA's next generation mission to measure evapotranspiration from the international space station. *Water Resources Research*, 56(4), e2019WR026058.
- Foale, M. A., Probert, M. E., Carberry, P. S., Lack, D., Yeates, S., Brimblecombe, D., Shaw, R., & Crocker, M. (2004). Participatory research in dryland cropping systems—monitoring and simulation of soil water and nitrogen in farmers' paddocks in Central Queensland. *Australian Journal of Experimental Agriculture*, 44, 321-331. doi: 10.1071/EA02205
- García-Tejero, I. F., Gutiérrez-Gordillo, S., Ortega-Arévalo, C., Iglesias-Contreras, M., Moreno, J. M., Souza-Ferreira, L., & Durán-Zuazo, V. H. (2018). Thermal imaging to monitor the crop-water status in almonds by using the non-water stress baselines. *Scientia Horticulturae*, 238, 91-97.
- Garden, D., Jones, C., Friend, D., Mitchell, M., & Fairbrother, P. (1996). Regional research on native grasses and native grass - based pastures. *New Zealand Journal of Agricultural Research*, 39(4), 471-485.
- Garden, D., Lodge, G., Friend, D., Dowling, P., & Orchard, B. (2000). Effects of grazing management on botanical composition of native grass-based pastures in temperate south-east Australia. *Australian Journal of Experiment Agriculture*, P225-245.

Gardner, B. R., Nielsen, D. C., & Shock, C. C. (1992). Infrared thermometry and the crop water stress index. I. History, theory, and baselines. *Journal of production agriculture*, 5(4), 462-466.

Garre, P., & Harish, A. (2018, December). Autonomous agricultural pesticide spraying uav. In *IOP Conference Series: Materials Science and Engineering* (Vol. 455, p. 012030). IOP Publishing.

Gerhards, M., Schlerf, M., Rascher, U., Udelhoven, T., Juszczak, R., Alberti, G., ... & Inoue, Y. (2018). Analysis of airborne optical and thermal imagery for detection of water stress symptoms. *Remote Sensing*, 10(7), 1139.

Gerhards, M., Schlerf, M., Mallick, K., & Udelhoven, T. (2019). Challenges and future perspectives of multi-/Hyperspectral thermal infrared remote sensing for crop water-stress detection: A review. *Remote Sensing*, 11(10), 1240.

Golgul, I., Kirnak, H., Irik, H. (2022) Yield components and crop water stress index (CWSI) of Mung Bean Grown under deficit irrigations. *Gesunde Pflanzen*. 75(10):1-11. DOI: 10.1007/s10343-022-00698-z

Gonzalez-Dugo, V., Lopez-Lopez, M., Espadafor, M., Orgaz, F., Testi, L., Zarco-Tejada, P., ... & Fereres, E. (2019). Transpiration from canopy temperature: Implications for the assessment of crop yield in almond orchards. *European Journal of Agronomy*, 105, 78-85.

Gonzalez-Dugo, V., Zarco-Tejada, P., Nicolás, E., Nortes, P. A., Alarcón, J. J., Intrigliolo, D. S., & Fereres, E. J. P. A. (2013). Using high resolution UAV thermal imagery to assess the variability in the water status of five fruit tree species within a commercial orchard. *Precision Agriculture*, 14, 660-678.

Gonzalez-Dugo, V., Zarco-Tejada, P., & Intrigliolo, D. (2021). Normalization of crop water stress index to assess the within-field spatial variability of water stress sensitivity. *Precision Agriculture*, 22, 964-983.

Gonzalez-Dugo, V., & Zarco-Tejada, P. J. (2022). Assessing the impact of measurement errors in the calculation of CWSI for characterizing the water status of several crop species. *Irrigation Science*, 1-13.

Grüner, E., Astor, T., & Wachendorf, M. (2019). Biomass prediction of heterogeneous temperate grasslands using an SfM approach based on UAV imaging. *Agronomy*, 9(2), 54.

Guereña, A., Ruiz - Ramos, M., Díaz - Ambrona, C. H., Conde, J. R., & Mínguez, M. I. (2001). Assessment of climate change and agriculture in Spain using climate models. *Agronomy Journal*, 93(1), 237-249.

Guobin, L., Kemp, D. R., & Liu, G. B. (1992). Water stress affects the productivity, growth components, competitiveness and water relations of phalaris and white clover growing in a mixed pasture. *Australian journal of agricultural research*, 43(3), 659-672.

Haghverdi, A., Reiter, M., Singh, A., & Sapkota, A. (2021). Hybrid bermudagrass and tall fescue turfgrass irrigation in central California: II. Assessment of NDVI, CWSI, and canopy temperature dynamics. *Agronomy*, 11(9), 1733.

Han, C. W., Lee, S. Y., Hong, Y. K., & Kweon, G. (2019). Development of a variable rate applicator for uniform fertilizer spreading. *International Journal of Agricultural and Biological Engineering, 12*(2), 82-89.

Handcock, R. N., Gobbett, D. L., González, L. A., Bishop-Hurley, G. J., & McGavin, S. L. (2016). A pilot project combining multispectral proximal sensors and digital cameras for monitoring tropical pastures. *Biogeosciences, 13*(16), 4673-4695.

Harrison, M., Cullen, B., & Rawnsley, R. (2016). Modelling the sensitivity of agricultural systems to climate change and extreme climatic events. *Agricultural systems, 148*, 135-148.

Hassler, S. C., & Baysal-Gurel, F. (2019). Unmanned aircraft system (UAS) technology and applications in agriculture. *Agronomy, 9*(10), 618.

Hayman, P., Whitbread, A., & Gobbett, D. (2008, September). Practicing agronomy in an uncertain climate—Using simulation modelling to study seasonal drought and the impact of ENSO in the Southern Australian grains belt. In *Proceedings of the 14th ASA Conference, Adelaide, South Australia*.

Heady, E. (1957). An economic investigation of the technology of Agricultural Production Functions. *Econometrica, 25*(2), 249-268.

Higgins, S., Schellberg, J., & Bailey, J. S. (2019). Improving productivity and increasing the efficiency of soil nutrient management on grassland farms in the UK and Ireland using precision agriculture technology. *European Journal of Agronomy, 106*, 67-74.

Hill, M. J., Donald, G. E., Hyder, M. W., & Smith, R. C. (2004). Estimation of pasture growth rate in the southwest of Western Australia from AVHRR NDVI and climate data. *Remote sensing of environment, 93*(4), 528-545.

Hipps, L. E., Asrar, G., & Kanemasu, E. T. (1985). A theoretically based normalization of environmental effects on foliage temperature. *Agricultural and Forest Meteorology, 35*(1-4), 113-122.

Hochman, Z., van Rees, H., Carberry, P., Hunt, J., McCown, R., Gartmann, A., Holzworth, D., van Rees, S., Dalgliesh, N., Long, W., Peake, A., Poulton, P., & McClelland, T. (2009). Reinventing model-based decision support with Australian dryland farmers. 4 Yield Prophet helps farmers monitor and manage crops in variable climate. *Crop and Pasture Science, 60*, 1057-1070.

Hornero, A., Zarco-Tejada, P.J., Quero, J.L., North, P.R.J., Ruiz-Gomez, F.J., Sanchez-Cuesta, R., Hernandez-Clemente, R. (2021) Modelling hyperspectral- and thermal-based plant traits for the early detection of Phytophthora-induced symptoms in oak decline, *Remote Sensing of Environment, 263*, 112570.

Horst, G., O'Toole, J., Faver, K. (1989) Seasonal and Species variation in baseline functions for determining Crop Water Stress Indices in Turfgrass. *Crop Science Vol 29, Issue 5. P 1227-1232.*

Hughes, N., Ying Soh, W., Boult, C., Lawson, K., Donoghue, M., & Valle, H. (2019). Abares working paper. www.agriculture.gov.au

- Hunt, J., Van Rees, H., Hochman, Z., Carberry, P., Holzworth, D., Dalgliesh, N., ... & Peake, A. (2006, September). Yield Prophet®: An online crop simulation service. In *Proceedings of the 13th Australian Agronomy Conference* (pp. 10-14).
- Hunt, J., & Kirkegaard, J. (2011). Re-evaluating the contribution of summer fallow rain to wheat yield in southern Australia. *Crop and Pasture Science*, 62(11), 915-929.
- Hutchinson, K. J. (1970). The persistence of perennial species under intensive grazing in a cool temperate environment. Proceedings 11th int. Grassld Congr., Surfers Paradise, 1970, 611-14.
- Idso, S., Jackson, R., Pinter, J., Reginato, R., & Hatfield, J. (1981). Normalizing the stress-degree-day parameter for environmental variability. *Agricultural and Forest Meteorology*, 24, 45-55.
- Idso, S. (1982). Non water stressed baselines: A key to measuring and interpreting plant water stress. *Agricultural and Forest Meteorology*, 27, 59-70.
- Idso, S. B., Reginato, R. J., Clawson, K. L., & Anderson, M. G. (1984). On the stability of non-water-stressed baselines. *Agricultural and Forest Meteorology*, 32, 177-182.
- Invest in Victorian Agriculture and Food. (August 2018). Economic Development, Jobs, Transport and Resources.
- Irmak, S., Haman, D., & Bastug, R. (2000). Determination of crop water stress index for irrigation timing and yield estimation of corn. *Agronomy Journal*, 92, 1221-1227.
- Ishimwe, R., Abutaleb, K., & Ahmed, F. (2014). Applications of thermal imaging in agriculture—A review. *Advances in remote Sensing*, 3(03), 128.
- Jackson, R., Reginato, R., & Idso, S. (1977). Wheat canopy temperature; a practical guide tool for evaluating water requirements. *Water Resources Research*, 13(3), 651-656.
- Jackson, R. D., Idso, S. B., Reginato, R. J., & Pinter Jr, P. J. (1981). Canopy temperature as a crop water stress indicator. *Water resources research*, 17(4), 1133-1138.
- Jalali-Farahani, H., Slack, D., Kopec, D., & Matthias, A. (1993). Crop water stress index models for bermudagrass Turf: A comparison. *Agronomy Journal*, 85(6), 1210-1217.
- Jensen, H., Svendsen, H., & Mogensen, V. (1990). Canopy-air temperature of crops grown under different irrigation regimes in a temperate humid climate. *Irrigation Science*, 11(3), 181-188.
- Jeffrey, S. J., Carter, J. O., Moodie, K. B., & Beswick, A. R. (2001). Using spatial interpolation to construct a comprehensive archive of Australian climate data. *Environmental Modelling & Software*, 16(4), 309-330.
- Jin, X., Zarco-Tejada, P. J., Schmidhalter, U., Reynolds, M. P., Hawkesford, M. J., Varshney, R. K., ... & Li, S. (2020). High-throughput estimation of crop traits: A review of ground and aerial phenotyping platforms. *IEEE Geoscience and Remote Sensing Magazine*, 9(1), 200-231.

Jochec, K. G., Mjelde, J. W., Lee, A. C., & Conner, J. R. (2001). Use of seasonal climate forecasts in rangeland-based livestock operations in West Texas. *Journal of Applied Meteorology and Climatology*, 40(9), 1629-1639.

Jochinke, D. C., Noonan, B. J., Wachsmann, N. G., & Norton, R. M. (2007). The adoption of precision agriculture in an Australian broadacre cropping system—Challenges and opportunities. *Field Crops Research*, 104(1-3), 68-76.

Johnson, I. R., Lodge, G. M., & White, R. E. (2003). The sustainable grazing systems pasture model: description, philosophy and application to the SGS National Experiment. *Australian Journal of Experimental Agriculture*, 43(8), 711-728.

Johnson, I. R., Chapman, D. F., Snow, V. O., Eckard, R. J., Parsons, A. J., Lambert, M. G., & Cullen, B. R. (2008). DairyMod and EcoMod: biophysical pasture-simulation models for Australia and New Zealand. *Australian journal of experimental agriculture*, 48(5), 621-631.

Johnston, W. H. (1996). The place of C4 grasses in temperate pastures in Australia. *New Zealand Journal of Agricultural Research*, 39(4), 527-540.

Jones, H. G. (1998). Stomatal control of photosynthesis and transpiration. *Journal of experimental botany*, 387-398.

Jones, H. G. (1999). Use of infrared thermometry for estimation of stomatal conductance as a possible aid to irrigation scheduling. *Agricultural and forest meteorology*, 95(3), 139-149.

Jones, H. G., Stoll, M., Santos, T., Sousa, C. D., Chaves, M. M., & Grant, O. M. (2002). Use of infrared thermography for monitoring stomatal closure in the field: application to grapevine. *Journal of experimental botany*, 53(378), 2249-2260.

Jones, H. (1992). Plants and microclimate: A quantitative approach to environmental plant physiology (2nd ed.). Cambridge University Press.

Jones, H. G. (2004). Irrigation scheduling: advantages and pitfalls of plant-based methods. *Journal of experimental botany*, 55(407), 2427-2436.

Jones, H. G., Serraj, R., Loveys, B. R., Xiong, L., Wheaton, A., & Price, A. H. (2009). Thermal infrared imaging of crop canopies for the remote diagnosis and quantification of plant responses to water stress in the field. *Functional Plant Biology*, 36(11), 978-989.

Jones, H. G., & Vaughan, R. A. (2010). *Remote sensing of vegetation: principles, techniques, and applications*. Oxford University Press, USA.

Jones, J. W., Antle, J. M., Basso, B., Boote, K. J., Conant, R. T., Foster, I., ... & Wheeler, T. R. (2017). Toward a new generation of agricultural system data, models, and knowledge products: State of agricultural systems science. *Agricultural systems*, 155, 269-288.

Jones, J. W., Antle, J. M., Basso, B., Boote, K. J., Conant, R. T., Foster, I., ... & Wheeler, T. R. (2017). Brief history of agricultural systems modelling. *Agricultural systems*, 155, 240-254.

- Jung, J., Maeda, M., Chang, A., Landivar, J., Yeom, J., & McGinty, J. (2018). Unmanned aerial system assisted framework for the selection of high yielding cotton genotypes. *Computers and Electronics in Agriculture*, 152, 74-81.
- Kar, G., Kumar, A. (2010) Energy balance and crop water stress in winter maize under phenology-based irrigation scheduling. *Irrigation Science*. 28(3):211-220. DOI: 10.1007/s00271-009-0192-x
- Keating, B. A., Gaydon, D., Huth, N. I., Probert, M. E., Verburg, K., Smith, C. J., & Bond, W. (2002). Use of modelling to explore the water balance of dryland farming systems in the Murray-Darling Basin, Australia. *European Journal of Agronomy*, 18(1-2), 159-169.
- Keating, B., Carberry, P., Hammer, G., Probert, M., Robertson, M., Holzworth, D., ... McLean, G. (2003). An overview of APSIM, a model designed for farming systems simulation. *European Journal of Agronomy*, 18, 267-288.
- Keogh, D. U., Watson, I. W., Bell, K. L., Cobon, D. H., & Dutta, S. C. (2005). Climate information needs of Gascoyne-Murchison pastoralists: A representative study of the Western Australian grazing industry. *Australian Journal of Experimental Agriculture*, 45, 1613-1625.
- Khanal, S., Kc, K., Fulton, J. P., Shearer, S., & Ozkan, E. (2020). Remote sensing in agriculture—accomplishments, limitations, and opportunities. *Remote Sensing*, 12(22), 3783.
- Kiem, A. S., Johnson, F., Westra, S., van Dijk, A., Evans, J. P., O'Donnell, A., ... & Mehrotra, R. (2016). Natural hazards in Australia: droughts. *Climatic Change*, 139, 37-54.
- King, A. D., Pitman, A. J., Henley, B. J., Ukkola, A. M., & Brown, J. R. (2020). The role of climate variability in Australian drought. *Nature Climate Change*, 10(3), 177-179.
- Knipper, K. R., Kustas, W. P., Anderson, M. C., Alsina, M. M., Hain, C. R., Alfieri, J. G., ... & Sanchez, L. A. (2019). Using high-spatiotemporal thermal satellite ET retrievals for operational water use and stress monitoring in a California vineyard. *Remote Sensing*, 11(18), 2124.
- Kölling, K., George, G. M., Künzli, R., Flütsch, P., & Zeeman, S. C. (2015). A whole-plant chamber system for parallel gas exchange measurements of *Arabidopsis* and other herbaceous species. *Plant Methods*, 11, 1-12.
- Kumar, N., Poddar, A., Shankar, V., Ojha, C. S. P., & Adeloye, A. J. (2020). Crop water stress index for scheduling irrigation of Indian mustard (*Brassica juncea*) based on water use efficiency considerations. *Journal of Agronomy and Crop Science*, 206(1), 148-159.
- Ledgard, S., & Steele, K. (1992). Biological nitrogen fixation in mixed legume/grass pastures. *Plant and Soil*, 141, 137-153.
- Lee, W. S., Schueller, J. K., & Burks, T. F. (2005). Wagon-based silage yield mapping system. *Agricultural Engineering International: CIGR Journal*.

Leinonen, I., & Jones, H. G. (2004). Combining thermal and visible imagery for estimating canopy temperature and identifying plant stress. *Journal of experimental botany*, 55(401), 1423-1431.

Leith, P. B. (2006). Conversations about climate: Seasonal variability and graziers' decisions in the eastern rangeland. School of Geography and Environmental Studies, University of Tasmania.

Liu, N., Deng, Z., Wang, H., Luo, Z., Gutierrez-Jurado, H., He, X., Guan, H. (2020) Thermal remote sensing pf plant water stress in natural ecosystems. *Forest Ecology and Management*. Volume 476, 15 November 2020, 118433

Lleida University Research Group In AgroTIC and Precision Agriculture. (n.d.). In Springer.com. Retrieved from <https://www.springer.com/journal/11119/updates/17240272>

Lugojan, C., & Ciulca, S. (2011). Evaluation of relative water content in winter wheat. *Journal of Horticulture, Forestry and Biotechnology*, 15(2), 173-177.

Maes, W. H., & Steppe, K. (2012). Estimating evapotranspiration and drought stress with ground-based thermal remote sensing in agriculture: A review. *Journal of Experimental Botany*, 63, 4671-4712.

Maes, W. H., Baert, A., Huete, A. R., Minchin, P. E., Snelgar, W. P., & Steppe, K. (2016). A new wet reference target method for continuous infrared thermography of vegetations. *Agricultural and Forest Meteorology*, 226, 119-131.

Maes, W. H., & Steppe, K. (2019). Perspectives for remote sensing with unmanned aerial vehicles in precision agriculture. *Trends in plant science*, 24(2), 152-164.

Masoud, M., Hsieh, J., Helmstedt, K., McGree, J., & Corry, P. (2023). An integrated pasture biomass and beef cattle liveweight predictive model under weather forecast uncertainty: An application to Northern Australia. *Food and Energy Security*, e453.

McCown, R. L., Hammer, G. L., Hargreaves, J. N. G., Holzworth, D., & Huth, N. I. (1995). APSIM: an agricultural production system simulation model for operational research. *Mathematics and computers in simulation*, 39(3-4), 225-231.

McDonnell, J., Brophy, C., Ruelle, E., Shalloo, L., Lambkin, K., & Hennessy, D. (2019). Weather forecasts to enhance an Irish grass growth model. *European Journal of Agronomy*, 105, 168-175.

McIntosh, P. C., Ash, A. J., & Smith, M. S. (2005). From oceans to farms: the value of a novel statistical climate forecast for agricultural management. *Journal of Climate*, 18(20), 4287-4302.

Messina, G., & Modica, G. (2020). Applications of UAV thermal imagery in precision agriculture: State of the art and future research outlook. *Remote Sensing*, 12(9), 1491.

Michez, A., Lejeune, P., Bauwens, S., Herinaina, A. A. L., Blaise, Y., Castro Muñoz, E., ... & Bindelle, J. (2019). Mapping and monitoring of biomass and grazing in pasture with an unmanned aerial system. *Remote Sensing*, 11(5), 473.

Mitchell, P., Kane, V., Lieschke, M. (2022) Farming Forecaster: integrating multiple sources of information for livestock producers. CSIRO. Farming Forecaster: integrating multiple sources of information for livestock producers. In: Australian Agronomy Conference; 19 to end of 22 Sep 2022; Toowoomba. CSIRO; 2022. 4. CSIRO: EP2022-2361.

Mohammed, B., Bekkay, H., Hassan, M., & Khalid, C. (2022, May). Neural Network-Based Precision Irrigation Scheduling and Crop Water Stress Index (CWSI) Assessment. In *International Conference on Electronic Engineering and Renewable Energy Systems* (pp. 661-669). Singapore: Springer Nature Singapore.

Moore, R. (1970). South-eastern temperate woodlands and grasslands. In *Australian Grasslands* (1st ed.).

Moore, A. D., Donnelly, J. R., & Freer, M. (1997). GRAZPLAN: decision support systems for Australian grazing enterprises. III. Pasture growth and soil moisture submodels, and the GrassGro DSS. *Agricultural systems*, 55(4), 535-582.

Mu, J., McCarl, B., & Wein, A. (2013). Adaptation to climate change: Changes in farmland use and stocking rate in the US. *Mitigation and Adaptation Strategies for Global Change*, 18, 713-730.

Mulla, D. (2013). Twenty-five years of remote sensing in precision agriculture: Key advances and remaining knowledge gaps. *Biosystems Engineering*, 114, 358-371.

Murphy, B. F., & Timbal, B. (2008). A review of recent climate variability and climate change in southeastern Australia. *International Journal of Climatology: A Journal of the Royal Meteorological Society*, 28(7), 859-879.

Myeni, L., Moeletsi, M., & Clulow, A. (2021). Field calibration of DFM capacitance probes for continuous soil moisture monitoring. *Water SA*, 47(1), 88-96.

NDVI from Landsat 8 vegetation indices to study movement dynamics of CAPRA IBEX in mountain areas.

Nielsen, D. C. (1990). Scheduling irrigations for soybeans with the crop water stress index (CWSI). *Field Crops Research*, 23(2), 103-116.

O'Reilly, D., Herdrich, G., & Kavanagh, D. F. (2021). Electric propulsion methods for small satellites: A review. *Aerospace*, 8(1), 22.

O'Shaughnessy, S., Evett, S., Colaizzi, P., & Howell, T. (2012). A crop water stress index and time threshold for automatic irrigation scheduling of grain sorghum. *Agricultural Water Management*, 107, 122-132.

O'Shaughnessy, S. A., Kim, M., Andrade, M. A., Colaizzi, P. D., & Evett, S. R. (2020). Site-specific irrigation of grain sorghum using plant and soil water sensing feedback-Texas High Plains. *Agricultural water management*, 240, 106273.

Park, S., Nolan, A., Ryu, D., Fuentes, S., Hernandez, E., Chung, H., & O'Connell, M. (2015, November). Estimation of crop water stress in a nectarine orchard using high-resolution imagery from unmanned aerial vehicle (UAV). In *Proceedings of the 21st International Congress on Modelling and Simulation, Gold Coast, Australia* (Vol. 29).

- Park, S., Ryu, D., Fuentes, S., Chung, H., Hernández-Montes, E., & O'Connell, M. (2017). Adaptive estimation of crop water stress in nectarine and peach orchards using high-resolution imagery from an unmanned aerial vehicle (UAV). *Remote Sensing*, 9(8), 828.
- Park, S., Ryu, D., Fuentes, S., Chung, H., O'Connell, M., & Kim, J. (2021). Dependence of CWSI-based plant water stress estimation with diurnal acquisition times in a nectarine orchard. *Remote Sensing*, 13(14), 2775.
- Parkash, V., & Singh, S. (2020). A review on potential plant-based water stress indicators for vegetable crops. *Sustainability*, 12(10), 3945.
- Payero, J. O., Neale, C. M. U., & Wright, J. L. (2005). Non-water-stressed baselines for calculating crop water stress index (CWSI) for alfalfa and tall fescue grass. *Transactions of the ASAE*, 48(2), 653-661.
- Pembleton, K. G., Cullen, B. R., Rawnsley, R. P., Harrison, M. T., & Ramilan, T. (2016). Modelling the resilience of forage crop production to future climate change in the dairy regions of Southeastern Australia using APSIM. *The Journal of Agricultural Science*, 154(7), 1131-1152.
- Perera, R., Cullen, B., & Eckard, R. (2020). Changing patterns of pasture production in south-eastern Australia from 1960 to 2015. *Crop and Pasture Science*, 71, 70-81.
- Pinter, J., Ritchie, J., Hatfield, J., & Hart, J. (2003). The agricultural research services remote sensing program: An example of interagency collaboration. *Photogrammetric Engineering & Remote Sensing*, 69(6), 615-618.
- Pungulani, L., Millner, J., Williams, W., & Banda, M. (2013). Improvement of leaf wilting scoring system in cowpea (*Vigna unguiculata* (L) Walp.): From qualitative scale to quantitative index. *Australian Journal of Crop Sciences*, 7(9), 1262-1269.
- Prakash, A. (2000). Thermal remote sensing: concepts, issues and applications. *International Archives of Photogrammetry and Remote Sensing*, 33(B1; PART 1), 239-243.
- Presentation by Cullen, B. (2019). Outlook for spring pasture growth: using soil moisture and temperature data.
- Quebrajo, L., Perez-Ruiz, M., Pérez-Urrestarazu, L., Martínez, G., & Egea, G. (2018). Linking thermal imaging and soil remote sensing to enhance irrigation management of sugar beet. *Biosystems Engineering*, 165, 77-87.
- Rawnsley, R. P., Chapman, D. F., Jacobs, J. L., Garcia, S. C., Callow, M. N., Edwards, G. R., & Pembleton, K. P. (2013). Complementary forages-integration at a whole-farm level. *Animal Production Science*, 53(9), 976-987.
- Rawnsley, R. P., Smith, A. P., Christie, K. M., Harrison, M. T., & Eckard, R. J. (2019). Current and future direction of nitrogen fertiliser use in Australian grazing systems. *Crop and Pasture Science*, 70(12), 1034-1043.
- Reed, K. F. M., Nie, Z. N., Miller, S., Hackney, B. F., Boschma, S. P., Mitchell, M. L., ... & Dear, B. S. (2008). Field evaluation of perennial grasses and herbs in southern Australia. 1. Establishment and herbage production. *Australian Journal of Experimental Agriculture*, 48(4), 409-423.

Rehman, A., Abbast, A., Islam, N., & Shaikh, Z. (2014). A review of wireless sensors and networks applications in agriculture. *Computer Standards & Interfaces*, 263-270.

Robinson, G. G., & Simpson, I. H. (1966). Performance of three perennial grass species during the winter drought, 1965 at Shannon Vale Nutrition Station. *Agricultural Gazette of New South Wales*, 77, 743-747.

Rogiers, S. Y., Greer, D. H., Hutton, R. J., & Landsberg, J. J. (2009). Does night-time transpiration contribute to anisohydric behaviour in a *Vitis vinifera* cultivar?. *Journal of Experimental Botany*, 60(13), 3751-3763.

Rud, R., Cohen, Y., Alchanatis, V., Cohen, A., Sprintsin, M., Levi, A., ... & Nigon, T. (2012). Evaluating water status in potato fields using combined information from RGB and thermal aerial images. *Proceedings of 10th ICPA, ISPA, Monticello, IL, USA. CD-ROM*.

Sandler, H. A. (2018). Weed management in cranberries: A historical perspective and a look to the future. *Agriculture*, 8(9), 138.

Scholander, P. F., Bradstreet, E. D., Hemmingsen, E. A., & Hammel, H. T. (1965). Sap Pressure in Vascular Plants: Negative hydrostatic pressure can be measured in plants. *Science*, 148(3668), 339-346.

Schott, J. R. (2007). *Remote sensing: the image chain approach*. Oxford University Press.

Schultz, H. R. (2003). Differences in hydraulic architecture account for near - isohydric and anisohydric behaviour of two field - grown *Vitis vinifera* L. cultivars during drought. *Plant, Cell & Environment*, 26(8), 1393-1405.

Shimshi, D. (1967). Leaf chlorosis and stomatal aperture. *New Phytologist*, 66(3), 455-461.

Shovelton, J. (2017). Virtual Group – Real time estimation of biomass.

Silva, J., & Giller, K. (2021). Grand Challenges for the 21st century: What crop models can and can't (yet) do. *The Journal of Agricultural Science*, 158, 794-805.

Sinclair, D., & Williams, J. (1979). Components of variance involved in estimating soil water content and water content change using a neutron moisture meter. *Australian Journal of Soil Resources*, 17, 237-247.

Slayter, R. (1967). *Plant Water Relationships*. Academic Press Inc, London, 366p.

Smigaj, M., Gaulton, R., Suarez, J. C., & Barr, S. L. (2017). Use of miniature thermal cameras for detection of physiological stress in conifers. *Remote Sensing*, 9(9), 957.

Smith, M. S., Buxton, R., McKeon, G., & Ash, A. (2000). Seasonal climate forecasting and the management of rangelands: do production benefits translate into enterprise profits? *Applications of seasonal climate forecasting in agricultural and natural ecosystems*, 271-289.

Stavros, E. N., Schimel, D., Pavlick, R., Serbin, S., Swann, A., Duncanson, L., ... & Wennberg, P. (2017). ISS observations offer insights into plant function. *Nature Ecology & Evolution*, 1(7), 0194.

Steele, D., Stegman, E. C., & Gregor, B. (1994). Field comparison of irrigation scheduling methods for corn. *Transactions of the ASAE*, 37(4), 1197-1203.

Stern, P. C., & Easterling, W. E. (1999). *Making climate forecasts matter* (Vol. 175). Washington, DC: National Academy Press.

Stockle, C. O., & Dugas, W. A. (1992). Evaluating canopy temperature-based indices for irrigation scheduling. *Irrigation Science*, 13, 31-37.

Struthers, R., Ivanova, A., Tits, L., Swennen, R., & Coppin, P. (2015). Thermal infrared imaging of the temporal variability in stomatal conductance for fruit trees. *International Journal of Applied Earth Observation and Geoinformation*, 39, 9-17.

Sun, Y. G., Zhao, D. Z., Guo, W. Y., Gao, Y., Su, X., & Wei, B. Q. (2013). A review on the application of remote sensing in mangrove ecosystem monitoring. *Acta Ecologica Sinica*, 33(15), 4523-4538.

Tanner, C. (1963). Plant Temperature. *Agronomy Journal*, 55(3), 210-211.

Tsouros, D. C., Bibi, S., & Sarigiannidis, P. G. (2019). A review on UAV-based applications for precision agriculture. *Information*, 10(11), 349.

Verburg, K., Cocks, B., Manning, B., Truman, G., & Schwenke, G. D. (2017). APSoil plant available water capacity (PAWC) characterisation of select Liverpool Plain soils and their landscape context.

Veysi, S., Nasri, A., Hamzeh, S., & Bartholomeus, H. (2017). A satellite-based crop water stress index for irrigation scheduling in sugar canes. *Agricultural Water Management*, 189, 70-86.

Waha, K., Clarke, J., Dayal, K., Freund, M., Heady, C., Parisi, I., & Vogel, E. (2022). Past and future rainfall changes in the Australian midlatitudes and implications for agriculture. *Climatic Change*, 170(3-4), 29.

Wahab, I., Hall, O., & Jirström, M. (2018). Remote sensing of yields: Application of uav imagery-derived ndvi for estimating maize vigor and yields in complex farming systems in sub-Saharan Africa. *Drones*, 2(3), 28.

Waller, R. A., & Sale, P. W. G. (2001). Persistence and productivity of perennial ryegrass in sheep pastures in south-western Victoria: a review. *Australian Journal of Experimental Agriculture*, 41(1), 117-144.

Wan, R., Wang, P., Wang, X., Yao, X., & Dai, X. (2018). Modeling wetland aboveground biomass in the Poyang Lake National Nature Reserve using machine learning algorithms and Landsat-8 imagery. *Journal of Applied Remote Sensing*, 12(4), 046029-046029.

Wang, B., Liu, D. L., Evans, J. P., Ji, F., Waters, C., Macadam, I., ... & Beyer, K. (2019). Modelling and evaluating the impacts of climate change on three major crops in south-eastern Australia using regional climate model simulations. *Theoretical and Applied Climatology*, 138, 509-526.

Wang, E., He, D., Zhao, Z., Smith, C. J., & MacDonald, B. C. (2020). Using a systems modelling approach to improve soil management and soil quality. *Frontiers of Agricultural Science and Engineering*, 7(3), 289-295.

- Wang, J., Xiao, X., Bajgain, R., Starks, P., Steiner, J., Doughty, R. B., & Chang, Q. (2019). Estimating leaf area index and aboveground biomass of grazing pastures using Sentinel-1, Sentinel-2 and Landsat images. *ISPRS Journal of Photogrammetry and Remote Sensing*, 154, 189-201.
- Wanjura, D., Kelly, C., Wend, C., & Hatfield, J. (1984). Canopy temperature and water stress of cotton crops with complete and partial ground cover. *Irrigation Science*, 36-46.
- Wanjura, D., Upchurch, D., & Mahan, J. (2006). Behavior of temperature-based water stress indicators in BIOTIC-controlled irrigation. *Irrigation Science*, 24, 223-232.
- Weiss, M., Jacob, F., & Duveiller, G. (2020). Remote sensing for agricultural applications: A meta-review. *Remote sensing of environment*, 236, 111402.
- Xue, X., Lan, Y., Sun, Z., Chang, C., & Hoffmann, W. C. (2016). Develop an unmanned aerial vehicle based automatic aerial spraying system. *Computers and electronics in agriculture*, 128, 58-66.
- Zarco-Tejada, P. J., Poblete, T., Camino, C., Gonzalez-Dugo, V., Calderon, R., Hornero, A., ... & Navas-Cortes, J. A. (2021). Divergent abiotic spectral pathways unravel pathogen stress signals across species. *Nature Communications*, 12(1), 6088.
- Ziervogel, G., Bithell, M., Washington, R., & Downing, T. (2005). Agent-based social simulation: a method for assessing the impact of seasonal climate forecast applications among smallholder farmers. *Agricultural systems*, 83(1), 1-26.